THE UNIVERSITY *of* EDINBURGH

DIFFERENTIATION OF EXTRAEMBRYONIC ENDODERM STEM CELL LINES AND PARIETAL ENDODERM INTO VISCERAL ENDODERM: THE ART OF XEN CELLS

Agnieszka Maria Paca

Thesis submitted for the degree of Doctor of Philosophy

University of Edinburgh

2012

The work in this thesis is my own, except where otherwise stated.

Agnieszka Paca

Ab ovo.

1. Acknowledgements

Firstly, I would like to thank my supervisor Dr Tilo Kunath for giving me the opportunity to carry out this research project in his lab, for his guidance, never ending optimism and passion for science. I would also like to thank Dr Paul Whiting for giving me an opportunity to experience lab work from an industrial perspective. I would also like to acknowledge BBSRC and Pfizer who funded this project.

This work would have been impossible without members of TC staff: Jon, Marilyn and Helen; and Animal House Unit.

I will be eternally in debt to past and current members of Kunath, Chambers, Brickam, Blackburn, Medvinsky, Lowell and Kaji labs for their daily advice, lab meetings, conversations and making this experience unforgettable. Special thank you goes to Dr Owen Davies, Dr Maurice Canham, Dr Nick Bredenkamp and Dr Christele Gonneau. I would to thank Dr Adin Ross-Gillespie for his help with statistical analysis. I would like to in particular acknowledge help of Dr Andrew Smith with hES cell experiments. His generosity with sharing research experience and protocols is absolutely remarkable. I am also grateful Dr Keisuke Kaji thanks to whom my name appeared in Nature. I also thank Dr Jennifer Nichols for teaching me diapause embryo dissections.

I would also like to thank Alexis, who in particular put up with me at the time of write-up. Last but not least, I would like to thank my parents for their constant support and encouragement throughout the years. Dziękuję.

2. Abstract

The extraembryonic endoderm of mammals is essential for nutritive support of the foetus and patterning of the early embryo. Visceral and parietal endoderm are major subtypes of this lineage with the former exhibiting most, if not all, of the embryonic patterning properties. Extraembryonic endoderm (XEN) cell lines derived from the primitive endoderm of mouse blastocysts represent a cell culture model of this lineage, but are biased towards parietal endoderm in culture and in chimaeras. Here, I further characterise XEN cells and show that these cell lines exhibit high levels of heterogeneity. In an effort for XEN cells to adopt visceral endoderm character different aspects of the in vivo environment were mimicked. I found that BMP4 and laminin promote a mesenchymal-to-epithelial transition of XEN cells with upregulation of epithelial markers and downregulation of mesenchymal markers. Gene expression analysis showed the differentiated XEN cells most resembled extraembryonic visceral endoderm. Correspondingly, inhibition of Erk and BMP signalling drives XEN cells toward parietal endoderm fate. Finally, I show that BMP4 treatment of freshly isolated parietal endoderm from Reichert's membrane promotes its visceral endoderm differentiation. This suggests that parietal endoderm is still developmentally plastic and can be transdifferentiated to a visceral endoderm in response to BMP. Generation of visceral endoderm from XEN cells uncovers the true potential of these blastocyst-derived cells and is a significant step towards modelling early developmental events *ex vivo*.

3. Table of contents

4. List of abbreviations

AVE – anterior visceral endoderm

BMP – bone morphogenic protein

DVE – distal visceral endoderm

DM - Dorsomorphin

ICM – inner cell mass

EB – embryoid bodies

ECM – extracellular matrix

EMT – epithelial-to-mesenchymal transition

emVE – embryonic visceral endoderm

ExEc – extraembryonic ectoderm

ExEn – extraembryonic endoderm

exVE – extraembryonic visceral endoderm

FBS – foetal bovine serum

FGF – fibroblast growth factor

hES – human embryonic stem

MEF – mouse embryonic fibroblast

mES – mouse embryonic stem

MET- mesenchymal to endothelial transition

mRNA – messenger ribonucleic acid

PD03 – PD032519

PE – parietal endoderm

PrE – primitive endoderm

PYS – parietal yolk sac

SB43 – SB431542

VE – visceral endoderm

VYS – visceral yolk sac

TE - trophectoderm

TS – trophoblast stem

UPL – Universal Probe Library

XEN cells – extraembryonic endoderm stem cells

5. Introduction

5.1 General introduction

The early mouse embryo poses a very rewarding and inviting subject of study. It starts as a single cell that goes through a number of divisions and through a number of fate decisions. Each embryo executes exactly the same plan of growth and differentiation. At the time of implantation (~E4.5 = 4.5 days of gestation) the mouse embryo is a blastocyst composed of an outer layer of trophectoderm (TE) cells surrounding the blastocoel cavity, epiblast and layer of primitive endoderm (PrE) on the surface of the epiblast. These three lineages exhibit different developmental potentials: TE cells will give rise to ectoplacental cone and extraembryonic ectoderm (ExEc); the PrE will produce a transient parietal yolk sac and visceral yolk sac endoderm; and the epiblast will form foetal tissues and extraembryonic mesoderm (Fig.5.1) (reviewed in (Tam and Loebel, 2007).

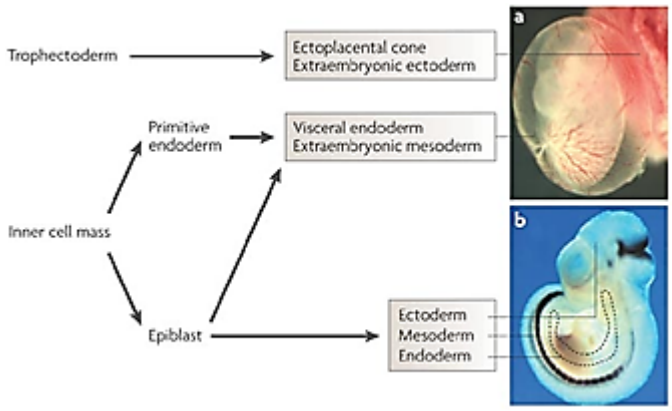

Figure 5.1 Extraembryonic lineages and germ layer derivatives contribution during embryo development. Trophectoderm cells make up part of the placenta (a). Extraembryonic endoderm cells together with epiblast derived extraembryonic mesoderm form the visceral yolk sac (a) and epiblast cells give rise to the foetus (b). Taken from (Tam and Loebel, 2007).

These early embryo lineages have their in vitro equivalents. The first to be derived were mouse embryonic stem (mES) cells, a discovery that proved to be remarkable breakthrough (Evans and Kaufman, 1981; Martin, 1981). To complete the in vitro picture trophoblast stem (TS) cells were subsequently derived from trophectoderm (Tanaka et al., 1998). Finally extraembryonic endoderm (XEN) stem cell lines were derived from the primitive endoderm of blastocysts (Kunath et al.,

2005). Together these cell lines represent models for all early embryonic lineages with each cell line having distinct properties and a lineage-specific chimaera contribution. Establishment of mES, TS and XEN cells allowed for studying of the early embryonic interactions and differentiation outside of the embryo.

5.2 Pre-implantation embryo development

5.2.1 ***Trophectoderm specification***

One of the earliest decisions that an embryo makes is establishing trophectoderm (TE) – its first extraembryonic lineage. Up to the 8-cell stage all blastomeres seemed to be equivalent. Should a single blastomere from 8-cell stage be aggregated with a host embryo it will contribute to all of the foetal and extraembryonic tissues (Kelly, 1977). This would suggest that 8-cell stage blastomeres are totipotent. However, when single 8-cell stage blastomeres were cultured in individual drops of media for up to 2 days, only about 20% of them formed a morula or blastocyst, with 42% forming a trophoblastic vesicle. In contrast, when single 4-cell stage blastomeres were cultured, 58% produced a morula or blastocyst and only 23% formed a trophoblastic vesicle (Tarkowski and Wroblewska, 1967). The discrepancy between chimaera experiments and results from in vitro culture of single blastomere has been attributed to insufficient number of cells for a later stage embryo to develop (Rossant, 1976). Additionally, a single 8-cell stage blastomere can give rise to either mES cell lines (5 cell lines out of 75 blastomeres, 7%) cells or TS cell lines (7 cell lines out of 50 blastomeres, 14%) (Chung et al., 2006). This further implies that, when cultured in vitro not all the blastomeres are equal and they have a greater propensity towards TE. Interestingly, it was shown recently that already at the 4- and 8-cell stage OCT4, a POU family transcription factor that is essential for maintenance of pluripotent state (Nichols et al., 1998b), has different nuclear import and export rates in blastomeres (Plachta et al., 2011). In this experiment OCT4 tagged with photoactivable GFP was activated in the nucleus and as a result two fluorescence decay kinetics were observed in the nuclei. Following this, a lineage tracing experiment assigned cells that have a higher rate of OCT4-paGFP nuclear export to extraembryonic lineage and the ones of lower rate to inner cell mass (ICM) (Plachta et al., 2011). Complementing this expression of

CDX2, a homeobox transcription factor characterising TE, was independently investigated. CDX2 is expressed in a mosaic manner already in an 8-cell stage embryo (Ralston and Rossant, 2008). This mosaic expression of CDX2 is not confirmed by single-cell gene expression analysis (Guo et al., 2010). However, Ralson and Rossant looked at the expression of protein, whilst Guo et al. investigated mRNA. Later in embryo development CDX2 and OCT4 antagonistic interactions have been proposed to reinforce TE and ICM fates (Niwa et al., 2005). *Oct4* null embryos are able to implant but die due to the lack of ICM derivatives (Nichols et al., 1998b). These embryos contain only trophoblast derivatives. In contrast, *Cdx2* mutant embryos continue to express *Oct4* in TE and die between E3.5 and E5.5 (Strumpf et al., 2005).

Unlike the 8-cell stage embryo, where all of the blastomeres have contact with the external environment, in a compacted morula (roughly a 32-cell stage) cells can either be inside the morula or stay in contact with the outer environment taking up position on its surface (Fig. 5.2a). The position of a cell has been proposed by Tarkowski and Wroblewska as driving factor in the commitment towards either ICM or TE (Tarkowski and Wroblewska, 1967). This inside-outside model was further validated by lineage tracing experiments the results of which suggest that inner cells will contribute to ICM, whereas outer cells will form TE (Fleming, 1987). According to this model the initial differentiation of TE is not driven by a transcription factor network, but by the position of a cell only. An alternative model proposes that it's not due to the position of the cell, but due to polarization that cells adopt TE fate (Johnson and Ziomek, 1981). In this model, as a result of cell divisions only outer cells are polarized and inner cells are devoid of polar structures. Indeed, PKC and Par proteins are expressed apically in compacted morula (Pauken and Capco, 2000; Vinot et al., 2005). Interesting evidence supporting in fact both models comes from analysis of Hippo pathway in TE formation (Nishioka et al., 2009). Hippo signalling is known to be dependent on cell-to-cell contact. TEAD4, transcription factor that is upstream of *Cdx2*, is involved in establishment of TE (Nishioka et al., 2008). TEAD4 is only transcriptionally active when it interacts with unphosphorylated Yap. If Yap is phosphorylated by Lats proteins it remains in cytoplasm and is degraded. Analysis of Yap expression show that Yap is phosphorylated in the inside cells, but not in the

outside cells therefore restricting the activity of TEAD4 to outer cells (Nishioka et al., 2009). This observation supports the inside-outside model. However, it is also possible that Hippo transmembrane receptors are differentially allocated between dividing cells of an early embryo (Nishioka et al., 2009). Single cell analysis shows that inner and outer cells of a morula start to diverge already at 16-cell stage and separate completely towards either TE or inner cell mass (ICM) fates by 32-cell stage (Guo et al., 2010).

Maintenance and further differentiation of TE is dependent on the presence of TE-specific transcription factors: *Cdx2*, *Eomes* (Strumpf et al., 2005), *Elf5* (Ng et al., 2008), *Gata3* (Ralston et al., 2010), *Ets2* (Yamamoto et al., 1998). Once the TE is formed the embryo reorganizes its structure. A blastocyst appears with a fluid-filled cavity and asymmetrically positioned ICM surrounded by TE (Fig.5.2b).

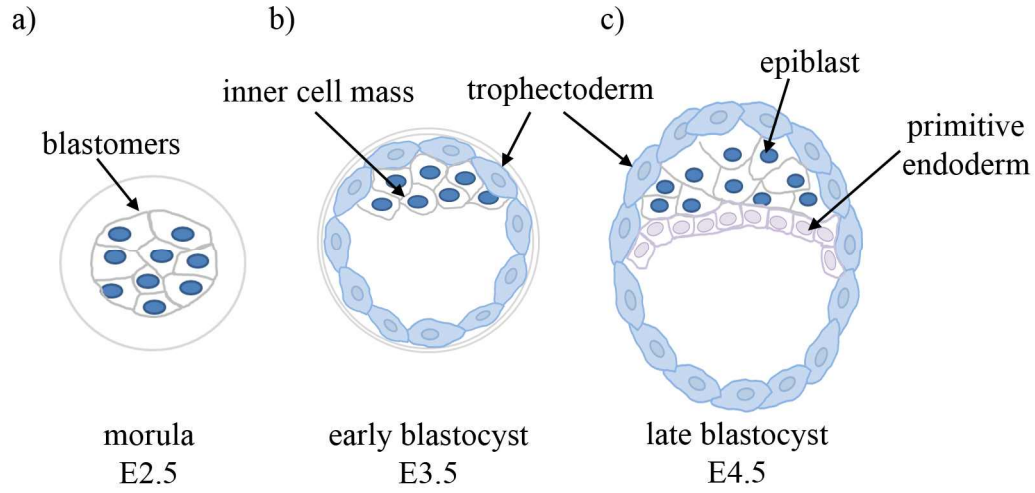

Figure 5.2 Embryo development until implantation. Between E2.5 and E4.5 the embryo establishes two extraembryonic lineages – trophectoderm and primitive endoderm. At the same time the embryo's organization changes from a clump of cells at E2.5 (morula, **a**), to an organized structure with an inner cavity at E3.5-E4.5 (blastocyst **b**, **c**).

5.2.2 Primitive endoderm formation

Following TE differentiation cells by E4.5 (4.5 days of gestation) cells within the ICM differentiate into *Nanog*, *Oct4* and *Sox2* expressing epiblast and *Gata6*, *Gata4* and *Pdgfrα* positive primitive endoderm (PrE). PrE forms an epithelium on the surface of epiblast and is in direct contact with blastocoele (Fig.5.2c). At E3.5 cells in the ICM express NANOG and GATA6 in a "salt-and-pepper" pattern

(Chazaud et al., 2006; Grabarek et al., 2012; Plusa et al., 2008; Yamanaka et al., 2010). The inverse correlation between expression of *Gata6* and *Nanog* is further confirmed by single-cell gene expression analysis of E3.5 ICM cells (Guo et al., 2010; Kurimoto et al., 2006). Analysis of *Pdgfrα*:H2B:GFP embryos, where *Pdgfrα*:H2B:GFP marks PrE precursors, together with careful staging of embryos (by the number of cells) showed that PDGFRα is present already at 16-cell stage (Plusa et al., 2008). Until the 64-cell stage (~E.3.5) PDGFRα, like Gata6, can be coexpressed with NANOG and positioned anywhere within ICM and it's not until a day later that the expression of PDGFRα is confined to PrE only (Plusa et al., 2008).

When a single E3.5 ICM labelled cell was injected into a blastocyst or aggregated with morula the contribution examined at E5.5 was very rarely in both epiblast and PrE (Chazaud et al., 2006), and PrE cells from E4.5 blastocyst would only give rise to PrE or its derivatives (Gardner, 1982; Grabarek et al., 2012). Grabarek et al. addressed the potential of ICM cells with a greater resolution (Grabarek et al., 2012). ICM cells from *Pdgfrα*:H2B:GFP embryos (from E3.25 to E4.5) express various levels of GFP that were assigned to 3 categories: negative, low and high GFP cells. Individual ICM cells from early to fully developed blastocysts were aggregated with morula and cultured for 48-hours in vitro. GFP negative cells were generally biased against PrE fate. GFP low cells presented a growing tendency towards epiblast contribution. GFP high cells showed a multi-lineage contribution that is gradually lost by E4.5 (Grabarek et al., 2012; Yamanaka et al., 2010). Surprisingly, GFP high expressing cells (PrE precursors) have greater plasticity than GFP negative cells (epiblast precursors). Furthermore, it was shown that loss of plasticity coincides with loss of OCT4 expression in PrE (Grabarek et al., 2012).

As the expression of epiblast and PrE markers in the ICM becomes mutually exclusive PrE cells take up position on the surface of epiblast. Observations of movement of cells in the blastocyst between 16-64 cell stage embryo showed ICM cells more frequently moved towards its surface rather than towards the inside (Morris et al., 2010). This has been suggested to happen predominantly through passive processes of division and expansion of the cavity rather through active migration of cells (Plusa et al., 2008). Cells expressing *Pdgfrα*:H2B:GFP deep within

ICM at the time of establishment of the PrE layer either undergo apoptosis or downregulate GFP and assume the epiblast fate (Plusa et al., 2008). The presumed change of fate of GFP-expressing cells in epiblast is also supported by developmental plasticity of early embryo *Pdgfrα*:H2B:GFP positive cells (Grabarek et al., 2012).

Chazaud et al. proposed that the sorting-out mechanism of epiblast and PrE cells is established by differences in adhesion preference of epiblast and PrE cells. This process is driven by Grb2, an adaptor protein involved in mitogen activated protein kinase (MAPK) pathway signal transduction (Chazaud et al., 2006). It has been previously shown that *Grb2* null embryos die by E7.5 and PrE is not formed (Cheng et al., 1998; Coffinier et al., 1999). Chazaud et al. examined closer *Grb2* null blastocysts more closely and observed no expression of GATA6 or GATA4 at E3.5, instead all ICM cells expressed NANOG (Chazaud et al., 2006). In the model proposed by Chazaud et al. the MAPK pathway downregulates *Nanog* and GATA6 levels elevate. Indeed, Nanog directly represses Gata6 (Singh et al., 2007) and MAPK Mek has been shown to downregulate NANOG (Hamazaki et al., 2006). Upregulation of GATA6 in return allows for the expression of its target genes, such as Dab2 and laminin, to be increased (Fig. 5.3). This is then followed by the respective differences in cell adherence to basement membrane of epiblast and PrE progenitors and finally results in sorting out of cells (Chazaud et al., 2006). Mutant embryos for another two members of MAPK signalling pathway - *Fgf4* and *FgfR2* - cannot form PrE exhibiting very similar early embryo phenotype to *Grb2* null embryos (Arman et al., 1998; Feldman et al., 1995). In addition, single-cell analysis showed that *FGF4* is expressed in epiblast-fated cells, whereas *FgfR2* is expressed in PrE precursors (Guo et al., 2010; Kurimoto et al., 2006). Finally, it was shown that manipulation of FGF signalling can change fate of cells within ICM. *Pdgfrα*:H2B:GFP-negative cells in control conditions are biased against PrE contribution, but once exposed to FGF4 they start to contribute to PrE (Grabarek et al., 2012). Conversely, *Pdgfrα*:H2B:GFP-high cells after treatment in PD03 (Mek inhibitor) and Chiron (GSK3β inhibitor) show an increase in epiblast contribution (Grabarek et al., 2012). Yamanaka et al. further clarified the effect of FGF signalling inhibition (Yamanaka et al., 2010). When embryos between E2.5 and E3.75 were

cultured in control conditions and then until E4.5 in the presence of PD03 and PD18 (FGF receptor inhibitor) expression of GATA6 was lost. Interestingly, when an embryo was cultured in the presence of PD03 and PD18 from E2.5 to E3.25 or E3.75 and then was released from inhibitors it recovered expression of GATA4 or GATA6, (Yamanaka et al., 2010). Nichols et al. showed that only NANOG and OCT4 are expressed in the ICM of an 8-cell stage embryo cultured for 2 days in PD03. However should an expanded blastocyst (E3.75) be cultured in the presence of PD03, PD18 and Chiron (GSK3β inhibitor) GATA4 is expressed in PrE layer and there is no difference between inhibitor cultured and control embryos (Nichols et al., 2009). The different source of embryos and treatments used may explain the different results obtained for E3.75 embryos. Nichols et al. used freshly flushed embryos, whilst Yamanaka et al. cultured embryos from 8-cell stage in vitro. Also Nichols et al. added Chiron. Though active-β-catenin is expressed at very low levels at late blastocyst stage and earlier is mainly localised on cell surface, presumably together with E-cadherin (Li et al., 2005), it is possible for Chiron to have an effect on preserving PrE precursors. Interestingly, GATA4 is expressed in an 8-cell stage embryo cultured up to the hatched blastocyst stage in the presence of Chiron (Nichols et al., 2009).

Also integrin β1 has been especially implied to be involved in the process of sorting out of ICM cells (Stephens et al., 1995). Integrin receptors bind to extracellular matrix (ECM). Integrin β1 null embryos die after implantation due to PrE and basement membrane defects. Mutant PrE does not form a layer on top of epiblast and rather remains as a clump of cells within ICM (Stephens et al., 1995). Interestingly, in integrin β1 null embryos blastocoel collapses suggesting that basement membrane plays also a structural role (Stephens et al., 1995).

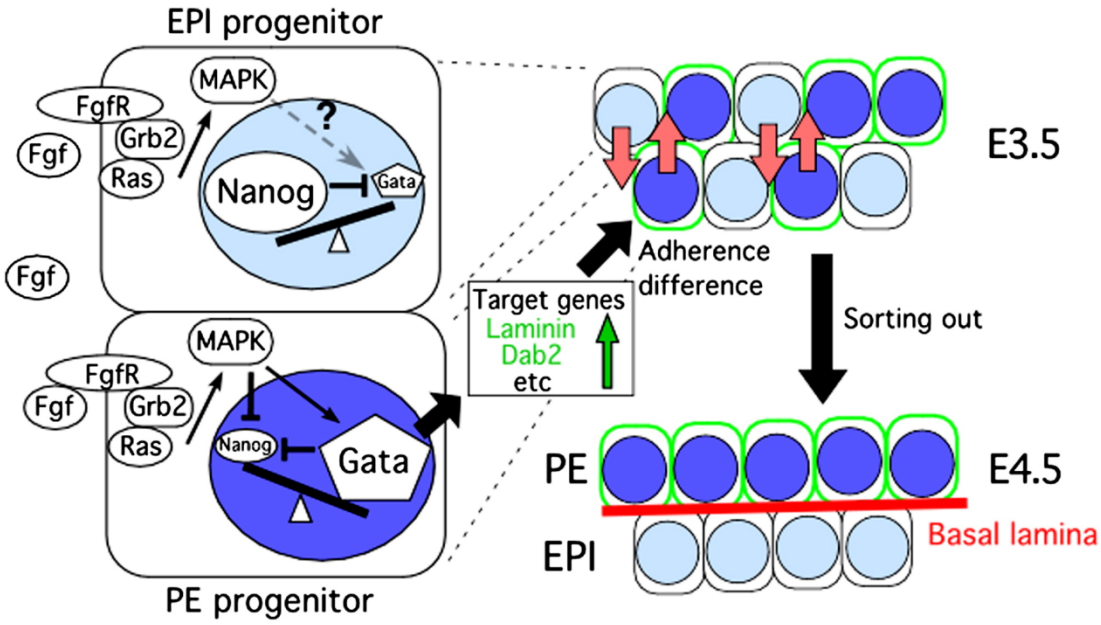

Figure 5.3 Model of epiblast and primitive endoderm formation and segregation. At E3.5 cells in ICM express epiblast and primitive endoderm (PrE) precursors in a mosaic manner. Upon upregulation of Gata6 expression due to activation of MAPK pathway, most likely through FGF signals, PrE precursors start to express laminin and Dab2 which consequently leads to sorting of the two lineages. At E4.5 basal lamina forms and separated PrE from epiblast. (Taken from (Chazaud et al., 2006)

GATA6 is one of the major transcriptional regulators of PrE fate. Stimulation of FGF/Erk pathway upregulates expression of GATA6 (Yamanaka et al., 2010). And once GATA6 expression reaches certain threshold ICM cells execute PrE differentiation program (Chazaud et al., 2006). GATA6 has been found to upregulate expression of Dab2, signal transduction protein (Capo-Chichi et al., 2005; Morrisey et al., 2000; Zhou et al., 2005). *Dab2* null embryos do not undergo gastrulation and are absorbed by E11.5 due to ExEn defects (Morris et al., 2002). PrE differentiates into visceral endoderm (VE) and parietal endoderm (PE), but in the absence of *Dab2* lacks organisation (Morris et al., 2002). Dab2 is coexpressed with other PrE markers: PDFGRα, GATA4 or GATA6 (Capo-Chichi et al., 2005; Plusa et al., 2008) and Dab2 regulates trafficking and signalling of Lrp2, an endocytic receptor present in polarized epithelium(Maurer and Cooper, 2005). Lrp2 was identified in PrE at the time when PrE becomes a polarized epithelium around E4.5 (Gerbe et al., 2008). *Lrp2* knockout mice manifest abnormalities in epithelial tissues and they die perinatally from respiratory insufficiency (Willnow et al., 1996). Another target of

GATA6 is laminin (Li et al., 2004). Mutants for *LamC1* die after implantation and have disorganised ExEn similarly to *Dab2* null embryos (Smyth et al., 1999). Once PrE is formed, epiblast and PrE are separated by basement membrane (basal lamina) of which laminin is a major component (Gersdorff et al., 2005).

Another transcription factor involved in PrE formation is Gata4. Gata4 appears to be downstream of Gata6 (Morrisey et al., 1998). Gata4 is upregulated when expression of Gata6 and Nanog becomes mutually exclusive (Plusa et al., 2008). It was shown at single cell level that expression of PrE markers is more consistent for *Gata4* and *Gata6* double positive cells than for *Gata6* only (Kurimoto et al., 2006; Plusa et al., 2008). Interestingly, *Gata6* mutant embryos exhibit abnormalities in later stages of ExEn differentiation and die after implantation (Koutsourakis et al., 1999; Morrisey et al., 1998). This is perhaps due to some degree of redundancy between Gata6 as Gata4 continues to be expressed in Gata6 null embryo (Morrisey et al., 1998). However, Gata4 cannot fully substitute for Gata6 as it was unable upregulate expression of Dab2 (Capo-Chichi et al., 2005). Gata4 null embryo die around E9.5 due to defects in ventral morphogenesis (Narita et al., 1997).

PrE is also characterised by expression of Sox17. Sox17 expression is observed already at 16-32-cell stage (Artus et al., 2011b; Morris et al., 2010; Niakan et al., 2010). Sox7, another member of Sox transcription factor family, is only expressed at later stages of PrE differentiation in cells already exposed to blastocoel (Artus et al., 2011b). *Sox17* deficient mice show morphological defects in gut definitive endoderm, whilst differentiation of PrE is not affected (Kanai-Azuma et al., 2002). However, when *Sox17*$^{-/-}$ implantation delayed diapause embryos were examined PrE epithelium differentiation was disrupted and some cells were prematurely migrating away (Artus et al., 2011b). Sox7 and Sox17 have been shown to upregulate expression of *Lama1* (laminin α1) (Niimi et al., 2004).

5.3 Extraembryonic endoderm after embryo implantation

5.3.1 Differentiation into visceral and parietal endoderm

After implantation PrE differentiates into two major subtypes – parietal endoderm (PE) and visceral endoderm (VE) (Fig. 5.4) (Enders et al., 1978; Hogan and Tilly, 1981). PE cells migrate along the inner surface of the trophectoderm and together with trophoblast giant cells form parietal yolk sac (PYS) (Hogan et al., 1980). PYS consists of PE cells, giant cells and Reichert's membrane (Salamat et al., 1995; Smith and Strickland, 1981). VE remains in direct contact with the epiblast and is essential for nutritive support of the embryo, but also plays a significant patterning role (Bielinska et al., 1999). Once the embryo is implanted TE, under the influence of FGF4, starts to proliferate rapidly and forms trophoblast consisting of ExEc and the ectoplacental cone (Tanaka et al., 1998). This fast growth pushes epiblast into the cavity and additional proliferation of epiblast results in a cup-like shape structure, an arrangement of tissues characteristic for rodents (Srinivas, 2006). Initially the VE overlays only the epiblast, but as the ExEc increases in size the VE quickly expands to also cover the ExEc. The VE covering the epiblast is called embryonic VE (emVE), whilst the VE on the surface of the ExEc is called extraembryonic VE (exVE) (Fig. 5.4). Throughout early postimplantation development emVE cells contribute to the exVE (Perea-Gomez et al., 2007). The characteristics of VE epithelium are region specific and very dynamic during development. The emVE and exVE show different morphologies; the emVE is a squamous epithelium while the exVE a columnar epithelium (Takito and Al-Awqati, 2004). Until recently, it had been assumed that, later in development, VE is displaced proximally by the cells from anterior primitive streak and its final destination is visceral yolk sac (VYS) (Cross et al., 1994; Lawson et al., 1986; Lawson and Pedersen, 1987). However, a recent report showed that visceral endoderm cells remain associated with the epiblast, intercalate with definitive endoderm and contribute to early gut tube (Kwon et al., 2008).

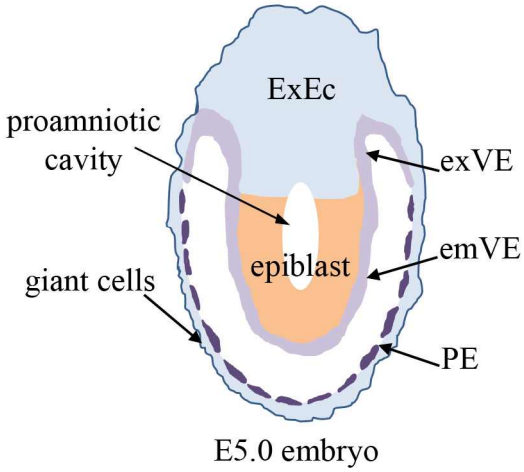

Figure 5.4 Primitive endoderm in an E5.0 embryo differentiates into embryonic and extraembryonic visceral endoderm and parietal endoderm.

After implantation expression of PrE markers Gata4 and Gata6 diverge. At E7.0 Gata6 and Gata4 are present in PE cells and allantois, but only Gata4 is expressed in VE (Koutsourakis et al., 1999; Morrisey et al., 1996). After implantation, Sox7 and Sox17 mark exVE and PE, but Sox17 is also present in a portion of emVE – anterior visceral endoderm (AVE) (Kanai-Azuma et al., 2002). PDGFRα follows a similar expression pattern to Gata6, Sox7 and Sox17. PDGFRα is mostly expressed in exVE and PE and only faintly in emVE (Orr-Urtreger and Lonai, 1992; Plusa et al., 2008; Takakura et al., 1997). Interestingly, though PDGFRα is expressed from early stages of PrE differentiation homozygotes for PDGFRα deletion mutation *Patch* present only growth retardation, deficiencies in mesodermal differentiation and die at birth. They also lack intraplacental yolk sac (IPYS) (Ogura et al., 1998). The IPYS has not been well characterized, but it has been proposed to be a PE and VE derivative (Gasperowicz and Natale, 2011; Kovacs et al., 2002). Deletion of PDGFRα only appears to affect very late ExEn differentiation.

vHnf1 has been identified as an essential transcription factor involved in differentiation of PrE into VE. *vHnf1*$^{-/-}$ embryos die before gastrulation and lack VE, however PE cells are present (Barbacci et al., 1999; Coffinier et al., 1999). vHnf1 induces expression of Hnf4α (Barbacci et al., 1999). Hnf4α is a transcription factor initially expressed at E3.5 and E4.5 in PrE (Kurimoto et al., 2006). Hnf4α expression requires the presence of Gata6 (Morrisey et al., 1998). After implantation Hnf4α

marks emVE and continues to be expressed in yolk sac, but also later in development it is present in the liver and kidneys (Duncan et al., 1994). Interestingly, Hnf4a together with FoxA1, FoxA2 or FoxA3 can directly convert fibroblasts into hepatocytes (Sekiya and Suzuki, 2011). Hnf4α induces expression of Afp (α-fetoprotein), ApoAI, ApoAIV, ApoB proteins and Tfn (Transferrin) (Morrisey et al., 1998). The Hnf4α null embryo has a smaller epiblast, which fails to undergo gastrulation leading to death. The VE is not correctly specified in the Hnf4α null embryo and Afp and Apo proteins are not expressed (Chen et al., 1994; Duncan et al., 1997). The emVE is characterised not only by expression of Hnf4α, but also by Afp (Dziadek and Adamson, 1978; Kwon et al., 2006; Kwon et al., 2008). Afp expression in emVE explants can be downregulated by co-culture with ExEc explants (Dziadek, 1978). Similarly, like Hnf4α, Afp continues to be expressed in the columnar VE epithelium of the yolk sac (Dziadek and Adamson, 1978; Kwon et al., 2006). Other markers of emVE include Bmp2, Fgf5, Fgf8, FoxA2, and Lim1 (Madabhushi and Lacy, 2011; Mesnard et al., 2006; Perea-Gomez et al., 1999).

PrE and VE that are no longer in contact with epiblast or ExEc quickly differentiate into PE. PE cells grow with minimal cell-to-cell contact and are dispersed over the inner surface of Reichert's membrane. PE cells are smooth, scatter individually and have filopodia (Enders et al., 1978; Hogan and Newman, 1984). Whereas VE cells have numerous microvilli on the surface exposed to the cavity and form continuous epithelium (Enders et al., 1978; Hogan and Newman, 1984). VE and PE cells produce laminin α1, β1 and γ1 chains, but PE cells additionally express α2, α3, β2 and γ2 chains (Gersdorff et al., 2005). PrE and VE express E-cadherin, an epithelial marker (Kadokawa et al., 1989). PE cells express Vimentin, a mesenchymal marker (Lane et al., 1983). Differentiation of PrE and VE into PE is the first epithelial-to-mesenchymal transition (EMT) during embryo development (van de Stolpe et al., 1993; Veltmaat et al., 2000; Verheijen et al., 1999a). Already at E4.5 cells start to delaminate from basement membrane and migrate along TE (Grabarek et al., 2012). At E7.5 EMT takes place at the marginal zone around 20 cells long (Hogan and Newman, 1984). EMT is process primarily regulated by expression of Snail (Carver et al., 2001). In order for cells to lose their cell-to-cell adhesion E-cadherin needs to be downregulated. Snail directly represses E-cadherin

by binding to epithelial specific E-box sequences (Batlle et al., 2000; Cano et al., 2000). Snail is upregulated via cAMP by PTHrP (parathyroid hormone related peptide) signalling (Veltmaat et al., 2000). PTHrP binds to PTHR (parathyroid hormone receptor). PTHR is already expressed at E3.5 in PrE cluster(Kurimoto et al., 2006) and later is expressed by exVE and PE (Verheijen et al., 1999a; Verheijen et al., 1999b). PTHrP on the other hand is secreted by TE at the blastocyst stage and later by trophoblast giant cells (Verheijen et al., 1999a; Verheijen et al., 1999b). Interestingly, PTHrP can be observed in the PrE cells that are adjacent to the TE, probably as a result of internalization of secreted PTHrP into the PrE cells (van de Stolpe et al., 1993). However, either due to redundancy or alternative signalling pathway driving PE differentiation mutations in PTHrP or PTHR do not result in impaired PE differentiation (Karaplis and Kronenberg, 1996; Lanske et al., 1996). PTHrP and PTHR null embryos are smaller and exhibit chondrocyte differentiation abnormalities (Karaplis and Kronenberg, 1996; Lanske et al., 1996; Verheijen et al., 1999a).

5.3.2 Appearance and origin of distal and anterior visceral endoderm

At around E5.5 a group of cells at the distal tip of the epiblast differentiates into a morphologically distinguishable tissue – distal visceral endoderm (DVE) (Rivera-Perez et al., 2003; Srinivas et al., 2004). Appearance of DVE marks formation of the distal-proximal axis, an axis of the embryo that translates into the anterior-posterior body axis, (Fig. 5.5a). DVE cells express several marker genes such as *Cer1* (Belo et al., 1997), *Hex* (Thomas et al., 1998), *Lefty1* (Perea-Gomez et al., 1999), *Otx2* (Ang et al., 1994; Perea-Gomez et al., 2001a), *Dkk1* (Kimura-Yoshida et al., 2005), *Hesx* (Thomas and Beddington, 1996), *FoxA2* and *Lim1* (Kimura-Yoshida et al., 2007; Mesnard et al., 2006; Perea-Gomez et al., 1999). *FoxA2* and *Lim1* are initially expressed in emVE their expression is later confined to DVE. Within 4-5 hours (between ~E5.75 and ~E6.0) the DVE migrates proximally as a continuous epithelial sheet to the prospective anterior pole of the embryo. The underlying mechanism of this migration is yet to be fully characterised and both active migration and differences in the proliferation rate of anterior versus posterior epiblast have been implied (Migeotte et al., 2010; Srinivas et al., 2004; Stuckey et al., 2011; Trichas et al., 2011). The unilateral movement of the DVE changes the

distal-proximal axis into the anterior-posterior axis of the embryo (Fig. 5.5b). Once the DVE has moved to the anterior side it is now called anterior visceral endoderm (AVE). AVE expresses a very similar set of markers compared to DVE (Pfister et al., 2007).

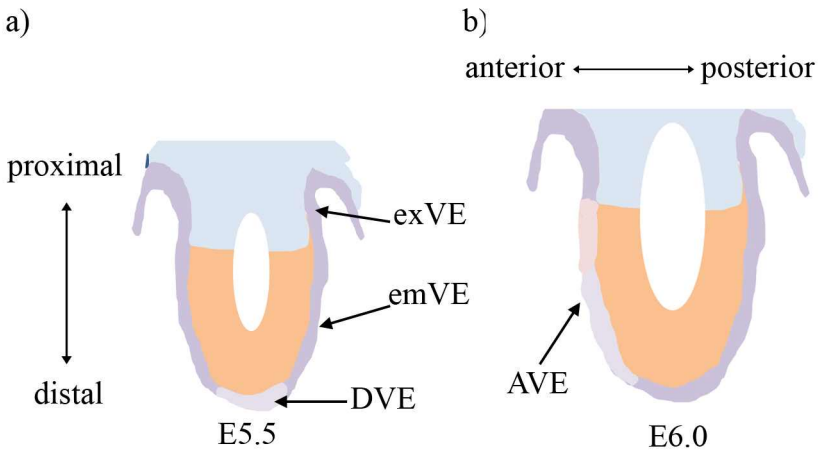

Figure 5.5 Distal and anterior visceral endoderm formation. Between E5.5 and E6.0 DVE cells migrate to the future anterior side of the embryo and form AVE. This results in the transformation of the distal-proximal axis into anterior-posterior axis.

The DVE and AVE are distinguished in the embryo by their locations. However, recently it was shown that not all DVE cells give rise to AVE (Takaoka et al., 2011). *Lefty1* and *Cer1* are already expressed asymmetrically in PrE (Mesnard et al., 2006; Takaoka et al., 2011; Takaoka et al., 2006; Torres-Padilla et al., 2007). Cer1 positive cells in a peri-implantation embryo also express *Lefty1* (Torres-Padilla et al., 2007). Frequently, a couple of cells within the ICM at E3.5 express Lefty1, but tracing experiments showed that these cells contribute to epiblast (Takaoka et al., 2011). Asymmetrical expression of Lefty1 in the VE continues after implantation (Takaoka et al., 2006). Further analysis of *Lefty1*:CreER^{T2}xRosa26R embryos, where transient exposure to tamoxifen allowed cells to be traced with greater resolution, showed that PrE Lefty1-positive cells exclusively give rise to a portion of the DVE (Takaoka et al., 2011). However, surprisingly these cells do not contribute to AVE, but after migration towards the anterior side of the embryo they lose expression of Lefty1 and can be found in lateral VE (Takaoka et al., 2011). Lefty1 and Cer1 positive DVE cells, a subpopulation of DVE, guide the migration of DVE/AVE cells towards the anterior side of the embryo (Takaoka et al., 2011; Takaoka et al., 2006). Genetic ablation of early Lefty1 expressing cells results in lack of DVE migration

(Takaoka et al., 2011). Also surgical removal or laser ablation of DVE affects migration of labelled cells to the anterior side (Miura and Mishina, 2007; Morris et al., 2012). Lefty1 and Cer1 are known antagonists of Nodal signalling (Piccolo et al., 1999; Sakuma et al., 2002). Overexpression of Lefty1 and Cer1 in the anterior portion of the embryo attracts migration of DVE cells towards the anterior. Conversely, upon overexpression of Nodal in the anterior side of an embryo DVE cells migrate in the opposite direction (Yamamoto et al., 2004). These experiments show that lower activity of Nodal signalling, as a result of Lefty1 and Cer1 expression, drives migration of DVE cells towards the anterior portion of the embryo. A live tracing experiment with *Cer1*-GFP positive PrE cells showed that they give rise to DVE and AVE, but also that a portion of *Cer1*-GFP positive DVE and AVE is formed de novo from the emVE after implantation (Torres-Padilla et al., 2007). Also the AVE has been shown not to be a descendent of a single ICM cell (Perea-Gomez et al., 2007). Hex is another marker of DVE and AVE, but is also expressed earlier in PrE (Rodriguez et al., 2001; Thomas et al., 1998). Contrary to asymmetrical Lefty1 and Cer1 expression, Hex is present in all of the PrE cells and has broader and a symmetrical expression in DVE (Mesnard et al., 2006; Thomas et al., 1998; Torres-Padilla et al., 2007). Moreover, in an *Hnf4α* null embryo VE defects do not influence expression of FoxA2 in the DVE, suggesting that proper VE specification is not needed for DVE formation (Chen et al., 1994). It has been recently reported that by the blastocyst stage Nodal signalling can be differentially received (Granier et al., 2011). The activity of the intronic enhancer (ASE) in only a portion of PrE cells could explain upregulation of Lefty1 and Cer1 in a subset of PrE (Granier et al., 2011; Mesnard et al., 2006; Takaoka et al., 2011; Takaoka et al., 2006; Torres-Padilla et al., 2007). Altogether these various experiments suggest polyclonal origin of the DVE and AVE and they show that an early specialized subset of DVE cells is necessary to guide the migration of DVE cells. The polyclonal origin of the DVE and AVE includes precursors already formed in the PrE, but there are also PrE cells that are destined to become DVE and AVE because of their location in the embryo.

Specification of the DVE/AVE requires an equilibrium between Nodal and BMP, members of the TGFβ signalling family, expressed by the epiblast and ExEc,

respectively (Yamamoto et al., 2009). Nodal and BMP signal transduction requires a common co-Smad4 (Massague, 2008). The *Smad4*$^{-/-}$ embryo dies at E7.5 due to gastrulation failure (Sirard et al., 1998). Mutant embryos have poorly differentiated VE and severely reduced expression of *Hnf4α*, however differentiation of PrE and PE seems to be unaffected (Sirard et al., 1998).

Nodal activity is regulated at various levels. Firstly, Nodal precursor needs to be cleaved by proprotein convertases, Furin or Pace4, to generate functional ligand (Beck et al., 2002). Nodal binds to type II receptors ActR-IIA or ActR-IIB and type I receptor ALK4 (ActR-Ib) and may require presence of its co-receptor Cripto which expression in turn is induced by Nodal (Kruithof-de Julio et al., 2011; Shen, 2007; Yeo and Whitman, 2001). Following receptor activation Smad2 or Smad3 are phosphorylated and together with Smad4 mediate transcriptional response in the nucleus (Yeo and Whitman, 2001). Particularly in early embryo development the presence of FoxH1 transcription factor is required for proper translation of Nodal signalling (Norris et al., 2002). FoxH1 also binds to Nodal's intronic enhancer element (ASE) and thus maintains and amplifies Nodal transcription (Norris et al., 2002). Nodal also induces expression of itself (Shen, 2007). Additionally, Nodal phosphorylates p38 which in turn enhances Smad2 activation (Clements et al., 2011).

Nodal is already expressed in the pre-implantation embryo in the epiblast and PrE and after implantation Nodal is maintained throughout the epiblast and VE. Eventually at the time of gastrulation Nodal expression is restricted to the proximal epiblast (Beck et al., 2002; Mesnard et al., 2006). Pro-Nodal convertases have a distinct expression pattern. Pace4 is mainly secreted by ExEc, whilst Furin is present in PrE, emVE and finally in exVE and ExEc (Mesnard et al., 2006). Although in the beginning ALK4, Nodal receptor, is expressed at low levels in the VE, it is upregulated in the DVE (Gu et al., 1998). Smad2 is expressed in the embryo and its extraembryonic tissues, but Smad3 is initially confined to ExEc and although after gastrulation its expression expands into mesoderm and endoderm, it is not present in VE or VYS (Tremblay et al., 2000). Cripto expression is confined to epiblast and later to the proximal portion of the epiblast (Mesnard et al., 2006; Robertson et al., 2003; Takaoka et al., 2006).

Embryos lacking Smad2, ALK4, Nodal, FoxH1 and Furin:Pace4 (double mutant) fail to properly pattern the DVE and die at the time of gastrulation (Beck et al., 2002; Ben-Haim et al., 2006; Brennan et al., 2001; Gu et al., 1998; Nomura and Li, 1998; Waldrip et al., 1998; Yamamoto et al., 2001). The DVE of mutant embryos lacks expression of various markers such as Cer1, Otx2, Lim1, Hesx, FoxA2. These embryos also fail to establish an anterior-posterior axis. Before specifying the AVE Nodal defines the emVE. In Nodal null embryos expression of the exVE marker Ttr is upregulated throughout the VE and expression of emVE markers such as Lim1, Fgf5, Fgf8 and Bmp2 is downregulated (Mesnard et al., 2006). However, formation of the PYS and VYS appears to be unaffected by Smad2 ablation (Nomura and Li, 1998) and differentiation of the PE is unaffected by lack of ALK4 (Gu et al., 1998). Moreover, reduced levels of Nodal signalling prevent the DVE from migrating (Norris et al., 2002). In *Cripto*$^{-/-}$ embryos the DVE is formed but fails to migrate towards the anterior and as a result the anterior-posterior axis is not established (Ding et al., 1998). *Furin*$^{-/-}$:*Pace4*$^{-/-}$ embryos also show delayed onset of Nodal signalling (Beck et al., 2002). Interestingly, in Nodal, ALK4 or Furin:Pace4 mutant embryos the VE cells at the distal tip form an outgrowth towards the cavity (Beck et al., 2002; Ben-Haim et al., 2006; Mesnard et al., 2006). This is probably due to detachment of cells and lack of their anterior migration. However, since these cells have most likely an exVE character they might produce an extensive basement membrane component, which in turn leads to a disorganised architecture of distal tip. Also, since expression of Lefty1 and Cer1 is meant to reduce proliferation rate of cells, the lack of Lefty1 and Cer1 in mutant embryos could affect the number of cells in the VE at the distal end of an embryo (Yamamoto et al., 2004). A similar bulging DVE phenotype is also observed in *Dab2*$^{-/-}$ embryo, which might suggest an additional function of Dab2 in post-implantation embryo development (Morris et al., 2002). In fact, Dab2 has been implied to stabilize interactions between the TGFβ receptor and Smad2 or Smad3 (Derynck and Zhang, 2003).

BMP4 and to a lesser extent BMP2 are other members of the TGF-β family that are involved in formation of the VE, DVE and AVE (Coucouvanis and Martin, 1995; Coucouvanis and Martin, 1999; Soares et al., 2005; Soares et al., 2008; Yamamoto et al., 2009). In an early embryo *Bmp4* is first expressed weakly in the

ICM then in the epiblast and TE and finally in the ExEc (Coucouvanis and Martin, 1999). *BMP2* is present mainly in the VE and weakly in the epiblast of postimplantation embryos (Coucouvanis and Martin, 1999; Mesnard et al., 2006; Yamamoto et al., 2009). BMPs bind to dimers of type I receptors (ALK2 (Actr1), Bmpr1a (ALK3), Bmpr1b (ALK6)) and type II receptor (Bmpr2). ALK2 and Bmpr1a are present in the VE and Bmpr1a is also expressed in the epiblast (de Sousa Lopes et al., 2004; Di-Gregorio et al., 2007). BMP signalling is transduced by phosphorylation of Smad1, Smad5 or Smad8 proteins. In pre-gastrulation embryo Smad1 is highly expressed in VE and at lower levels in epiblast. Smad5 is present at low levels, whereas Smad8 in undetected until gastrulation when it's expressed in extraembryonic mesoderm and epiblast. After gastrulation Smad1, Smad5 and Smad8 are expressed in similar patterns throughout the embryo (Tremblay et al., 2001).

Surprisingly, absence of BMP2 or BMP4 in embryos does not result in defective VE differentiation, which could imply a level of functional redundancy between BMP molecules (Lawson et al., 1999; Zhang and Bradley, 1996). However, more detailed analysis of knocking down BMP4 showed that BMP4 is required at E5.25 for correct DVE migration (Soares et al., 2005; Soares et al., 2008). Embryos lacking expression of ALK2, Bmpr1a or Bmpr2 all exhibit various VE defects. VE in *ALK2*$^{-/-}$ embryos is disrupted and expresses *Hnf4α* at lower levels, whilst PE differentiation is unaltered (Gu et al., 1999). *Bmpr2*$^{-/-}$ embryos show lower levels of phosphorylated Smad1 and an impaired differentiation of emVE (Yamamoto et al., 2009). Additional removal of one copy of *Actr2b* from a *Bmpr2*$^{-/-}$ embryo results in complete loss of phosphorylated Smad1 and emVE differentiation, but exVE is successfully specified (Yamamoto et al., 2009). In *Bmpr1a*$^{-/-}$ embryos even though VE is only slightly thinner and DVE is formed, DVE fails to migrate (Mishina et al., 1995; Miura et al., 2010). In contrast to VE, PE in *Bmpr1a*$^{-/-}$ embryos is unaffected (Mishina et al., 1995). Furthermore, expression of dominant negative Bmpr1b, which does not transduce the BMP signal, blocks VE but not PE differentiation in vitro (Coucouvanis and Martin, 1999). *ALK2*$^{-/-}$, *Bmpr1a*$^{-/-}$ and *Bmpr2*$^{-/-}$ embryos all exhibit mesoderm differentiation defects (Di-Gregorio et al., 2007; Gu et al., 1999; Mishina et al., 1995). *Smad1*$^{-/-}$ embryos proceed through gastrulation and the anterior-

posterior axis is correctly positioned, but the VE is abnormally ruffled in the extraembryonic region (Tremblay et al., 2001). *Smad5*$^{-/-}$ embryos do not exhibit any VE defects, but like *Smad1*$^{-/-}$ embryos, they die after gastrulation due to mesoderm defects (Chang et al., 1999; Tremblay et al., 2001).

In a pre-gastrulation embryo the ExEc is the source of BMP4. Interestingly, it was noticed that the DVE is only formed when the size of egg cylinder reaches 70µm and the size of conceptus is 170µm at around E5.5 (Mesnard et al., 2006). Also the initial broad expression of *Lefty1*, *Cer1* and *Hex* is downregulated between implantation and E5.5 when the DVE is formed (Mesnard et al., 2006). Formation of the DVE correlates with the lack of phosphorylated Smad1 in distal portion of VE at E5.5 (Yamamoto et al., 2009). Moreover, when the ExEc was microsurgically removed from the pre-gastrulation embryo all of the VE acquires DVE/AVE character and the DVE fails to migrate (Mesnard et al., 2006; Richardson et al., 2006; Rodriguez et al., 2005). This has been further attributed to removal of only the posterior part of the ExEc (Richardson et al., 2006). Also additional support comes from introducing BMP4 RNAi into ExEc at E5.25 which resulted in abnormal expansion of *Cer1*-GFP expression (Soares et al., 2008). Moreover, when embryos lacking ExEc were cultured in the presence of SB43154, Activin signalling inhibitor, DVE formation was abolished (Mesnard et al., 2006). To summarize, importantly for correct DVE specification, Nodal together with BMP signalling is required to promote differentiation of PrE/VE into emVE. However, later for DVE differentiation BMP signalling needs to be reduced, but Nodal signalling needs to be maintained at substantial levels (Mesnard et al., 2006; Yamamoto et al., 2009).

Another pathway, involved in DVE and AVE formation is Wnt signalling. In the canonical pathway in the absence of Wnt ligand, β-catenin is phosphorylated by Axin complex (composed of Axin, APC, CK1, and GSK3) and β-catenin is degraded. When Wnt binds to its receptor, the Axin complex is recruited to the receptor and β-catenin inhibition is released and β-catenin can accumulate in nucleus. Wnt can also non-canonically activate other signalling pathways (MacDonald et al., 2009). Analysis of *Apc*$^{min/min}$ mutant, where β-catenin is constitutively active, showed no formation of DVE and expansion of proximal markers (Chazaud and Rossant,

2006). Chimaeras between *Apc*$^{min/min}$ embryos and wild-type ES cells, where ES cells contribute to epiblast, but not visceral endoderm, showed expanded *Hex* expression throughout the VE, but no expression of *Lefty1* and *Cer1* (Chazaud and Rossant, 2006). In addition, when Dkk1, β-catenin antagonist, is not expressed by the DVE the anterior-posterior axis is not formed as DVE cells fail to migrate to the future anterior side (Kimura-Yoshida et al., 2005). A similar phenotype can be observed for *Otx2*$^{-/-}$ embryo where DVE migration, but not differentiation is impaired (Kimura et al., 2000). Dkk1 is a direct target of Otx2 and Otx2 deficiency can be rescued by overexpression of Dkk1 (Kimura-Yoshida et al., 2005). Dkk1, similar to Lefty1, is thought to be guiding DVE migration towards the anterior portion of the embryo (Kimura-Yoshida et al., 2005). Expression of Dkk1 could form a gradient of Wnt3 and hence attract migration of cells towards the anterior (Kimura-Yoshida et al., 2005). Interestingly, loss of migration of the DVE in *Bmpr1a*$^{-/-}$ embryos has also been related to loss of Dkk1 expression (Miura et al., 2010). Furthermore, overexpression of Dkk1 on both anterior and posterior sides of the embryos attracts bilateral DVE migration (Miura et al., 2010). Also β-catenin deficient embryos exhibit defects in DVE migration (Huelsken et al., 2000). However, Wnt3$^{-/-}$ embryos seem to correctly specify both DVE and AVE suggesting that there may be redundancy between other members of the Wnt family during AVE formation (Barrow et al., 2007; Liu et al., 1999). Also, the non-canonical Wnt signalling pathway could be involved in DVE migration. DVE of embryos lacking effectors of non-canonical Wnt signalling - Rac1 or Prickle 1 - fails to migrate (Migeotte et al., 2010; Tao et al., 2009).

Interestingly, all of the described pathways are connected. For instance, Nodal has been implicated in regulation of BMP4 expression as in a *Nodal*$^{-/-}$ embryo BMP4 expression is lower (Beck et al., 2002; Robertson et al., 2003). BMP4 expression from ExEc in turn is required to reinforce Wnt3 expression which in turn maintains expression of Nodal (Ben-Haim et al., 2006; Miura et al., 2010). A perfect balance between pathway interactions and signalling is required for correct axis specification and embryo patterning.

5.3.3 Role and function of extraembryonic endoderm

Descendants of PrE perform crucial functions during embryogenesis. Before formation of the chorioallentoic placenta, the VYS and PYS provide nutrient, gas and waste exchange system for developing embryo (Bielinska et al., 1999). Moreover, VE and its derivatives impart crucial differentiating and patterning cues upon epiblast. Especially, DVE and AVE play critical roles in embryo axis formation and development of anterior structures (Rossant and Tam, 2004; Thomas and Beddington, 1996).

The PYS, composed of PE cells, trophoblast cells and Reichert's membrane, is a transient structure that appears in the embryo after implantation at ~E5.0 and usually disappears by E18 (Dickson, 1979; Salamat et al., 1995). Reichert's membrane is formed by PE and trophoblast giant cells and is mainly composed of collagen IV, laminins, nidogen and perlecan (Gersdorff et al., 2005; Smith and Strickland, 1981). PYS has been implied to act as a filtration barrier (Jollie, 1990). Furthermore, expression of calcitropic genes in PYS suggests its function in calcium transport between a mother and her foetus (Gasperowicz and Natale, 2011; Kovacs et al., 2002).

In contrast to PE, VE is one of key players in early embryo development. Post gastrulation blocking of VYS cells with antibodies results in congenital malformations of embryo (Jensen et al., 1975). At E5.0 VE surrounds the egg cylinder and acts as a barrier between the maternal environment and the embryo. At later stages (~E8.0), together with extraembryonic mesoderm, the VE forms the VYS and by the 14-16 somite stage the VYS entirely enfolds the embryo (Pereira et al., 2011). The VE in the pre-gastrulation embryo expresses proteins that are later found in an adult organism in the tissues interposed between the internal and external environments (Bielinska et al., 1999; Duncan et al., 1994). For example, Hnf4α found in VE is also expressed in hepatocytes, intestinal epithelium and kidney tubules (Duncan et al., 1994). VE also secretes many of the proteins that are later produced by hepatocytes: albumin, transferrin, Afp, apolipoproteins (Dziadek and Adamson, 1978; Meehan et al., 1984; Shi and Heath, 1984). By expression of these molecules VE acts as a gas, nutrient and waste exchange system that is later in

development replaced by the chorioallantois (Bielinska et al., 1999; Cross et al., 1994; Jollie, 1990). After placenta formation the VYS continues to play an essential role in retinol transport (Johansson et al., 1997). Moreover, the VYS is the first site of haematopoiesis in the embryo (McGrath and Palis, 2005; Toles et al., 1989). Through expression of Indian hedgehog (Ihh) and VEGF the VYS induces formation of blood islands and endothelial cells (Byrd et al., 2002; Damert et al., 2002; Dyer et al., 2001). Additionally, proximal VE was shown to be involved in early primordial germ cell differentiation (de Sousa Lopes et al., 2007; de Sousa Lopes et al., 2004).

5.3.3.1 Distal and anterior visceral endoderm as an anterior organizer

In amphibians Spemann and Mangold established the presence of an organizer that is able to induce complete second axis in an embryo (Spemann and Mangold, 1924). Similar organizer structures were subsequently discovered in other organisms - Hensen's node in chick (Waddington, 1932; Waddington, 1933) and the node in mouse (Fig. 5.6) (Beddington, 1994). However, transplantation of the mouse node resulted in formation of an incomplete axis lacking anterior structures (Beddington, 1994). Later in both mouse and chicken additional signalling centres specialised in neural induction called AVE and hypoblast, respectively, were discovered (Bertocchini and Stern, 2002; Chapman et al., 2003; Thomas and Beddington, 1996). AVE plays a significant role in the anterior patterning of the embryo during gastrulation (Beddington and Robertson, 1998; Madabhushi and Lacy, 2011; Perea-Gomez et al., 2001b; Perea-Gomez et al., 2002; Thomas and Beddington, 1996; Yamamoto et al., 2004; Yang and Klingensmith, 2006).

At around E6.0, after formation of anterior posterior axis firstly cells in the proximal posterior epiblast of the embryo start to form the primitive streak (Fig. 5.6). Cells from the epiblast will then migrate through the primitive streak and form germ layers: endoderm and mesoderm. First to migrate is the most posterior mesoderm that is patterned by BMP4 expressed in ExEc and this will give rise to extraembryonic mesoderm. Anterior and lateral levels of streak give rise to other types of mesoderm (lateral plate and paraxial mesoderm). Cells migrating through the most anterior part of the primitive streak will contribute to node, notochord and definitive endoderm. Over the next 36hrs primitive streak will elongate along the posterior towards

anterior portion of the embryo. As gastrulation progresses AVE is displaced by definitive endoderm (reviewed in (Arnold and Robertson, 2009; Tam and Loebel, 2007).

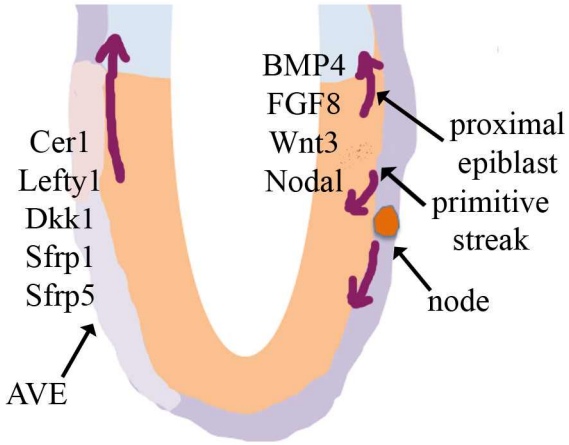

Figure 5.6 Early gastrulation embryo. Anterior visceral endoderm (AVE) synergistically with primitive streak and node patterns the embryo during gastrulation. Magenta arrows mark prospective cell movement through the primitive streak and eventual displacement of AVE by anterior definitive endoderm.

The AVE imparts patterning information onto epiblast by producing agonists and antagonists of TGF-β superfamily and Wnt signalling (Brennan et al., 2001; Perea-Gomez et al., 2001b; Takaoka et al., 2006; Yamamoto et al., 2004). Firstly however, before becoming the anterior organizer, the DVE/AVE is involved in axis formation (Fig. 5.5). Appearance of the DVE, as a subset of the emVE, characterises the distal-proximal axis. The DVE's migration to the anterior side marks the appearance of the anterior-posterior axis (Robertson et al., 2003; Takaoka et al., 2011; Takaoka et al., 2006; Yamamoto et al., 2004). The evidence for the DVE/AVE's crucial role in embryo patterning comes predominantly from the loss of function analysis. Microsurgical removal of AVE resulted in anterior neural structures truncations (Thomas and Beddington, 1996). As a consequence of DVE ablation primitive streak is mispositioned and the expression of posterior markers, *Wnt3*, *Nodal* and *Cripto* expands (Miura and Mishina, 2007).

The DVE/AVE expresses various modulators of signalling pathways: Cer1, Lefty1, Dkk1, Sfrp1 and Sfrp5. Cer1 and Lefty1 are TGF-β signalling inhibitors. Lefty1 binds competitively to ActR-IIA or ActR-IIB receptors (Sakuma et al., 2002).

Cer1 binds directly to Nodal inhibiting its interactions with receptor (Piccolo et al., 1999). Cer1 can also bind and block signalling of BMP and Wnt molecules (Piccolo et al., 1999). Dkk1 is a potent Wnt antagonist that binds to Wnt receptor subunit (Glinka et al., 1998; Kawano and Kypta, 2003). Sfrps molecules directly bind and inactivate Wnt (Kawano and Kypta, 2003). Cooperatively, these inhibitors neutralize Nodal, BMP and Wnt signalling in the anterior epiblast.

Nodal signalling through Smad2 is required for AVE differentiation (Yamamoto et al., 2009). In *Smad2*$^{-/-}$ embryos epiblast assumes proximal character as a result of failure to establish anterior posterior axis (Waldrip et al., 1998). FoxA2 is known to induce expression of *Otx2*, *Dkk1*, *and Cer1* in AVE (Kimura-Yoshida et al., 2007). *FoxA2*$^{-/-}$ embryos fail to express *Otx2* and the expression of *Dkk1* and *Cer1* is downregulated. This in turn upregulates β-catenin signalling in the DVE and results in failure of DVE migration (Kimura-Yoshida et al., 2005; Perea-Gomez et al., 1999). *FoxA2*$^{-/-}$ embryos lack correct anterior-posterior patterning and the primitive streak does not elongate (Dufort et al., 1998). Mutations in other markers of AVE, *Lim1* and *Otx2*, result in severe anterior neural truncations (Kimura et al., 2000; Shawlot et al., 1999). The *Otx2*$^{-/-}$ embryo can be rescued by expression of *Dkk1* (Kimura-Yoshida et al., 2005). Even though single mutant embryo for either *Cer1* or *Lefty1* seems to undergo normal gastrulation, embryos lacking both *Cer1* and *Lefty1* show a plethora of phenotypes ranging from an expanded primitive streak to multiple primitive streak formation (Perea-Gomez et al., 2002; Yamamoto et al., 2004). Interestingly, removal of one copy of *Nodal* rescues this phenotype (Perea-Gomez et al., 2002). The AVE reduces BMP signalling in surrounding tissues (Yang and Klingensmith, 2006). Likewise, epiblast of *Bmpr1a*$^{-/-}$ embryos loses expression of proximal markers such as *Brachyury*, *Fgf8*, *Cripto*, *Wnt3* and *Nodal*, but upregulates expression of early neural markers – *Six3* and *Sox1* (Di-Gregorio et al., 2007).

However, even though AVE explants on their own are not sufficient to induce any ectopic neural tissue in E6.5 epiblast, AVE is able to suppress expression of *Brachyury* and *Cripto*, posterior markers, in anterior epiblast (Kimura et al., 2000; Tam and Steiner, 1999). As stated previously, node transplantations result in

incomplete secondary axis formation (Beddington, 1994). However, when AVE and primitive streak with node where transplanted together strong induction of anterior markers was observed (Tam and Steiner, 1999). Moreover, *Wnt3*$^{-/-}$ embryos lacking primitive streak and node but with properly established AVE do not form neural tissue (Liu et al., 1999). More careful staging of AVE inductive properties showed that AVE can induce expression of Six3, a neural anterior marker, in anterior explants of E6.5-E7.0, but not E6.0-E6.5 embryo. The ability to induce Six3 coincides with the appearance of the node at around E6.5 (Yang and Klingensmith, 2006). Similarly, experiments in chick showed that removal of the AVE caused the appearance of multiple primitive streaks and ectopic grafts of hypoblast can induce transient expression of neural markers (Albazerchi and Stern, 2007; Bertocchini and Stern, 2002).

Recently, BMP2 expression in the AVE has been shown to not only take part in neural induction, but also in heart positioning and foregut invagination (Madabhushi and Lacy, 2011). Similarly, epiblast cultured with VE frequently gives rise to cardiomyocytes and addition of BMP2 enhances cardiomyocyte differentiation (Bin et al., 2006; Hogan and Tilly, 1981).

Altogether all the described experiments indicate that the AVE's function in neural induction in the early embryo is to protect anterior neural tissue from posteriorisation. This happens through repression of posteriorising signals rather than by sending out a positive signal (Fig. 5.6) (Kimura et al., 2000; Perea-Gomez et al., 2002). At the same time the AVE actively takes part in positioning of other anterior structures (Madabhushi and Lacy, 2011).

5.4 In vitro models of blastocyst lineages

5.4.1 Introduction

Mouse ES (mES) cells derived from epiblast (Evans and Kaufman, 1981; Martin, 1981), TS cells derived from trophectoderm (Tanaka et al., 1998) and XEN cells derived from primitive endoderm (Kunath et al., 2005) represent models for all the early embryonic lineages with each cell line representing a different potential for chimaera contribution (Fig. 5.7). mES cells will contribute to the embryo proper

(Beddington and Robertson, 1989; Bradley et al., 1984) TS cells to trophoblast derivatives (Tanaka et al., 1998) and XEN cells to PYS and very rarely to VYS (Kunath et al., 2005). mES require LIF and BMP signalling for self-renewal (Ying et al., 2003). TS cells depend on the presence of FGF4 (Tanaka et al., 1998). Culture conditions for XEN cells have not been yet precisely defined and as a general rule these cells require presence of the serum. Also in culture, both ES and TS cells form epithelial colonies, the presence of which is rare in XEN cells (Fig. 5.7).

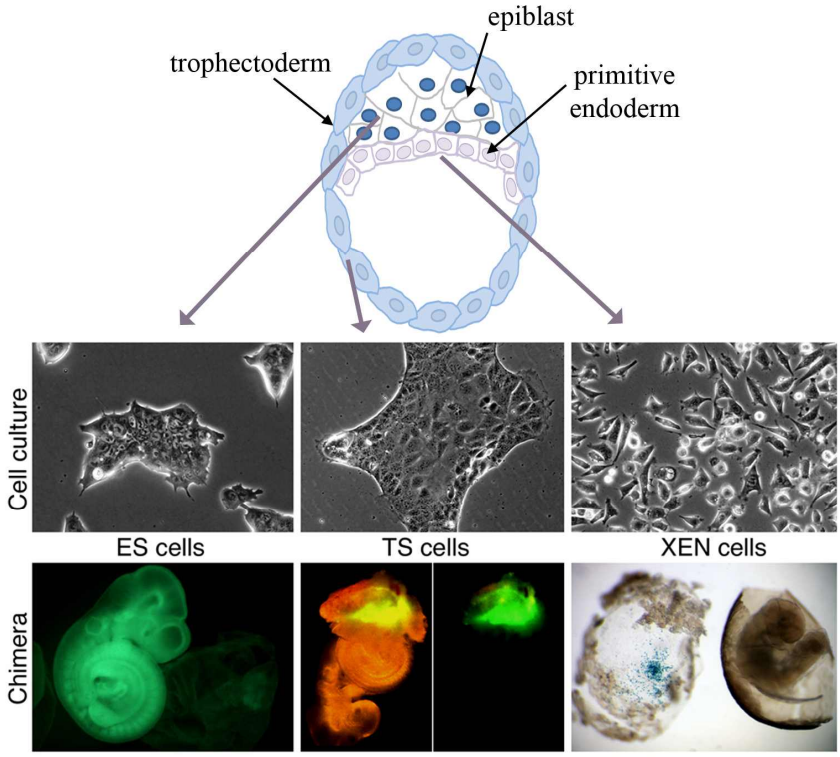

Figure 5.7 Blastocyst-derived stem cell lines contribute to unique, non-overlapping lineages in chimaeras. ES cells derived from epiblast of pre-implantation embryo contribute to the embryo proper and extraembryonic mesoderm. TS cells derived from trophectoderm contribute to trophoblast derivatives, whilst primitive endoderm derived XEN cells contribute to ExEn (modified figure from T. Kunath, unpublished).

5.4.2 Extraembryonic endoderm in vitro models

mES cells rarely contribute to the ExEn in chimaera contribution assays (Beddington and Robertson, 1989; Canham et al., 2010). However when ES cells are cultured in aggregates – embryoid bodies (EBs) - they replicate ICM differentiation and form a layer of PrE on the surface of an aggregate (Coucouvanis and Martin,

1995). EBs reproduce many of the various ExEn differentiation defects that are observed in vivo. *vHnf1*$^{-/-}$ embryos fail to make VE and so do mES *vHnf1*$^{-/-}$ EBs (Coffinier et al., 1999). ExEn of *Lamγ1*$^{-/-}$ EB cells fails to differentiate beyond PrE (Smyth et al., 1999). FGF/Grb2/Erk signalling is crucial for PrE formation from ICM (Arman et al., 1998; Feldman et al., 1995; Nichols et al., 2009; Wang et al., 2011b; Yamanaka et al., 2010). Similarly, in *Grb2*$^{-/-}$ and *Fgf4*$^{-/-}$ EBs PrE is not formed. However, expression of Gata6 in mES cells during *Grb2*$^{-/-}$ EB differentiation fully restores PrE formation (Wang et al., 2011b) and constitutively active Mek overexpression in mES cells drives them toward PrE lineage (Hamazaki et al., 2006).

Until derivation of mES cells embryonal carcinoma (EC) cells were used as a model to study early embryo differentiation (Brinster, 1974; Martin and Evans, 1975; Papaioannou et al., 1975). Similarly until derivation of XEN cells different EC cell lines were analysed as a model of ExEn differentiation (Sato et al., 1985). Especially, the F9 EC cell line was a prominent object of study (Futaki et al., 2004; Grover et al., 1983; Harris and Childs, 2002; Niimi et al., 2004; Strickland et al., 1980; Veltmaat et al., 2000; Verheijen and Defize, 1999; Verheijen et al., 1999b; Verheijen et al., 1999c). Importantly, this work validated PTHrP role in PE differentiation (van de Stolpe et al., 1993; Veltmaat et al., 2000; Verheijen et al., 1999a) and also stressed the importance of Erk signalling in PrE differentiation (Verheijen et al., 1999b; Verheijen et al., 1999c).

Fowler et al. reported derivation of parietal endoderm cell (PEC) lines from mouse embryos (Fowler et al., 1990). These cell lines were derived from mouse delayed and non-delayed blastocysts. PEC cells produced substantial amounts of ECM proteins in aggregates and have been suggested as a potential source of ECM. Their chimaera contribution potential was not assessed.

5.4.3 XEN cells

XEN (e**X**traembryonic **EN**doderm) cell lines are an in vitro model of PrE (Kunath et al., 2005). They were derived from ICM or blastocyst outgrowths in serum containing media. Though initially also LIF or FGF4 were present in derivation media, these ligands are not necessary for their subsequent culture. XEN cells express major regulators of ExEn – Gata6, Gata4, Sox7 and Sox17 (Kunath et

al., 2005). XEN cells share many characteristics with PE, but little of VE. Already in early post derivation culture only a minority of cells is able to maintain epithelial character. As shown by microarray analysis different XEN cell lines express both markers for VE and PE, with PE markers at much higher levels (Brown et al., 2010a; Kunath et al., 2005). Also chimaera contribution is strongly biased towards PE and in the initial characterisation a XEN cell contribution to VYS was found in 1 out of 50 chimaeras (Kunath et al., 2005). Interestingly, similar to PrE derivatives in vivo XEN cells also exclusively inactivate paternal the X chromosome (Kunath et al., 2005; Takagi and Sasaki, 1975). And equally like ExEn in vivo, chromatin of XEN cell is hypomethylated (Chapman et al., 1984; Gardner and Davies, 1992; Monk et al., 1987; Rugg-Gunn et al., 2010).

XEN cells cannot be derived from Sox17 null (Niakan et al., 2010). Even though Sox17 null mES derived EBs could form PrE, the PrE failed to differentiate further into VE and PE (Niakan et al., 2010; Shimoda et al., 2007). *PDGFRα*$^{-/-}$ blastocysts also cannot give rise to XEN cells, which suggests a role of PDGF signalling in expansion of XEN cells (Artus et al., 2010). XEN cells also cannot be derived from Dicer null embryos and as a result of Dicer knock-out in XEN cells stop to proliferate which indicates a role of microRNA in maintenance of XEN cells (Spruce et al., 2010). Lim et al. showed that Sall4 RNAi knockdown XEN cells behave similarly as Dicer null knock-out (Lim et al., 2008). Sall4 has been shown to occupy promoters of Gata4, Gata6, Sox7 and Sox17 and in the absence of Sall4 expression of those ExEn regulators is downregulated and large vacuoles appear inside the cells (Lim et al., 2008).

XEN cells have also been derived from rat. Rat XEN cells continue to express Oct4 (Chuykin et al., 2010; Debeb et al., 2009). Interestingly, expression of Oct4 in extraembryonic derived cell lines is also characteristic for bovine TE cells. These cells not only continue to express OCT4, but can also contribute to ICM (Berg et al., 2011). The tighter regulation of Oct4 in mouse is due to acquired and murine specific regulatory sites (Berg et al., 2011).

mES cells, previously shown to be able to differentiate into PrE and its derivatives in an aggregate culture, can also give rise to XEN cells. Over expression

of *Gata4* or *Gata6* transcription factors in mES cells resulted in their differentiation into XEN cells (Fujikura et al., 2002; Shimosato et al., 2007). mES cells derived XEN cells share characteristics of embryo derived XEN cells with the respect to morphology, gene expression profile and chimaera contribution (Fujikura et al., 2002; Shimosato et al., 2007). Similarly, upregulation of Cdx2 in mES drives them towards TS cell differentiation (Niwa et al., 2005). However, mES derived extraembryonic stem cell lines, in contrast to their embryo derived counterparts, exhibit random X chromosome inactivation (Murakami et al., 2011).

XEN cells are to date the best ExEn in vitro model. It has already been shown that XEN cells have similar differentiation inducing properties to VE. XEN cells, like AVE, are able to induce cardiomyocytes differentiation (Brown et al., 2010a). This is most likely due to the high BMP2 expression in XEN cells (Brown et al., 2010b). Other differentiation inducing properties of XEN cells still remain to be elucidated, but potentially due to the biased PE and exVE character of XEN cells in current culture conditions such properties are restricted.

5.5 Project goals

The propensity of XEN cells to differentiate towards PE in culture limits their potential. Uncovering ways of maintaining a naive character of cells and reinforcing both PrE and VE character of XEN cells would greatly increase their application.

The overall aim of this research was to identify conditions enhancing epithelial, i.e. PrE and VE, character and differentiation of XEN cells. The specific aims were:

- to further characterize the extent of heterogeneity within XEN cell culture;
- to recreate various aspects of in vivo PrE and VE context, with a special focus on TGFβ signalling ligands and to establish culture conditions driving VE differentiation;
- to assess ExEn explants behaviour in an in vitro culture;
- to construct *SIX3* human embryonic stem cell reporter line that would allow the study of potential neural inducing properties of XEN cells (results can be found in Appendix 11.2).

6. Material and Methods

6.1 Cell culture reagents

6.1.1 Cell lines

XEN1.3 passage 20-35

IM8A1 passage 42-52

IM8A1-GFP passage 48-62

MEF passage 1-5 (kind gift from Dr Keisuke Kaji)

6.1.2 Cell culture media

Standard medium to culture XEN cells and MEFs: GMEM Complete: Glasgow Minimal Essential Medium (GMEM, Sigma G5154) + Foetal Calf Serum (10%, FCS) + non-essential amino acids (1x, Gibco 11140-035) + L-Glutamine (2mM, Invitrogen), sodium pyruvate (Invitrogen), β-mercaptoethanol (100µM, BDH 441413)

N2B27 serum-free complete medium (Stem Cell Sciences SCS-SF-NB-02)

Freezing medium: standard medium supplemented with 10% DMSO

6.1.3 Cytokines and inhibitors

BMP4: Recombinant human (Peprotech 120-05)

Activin A: Recombinant human (Peprotech, 120-14)

FGF2: Recombinant human, 10ng/ml (Peprotech, 100-18B)

PD0325901 (PD03): Mek inhibitor (Signalling Technologies, University of Dundee)

Dorsomorphin (DM): Bmpr inhibitor (Sigma, P5499)

SB431542 (SB43): Activin receptor inhibitor (Ascent, Asc-163)

6.1.4 Other reagents

Gelatin (0.1% in PBS) (Sigma G5154)

Trypsin: 0.25% Trypsin (Gibco, 15090-046)

PBS (Sigma D8537)

DMSO (VWR International)

Poly-L-ornithine solution (Sigma P4957)

Laminin from EHS murine sarcoma basement membrane (Sigma L2020)

Fibronectin (Invitrogen 33010-018)

6.2 Cell culture techniques

6.2.1 Routine culture conditions

All XEN cell lines and MEFs cells were cultured at 37°C in a humidified atmosphere of 95% air and 5% CO_2 and were maintained in standard medium on gelatinised plates. XEN cells were routinely passaged using trypsin and split every two or three days at 1:10-1:20 ratio.

6.2.2 Cell freezing

Cells after trypsin treatment where spun down at 300g and resuspended in freezing medium. Cells were then stored first at -80^{o}C and after a couple days transferred to liquid nitrogen.

6.2.3 MEF irradiation

MEF cells were cultured until confluent. Cells were then lifted with trypsin. MEF irradiation was carried out by Tissue Culture Staff. γMEFs were plated at $6x10^4$cells/cm^2 or frozen down in freezing medium.

6.2.4 MEF conditioned media

To make MEF conditioned media (MEF-CM) standard media was added to confluent MEFs flasks and media was collected 24h later. Media was then sterile filtered, aliquoted and stored at -80^{o}C.

6.2.5 Gelatin coating

For routine culture, gelatin coated plates were prepared by coating with 0.1% porcine gelatin solution for 5 minutes at room temperature. For treatment experiments and clonal plates were incubated with gelatin solution overnight at room temperature.

6.2.6 Laminin coating

Laminin coasted plates were prepared by coating with poly-L-ornithine (10μg/cm^2) for 30min at room temperature, followed by laminin coating (0.15μg/cm^2) overnight at room temperature.

6.2.7 Fibronectin coating

Fibronectin coated plates were prepared by incubating with fibronectin solution (0.15μg/cm^2) overnight at room temperature.

6.2.8 Clonal density assay

Clonal analysis was performed by plating XEN cells at 50 or 100cells/cm^2 on gelatin, laminin or fibronectin. The plating density was based on the standard colony forming assay used for mES cells. After 5 days cells were fixed and incubated with anti-E-cadherin antibody and colonies were scored according to the proportion of E-cadherin positive cells within the colony. For each cell line, results represent an average from 6 wells (triplicate for each of the two clonal densities) and the error bar represents standard deviation of 6 replicates. For subclonal IM8A1 cell lines cells were plated at 100cells/cm^2 and results represent average from 2 wells; and p-values were calculated using a Chi-square test.

For clonal analysis of cells in serum free conditions XEN cells were plated at 100 cells/cm^2 overnight in N2B27+1%FCS. The following day medium was changed to N2B27 only or N2B27 supplemented with Activin A (50ng/ml) or BMP4 (50ng/ml) and cells were cultured for another 4 days. The results represent an average of 3 wells and p-values were calculated using a Chi-square test.

For each clonal density assay at least 20-30 colonies per well were scored.

6.2.9 Derivation of IM8A1 XEN cell line subclones

IM8A1 XEN cell line p42 and p44 was subcloned by limiting dilution method, where approximately 50 or 100 cells were suspended in 25ml of standard medium and 200µl of cell suspension was added per well in a 96-well gelatinised plate. Clones arising from single cell only were expanded.

6.2.10 Aggregate culture

IM8A1-GFP and XEN1.3 cells were suspended as single cells. 20µl drops containing approx. 300 cells were then deposited on the lid of dish and were cultured in hanging drops for 10 days.

6.2.11 Culture of cells on gelatin, laminin or fibronectin

XEN cells were plated at low density (~10^3cells/cm^2) either on gelatin, laminin or fibronectin and were cultured in standard medium for 4 days.

6.2.12 BMP4 and Activin A treatment

XEN cells were plated at low density (~10^3cells/cm^2) either on gelatin or laminin in N2B27+1% FCS overnight. The media was then changed to either N2B27 only or N2B27 supplemented with BMP4 (10ng/ml or 50ng/ml) or Activin A (50ng/ml) and cells were cultured for 4 to 8 days. Media was changed on day 3, 5 or 7 of treatment.

6.2.13 Inhibitor treatment

XEN cells were plated at low density (~10^3cells/cm^2) either on gelatin or laminin in standard medium supplemented with DMSO (vehicle), Dorsomorphin (DM) at the final concentration of 2µM, PD0325901 (PD03) at 1µM, or SB431542 (SB43) at 10µM. Cells were cultured for 4 days.

For BMP4/inhibitor treatment XEN cells were plated at low density (~10^3cells/cm^2) on laminin in N2B27+1% FCS overnight. The media was then changed to either N2B27 with BMP4 (50ng/ml) and DMSO (vehicle), or DM(2µM), or PD03 (1µM) or SB43 (10µM). Cells were cultured for 7 days.

For the gene induction experiments XEN cells were cultured in N2B27 alone for 6hrs, then pre-incubated for 15min with DMSO, DM (2µM), PD03 (1µM) or SB43 (10µM) followed by 45min stimulation with BMP4 (10ng/ml), Activin A (20ng/ml), FGF2 (10ng/ml) or 10% FCS.

6.2.14 Flow cytometry

XEN cells were dissociated with trypsin, washed with PBS+2% FBS, incubated with anti-E-CADHERIN antibody at 1:400 (ECCD2, Invitrogen, 13-1900) and labelled with a secondary antibody (anti-rat IgG-APC, Jackson Immunoresearch, 712-136-153) before analysis on a Beckman Coulter CyAn flow cytometer.

6.3 Embryonic tissue isolation

6.3.1 Mice

MF1 and 129 mice were maintained on a 14-hour light, 10-hour dark cycle and were housed and bred within the University of Edinburgh animal house and according to the regulations of the Animals Scientific Procedures Act, UK, 1986. Overnight matings were set up. Noon on the day of finding a vaginal plug was designated as E0.5.

6.3.2 Isolation of primitive endoderm

Diapause blastocysts were flushed from uteri of pregnant females 4 days after Tamoxifen (Sigma, T5648-1G; 10µg per mouse) and Depo Provera (Pharmacia, MEDEP01; 3mg per mouse) injections on E2.5. Diapause embryos subsequently underwent immunosurgery. Diapause blastocysts were incubated in N2B27 with 20% whole mouse antiserum (400µl N2B27 + 100µl of antiserum, Sigma M5774) for one hour at 37^{o}C and 7% CO_2. Then they were rinsed three times in N2B27 (400µl) alone and incubated for twenty minutes in N2B27 with 20% rat serum (400µl N2B27 + 100µl rat serum, prepared in house and provided by Transgenic Facility), then transferred to N2B27 (400µl) alone for approximately 10-20min before removal of the lysed trophectoderm by repeated aspiration with a finely drawn glass needle. Isolated ICMs were then incubated in 37^{o}C and 7% CO_2overnight in hanging drops (approximately 15-20µl) of N2B27 supplemented with LIF to allow

the PrE to envelop the epiblast to produce a ‘rind and core’ structure. Using a finely flame drawn glass needle with a tip diameter wider than the epiblast, but narrower than the entire ICM, the PrE was removed by repeated aspiration.

6.3.3 Isolation of visceral endoderm

Visceral endoderm was isolated from E6.5 embryos. After removal of Reichert’s membrane and a cut was made along embryonic-extraembryonic border. After trypsin/pancreatin (0.5% and 2.5%, respectively in PBS) treatment of the remaining epiblast VE was removed away by repeated aspiration. These dissections were performed by C.R.Osorno.

6.3.4 Dissection of parietal endoderm

Embryos were obtained at E7.5 and E8.5 and dissected from their decidua in PB1 medium. A cut was made with a mounted needle at the boundary between the ExEc and the epiblast. Reichert's membrane from E7.5 and E8.5 embryos was then reflected with forceps or mounted needles. Dissected pieces of Reichert’s membrane with PE and trophoblast giant cells were incubated at room temperature for 10-15min with Accutase (Sigma, A6964) before plating on γ-irradiated mouse embryonic fibroblasts (MEFs).

6.3.5 Explant culture

Dissected PrE, VE and PE explants were carefully deposited in the well on a layer of γ-irradiated MEFs in standard medium. After 5 days cells were fixed and immunostained.

6.3.6 BMP4 treatment of parietal endoderm cells

E7.5 and E8.5 PE cells from Reichert’s membrane were cultured on gelatin or laminin in 70% MEF-CM for 5 days to determine that only PE and trophoblast giant cells were present in the culture. Media was then changed either to N2B27, N2B27 + BMP4 (50ng/ml) or maintained in 70% MEF-CM for another 5 days before cells were fixed and immunostained.

6.4 Molecular biology techniques

6.4.1 RNA isolation

Total RNA was prepared using Tri Reagent (Sigma T9424) according to manufacturer's protocol. RNA was additionally purified by ethanol precipitation method. To RNA 1/10 volume of 3M NaOAC and 3 volume ethanol were added and incubated overnight at -20^{o}C. The mixture was then spun down at maximum speed (~14000 rpm) for 30min and the remaining RNA pellet was washed with 70% ethanol. Following this, after removal of liquid RNA was briefly air-dried and resuspended in RNase-free water (Invitrogen 10977-022). Concentration of RNA was measured using Nanodrop spectrophotometer according to manufacturer's instructions.

6.4.2 cDNA synthesis

Total RNA (2μg) was treated with DNaseI (NEB M0303S) following manufacturer's instructions before reverse transcription. cDNA was made using random primers (Thermo Fisher PCR-545-020T) and M-MLV Reverse Transcriptase (Invitrogen 28025013) according to manufacturer's instructions.

6.4.3 Quantitative reverse transcriptase (qRT)-PCR

Real-time PCR was performed with the LightCycler 480 using the Universal Probe Library (UPL) System (Roche). Primers, designed using UPL system online software, and UPL probes used in the assays are listed in Table 6.1.The amplification protocol consisted of denaturation step at 95°C for 5min followed by 45 cycles of 95°C, 10s; 61°C, 10s and a single data acquisition at the end of each extension cycle. qRT-PCR results were normalised to TBP expression and represent an average of biological duplicates, error bars are standard deviation between biological duplicates.

Biological replicates were used in most of the experiments and technical duplicates were used for initial screening of markers (Fig.7.2), analysis of various subclonal lines (Fig. 7.6), analysis of effect of density (Fig. 8.1) and analysis of aggregate culture (Fig. 8.2).

Gene	Primers	UPL
Tbp	F ggggagctgtgatgtgaagt	#97
	R ccaggaaataattctggctca	
Afp	F catgctgcaaagctgacaa	#63
	R ctttgcaatggatgctctctt	
Bmp2	F cggactgcggtctcctaa	#49
	R ggggaagcagcaacactaga	
Dab2	F gcagtcgaactttctggatctc	#51
	R ggtgttactgggaccgtacct	
Dkk1	F ccgggaactactgcaaaaat	#76
	R ccaaggttttcaatgatgctt	
E-cadherin	F atcctcgccctgctgatt	#18
	R accaccgttctcctccgta	
Egr1	F ccctatgagcacctgaccac	#22
	R tcgtttggctgggataactc	
Fgf5	F aaaacctggtgcaccctaga	#29
	R catcacattcccgaattaagc	
Fgf8	F gctgttgcacttgctggtt	#16
	R atgctgtgtaaaattaggtgagga	
FoxA2	F gagcagcaacatcaccacag	#77
	R cgtaggccttgaggtccat	
Gata6	F ggtctctacagcaagatgaatgg	#40
	R tggcacaggacagtccaag	
Gata4	F ggaagacacccaatctcg	#13
	R catggccccacaattgac	
Id3	F gaggagcttttgccactgac	#19
	R gctcatccatgccctcag	
Hex	F tcagaatcgccgactaaat	#2
	R gtccaacgcatccttttgt	
Hnf4α	F ccaagaggtccatggtgttta	#68
	R ccgagggacgatgtagtcat	
Ihh	F tgcattgctctgtcaagtctg	#83
	R gctccccgttctctaggc	
Lefty1	F actcagtatgtggccctgcta	#67
	R aacctgcctgccacctct	
Sox7	F cggagctcagcaagatgc	#97
	R ctgcctcatccacataggg	
Sox17	F cacaacgcagagctaagcaa	#97
	R cgcttctctgccaaggtc	
Snail	F cttgtgtctgcacgacctgt	#71
	R aggagaatggcttctcacca	
Thrombomodulin	F atgcgtggagcatgagtg	#81
	R ctggcatcgaggaaggtc	

Table 6.1 Primers sequence and UPL probe number used in qRT-PCR assays. F –forward primer, R – reverse primer.

6.4.4 Immunofluorescence

Cells were fixed in 4% paraformaldehyde (room temperature, 8-10 minutes), washed three times with PBS, then incubated for 30min at room temperature in blocking buffer (PBS, 2% donkey serum, 0.1% Triton X-100). Primary antibodies were diluted in blocking buffer and applied overnight at 4^{o}C, followed by three washes in PBS. Donkey secondary antibodies conjugated to AlexaFluor dyes (Molecular Probes) were diluted at 1:1000 in blocking buffer and applied for 1-1.5 hours at room temperature. Cells were then washed twice in PBS and a third time in PBS containing DAPI (10μg/ml) prior to imaging using an Olympus IX51 inverted fluorescence microscope. Negative control staining was performed using secondary antibody only and results are shown in Fig. 11.7 in Appendix 11.3.

Antigen	Clone	Isotype	Concentration	Conjugate	Supplier
E-CADHERIN	ECCD-2	rat IgG2a	1:300	-	Invitrogen
GATA4	L97-65	mouse $IgG_{1\kappa}$	1:100	AlexaFluor 555	BD
PDGFRα	C-20	rabbit IgG	1:50	-	Santa Cruz
VIMENTIN	40E-C	mouse IgM	1:50	-	DSHB
AFP	Ab-2	rabbit IgG	1:100	-	Thermo Scientific

Table 6.2 Table of primary antibodies used for immunofluorescence.

Antigen	Isotype	Conjugate	Concentration	Supplier
rat	Donkey IgG	AlexaFluor 488	1:1000	Molecular Probes
rat	Donkey IgG	AlexaFluor 568	1:1000	Molecular Probes
rabbit	Donkey IgG	AlexaFluor 555	1:1000	Molecular Probes
mouse IgM	Donkey IgG	AlexaFluor 568	1:1000	Molecular Probes

Table 6.3 Table of secondary antibodies used for immunofluorescence.

7. XEN cells are heterogeneous and contain progenitors of primitive, visceral and parietal endoderm.

7.1 Introduction

XEN cells derived through current derivation protocols show a significant degree of heterogeneity, with the observation of at least two distinctive cell morphologies. The first class of cells are highly refractile, spindle-like or rounded, whilst the second class are of an epithelial character (Fig. 7.1 and (Kunath et al., 2005). A key question is whether these cell represent different types of ExEn and furthermore whether they would respond differently to differentiation cues. It is therefore the aim of these experiments to fully define the nature and the extent of heterogeneity within XEN cell populations.

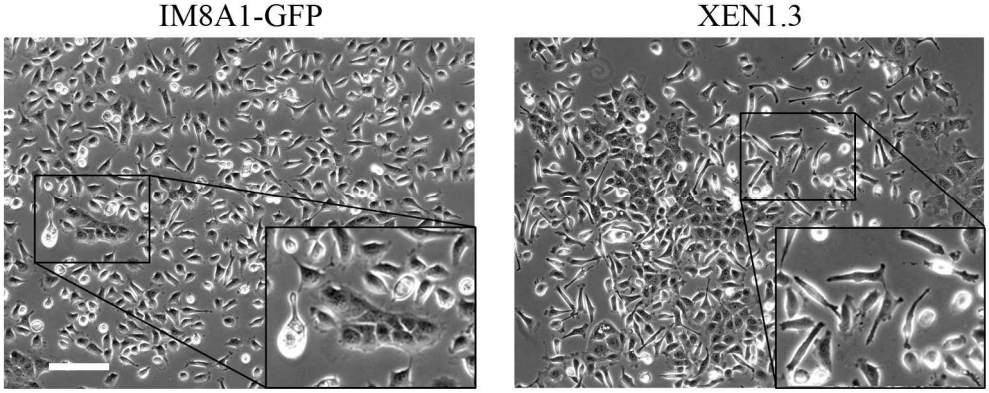

Figure 7.1 XEN cells exhibit several different types of morphology in culture. Two different XEN cell lines – IM8A1 and XEN1.3 were grown in standard condition for 3 days. Examples of epithelial cells (from IM8A1 cell line) and spindle cells (from XEN1.3 cell line) are presented in insets; scale bar: 200µm.

7.2 Heterogeneous character of XEN cell lines

7.2.1 XEN cells express markers of primitive, visceral and parietal endoderm

In previous work, XEN cells were extensively characterized by a microarray gene expression analysis (Brown et al., 2010b; Kruithof-de Julio et al., 2011; Kunath et al., 2005). This revealed that XEN cells express markers of PE and exVE at higher levels and the expression of emVE, DVE/AVE is at low or undetectable levels.

I validated some of the microarray results for different ExEn markers by qRT-PCR. This analysis was performed on two XEN cell lines (XEN1.3 and IM8A1), E14Tg2a mES cell line and day 7 embryoid bodies (EBs). The RNA samples of mES cell line and EBs were kind gifts from Dr K.Kaji and Dr S.N.Villegas, respectively (Fig. 7.2).

Both XEN cell lines and EB express *Gata4*, *Gata6*, *Sox7*, *Sox17*. These major regulators of PrE are absent or expressed at very low levels in mES cells. *Hex*, a marker of PrE and AVE, is expressed in IM8A1-GFP XEN cell line at the similar level to day 7 EBs. *Hex* is expressed at lower levels in mES cells and in XEN1.3 cell line. *Dab2*, another PrE marker, is expressed highly in XEN cell lines and EB, but absent in mES. *Bmp2* and *FoxA2*, markers of emVE, are expressed in XEN cells at similarly high level to those in EB, whilst at low levels in mES cells. Expression of emVE and exVE marker, *Hnf4α* in XEN cells is comparable with EB, whilst being absent in mES cells. Similarly, expression of exVE marker *Ihh*, is also at comparable levels with EB, whilst being absent in mES cells. Interestingly, *Afp*, a VE and exVE marker, is expressed highly in EB, but at a very low level in XEN cells and absent in mES cells. EMT-associated gene and a general VE marker *E-cadherin* is expressed at highest level in mES cells with a 6-fold lower level in XEN cells and EB. *Snail*, E-cadherin's negative regulator, is expressed highest in EB and at comparably lower levels in XEN cells; it is barely detectable in mES cells. *Thbd*, PE marker, is expressed highly in XEN1.3 cell line, at around 3 times lower levels in IM8A1-GFP and EB and is not detected in mES cells. *Dkk1*, AVE marker, is expressed at highest levels in EB, 3 times lower in IM8A1-GFP and at low levels in XEN1.3 and mES. Expression of *Lefty1* and *Cer1*, AVE markers, is not detected in XEN cells and is present at low levels in mES cells when compared to EB. Similarly, *Fgf5* and *Fgf8*, emVE markers are barely detected in XEN cell lines and mES, but are expressed at substantial levels in EB.

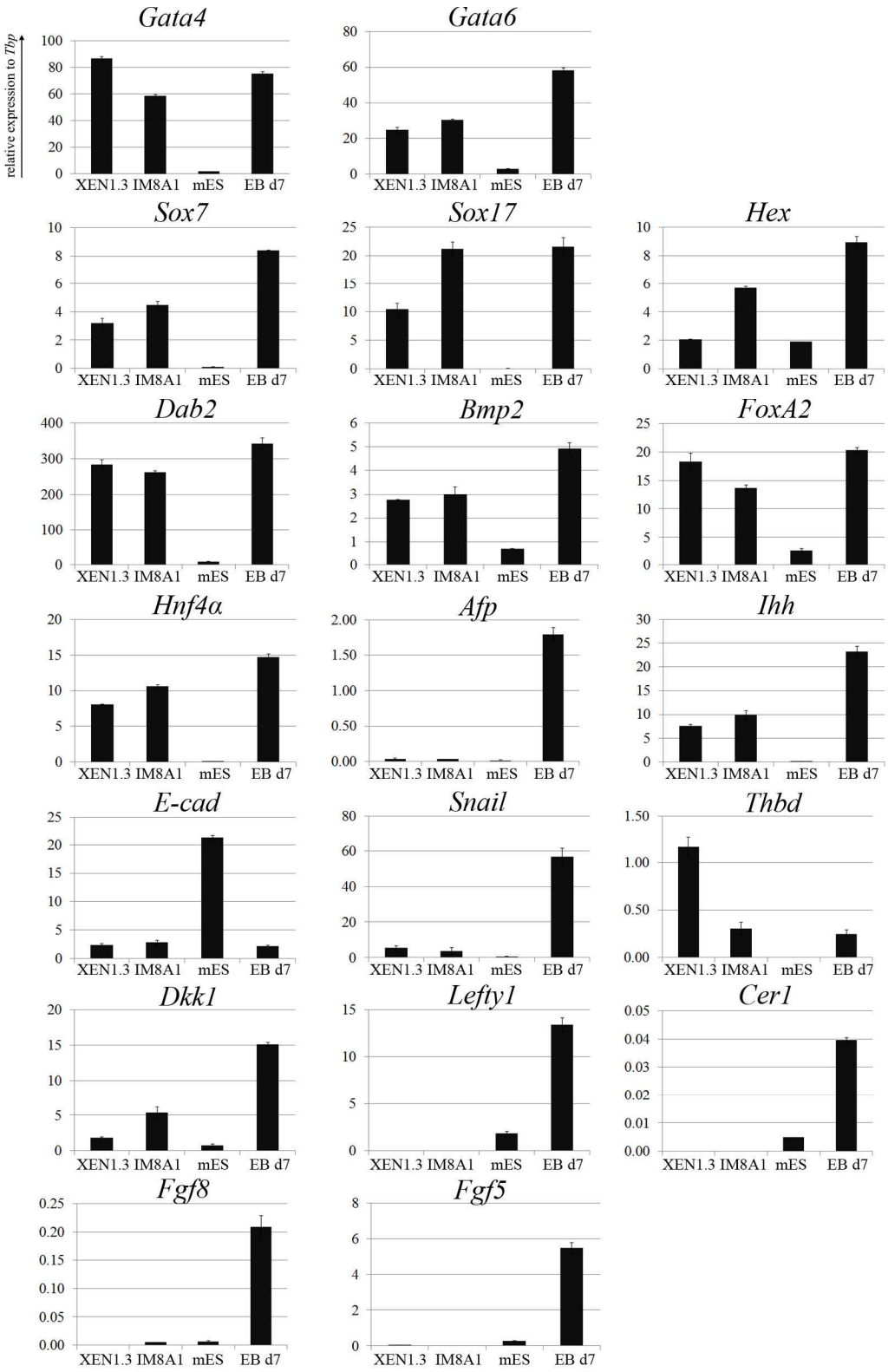

Figure 7.2 XEN cells express markers of primitive, visceral and parietal endoderm. qRT-PCR analysis of XEN cell lines: XEN1.3 and IM8A1-GFP, E14Tg2a mES cells and day 7 E14Tg2a embryoid body (EB) differentiation. qRT-PCR results were normalised to *Tbp* expression and represent an average of technical duplicates, error bars are standard deviation between technical duplicates.

In summary, XEN cells express different markers of PrE, VE and PE. XEN cells are characterised by substantially increased expression of PrE, exVE and PE markers such as *Gata6*, *Sox7* and *Sox17* and reduced expression of emVE or AVE markers like *Afp*, *Cer1*, *Lefty1*, *Fgf5*, *Fgf8* relative to the levels observed in ES cells and EBs. Surprisingly, expression of emVE *FoxA2* and *Bmp2* is detectable at substantial levels.

The results of this experiment and embryonic expression of various ExEn markers are summarised in Table 7.1.

	XEN cells	E4.5 PrE	E5.0 VE	emVE	exVE	DVE/AVE	PE	VYS
Gata4	yes	yes	yes	yes	yes	yes	yes	
Gata6	yes	yes	yes	lower	yes	yes	yes	
Sox7	yes	yes	yes	no	yes	no	yes	
Sox17	yes	yes	yes	no	yes	yes	yes	
Hex	yes	yes	yes	yes	no	yes		
Dab2	yes	yes	yes	yes	yes	yes	no	
Bmp2	yes	yes	yes	yes	no	yes	no	
FoxA2	yes		yes	yes	no	yes	no	
Hnf4α	yes		yes	yes	yes		no	yes
Afp	yes (low)		yes	yes	yes		no	yes
Ihh	yes							yes
E-cadherin	yes	yes	yes	yes	yes	yes	no	
Snail	yes						yes	
Thbd	yes						yes	
Dkk1	yes	yes			no	yes		
Lefty1	no	yes			no	yes		
Cer1	no	yes			no	yes		
Fgf8	yes (low)		yes	yes	no			
Fgf5	yes (low)		yes	yes	no			

Table 7.1 Expression of extraembryonic endoderm markers in XEN cells and various types of extraembryonic endoderm. The table summarise expression of various markers based on the results of qRT-PCR experiment and literature.

7.2.2 Expression of E-CADHERIN, GATA4, PDGFRa and VIMENTIN in XEN cells

To further investigate the heterogeneous nature of XEN cells I analysed expression of E-CADHERIN (epithelial, PrE VE marker (Chen et al., 2005; Kadokawa et al., 1989)), GATA4 (ExEn marker (Arceci et al., 1993)), PDGFRα (PrE, exVE and PE marker (Plusa et al., 2008)) and VIMENTIN (PE and mesenchymal marker (Lane et al., 1983)) in XEN1.3 XEN cells grown in standard conditions (i.e. on gelatin in serum).

When XEN cells were cultured on gelatin, all cells showed expression of GATA4, whilst only a portion expressed E-CADHERIN (Fig. 7.3a). The E-CADHERIN and GATA4 double positive cells are confined to certain areas, suggesting they may be growing in patches. This is true for all the E-CADHERIN stained samples (Fig. 7.3a-c). Staining for E-CADHERIN and PDGFRα revealed that whilst the majority of cells are PDGFα positive (with localisation to the cell membrane, cytoplasm or around the nucleus), it is the subpopulation of E-CADHERIN+ cells that show reduced or no expression of PDGFRα. Finally, the expression of E-CADHERIN and VIMENTIN, an intermediate filament and a mesenchymal marker, is almost mutually exclusive, with only a few cells expressing low levels of VIMENTIN whilst being E-CADHERIN positive (Fig. 7.3c).

In conclusion, all XEN cells express GATA4, with a small subpopulation also expressing E-CADHERIN; expression of PDGFRα and VIMENTIN is heterogeneous and remarkably has very little if any overlay with E-CADHERIN.

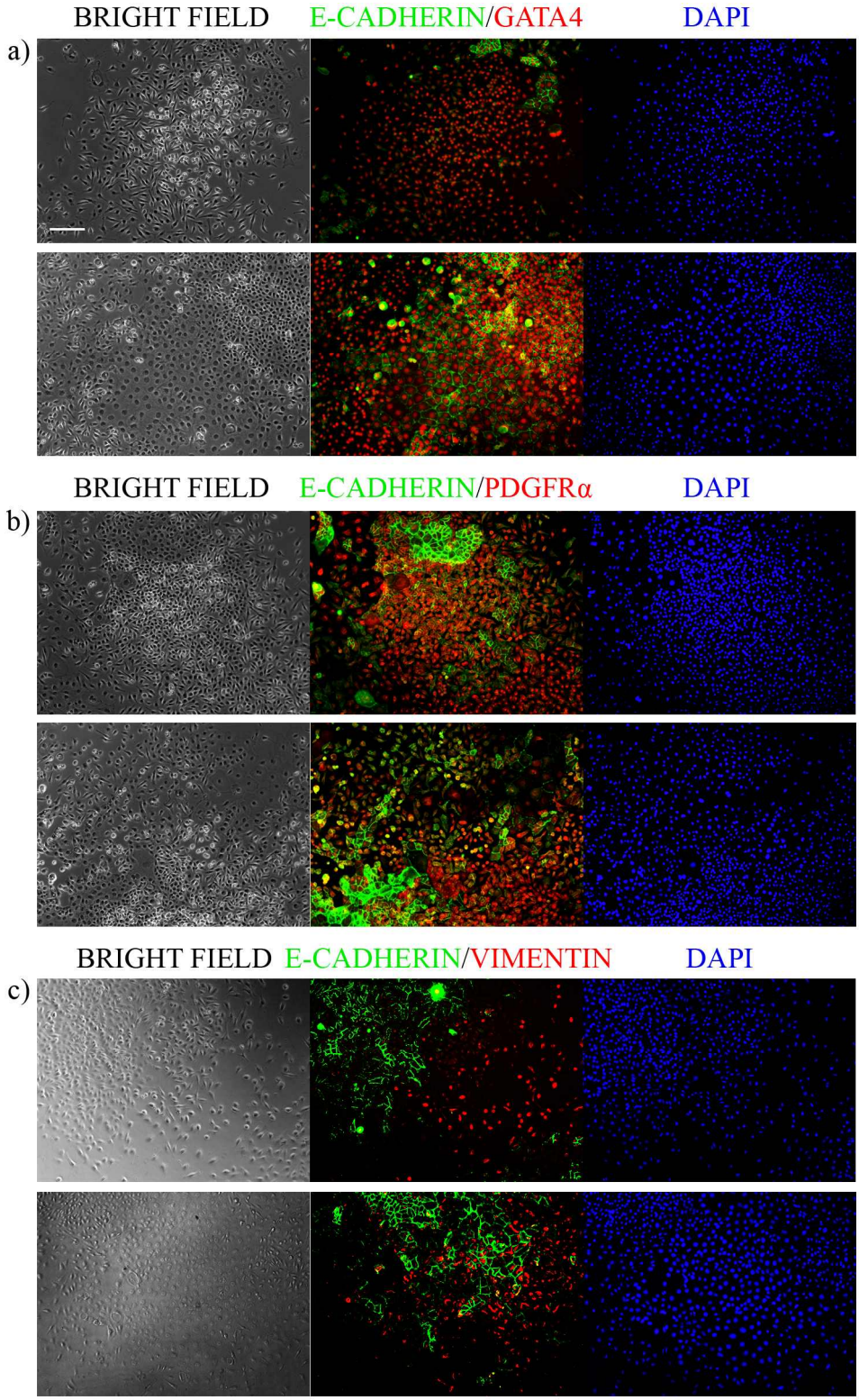

Figure 7.3 XEN cells are positive for GATA4 and PDGFRα and express E-CADHERIN and VIMENTIN in a heterogeneous manner. XEN1.3 cells were plated at low density and cultured on gelatin in FBS for 4 days after which they were fixed and immunostained with appropriate antibodies. Two representative images for each staining are presented; scale bar: 200µm.

7.2.3 Clonal assay

In order to further examine the heterogeneous nature of XEN cell cultures at a single cell level, I established a clonal assay.

Cells were plated at low, clonal densities for 5 days and three types of colonies were distinguished and classified: E-CADHERIN-low colonies (Fig. 7.4a), mixed colonies, which contained both E-cadherin-positive and negative cells (Fig. 7.4b), and uniformly E-cadherin-high compact colonies (Fig. 7.4c). I compared the ratio of these three different types of colonies for IM8A1-GFP and XEN1.3 cell lines plated on gelatin. For the IM8A1-GFP XEN cell line, 85% of colonies were E-CADHERIN-low, 12% mixed and 3% E-CADHERIN-high (Fig. 7.4d). For the XEN1.3 cell line, 60% of colonies were E-CADHERIN-low, 30% mixed and 10% E-CADHERIN-high (Fig. 7.4d). The difference in the ratio of different types of colonies between these two cell lines is statistically significant ($p_{\chi 2}<0.0001$).

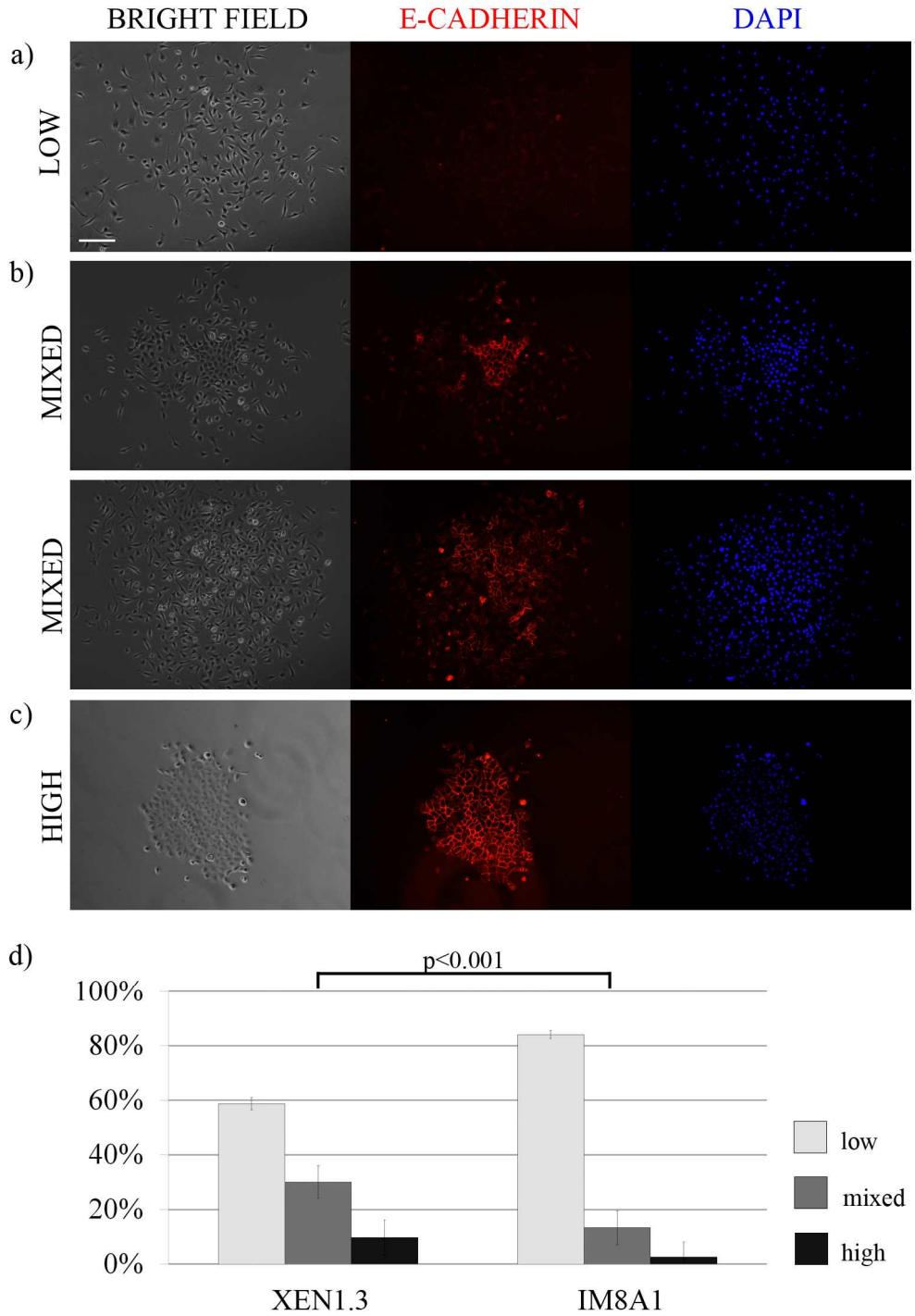

Figure 7.4 At clonal density XEN cells form 3 different types of E-CADHERIN expressing colonies. a-c) Examples of XEN cell colonies on gelatin expressing different levels of E-CADHERIN: low (a), mixed (b) and high (c); scale bar: 100µm. **d)** XEN1.3 and IM8A1-GFP XEN cell lines have different ratios of low, mixed and high E-CADHERIN positive colonies ($n_{IM8A1\text{-}GFP}$=195, $n_{XEN1.3}$=193; $p_{\chi 2}$<0.0001).

7.2.4 Derivation and morphological characterisation of IM8A1 XEN cell line subclones

The XEN clonal assays revealed that at least 3 different types of colonies could be formed from single XEN cells. This leads then to the question whether a single cell can generate a subclonal cell line sharing only a subset of characteristics with the parental cell line.

To address question IM8A1 cell line subclones were derived using a limiting dilution method. In the first round, around 50 cells were plated in 96-well plate, but only 6 subclones were derived. The second time, approximately 80 cells were plated in a 96-well plate giving an average of 0.8 cell per well. Care was taken to ensure that only subclones arising from a single cell were expanded. In over half of the wells clones were growing, but in the end only 14 clones were successfully expanded and characterised giving a total number of 20 subclones.

The first step of characterisation involved daily observation using transmitted light microscopy over the 2-3 week course of subclone expansion. The presence and the ratio of epithelial and refractile cells in the culture were assessed. As a result 4 different categories of morphologies were established.

- The first category called “XEN-like” includes 6 subclones and showed substantial resemblance to the parental XEN cell line. These subclones, A11, B6, C6, F4, F7 and G10, consisted of two characteristic types of cells: spindle-like refractile cells (majority) and some more epithelial looking cells. Interestingly, one of the subclones, clone C6, started initially as cells of epithelial-like morphology, but over the time of expansion, spindle-like cells started to appear (Fig. 7.5a).
- The second “spindle-like” category contained highly refractile, spindle-like cells (Fig. 7.5b). This was observed for 7 subclones (A8, D11, E11, F3, G3, H4 and H12).
- The third category, called “epithelial-like” subclones contained some spindle-like cells are present, but with a majority of epithelial cells (Fig. 7.5c).This category included 4 subclones (C1, F9, F12 and H3).

- Last, but not least a “flat cells” category where cells are similar to XEN-like or epithelial-like subclones, but with the presence of large flat cells that are occasionally noticed in the parental XEN cell (Fig. 7.5d). This was observed for 3 subclones: B3, H5 and H7.

To summarise, a single XEN cell can give rise to subclonal lineage that has different morphological properties. These properties, however, are collectively present in the IM8A1 parental cell line.

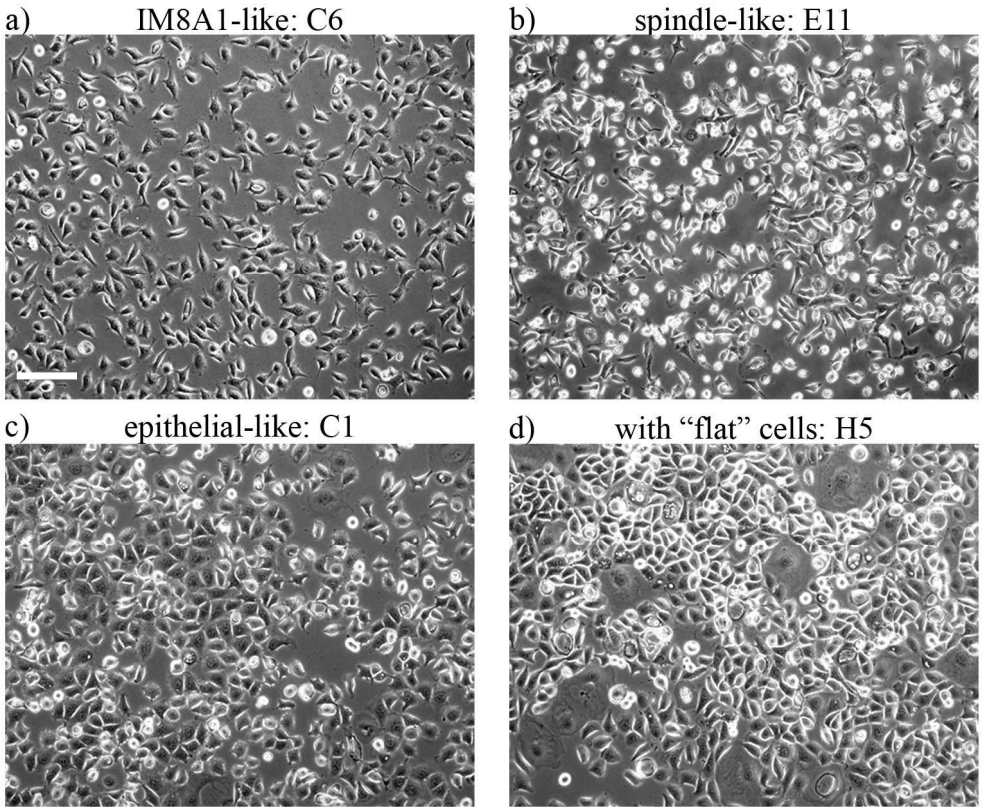

Figure 7.5 Examples of IM8A1 subclones assigned to 4 different categories. Bright-field pictures of cells growing on gelatin in FBS. **a)** XEN-like, subclone C6, **b)** spindle-like, subclone E11, **c)** epithelial-like, subclone C1 and **d)** subclone H5 with “flat” cells; scale bar: 200µm.

7.2.5 qRT-PCR analysis of XEN cell subclones

Given the morphological differences between derived subclones I next addressed the question of whether these subclones show differential expression of various ExEn markers. To achieve that IM8A1 subclones were analysed by qRT-PCR (Fig. 7.6).

Gata4 and *Gata6*, general ExEn markers, are expressed by all subclones. *Gata4* expression is higher in XEN-like, epithelial-like and subclones with "flat" cells than in spindle-like subclones, whilst expression of *Gata6* is on average lowest in epithelial-like subclones. *Snail*, PE markers, is upregulated in spindle-like subclones compared to IM8A1 or epithelial-like subclones ($p=0.0078$); expression is similar to IM8A1 or reduced in XEN-like subclones and subclones with "flat" cells. *Thbd*, another PE marker, is downregulated in all of the epithelial subclones and is expressed at higher levels in 4 out of 7 spindle-like subclones. Also, one of the XEN-like subclones expresses *Thbd* higher level than IM8A1. The expression of *E-cadherin*'s expression is quite variable between the clones. None of the spindle-like subclones expresses it at higher level than IM8A1. However, 3 out of 6 XEN-like subclones, 2 out of 4 epithelial-like subclones and 1 out 3 of subclones with "flat" cells express it at levels that are higher than in IM8A1. *Hex*, PrE and AVE marker, is expressed at similar level to IM8A1 in spindle-like subclones, but is expressed at higher levels in XEN-like subclones, most of epithelial-like subclones and 2 out of 3 subclones with "flat" cells. *Ihh*, VE marker, is expressed without any particular pattern between the subclones, though it seems to be higher in XEN-like and spindle-like subclones than in epithelial-like subclones. *Hnf4α*, VE marker, is expressed in a similar manner to *Hex*. Its expression is on average higher in XEN-like and epithelial-like subclones and subclones with "flat" cells than it is in spindle-like subclones. Finally, *Afp*, VE marker, is expressed at lower levels than in IM8A1 in all of the derived subclones, but two: epithelial-like subclone C1 and B3 subclone with "flat" cells.

These findings suggest that, in keeping with their morphological differences, IM8A1 subclones show distinct expression of different VE or PE markers.

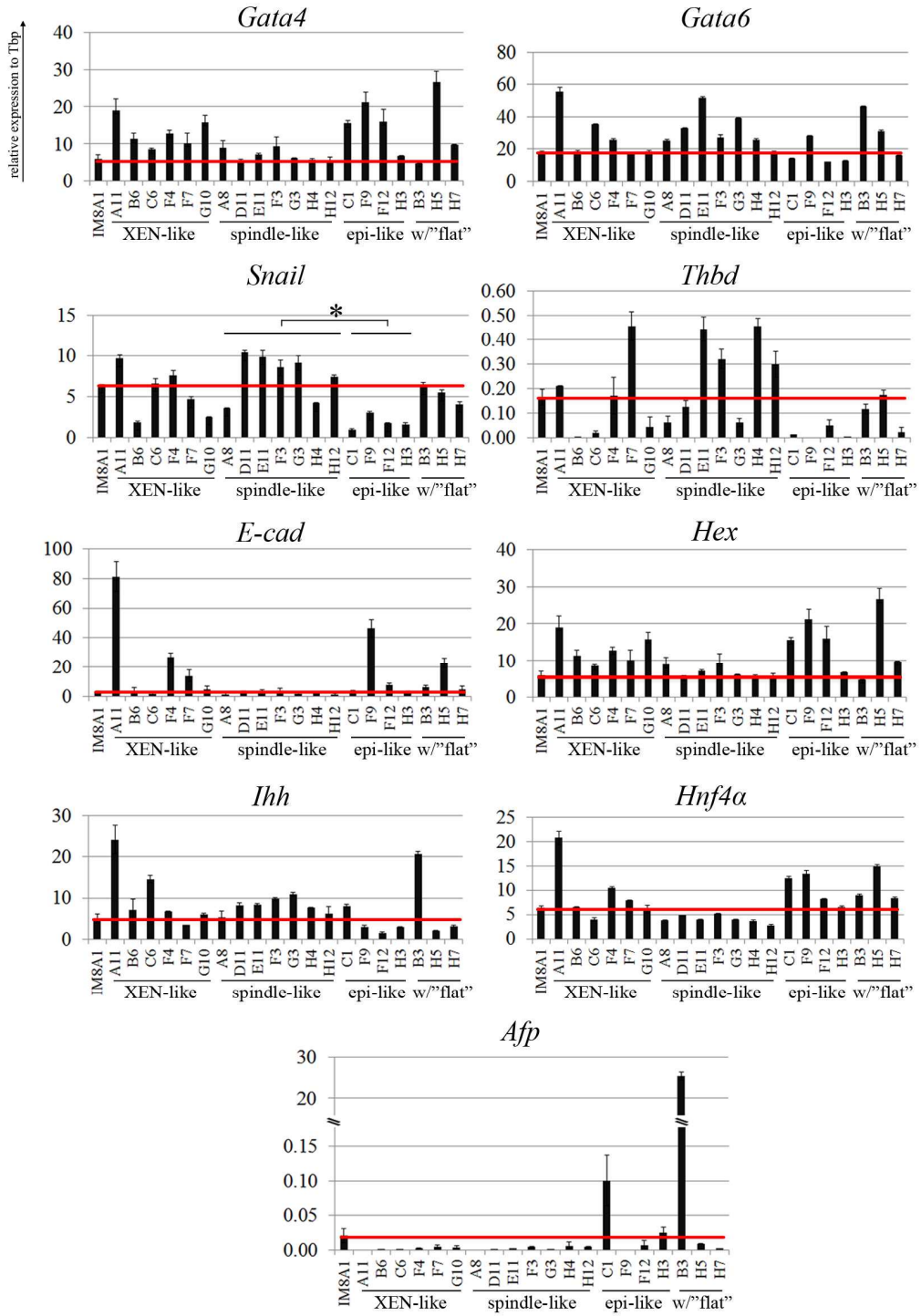

Figure 7.6 IM8A1 subclones show variable expression of visceral and parietal endoderm markers. qRT-PCR analysis of 20 different subclonal cell lines and paternal line (IM8A1) for various ExEn markers. qRT-PCR results were normalised to *Tbp* expression and represent an average of technical duplicates, error bars are standard deviation between technical duplicates. One-way analysis of variance for the results of *Snail* expression showed that there were significant differences among the different morphological types of subclones (p=0.014). * Tukey's post-hoc statistical test showed that the mean value of *Snail* expression is different between spindle-like and epithelial-like subclones (p=0.0078).

7.2.6 Expression of E-CADHERIN in selected subclones

Following qRT-PCR analysis, the expression of E-CADHERIN was examined in 3 subclones representative of different classes.

The parental IM8A1 cell line expresses E-CADHERIN in a heterogeneous manner, with cells expressing E-CADHERIN are surrounded by E-CADHERIN-negative cells (Fig. 7.7a). A8 subclone, assigned to spindle-like category, does not express E-CADHERIN (Fig. 7.7b). Another subclone called B3 belonging to special category of subclones with "flat cells", expresses E-CADHERIN at very low level (Fig. 7.7c). On the other hand, F9 subclone, epithelial subclone shows a high E-CADHERIN expression with the majority of cells expressing E-CADHERIN (Fig. 7.7d). This is in agreement with qRT-PCR data (Fig. 7.6).

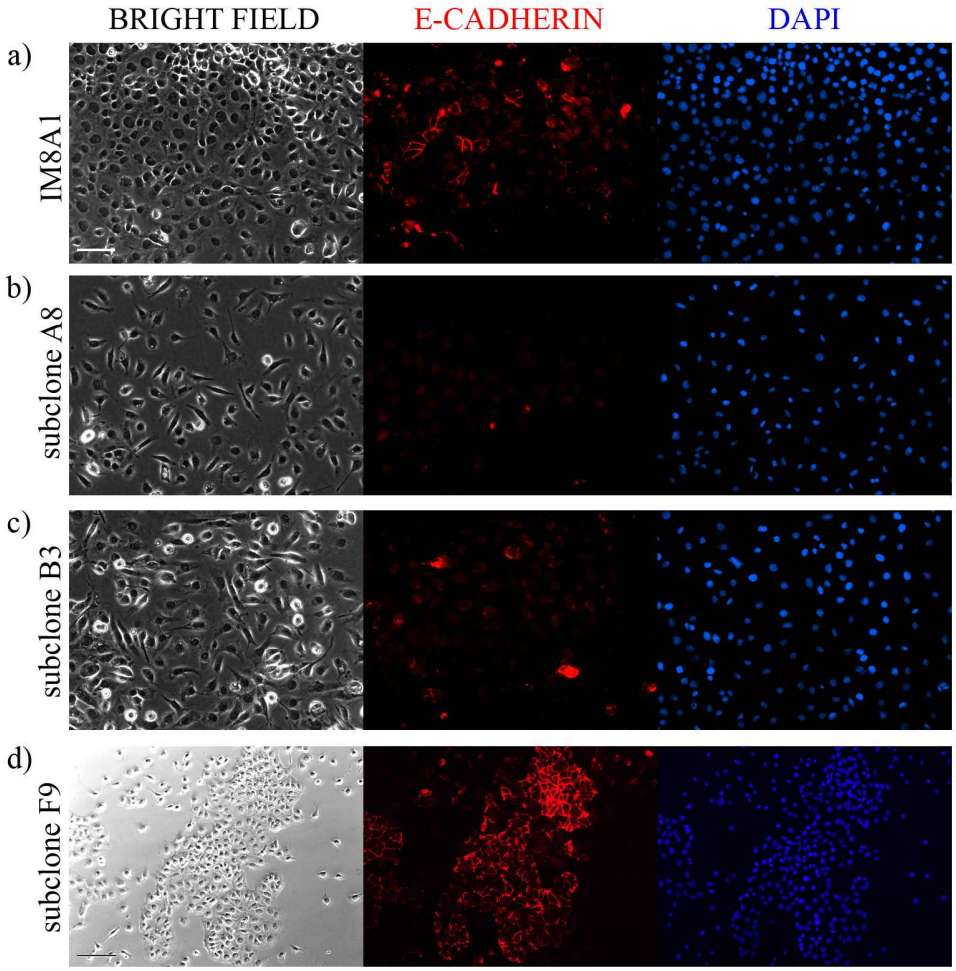

Figure 7.7 E-CADHERIN expression in selected subclones. Cells were grown on gelatin in serum for 3 days: **a)** IM8A1 parental cell line; **b)** spindle-like A8 subclone; **c)** B3 subclone from special category of subclones with "flat cells" **d)** epithelial-like subclone F9; scale bar: 100µm (a-c), 200µm (d).

7.2.7 Clonal assay for selected IM8A1 subclones.

To gain further insight into subclones I took advantage of the clonal assay allowing the ratios of different types of E-CADHERIN expressing colonies to be determined (Fig7.4.a-c). I chose two different spindle-like subclones: E11 and G3; and two epithelial-like subclones: C1 and F9.

For E11 subclone 82% of colonies are E-CADHERIN-low, 18% mixed and 0% E-CADHERIN. Very similarly, for subclone G3 86% of colonies are E-CADHERIN-low, 14% E-CADHERIN-mixed and 0% E-CADHERIN-high (Fig. 7.8a).

In contrast, C1 epithelial-like subclone has 13% of E-CADHERIN-low, 52% of E-CADHERIN-mixed and 35% of colonies is E-CADHERIN-high colonies. For F9 subclone 4% of colonies are E-CADHERIN-low, 41% mixed and 55% E-CADHERIN (Fig. 7.8b). The difference in the ratio of different types of colonies between these two epithelial-like subclones is statistically significant ($p_{\chi 2}<0.0001$).

Different IM8A1 subclones have different ratio E-CADHERIN expressing colonies. The majority of colonies in spindle-like subclones is E-CADHERIN low expressing colonies, whilst the majority of colonies in epithelial-like subclones is either E-CADHRIN-mixed or E-CADHERIN-high. The overall difference in the ratio of different types of colonies between PE subclones (E11 or G3) and VE subclones (C1 or F9) is statistically significant ($p_{\chi 2}<0.0001$).

Interestingly, at clonal level two compared PE-like subclones are similar, but two compared VE-like subclones are not suggesting that PE-like subclones are more homogenous.

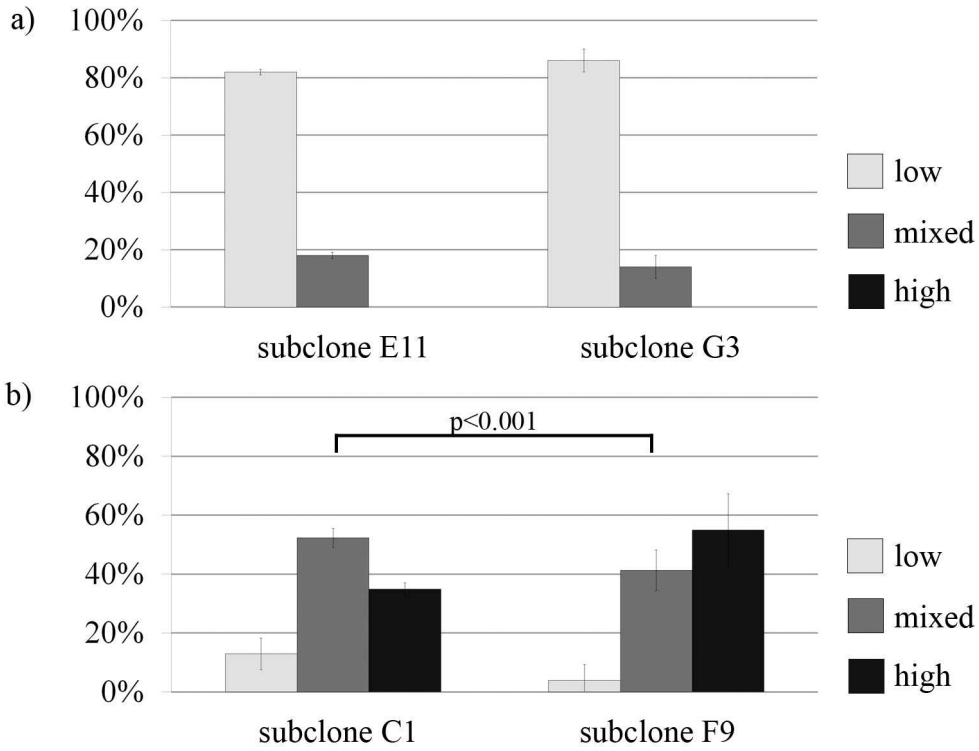

Figure 7.8 Spindle-like subclones and epithelial-like subclones have different ratio of 3 types of E-CADHERIN expressing colonies. a) E11 and G3, spindle like subclones, p=0.86; **b**) C1 and F9 epithelial-like subclones, p<0001. Cells were plated at clonal density and cultured for 5 days ($_{nE11}$=48, n_{G3}=42, n_{C1}=31, n_{F9}=39).

7.3 Discussion

XEN cells are heterogeneous cells lines containing mixed derivatives of PrE. The heterogeneity is already evident under the light microscope and at least two types of cells can be distinguished – spindle-like, mesenchymal cells of PE nature and epithelial-like VE cells (Fig 7.1). Patchy-like expression of E-CADHERIN and VIMENTIN, VE and PE markers, respectively (Kadokawa et al., 1989), or PDGFRα – expressed in PrE, exVE and PE (Takakura et al., 1997) - further underlines heterogeneity (Fig. 7.3). At clonal density a single cell can give rise to a colony expressing various levels of E-CADHERIN (Fig. 7.4). Moreover, single cells can give rise to subclonal cell lines that have distinctive properties. These subclones include cell lines similar to parental cell line, subclones of epithelial VE-like properties and subclones of mesenchymal, i.e. PE-like character (Fig. 7.5 and Fig. 7.6).

Furthermore, gene expression analysis of genes such as *Snail, Thbd, Sox7, Fgf5, Fgf8* showed that XEN cells are biased towards PE and exVE (Fig. 7.2 and

Table 7.1) confirming previous microarray analysis results (Brown et al., 2010b; Kunath et al., 2005). Though it is expected for XEN-like subclones to contain cells of both epithelial and mesenchymal morphology, also such cells were present in epithelial-like and spindle-like subclones suggesting the general propensity of even differentiated subclones towards heterogeneity. XEN cells are not only heterogeneous within culture, but also two XEN cell lines show a level of variability between each other. XEN1.3 cell line expresses *Thbd*, PE marker, at 3 times higher levels than IM8A1-GFP, but expresses *Dkk1* and *Hex* at lower levels than IM8A1-GFP (Fig. 7.2). Also, the ratio of 3 types of E-CADHERIN expressing colonies between XEN1.3 and IM8A1-GFP is significantly different (Fig. 7.4d). These two cell lines were derived from different mouse strains and were derived from ICM pairs (IM8A1-GFP) or from blastocyst outgrowth (XEN1.3) (Kunath et al., 2005).

It is essential to appreciate that already PrE exhibits heterogeneous expression of some of DVE/AVE markers, such as Cer1, Lefty1 (Takaoka et al., 2011; Takaoka et al., 2006; Torres-Padilla et al., 2007). Nodal/Activin and signalling can be differentially perceived within PrE (Granier et al., 2011). This would imply that at the time of maturation of signalling pathways PrE cells are sensitive to even minor changes in signalling intensity. After implantation VE can be classified into a number of different subtypes depending on the developmental stage and location in the embryo. These different types of VE respond to the signal received from underlying tissue. For instance only proximal VE, overlying proximal epiblast expressing high levels of Wnt3, has high levels of nuclear β-catenin (Kimura-Yoshida et al., 2005). Equally, in exVE that is in direct contact with ExEc, a source of BMP4, phosphorylated Smad1 is higher than in the emVE portion. Conversely, the levels of phosphorylated Smad2 are higher in emVE, that overlies epiblast, than in exVE (Yamamoto et al., 2009). Following the changes in the signals received from epiblast and ExEc the expression of various ExEn markers is also dynamic (Pfister et al., 2007). For example, Sox17 is expressed in PrE and its expression is later confined to exVE and PE, but also Sox17 is observed in AVE (Artus et al., 2011b; Kanai-Azuma et al., 2002). Similarly, Gata6 initially present in PrE later is downregulated in emVE, but maintained in exVE and PE (Chazaud et al., 2006; Koutsourakis et al., 1999; Morrisey et al., 1996).

XEN cells are derived from PrE, but whilst in culture they upregulate expression of VE and PE markers (Kunath et al., 2005). To be able to differentiate into PE PrE must undergo EMT driven by PTHrP and cAMP (van de Stolpe et al., 1993; Veltmaat et al., 2000; Verheijen et al., 1999a). In vivo PrE and VE subtypes exist in certain context and are influence by signalling from epiblast and ExEc. It is therefore possible that the current culture conditions favour PE differentiation of PrE and VE and that epithelial phenotype of XEN cells in culture is unsustainable. Indeed, Gardner suggested that PE is the default phenotype for ExEn (Gardner, 1982). However, the data confirming this bias stems from chimaera contribution of PrE, VE and PE cells. In vivo dissected E5.5 VE cells injected immediately back into blastocyst would contribute preferentially to PE (19/23 chimaeras) (Gardner, 1982). Chimaera contribution analysis (blastocyst injection and morula aggregation) of XEN cells showed similar tendency (Kunath et al. 2005, Artus et al. 2011, Kruithof et al 2011). However, is chimaera contribution then a right type of analysis to assess their potential? It is likely that such assay is only appropriate for cells of an equivalent embryonic stage cell, i.e. pre-PrE cells. It is probable that due to adhesion differences VE cells fail to integrate with nascent layer of PrE and preferentially would attach to mural portion of TE layer and later contribute to PYS. Similarly, post-implantation mouse stem cells, though can differentiate towards all three germ layers, when injected into blastocyst fail to contribute to epiblast derivatives (Brons et al., 2007; Tesar et al., 2007). Therefore, I believe that until truly PrE-XEN cell derivation conditions are established chimaera contribution is not an appropriate assay to uncover XEN cell potential.

Another piece of evidence supporting preferential PE differentiation of XEN cells comes from subclones derivation. 7 out of 20 expanded subclones were of a mesenchymal, i.e. PE, character. Moreover, during subclone expansion one of the initially epithelial looking subclones gave rise to subclone of XEN-like properties which includes cells of both epithelial and mesenchymal character. Moreover in XEN-like subclones (6/20) mesenchymal looking cells were in majority (Fig. 7.5b). Also, PE-like cells were present in epithelial-like subclones (Fig. 7.8b). Nevertheless, spindle-like subclones could still give rise to small proportion of E-CADHERIN expressing colonies and conversely some colonies in epithelial-like subclones did not

express E-CADHERIN (Fig. 7.8a). Basing on the characterised expression of ExEn markers and on morphology of subclones it can generally assumed that spindle-like subclones resemble PE cells, whilst epithelial-like subclones VE.

Kunath et al. reported that during their subclonal analysis the expanded subclones contained cell of two distinct morphologies (Kunath et al., 2005). I observed the morphological changes over 2-3 week period and further classified the subclones. The differences in morphology were also translated into variable levels of expression of PE markers and to a certain extent of VE markers (Fig. 7.6). In particular, expression of *Snail* and *Thbd* was downregulated in epithelial-like subclones. Intriguingly, expression of Ihh, VE marker was on average higher in spindle-like subclones than in epithelial-like subclones (Fig. 7.6). Ihh expression was reported in VYS and Ihh is thought to indicate late differentiation of ExEn (Maye et al., 2000).

In summary, XEN cell are clonal and heterogeneous cell lines. They contain progenitors of VE and PE like cells. But importantly subclones of similar properties as parental cell line are present. These would be then cells responsible for self-renewal of cell line and they are most likely responding to current culture conditions by giving rise to more differentiated progenitors.

8. BMP4 and laminin promote differentiation of XEN cells into visceral endoderm.

8.1 Introduction

In culture and in chimaera contribution analysis XEN cells are heavily biased against PrE and VE. It is accepted that signals from epiblast, ExEc and ECM are required for cells to maintain their VE identity (Gardner, 1982; Hogan and Tilly, 1981; Smyth et al., 1999; Yamamoto et al., 2009). In an effort to promote XEN cells to adopt VE character different aspects of the in vivo environment were mimicked.

ECM components, such as laminin and fibronectin were previously implied in differentiation of PrE (Behrendtsen et al., 1995; Liu et al., 2009; Smyth et al., 1999). Furthermore, specification and formation of VE and its subtypes in embryo also requires Nodal and BMP signalling, members of TGFβ signalling family (Yamamoto et al., 2009). Nodal and BMP4 after implantation are expressed by epiblast and ExEc, respectively (Beck et al., 2002; Coucouvanis and Martin, 1995; Mesnard et al., 2006). Mutants embryos for receptors and ligands of these pathways were shown to exhibit various VE differentiation defects (Beck et al., 2002; Ben-Haim et al., 2006; Brennan et al., 2001; Gu et al., 1998; Mishina et al., 1995; Miura et al., 2010; Sirard et al., 1998; Waldrip et al., 1998; Yamamoto et al., 2009). For this reason BMP4 and Activin A (a Cripto-independent equivalent of Nodal) were chosen for studies of their effects on XEN cells.

8.2 The effect of cell density on XEN cells

XEN cells are strikingly similar to PE cells when cultured at subconfluent densities. Cells are motile, infrequently forming epithelial sheets and very few cells express E-CADHERIN (Fig 7.1 and Fig. 8.1a). However, when cultured to high cell densities some cells form epithelial sheets and upregulate E-CADHERIN at cell-to-cell junctions (Fig. 8.1b).

I then analysed gene expression of ExEn markers in XEN cells cultured at low and high densities (Fig. 8.1c). Cells were plated at two different starting densities (low: 10^3cells/cm^2 and high: 10^4cells/cm^2) and cultured for 3 days. Whether

at low or high density the IM8A1-GFP XEN cell line expressed *Gata4*, albeit its expression is lower at high density. Expression of *Gata6* remained unchanged between low and high density conditions. *Snail*, a PE marker, is downregulated by 3-fold at high density. Downregulation of Snail agrees with observed upregulation of E-CADHERIN (Fig. 8.1b). *Hex* and *Hnf4α* were expressed at slightly lower levels at higher density than at low density. Interestingly, expression of *Afp* and *Ihh*, VE markers, was upregulated by 2- and 2.5-fold, respectively, at high cell densities. Expression of *Dkk1*, AVE marker, is the same between low and high density. Also expression of *Fgf8*, emVE marker, remained at a relatively low level whether at low or high density.

To summarize, XEN cells at high cell density readily upregulate expression of E-CADHERIN, *Afp*, *Ihh* (VE markers) and downregulate expression of *Snail* (PE marker).

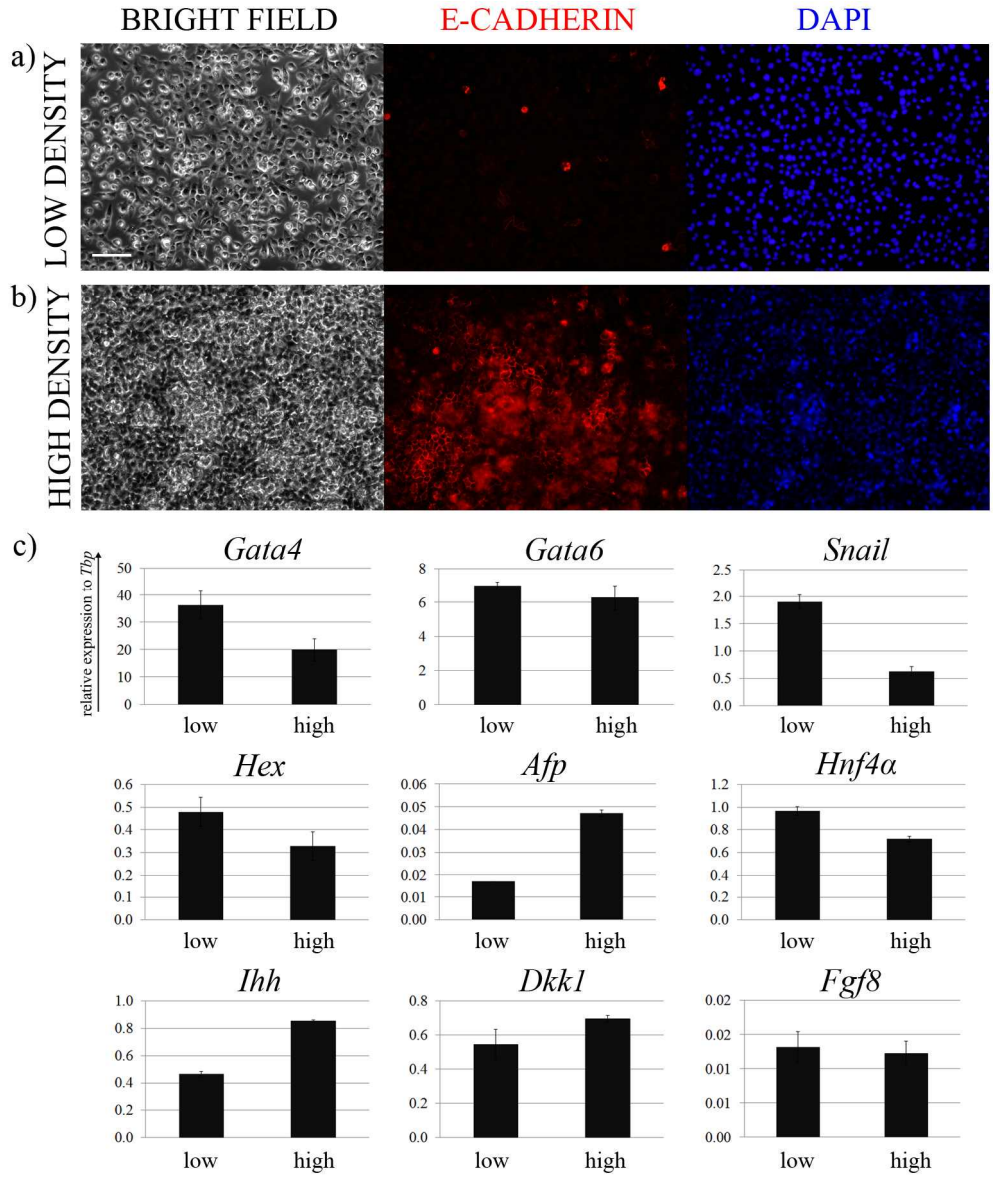

Figure 8.1 XEN cells upregulate expression of E-CADHERIN and some of the visceral endoderm markers at high cell densities and downregulate expression of *Snail*, parietal endoderm marker. a-b) Immunostaining of E-cadherin in XEN cells cultured at low (a) and high (b) density on gelatin for 4 days; scale bar: 100µm; **c**) qRT-PCR for selected markers were normalised to *Tbp* expression and represent an average of technical duplicates, error bars are standard deviation between technical duplicates..

8.3 XEN cell aggregates

The changes in XEN cells at high cell density prompted me to ask whether this is due to forced cell-to-cell interactions between cells. In order to investigate this I established a XEN cell aggregate culture. Cells were suspended as single cells and were cultured in hanging drops for 10 days.

Both IM8A1-GFP and XEN1.3 cells formed cohesive aggregates in hanging drops (Fig. 8.2a-b). These aggregates are not particularly regular and they frequently fused together forming a larger aggregate. Gene expression of XEN cell aggregates of two XEN cell lines (IM8A1-GFP and XEN1.3) was compared to the same XEN cell line grown in monolayer culture (Fig. 8.2c). *Gata4* was expressed higher in aggregates than in monolayer culture. *Gata6* was upregulated in XEN1.3 aggregates by 2-fold, but only mildly in IM8A1-GFP. A 3-fold upregulation of *Snail*, PE marker, was noted in aggregates compared to monolayer culture for both IM8A1-GFP and XEN1.3 cells. Another PE marker, *Thbd*, in contrast was downregulated in aggregate culture. The expression of *FoxA2*, *Hex* and *Ihh* was upregulated in aggregates. However, *Afp*, VE marker, was downregulated in aggregates and *Hnf4α* was unchanged between aggregate and monolayer culture.

Aggregate culture of XEN does not promote homogenous differentiation of XEN cells. Upregulation of some VE markers (*Gata4*, *Gata6*, *FoxA2*, *Hex* and *Ihh*) is observed, but another VE marker, *Afp*, is downregulated. Upregulation of Ihh might indicate maturation of ExEn (Maye et al., 2000). At the same time XEN cells in aggregate upregulate expression of *Snail*.

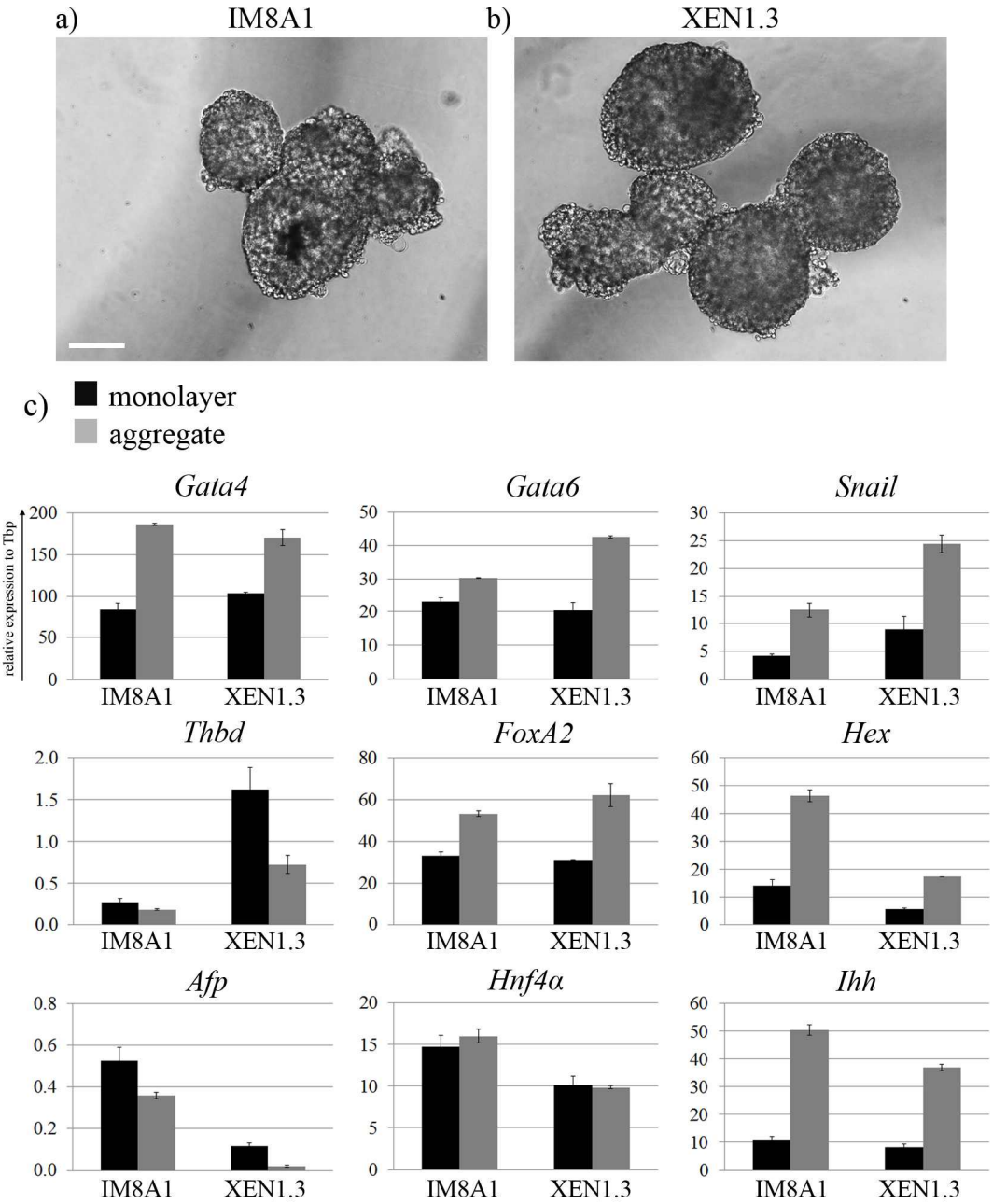

Figure 8.2 XEN cells upregulate a subset of visceral endoderm and parietal endoderm markers in aggregate culture. a-b) Bright field picture of XEN cell aggregates: IM8A1-GFP (a) and XEN1.3 (b); scale bar: 40µm; **c)** qRT-PCR assay for selected markers. qRT-PCR results were normalised to *Tbp* expression and represent an average of technical duplicates, error bars are standard deviation.

8.4 The effect of ECM components: laminin and fibronectin on XEN cells

8.4.1 Morphology of XEN cells and expression of E-CADHERIN on gelatin, laminin and fibronectin

The observation that XEN cells upregulate E-CADHERIN at high densities led to a hypothesis that XEN cells may be depositing extracellular matrix (ECM) components that promote epithelial formation. Indeed, XEN cells are known to express very high levels of laminin alpha 1 and beta 1 and other ECM components that are also present in the basement membrane of E7.0 embryos (Gersdorff et al., 2005; Kunath et al., 2005).

Consequently, I compared the morphology of XEN cells cultured on gelatin, laminin, and fibronectin (Fig. 8.3a). XEN cells cultured on laminin for 2 days readily formed epithelial colonies. In contrast, cells cultured on gelatin or fibronectin remained refractile and freely spread around the plate.

Subsequently, XEN cells cultured on gelatin, laminin or fibronectin were assessed for expression of E-CADHERIN and VIMENTIN (Fig. 8.3b-d). Cells were plated at low density and cultured for 4 days. Cells on laminin exhibited increased E-CADHERIN expression at cell junctions and decreased expression of VIMENTIN as compared to cells cultured on gelatin (Fig. 8.3b-c). However, XEN cells cultured on fibronectin did not form E-CADHERIN positive epithelial sheets and maintained expression of VIMENTIN (Fig. 8.3d).

Next, E-CADHERIN expression in IM8A1-GFP cells cultured on laminin and gelatin was quantified by flow cytometry (Fig. 8.3e). The number of E-CADHERIN-positive cells more than doubled (from 15% to 39%) when cells were cultured on laminin compared to gelatin.

Laminin, in contrast to fibronectin, has a very striking effect on XEN cells. Cells become more epithelial and upregulate E-CADHERIN.

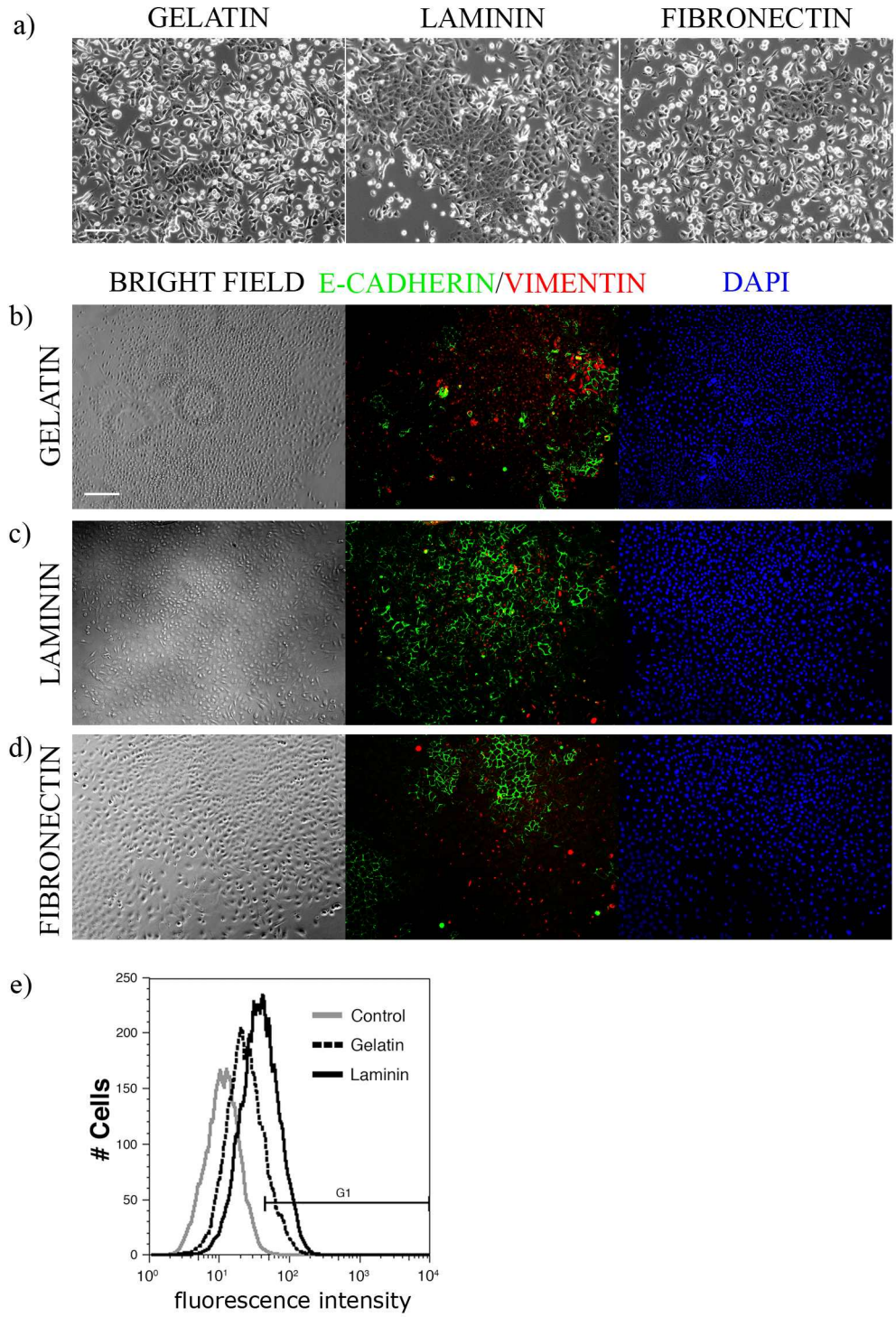

Figure 8.3 XEN cells form epithelial colonies and upregulate expression of E-CADHERIN and downregulate VIMENTIN on laminin. a) Bright field pictures of IM8A1-GFP cells cultured on gelatin, laminin or fibronectin for 2 days; **b-d)** XEN1.3 cells were plated at low density either on gelatin (b), laminin (c) or fibronectin (d), or after 4 days of culture immunostained for E-CADHERIN and VIMENTIN; scale bar: 200µm. **e**) Flow cytometry for E-cadherin expression of XEN cells cultured for 4 days on gelatin or laminin ($G1_{control}$=0.6%, $G1_{gelatin}$=15%, $G1_{laminin}$=39%); control sample: cells incubated with secondary antibody only.

8.4.2 Clonal assay for cells growing on laminin or fibronectin

In order to be able to further examine the heterogeneous nature of E-CADHERIN expression in XEN cells a clonal assay was carried out for XEN cells cultured on laminin and fibronectin.

On laminin less than half of the colonies (46%) were E-cadherin-low, 39% mixed and 15% E-cadherin-high for IM8A1-GFP (Fig 8.4a). Very similarly for XEN1.3 cell line the For XEN1.3 XEN cell line 41% of colonies were E-CADHERIN-low, 41% mixed and 18% E-CADHERIN-high (Fig. 8.4a).

On fibronectin the percentages of different types of colonies were very similar between cell lines. For IM8A1-GFP cell line 61% of colonies were E-cadherin-low, 34% mixed and only 5% E-cadherin-high (Fig 8.4b). For XEN1.3 cell line 62% of colonies were E-CADHERIN-low, 32% mixed and 6% E-CADHERIN-high (Fig 8.4b).

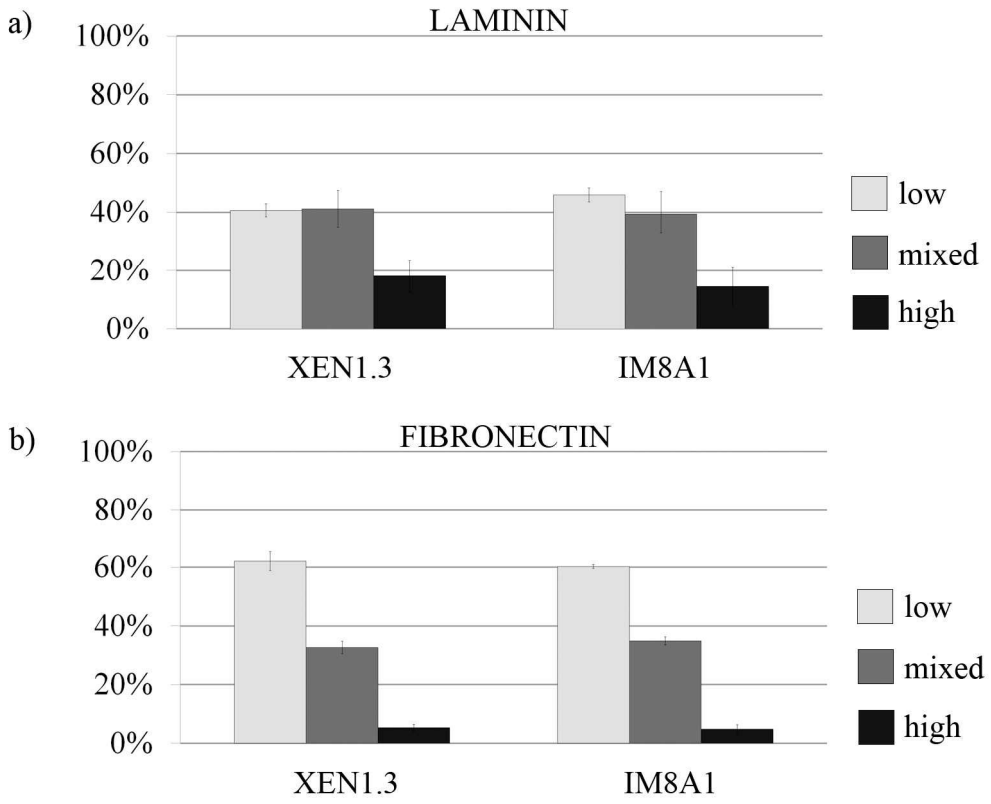

Figure 8.4 Laminin, but not fibronectin, increased the ratio of E-CADHERIN expressing colonies at clonal level. Cells were plated at clonal density and cultured for 5 days on: **a**) laminin ($n_{IM8A1\text{-}GFP}$=178, $n_{XEN1.3}$=203), $p_{\chi 2}$=0.5363; **b**) fibronectin ($n_{IM8A1\text{-}GFP}$=83, $n_{XEN1.3}$=95), $p_{\chi 2}$=0.9135.

XEN1.3 and IM8A1-GFP cell lines have different ratio of colonies when cultured on gelatin (Fig. 7.4d). Once on laminin or fibronectin the ratio becomes similar. The proportion of E-CADHERIN expressing colonies increases for both cell lines on laminin. The difference between types of XEN1.3 colonies on fibronectin and gelatin is not statistically significant ($p_{\chi 2}$= 0.2385). Yet, the difference in the ratio of types colonies in XEN1.3 cells cultured on gelatin and laminin or laminin and fibronectin are statistically different ($p_{\chi 2}$=0.0005 and $p_{\chi 2}$<0.0001, respectively). For IM8A1-GFP cell line on fibronectin the percentage of E-CADHERIN-mixed colonies is almost tripled when compared to gelatin, and the difference in the ratio of colonies on gelatin versus fibronectin is statistically different ($p_{\chi 2}$<0.0001). Similarly, the ratio of different types of colonies on gelatin versus laminin and fibronectin versus laminin is significantly different ($p_{\chi 2}$<0.0001 and$p\chi_2$=0.0022, respectively).

Overall, laminin has an epithelializing effect on XEN cells and more than half of colonies express E-CADHERIN.

8.4.3 qRT-PCR analysis of XEN cells on gelatin, laminin or fibronectin

I subsequently compared gene expression of various ExEn markers in XEN cells in two separated analyses comparing gelatin to laminin (Fig. 8.5a) and gelatin to fibronectin (Fig. 8.5b).

On gelatin and laminin the expression of *Gata4* was similar, whilst *Gata6* was downregulated on laminin. Also, PE markers, *Snail* and *Thbd*, were downregulated on laminin. *FoxA2* was unchanged on laminin for IM8A1-GFP cell line, but was downregulated for XEN1.3. *Hex*, *Afp* and *Ihh* were all expressed at higher and upregulated levels on laminin for IM8A1-GFP, but were lower for XEN1.3 on laminin compared to gelatin. *Hnf4α* was slightly upregulated on laminin in IM8A1-GFP cells, but again was downregulated in XEN1.3.

Similarly as on laminin, expression of *Gata4* is unchanged between cells cultured on gelatin and fibronectin and *Gata6* is downregulated on fibronectin. PE markers, *Snail* and *Thbd*, are downregulated on fibronectin, but only for XEN1.3 cell line and remain at the same level for IM8A1-GFP. All of the analysed markers of

different types of VE i.e., *FoxA2, Hex, Afp, Ihh* and *Hnf4α* are downregulated on fibronectin for both IM8A1-GFP and XEN1.3 cell lines.

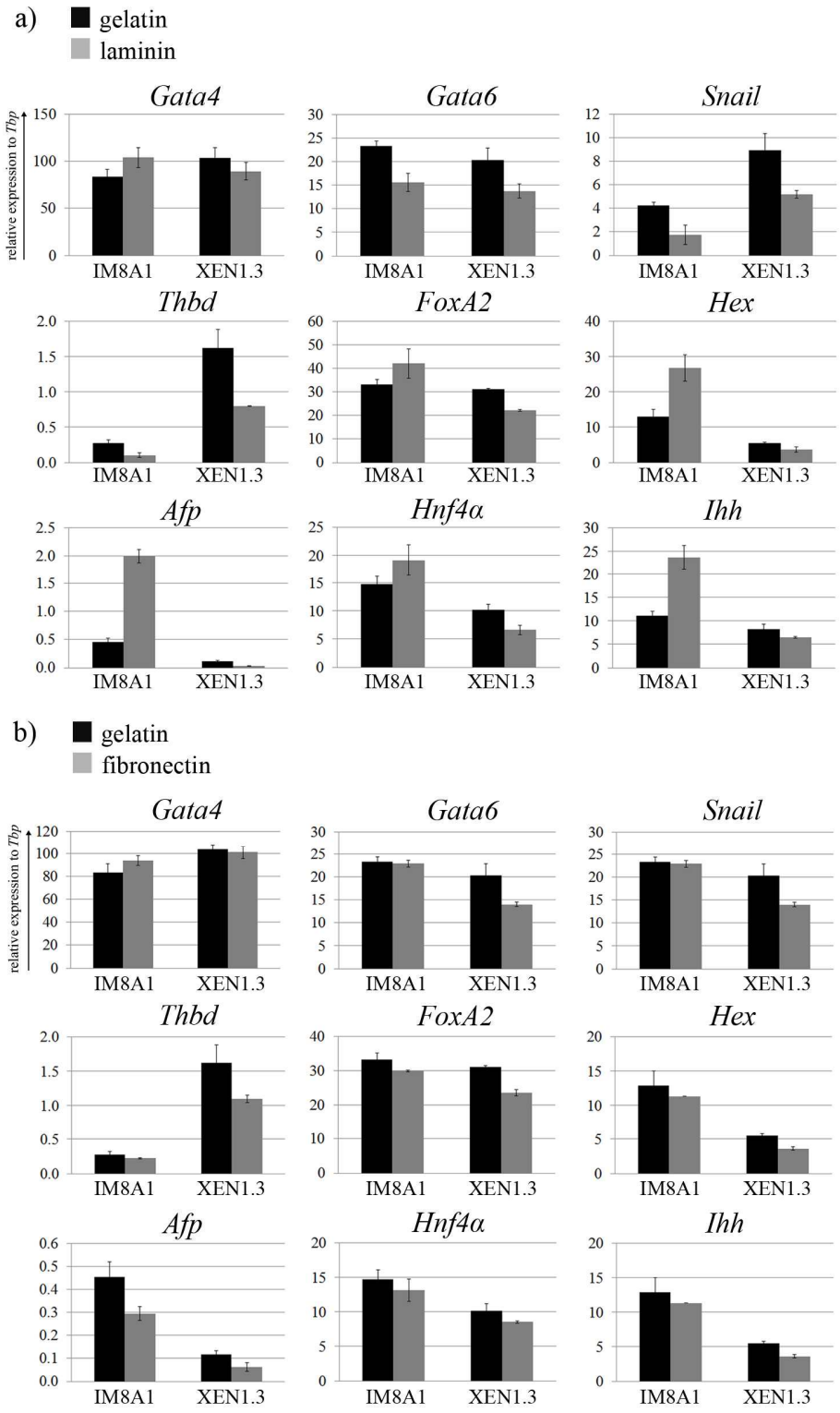

Figure 8.5 XEN cells on laminin downregulate expression of parietal endoderm markers for XEN1.3 and IM8A1-GFP cell lines, but upregulate expression of visceral markers for IM8A1-GFP cell line only. a-b) qRT-PCR assay for selected markers for XEN1.3 and IM8A1-GFP (IM8A1) cells growing on gelatin and laminin (a) or gelatin and fibronectin (b). qRT-PCR results were normalised to *Tbp* expression and represent an average of biological duplicates, error bars are standard deviation between biological duplicates.

Together with E-CADHERIN staining, gene expression analysis also supports the observation that XEN cells were induced to be more visceral in character when grown on laminin. Consistently with E-CADHERIN upregulation *Snail* and *Thbd*, PE markers, are downregulated on laminin. Fibronectin does not have such coherent effect on XEN cells and the response to fibronectin is different between XEN1.3 and IM8A1-GFP cell lines.

8.4.4 Expression of E-CADHERIN, GATA4, PDGFRa in XEN cells on laminin

I further analysed XEN cells cultured on laminin for expression of other ExEn markers. XEN cell-derived epithelial cells, whether on gelatin or laminin, continued to express GATA4 and PDGFRα (Fig. 8.6a-d), albeit the levels of PDGFRα were lower in the E-CADHERIN positive cells when compared to neighbouring E-CADHERIN negative cells (Fig. 8.6c-d). Lower PDGFRα has also been observed previously (Fig. 7.3b)

Taken together with previous results (Fig. 8.3-5), it is observed that laminin induces epithelialization of XEN cells and downregulation of parietal endoderm markers. Upregulation of VE markers is observed only for IM8A1-GFP cell line.

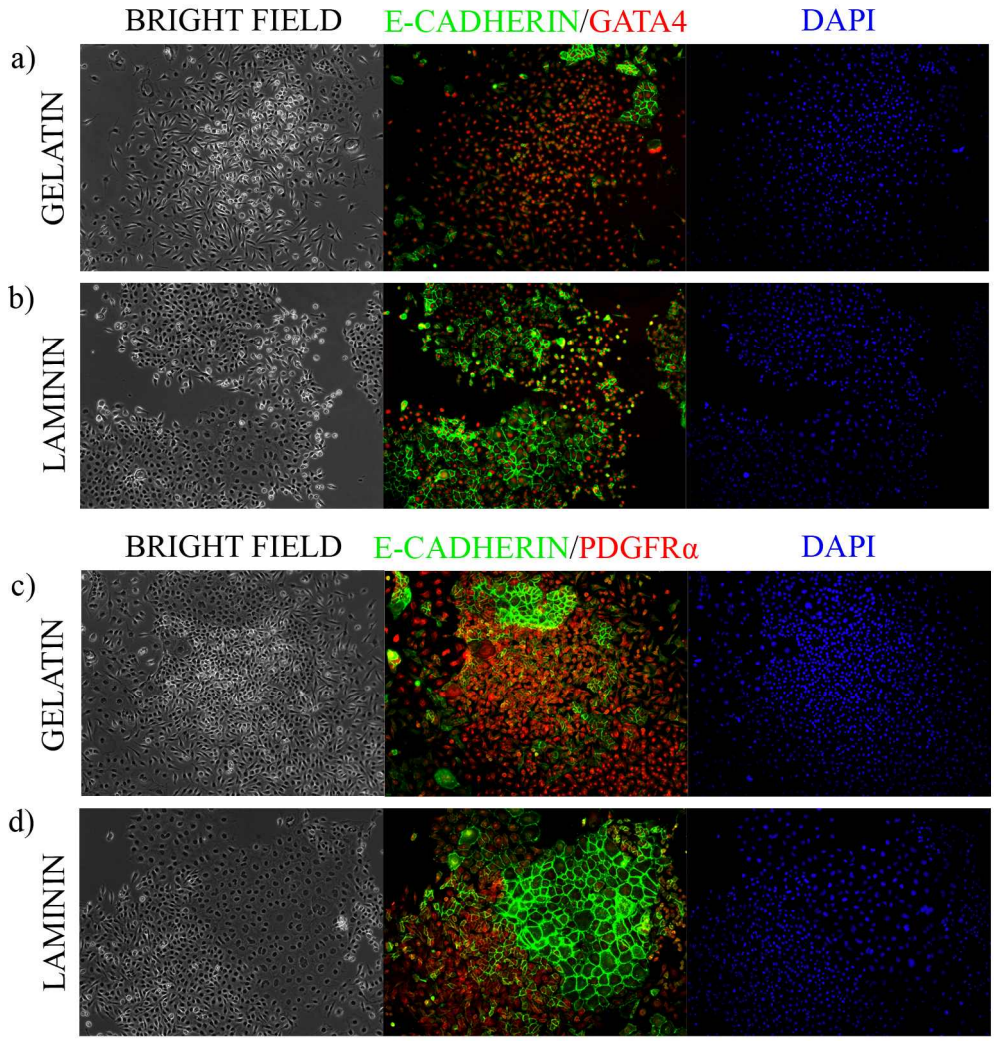

Figure 8.6 XEN cells on laminin continue to express GATA4 and express E-CADHERIN and PDGFRα in a heterogeneous and mutually exclusive manner. XEN1.3 cells were plated at low density and cultured on gelatin or laminin in serum for 4 days after which they were fixed and immunostained with indicated antibodies; scale bar: 200µm.

8.4.5 Clonal assay for selectedIM8A1 subclones cultured on laminin

Laminin has an epithelializing effect on XEN cells in bulk culture but also at clonal level (Fig. 8.3, Fig. 8.4). The ratio E-CADHERIN negative colonies is reduced when cells are plated on laminin, which indicates that either some of previously E-CADHERIN negative cells gave rise to E-CADHERIN expressing colonies or that the differentiation of E-CADHERIN non-expressing cells is prevented on laminin. To answer that question it is conceivable then to find out how more homogenous subclones derived from IM8A1 cell line also respond to laminin.

Two PE-like subclones (E11 and G3) and two VE-like subclones (C1 and F9) were chosen.

A typical colony of E11 or G3 subclone from spindle-like category grows on laminin as single, freely spreading cells not expressing E-CADHERIN (Fig. 8.7a-b). Colonies arising from epithelial-like subclones are more compact than from E11 or G3 subclone and express E-CADHERIN (Fig. 8.7c). Albeit the levels of E-CADHERIN are lower in a C1 colony than in a F9 colony (Fig. 8.7d).

For E11 subclone (Fig. 8.7e) on laminin 68% of colonies were E-CADHERIN-low, 32% mixed and 0% E-CADHERIN and is different from gelatin ($p_{\chi 2}$=0.0032) (Fig. 7.8a). Similarly, for subclone G3 (Fig. 8.7e) on laminin 71% of colonies are E-CADHERIN-low, 21% E-CADHERIN-mixed and 0% E-CADHERIN-high and is different from the ratio on gelatin ($p_{\chi 2}$=0.0003)

In contrast to spindle-like subclones, C1 epithelial-like subclone has 13% E-CADHREIN-low, 65% E-CADHERIN-mixed and 21% of colonies are E-CADHERIN-high colonies (Fig. 8.7f) and is different when compared to gelatin ($p_{\chi 2}$=0.0176). However the total percentage of E-CADHERIN expressing colonies remains the same for gelatin and laminin. For F9 subclone 4% of colonies are E-CADHERIN-low, 48% mixed and 48% E-CADHERIN-high (Fig. 8.8f). For F9 the ratio of different types of colonies on gelatin versus laminin is not significantly different ($p_{\chi 2}$=0.3603).

Surprisingly, laminin increased the ratio of E-CADHERIN expressing colonies in spindle-like subclones by almost a 2-fold. This indicates that laminin can upregulate expression of E-CADHERIN and thus promote mesenchymal to epithelial transition in seemingly differentiated and mesenchymal PE-like cells.

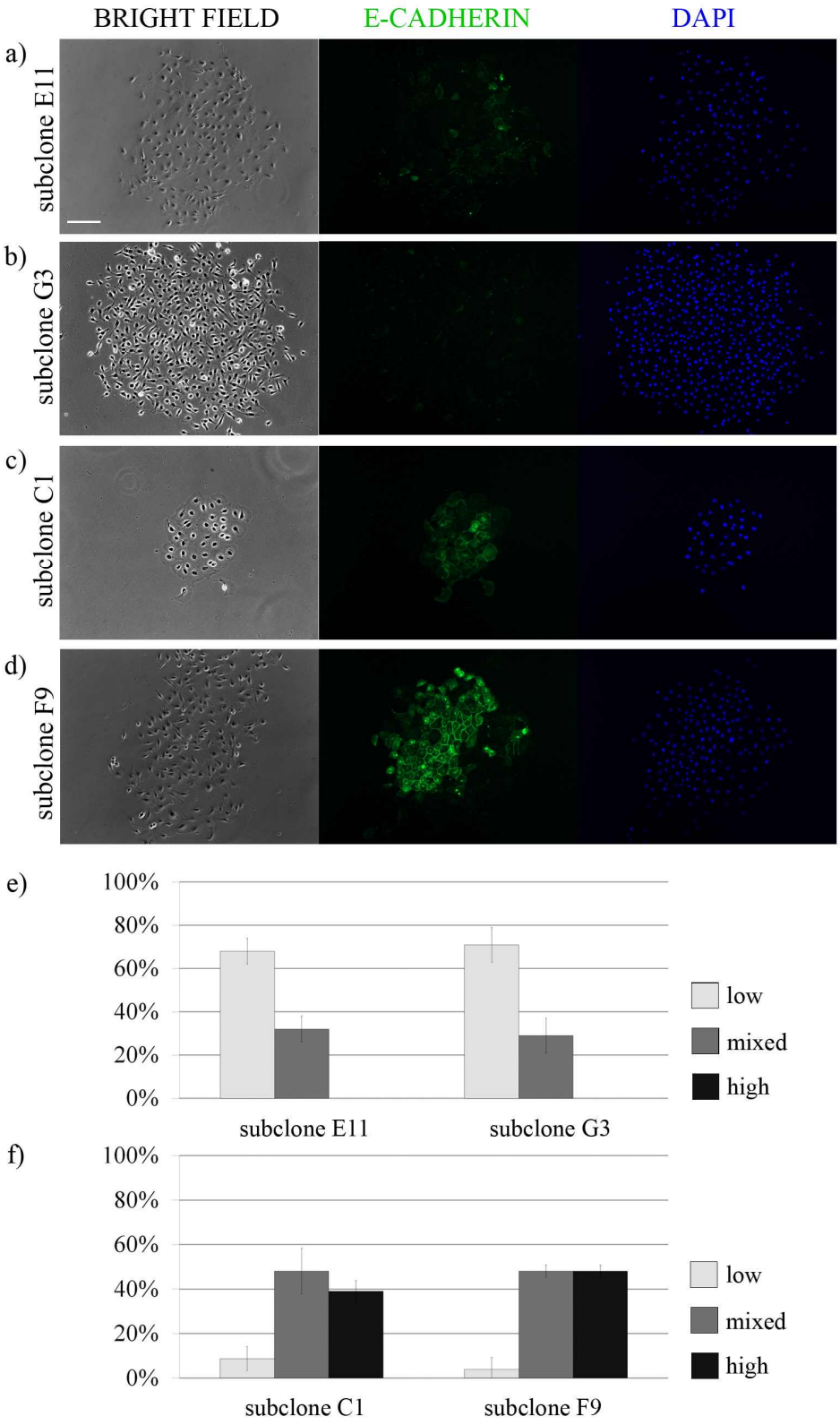

Figure 8.7 Laminin promotes upregulation of E-CADHERIN expression also in parietal endoderm like subclones. Cells were plated at clonal density on laminin and cultured for 5 days: **a-d**) Images of typical colony arising from various subclones; **e-f)** Clonal assay for PE-like subclones (n_{E11}=42, n_{G3}=51) (e) and VE-like subclones (n_{C1}=37, n_{F9}=41) (f).

8.5 BMP4 induced differentiation of XEN cells

8.5.1 Establishment of serum-free culture conditions for XEN cells

Firstly, in order to clearly elucidate the effect of added signalling molecules I decided to establish serum-free culture conditions for XEN cells. Primarily, because FBS often contains some BMP activity experiments conducted in serum-free medium would show less ambiguity. Also serum is likely to contain factors that could actively stimulate PE differentiation of XEN cells. I chose N2B27 serum-free medium that has previously been used in endoderm differentiation of mES cells (Morrison et al., 2008).

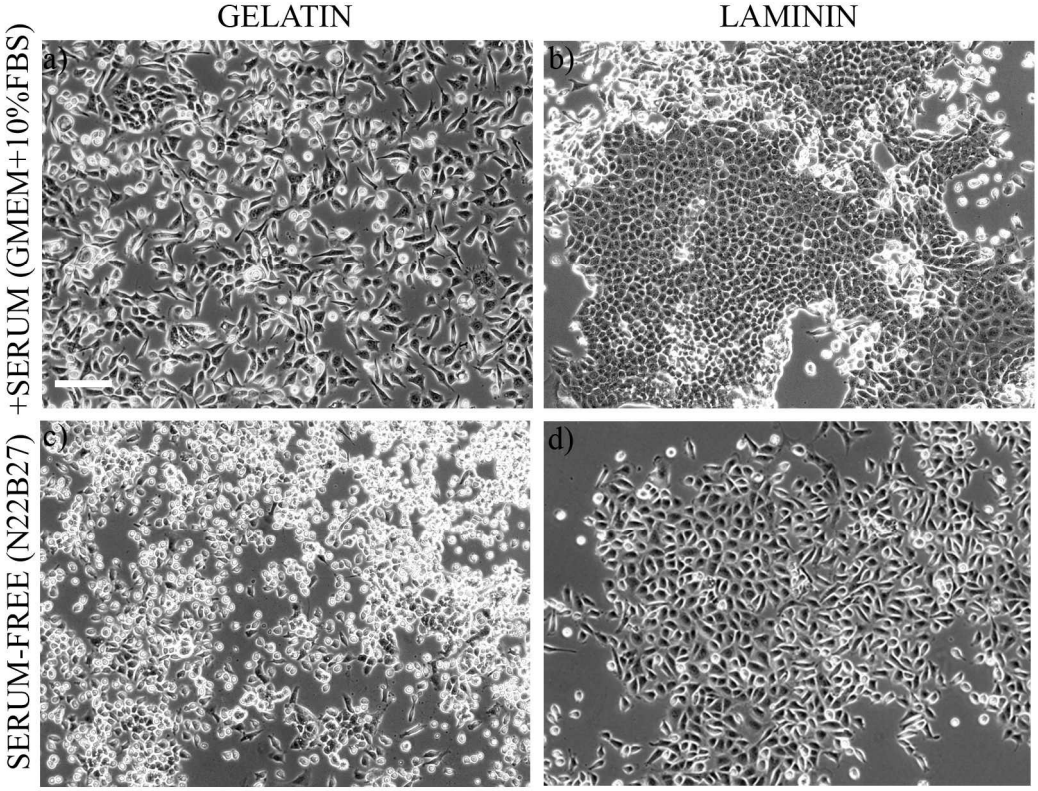

Figure 8.8 XEN cells cultured in serum-free conditions. Bright field images of IM8A1-GFP XEN cells cultured in standard (**a, b**) and serum-free (**c, d**) conditions either on gelatin (a, c) or laminin (b, d) for 3 days; scale bar: 200µm.

When XEN cells were plated in serum-free conditions on gelatin their morphology changed. Cells start to curl up and become very refractile comparing to serum-containing media (Fig. 8.8a and Fig. 8.8c). Whilst on laminin XEN cells retain their mixed morphology and look very similar to cells cultured in serum on gelatin

(Fig. 8.8d). Yet, when compared to serum-containing media (Fig. 8.8b) it becomes clear that in serum-free conditions these cells have potentially lost their epithelial character and the junctions between cells in a colony become loose.

The differences between cells cultured in serum-containing and serum-free media on laminin become even more apparent for IM8A1-GFP than XEN1.3 cell line in clonal assays. For IM8A1-GFP cell line in serum containing media 46% of colonies were E-cadherin-low, 39% mixed and 15% E-cadherin-high. While in serum-free conditions 67% of colonies were E-CADHERIN-low, 29% E-CADHERIN-mixed and only 4% E-CADHERIN-high (Fig. 8.9a). For XEN1.3 cell line in serum containing medium 41% of observed colonies were E-cadherin-low, 41% mixed and 18% E-cadherin-high. Whereas in serum-free medium 37% of colonies were E-CADHERIN-low, 39% E-CADHERIN-mixed and 26% E-CADHERIN-high (Fig. 8.9b).

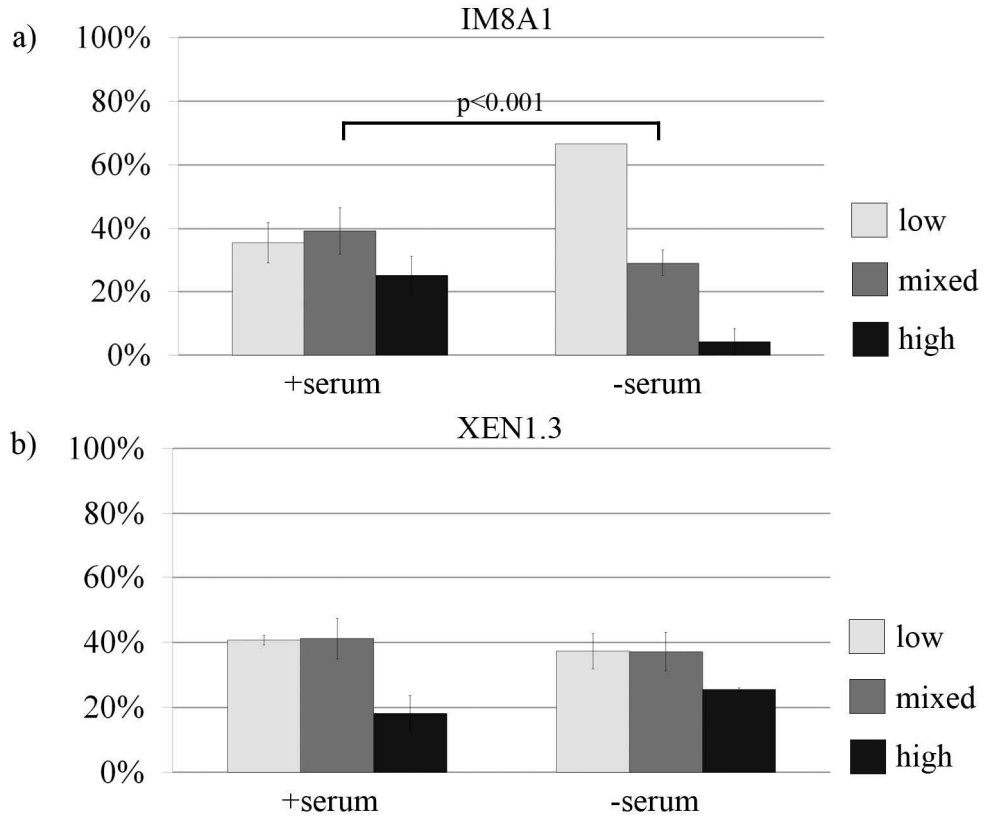

Figure 8.9 Clonal assay for IM8A1-GFP and XEN1.3 cell lines cultured on laminin in standard and serum-free conditions. Cells were plated on laminin at clonal density and cultured for 5 days. **a)** IM8A1-GFP (IM8A1) cell line ($n_{IM8A1\text{-}GFP+serum}$=178,$n_{IM8A1\text{-}GFP\text{-}serum}$=72; $p_{\chi 2}$<0.0001); **b)** XEN1.3 cell line, ($n_{XEN1.3+serum}$=203,$n_{XEN1.3\text{-}serum}$=77; $p_{\chi 2}$=0.1144).

Finally, I compared expression of a few markers between serum and serum-free conditions on laminin for IM8A1-GFP cell line (Fig. 8.10). *Gata4* and *Snail* levels are unchanged in different media. *Gata6* expression increases when serum is removed. *Afp* and *Hex* are both downregulated in serum-free conditions. However, the level of expression of another exVE marker, *Ihh*, increases in serum-free conditions.

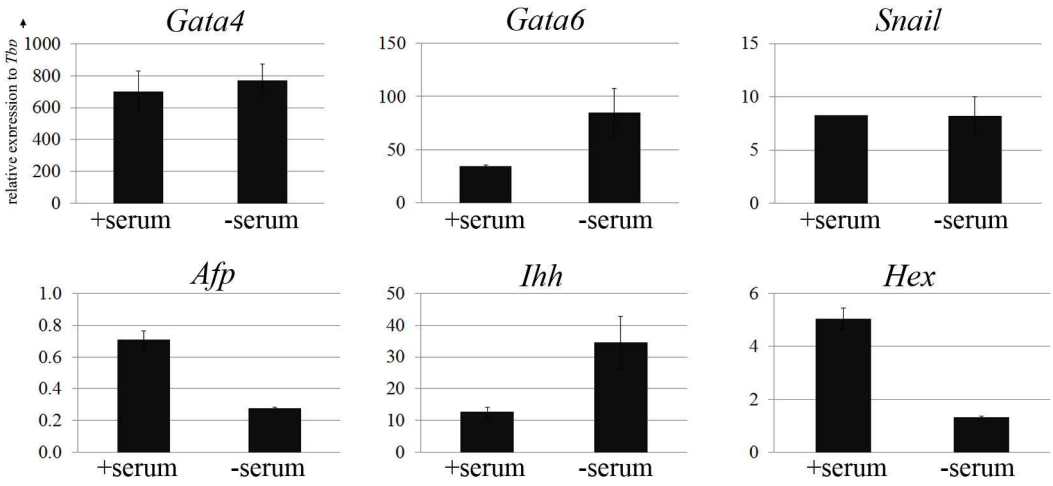

Figure 8.10 XEN cells continue to express various ExEn markers in serum-free conditions. qRT-PCR analysis of IM8A1-GFP XEN cells cultured on laminin in GMEM+10%FBS and N2B27. qRT-PCR results were normalised to *Tbp* expression and represent an average of biological duplicates, error bars are standard deviation between biological duplicates.

In contrast to gelatin, laminin is able to support robust cell attachment in serum free conditions. Absence of serum downregulates expression of some of the VE markers in IM8A1-GFP cell line. Serum-free conditions also reduce percentage of E-CADHERIN expressing cells in IM8A1-GFP, but not XEN1.3 cell line. Yet, the ratio of E-CADHERIN positive colonies is still higher than when cells are cultured in standard medium on gelatin ($p_{\chi 2}$=0.005).

8.5.2 Dose-dependent effect of BMP4 on E-CADHERIN, Afp and Hex expression

Having established serum-free culture conditions for XEN cells I treated XEN cells with BMP4. I initially tried two different BMP4 concentrations: 10ng/ml and 50ng/ml. Cells were plated in N2B27+1% FBS overnight and medium was changed the following day to N2B27 only or N2B27 supplemented with BMP4. Already on day 2 of culture cells in presence of BMP4 start to form small epithelial-looking colonies, when compared to cells in N2B27 only (Fig. 8.11a). By day 4 of BMP4 treatment E-CADHERIN was highly expressed in XEN cells cultured in either 10ng/ml or 50ng/ml BMP4 (Fig. 8.11b-d). Yet, only the high BMP4 concentration promoted upregulation of E-CADHERIN in nearly all XEN cells, whereas 10ng/ml of BMP4 resulted in fewer XEN cells upregulating E-cadherin (Fig. 8.11c,d). This dosage effect was also observed with the level of *Afp* and *Hex* expression, where increasing BMP4 concentrations resulted in higher induction (Fig. 8.11e). In subsequent experiment only high BMP4 concentration, i.e. 50ng/ml, is used.

8.5.3 Expression of E-CADHERIN, PDGFRa and VIMENTIN in BMP4 treated XEN cells

To further investigate BMP4 induced differentiation of XEN cells I then analysed expression of E-CADHERIN, PDGFRα and VIMENTIN in XEN1.3 cells cultured in N2B27 on laminin in the presence or absence of BMP4 on day 5 of culture.

When XEN cells are cultured in media supplemented with BMP4 they strongly upregulated E-CADHERIN as compared to non-supplemented N2B27 (Fig. 8.12a, b). In N2B27 the majority of cells expressed PDGFRα and it was expressed in a mutually exclusive fashion with E-CADHERIN (Fig. 8.12a). Cells exposed to BMP4 not only down-regulated PDGFRα (Fig. 8.12a), but also VIMENTIN (Fig. 8.12b) when compared to N2B27 only conditions. There were only a few cells that maintained VIMENTIN expression after BMP4 treatment.

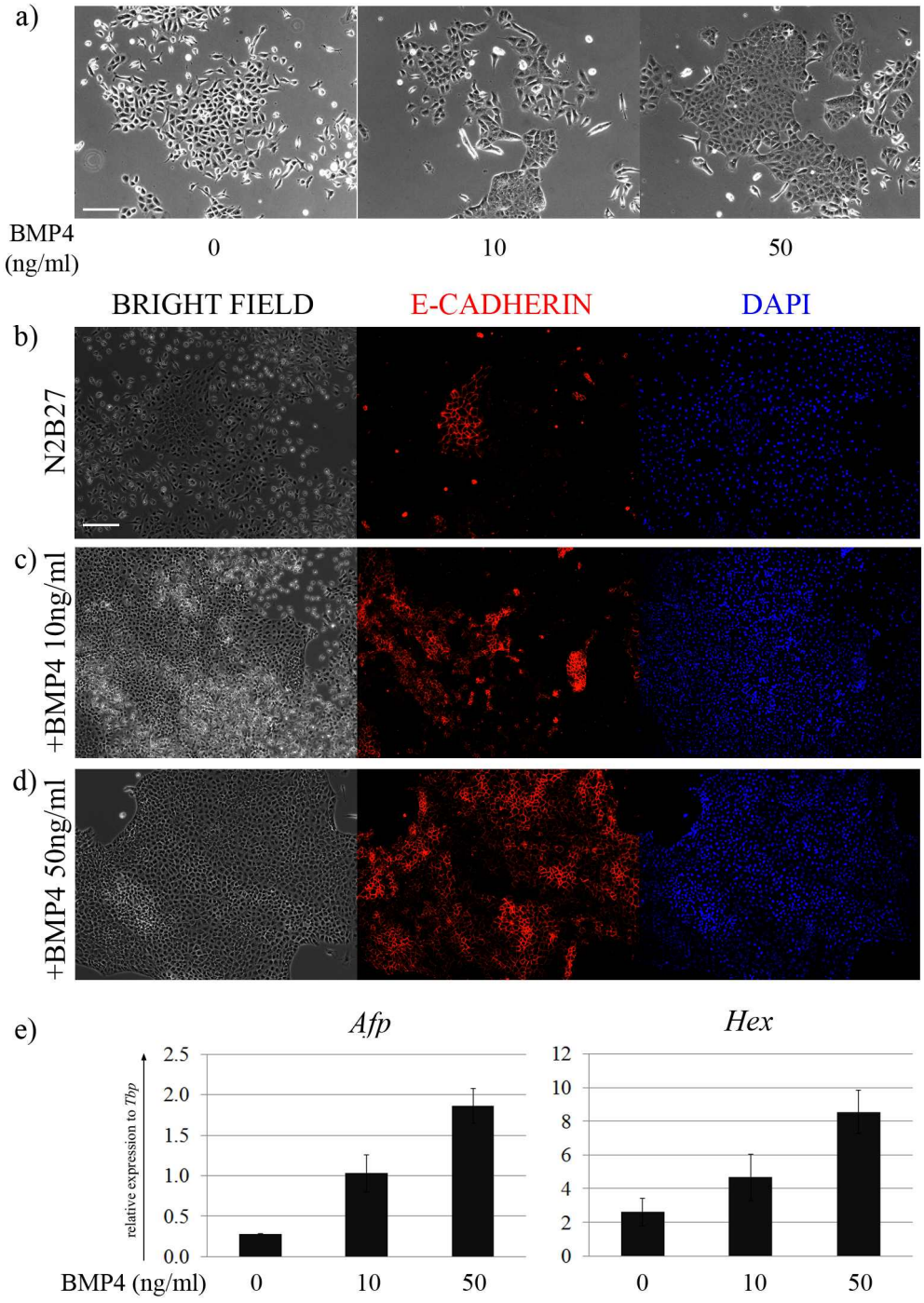

Figure 8.11 BMP4 acts in a dose-dependent manner. a) Bright field pictures of IM8A1-GFP XEN cells cultured with various BMP4 concentrations on laminin in N2B27 on day 3 of culture. **b**–**d**) Immunostaining of E-CADHERIN in IM8A1-GFP XEN cells cultured on laminin in N2B27 only (b) or N2B27 supplemented with BMP4 (c, d); scale bar: 200µm. **e**) qRT-PCR analysis of *Afp* and *Hex* expression in XEN cells cultured in N2B27 with or without BMP4 on laminin for 4 days. qRT-PCR results were normalised to *Tbp* expression and represent an average of biological duplicates, error bars are standard deviation between biological duplicates.

To conclude, BMP4 has a very prominent effect on XEN cells by robustly up-regulating expression of E-CADHERIN and down-regulating the expression of PDGFRα and VIMENTIN.

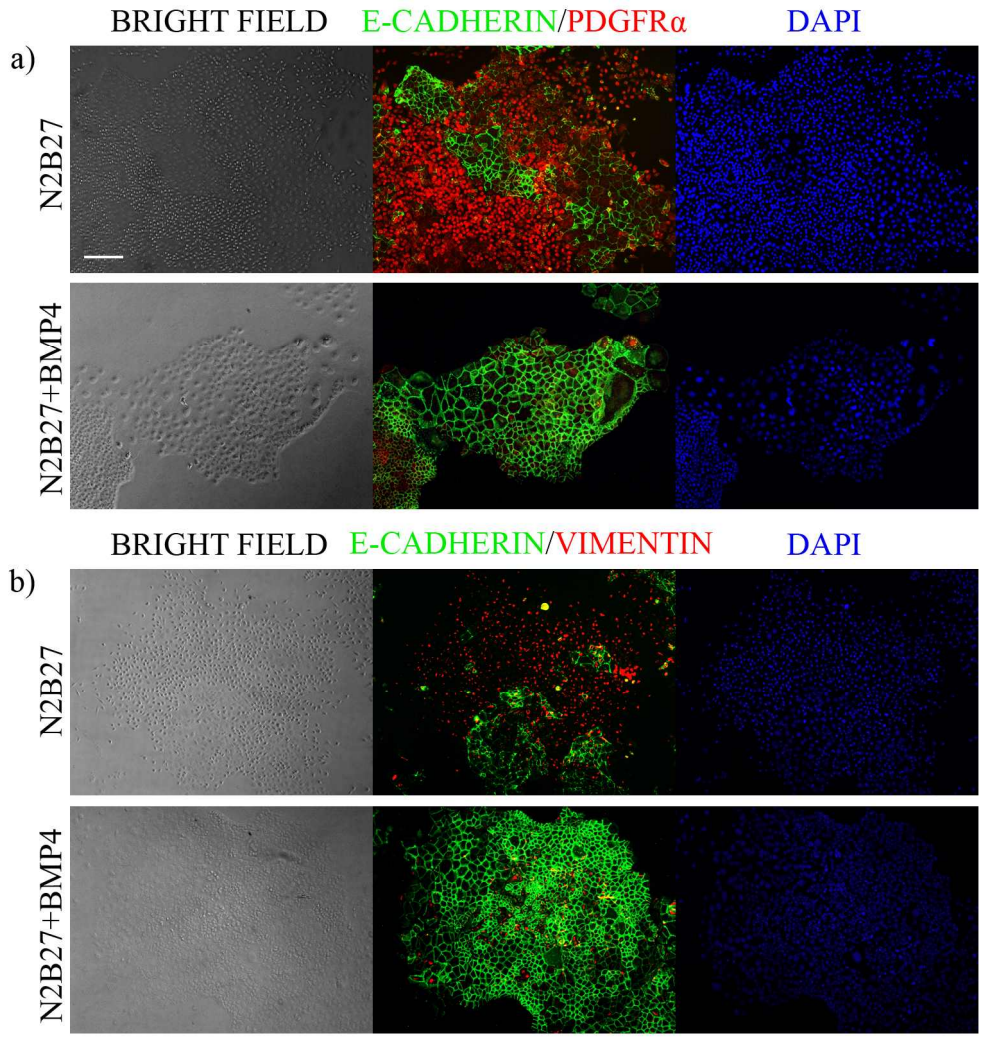

Figure 8.12 BMP4 upregulates E-CADHERIN expression and downregulates expression of PDGFRα and VIMENTIN. Immunostaining of **a**) E-CADHERIN and PDGFRα and **b**) E-CADHERIN and VIMENTIN of XEN1.3 cells cultured on laminin in N2B27 in presence or absence of BMP4 on day 5 of culture; Scale bar: 200µm.

8.5.4 Clonal assay for IM8A1-GFP XEN cell line cultured in the presence of BMP4 in serum-free media

Following the robust E-CADHERIN upregulation in bulk culture of BMP4-treated XEN cells I proceeded with the clonal assay. When IM8A1-GFP XEN cells were cultured in serum-free conditions on laminin 67% of colonies were E-CADHERIN-low, 29% E-CADHERIN-mixed and 4% E-CADHERIN-high. However, addition of BMP4 to IM8A1-GFP changed this ratio radically. The percentage of cells E-cadherin-high colonies is close to 60%, a third of colonies is E-CADHERIN-mixed and only 8% E-CADHERIN-low (Fig. 8.13a). In case of XEN1.3 cells the ratio between E-CADHERIN-low:mixed:high colonies changes from 37:37:26 in N2B27 to 18:40:42 in N2B27+BMP4 (Fig. 8.13b). The differences in the ratio of different types of colonies in these two cell lines is statistically significant ($p_{\chi 2}<0.0001$ for IM8A1-GFP and XEN1.3).

BMP4-treated XEN cells colonies cultured on laminin were mostly uniformly E-CADHERIN positive and VIMENTIN negative, and untreated cells were mostly negative for E-CADHERIN and expressed high levels of VIMENTIN (Fig. 8.21c-d).

BMP4 strongly promotes E-CADHERIN expression shifting the ratio of colonies in favour of E-CADHERIN-mixed and E-CADHERIN-high. The key observation is that the proportion of E-CADHERIN-low colonies was reduced to either from 29% to 8% (IM8A1-GFP) or from 37% to 18% (XEN1.3).

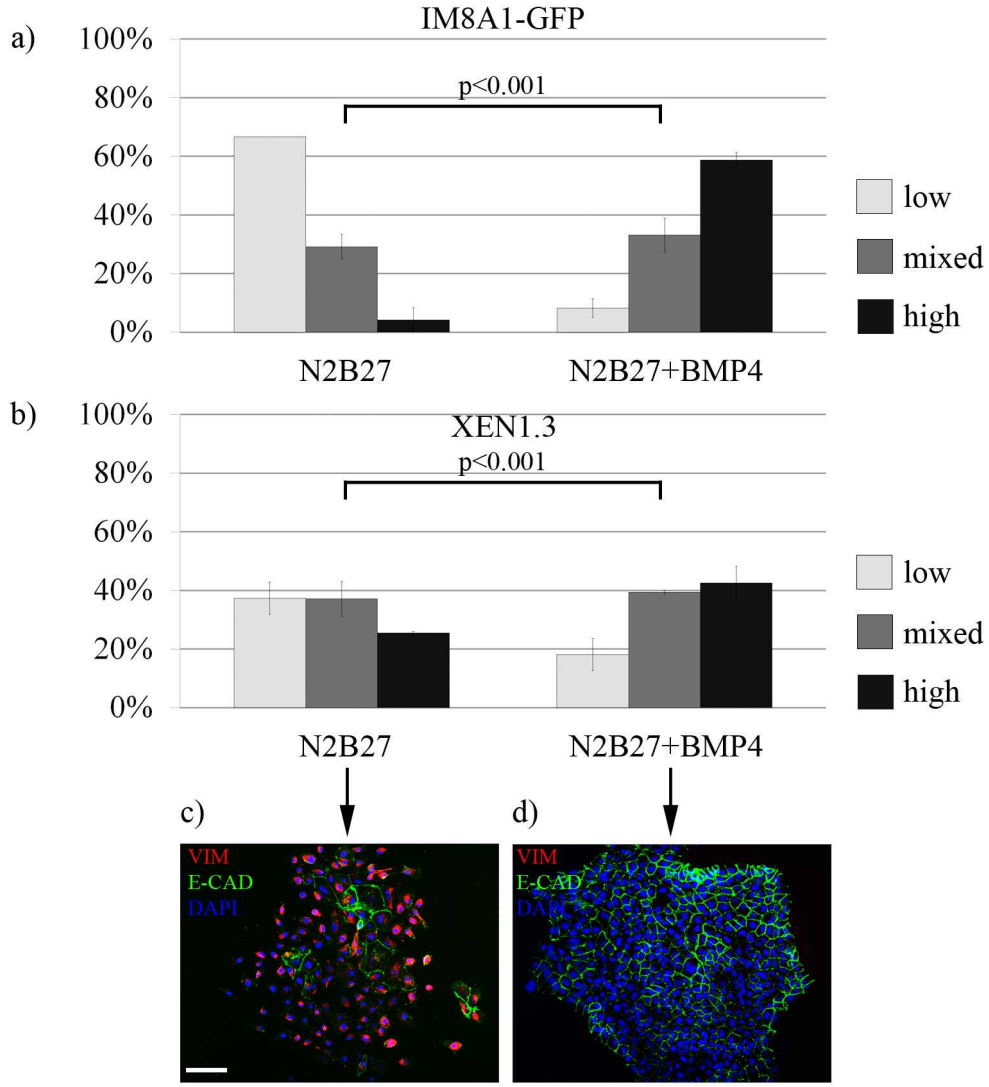

Figure 8.13 BMP4 increases the ratio of E-CADHERIN positive colonies. Cells were cultured on laminin in presence or absence of BMP4 (50ng/ml) at clonal density for 5 days. **a)** IM8A1-GFP cell line, $p_{\chi 2}<0.0001$; **b)** XEN1.3 cell line, $p_{\chi 2}<0.0001$; **c-d**) Examples of different types of colonies formed in N2B27 only (c) or N2B27+BMP4 (d) immunostained against E-CADHERIN and VIMENTIN; scale bar: 100µm.

8.5.5 qRT-PCR analysis of BMP4 treated XEN cells

I further analysed the changes in other ExEn markers upon BMP4 treatment of IM8A1-GFP and XEN1.3 cell lines by qRT-PCR.

For IM8A1-GFP (Fig. 8.14a) *Gata4* and *Gata6* levels remained relatively stable and did not change in response to BMP4 treatment. *Snail* and *Thbd*, PE markers, were downregulated in BMP4 treated cells.BMP4 treatment in serum-free conditions induced the most significant increase of *Afp* expression. *Hex* followed a

similar pattern to *Afp*, being second most upregulated in BMP4 treated cells in serum-free conditions. *Hnf4a* was only slightly induced by BMP4. However, another exVE marker, *Ihh*, did not respond significantly to BMP4 signalling. *FoxA2*, *Dkk1* and *Fgf8* were all downregulated in response to BMP4.

In XEN1.3 (Fig. 8.14b) *Gata4* expression also was upregulated in response to BMP4 treatment. However, *Gata6* levels remained unchanged. *Snail* and *Thbd*, were both upregulated in BMP4 treated cells.BMP4 induced expression of *Afp* and *Hex*. Upon BMP4 treatment expression of *Hnf4a* doubled. But *Ihh* was unchanged between BMP4 treated and control samples. Similarly expression of *FoxA2* and *Fgf8* expression remained at the same level. However, *Dkk1* was downregulated in response to BMP4.

When BMP4 treatment was extended up to 8 days expression of ExEn markers *Gata4* and *Gata6* is downregulated when compared to XEN cells in N2B27 with or without BMP4 on day 4 (Fig. 8.15). Expression of PE marker, *Thbd* and *Snail* is at similar levels between the samples on day 4 and day 8. *Hex* remained unchanged in N2B27 only, but was slightly increased between day 4 and day 8 of BMP4 treatment. *Afp* levels were strongly increased in BMP4 only conditions and there was a further 3-fold upregulation between day 4 and day 8. *Hnf4a* expression is upregulated (2-fold change) in the presence of BMP4 and the expression is similar between day 4 and day 8. Finally, *Ihh* was downregulated at day 8 of BMP4 differentiation.

Even though, there are differences between two XEN cell lines consistent upregulation of *Hex, Afp* and *Hnf4α* and E-CADHERIN indicates that BMP4 promotes VE-like differentiation of XEN cells. At clonal level increase in the expression of E-CADHERIN was observed for IM8A1-GFP and XEN1.3 cell line, but only IM8A1-GFP downregulated *Snail* expression according to qRT-PCR assay.

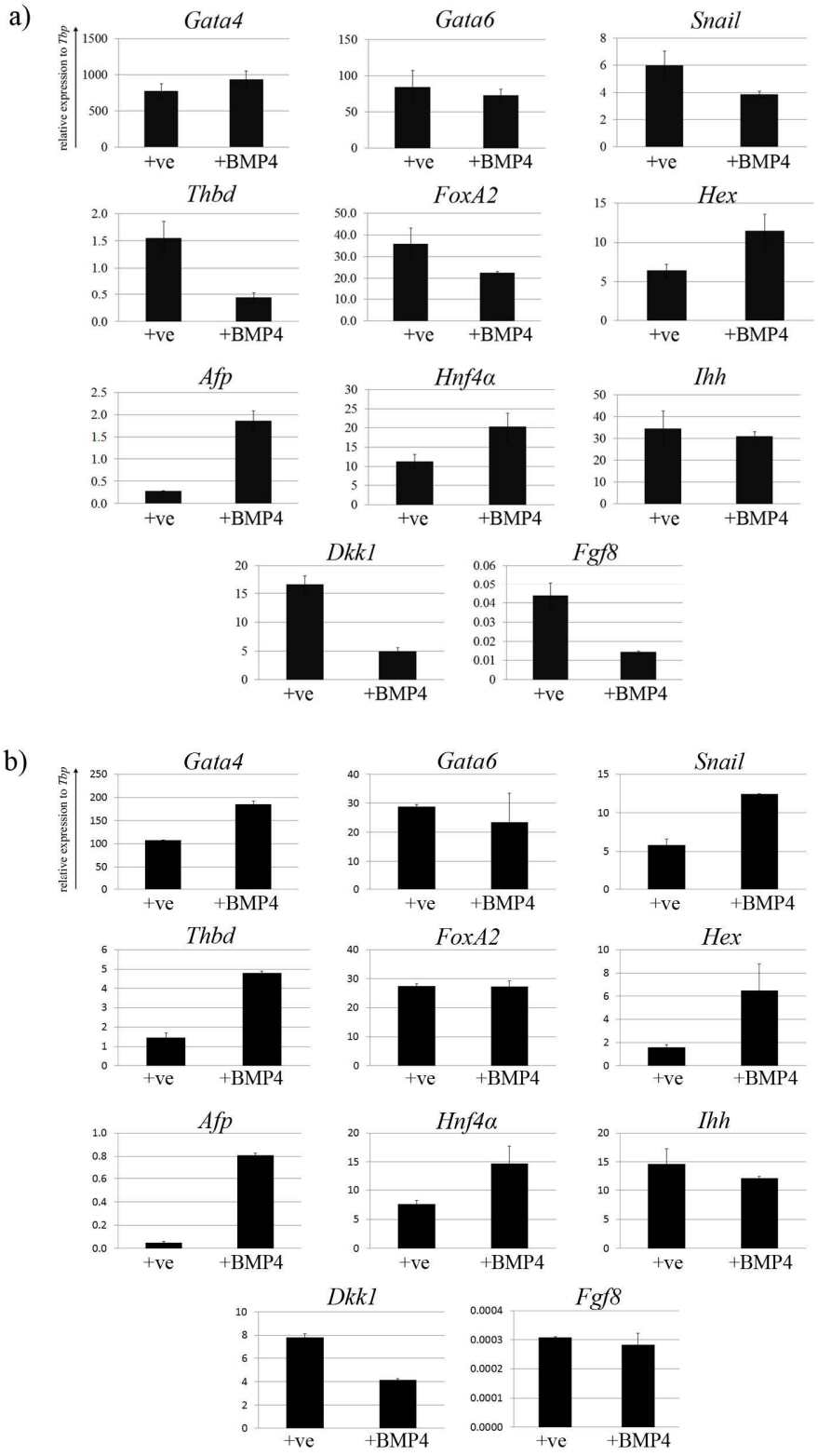

Figure 8.14 BMP4 induces expression of VE associated markers. Cells were cultured on laminin in presence or absence of BMP4 (50ng/ml) for 4 days. **a)** IM8A1-GFP cell line; **b)** XEN1.3 cell line; qRT-PCR results were normalised to *Tbp* expression and represent an average of biological duplicates, error bars are standard deviation between biological duplicates.

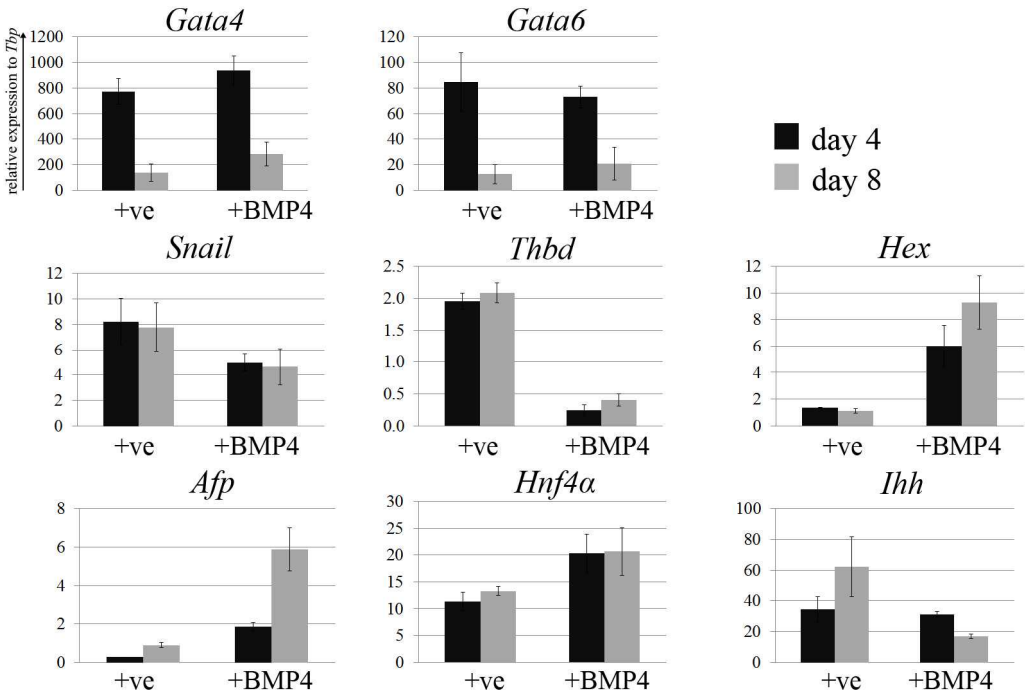

Figure 8.15 BMP4 upregulates expression of VE associated markers. IM8A1-GFP cells were cultured on laminin in presence of absence of BMP4 (50ng/ml) for 4 or 8 days. qRT-PCR results were normalised to *Tbp* expression and represent an average of biological duplicates, error bars are standard deviation between biological duplicates.

8.5.6 BMP4 treatment of selected IM8A1-GFP subclones

Following the observation that BMP4 greatly reduced the proportion of E-CADHERIN-low colonies in clonal assays I decided to test the effect of BMP4 on PE-like subclones.

Like IM8A1-GFP XEN cell line, E11 and G3 subclones were exposed to BMP4 in serum-free conditions on laminin for a total of 4 days. Cells were then immunostained with antibodies against E-CADHERIN and VIMENTIN and scored according to E-CADHERIN expression.

At clonal density in serum-free media on laminin for E11 subclone 60% of colonies are E-CADHERIN-low, 40% mixed and 0% E-CADHERIN-high (Fig. 8.16c). BMP4 has a profound effect on E11 subclone reducing the percentage off E-CADHERIN-low colonies by 4.6 times to only 13%. Almost two-thirds of colonies were E-CADHERIN-mixed and a quarter E-CADHERIN-high (Fig. 8.16c).

For G3 subclone on laminin in N2B27 73% of colonies are E-CADHERIN-low, 24% E-CADHERIN-mixed and only 3% E-CADHERIN-high (Fig. 8.16d). Upon BMP4 treatment the ratio between different types of E-CADHERIN colonies changes. BMP4 lowers the percentage of E-CADHERIN-low colonies to 20%, 47% of colonies are E-CADHERIN-mixed and the ratio of E-CADHERIN-high colonies rises by 11-fold reaching 33%.

To summarize, BMP4 treatment induced a fraction of cells (~25%-30%) in both subclones to adopt epithelial character and express E-CADHERIN. However, the majority of cells responded less robustly to BMP4 and maintained a high expression of VIMENTIN (Fig. 8.16a-b).

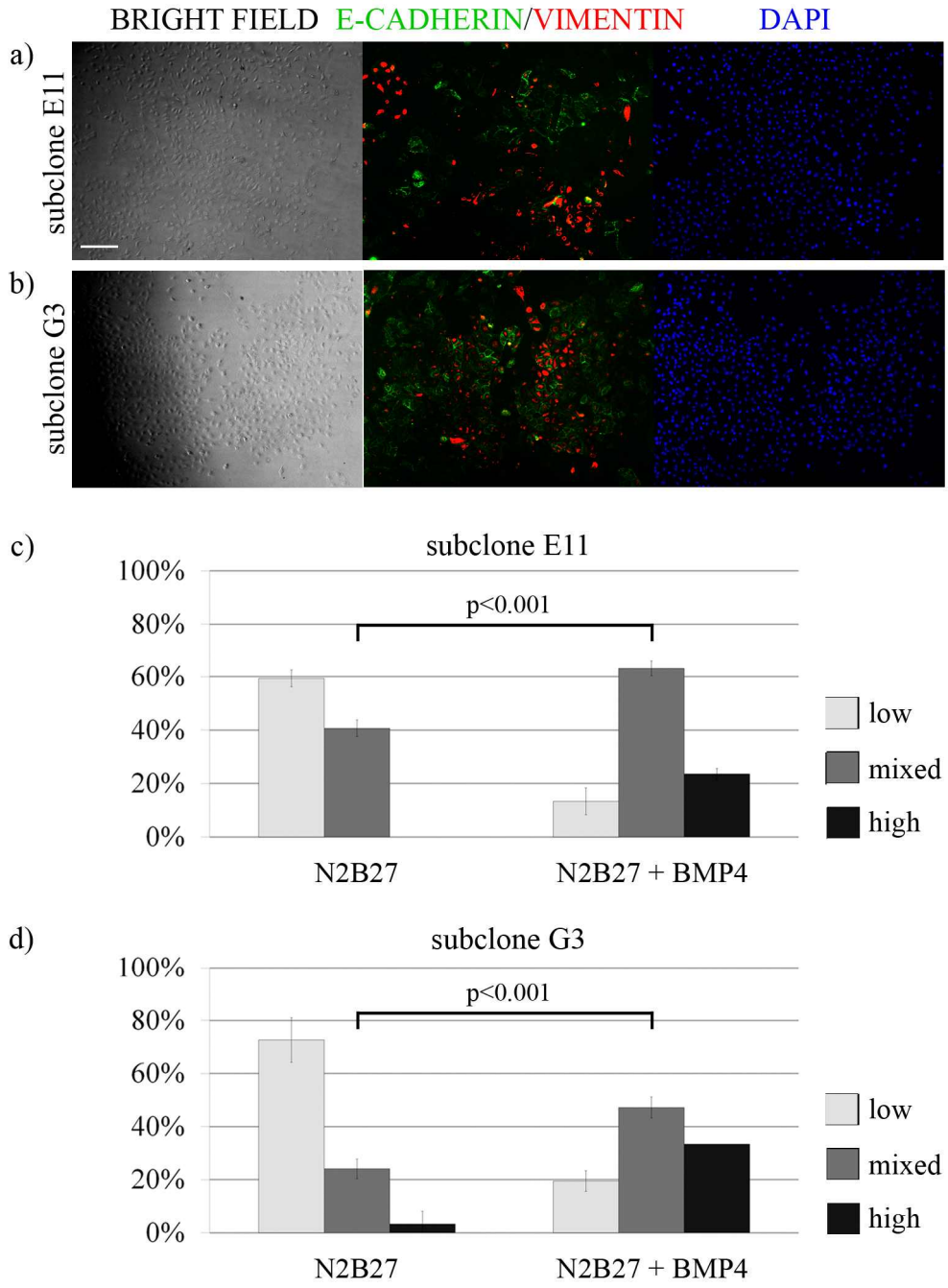

FIGURE 8.16 BMP4 induces E-CADHERIN expression in PE-like subclones. Cells were cultured on laminin in N2B27 in absence or presence of BMP4 (50ng/ml) for 5 days. **a-b)** Immunostaining against E-CADHERIN and VIMENTIN for E11, G3, scale bar: 200µm; **c-d)** Clonal assay for E11 (c) and G3 (d) subclones. ($n_{E11,N2b27}$=27, $n_{E11,N2B27+BMP4}$=38, $p_{\chi 2}$<0.0001; $n_{G3,N2b27}$=27, $n_{G3,N2B27+BMP4}$=36, $p_{\chi 2}$<0.0001).

8.6 Differentiation of XEN cells in presence of Activin A

8.6.1 Expression of E-CADHERIN, PDGFRα and VIMENTIN in Activin A treated XEN cells

Another ligand that was used to promote differentiation of XEN cells was Activin A. Activin A is an equivalent signalling molecule to Nodal, but in contrast to Nodal Activin A acts in a Cripto independent manner (Mesnard et al., 2006). XEN cells do not express Cripto (Kunath et al., 2005).

Similarly to BMP4 treatment, XEN cells were plated at low density on laminin in 1% FBS in N2B27 and the following day media was changed to N2B27 or N2B27 supplemented with Activin A (50ng/ml). On day 2 of treatment cells exposed to Activin A formed small colonies and fewer cells are refractile when compared to N2B27 only conditions (Fig. 8.17a). After 4 days in Activin A XEN cells formed colonies, but these were similar to the untreated cells (Fig. 8.17b).

After 4 days of Activin A treatment cells were fixed and analysed for expression of E-CADHERIN, PDGFRα and VIMENTIN. When XEN cells were cultured in media supplemented with Activin A expression of E-CADHERIN did not change when compared to non-supplemented N2B27 (Fig. 8.17c,d). In N2B27 only and N2B27 + Activin A the majority of cells expressed PDGFRα with just a few cells expressing low levels PDGFRα and E-CADHERIN or E-CADHERIN only (Fig. 8.17c). Expression of VIMENTIN appears to be unaffected by Activin A (Fig. 8.17d). Majority of cells remain VIMENTIN-positive with only a fraction of cells expressing E-CADHERIN.

To conclude, Activin A does not alter expression of E-CADHERIN, PDGFRα and VIMENTIN in XEN cells.

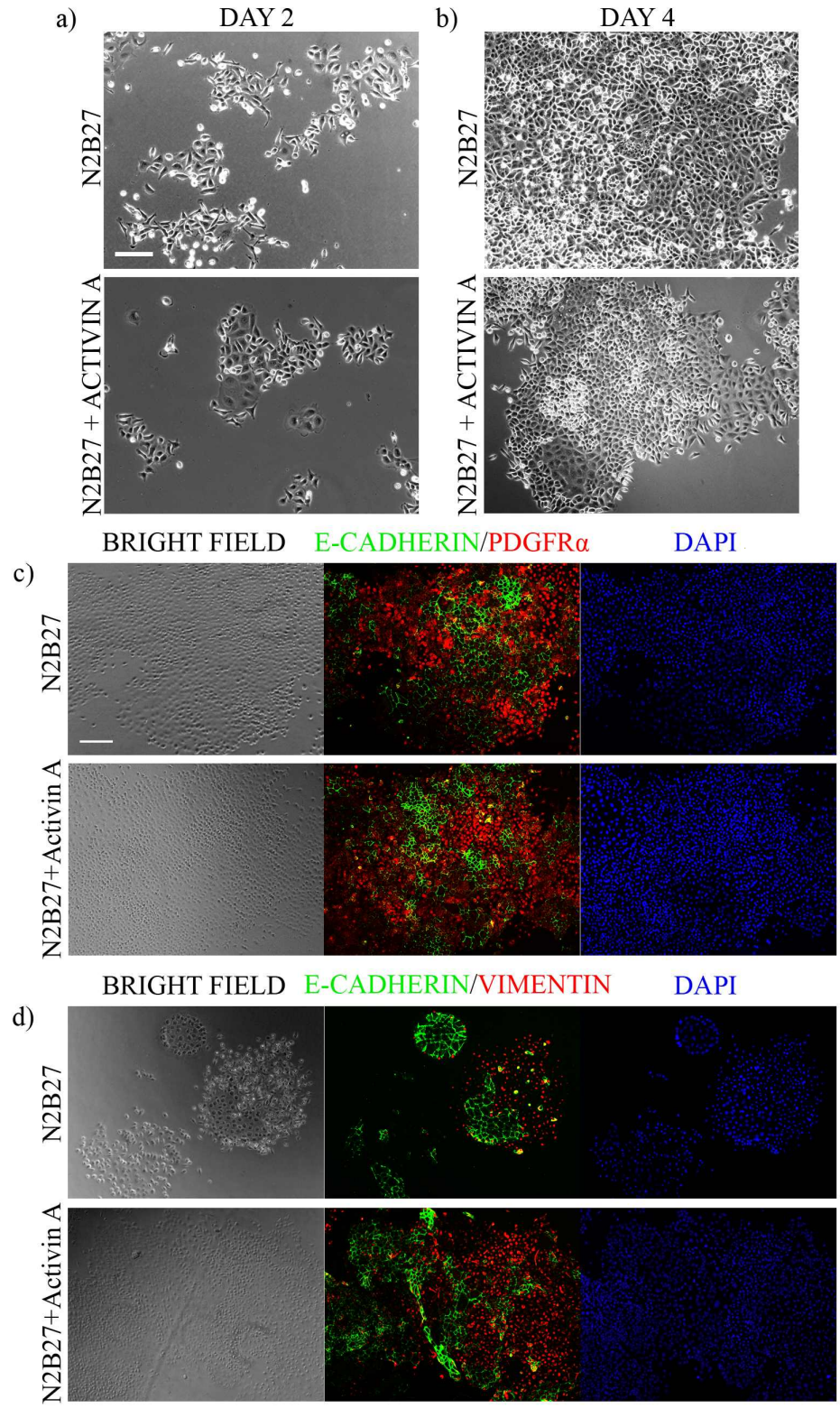

Figure 8.17 Activin A treatment does not alter expression of E-CADHERIN, PDGFRα and VIMENTIN in XEN cells. a-b) Bright field pictures of IM8A1-GFP XEN cells on day 2 (a) and 4 (b) of culture in presence or absence of Activin A (50ng/ml), scale bar: 200µm; **c-d**) Immunostaining of E-CADHERIN and PDGFRα (c) and E-CADHERIN and VIMENTIN (d) of XEN cells cultured on laminin in N2B27 in presence or absence of Activin A on day 5 of culture; scale bar: 200µm.

8.6.2 Clonal assay for IM8A1-GFP XEN cell lines cultured in the presence of Activin A in serum-free media

I next examined whether Activin A has an effect on XEN cells at clonal density. When IM8A1-GFP XEN cells were cultured in serum-free conditions on laminin 64% of colonies were E-CADHERIN-low, 29% E-CADHERIN-mixed and only 7% are E-CADHERIN-high. Supplementing N2B27 with Activin A changes this ratio in favour of E-CADHERIN-mixed and –high colonies. The percentage of cells E-cadherin-high colonies is close to 40%, while 44% of colonies are E-CADHERIN-mixed and 17% E-CADHERIN-low (Fig. 8.18). The differences in the ratio of different types of colonies in these two conditions is statistically significant ($p_{\chi 2}<0.0001$).

Activin A increases the proportion of E-CADHERIN expressing colonies with only a fifth of colonies remaining as E-CADHERIN negative.

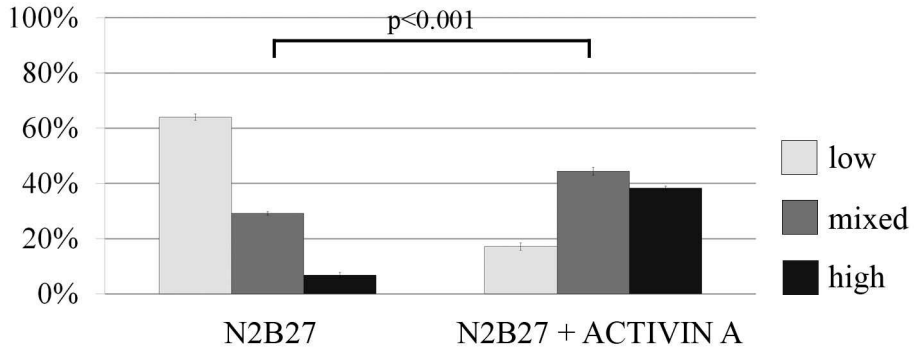

Figure 8.18 Activin A increases ratio of E-CADHERIN positive colonies. IM8A1-GFP XEN cells were cultured on laminin in presence of absence of Activin A (50ng/ml) at clonal density for 5 days; ($n_{N2b27=}89$, $n_{N2b27+ACTIVIN}=99$; $p_{\chi 2}<0.0001$)

8.6.3 qRT-PCR analysis of Activin A treated XEN cells

I subsequently analysed changes in expression of other ExEn markers upon Activin A treatment of IM8A1-GFP and XEN1.3 cell lines by qRT-PCR.

For IM8A1-GFP (Fig. 8.19a) *Gata4* levels remain relatively stable and do not change upon Activin A treatment, whilst *Gata6* is downregulated by Activin A. *Snail* expression is upregulated by Activin A. *Thbd* expression does not change in response to Activin A. *FoxA2* is decreased by Activin A while *Hex* remains at the same level. However, *Afp* expression is 3 times higher in Activin-treated sample. *Hnf4a* follows a similar pattern to *Hex* and its expression is unaltered by Activin A. Yet, *Ihh*, *Dkk1* and *Fgf8* were all downregulated in response to Activin A.

In XEN1.3 (Fig. 8.19b) expression of both *Gata4* and *Gata6* increases in response to Activin A treatment. *Snail* and *Thbd*, are both strongly upregulated in Activin A treated cells. *FoxA2* remains at the same level between Activin A treated and untreated sample. *Hex*, on the other hand, is only modestly upregulated. In contrast to IM8A1-GFP Activin A treatment in serum-free conditions reduced expression of *Afp* in XEN1.3 cells. Activin A has no effect on *Hnf4a* expression which levels were unchanged. Similarly expression of *Dkk1* and *Fgf8* expression remained at the same level. *Ihh* is decreased upon Activin A treatment.

In summary, Activin A has to a certain degree a mixed effect on XEN cells with IM8A1-GFP and XEN1.3 cell lines responding differently to the treatment. However, the common outcome of Activin A presence is upregulation of *Snail*.

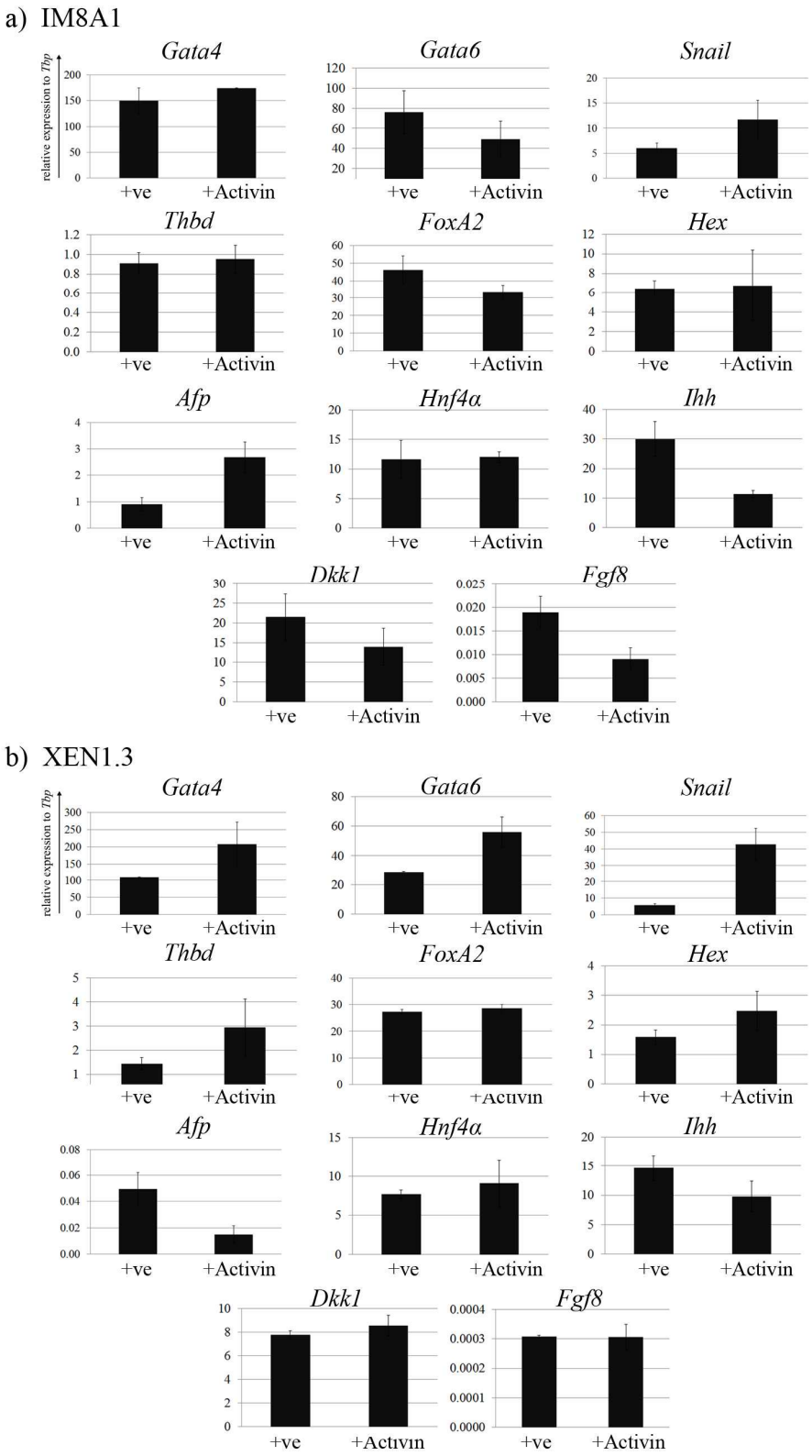

Figure 8.19 Activin A effect on XEN cells. Cells were cultured on laminin in presence of absence of Activin A (50ng/ml) for 4 days. **a)** IM8A1-GFPcell line; **b)** XEN1.3 cell line; qRT-PCR results were normalised to *Tbp* expression and represent an average of biological duplicates, error bars are standard deviation between biological duplicates.

8.7 Combined Bmp4 and Activin A effect on XEN cells

8.7.1 Introduction

The results of BMP4 and Activin A treatments prompted me to test the combined effect of these signalling molecules on XEN cells. Additionally, during in vivo PrE differentiation VE is exposed to simultaneous presence of Nodal and BMP4 and once emVE is formed BMP signalling is excluded from distal tip allowing for DVE specification (Mesnard et al., 2006; Yamamoto et al., 2009). To test this I designed two different protocols of combined treatment. The first one is when the medium is supplemented with both BMP4 and Activin A at the same time. In the other case Activin A follows BMP4 treatment.

8.7.2 Expression of E-CADHERIN, PDGFRα and VIMENTIN in simultaneously BMP4 and Activin A treated XEN cells

XEN cells were plated at low density and exposed to BMP4+Activin A for 4 days. After that cells were fixed and the expression of E-CADHERIN, PDGFRα and VIMENTIN was analysed.

In N2B27 only a minority of cells is E-CADHERIN positive, whilst most of cells express PDGFRα or VIMENTIN (Fig. 8.20a, c). When XEN cells were cultured in media supplemented with BMP4 and Activin A they upregulated E-CADHERIN and downregulated PDGFRα or VIMENTIN when compared to non-supplemented N2B27 (Fig. 8.20b, d).

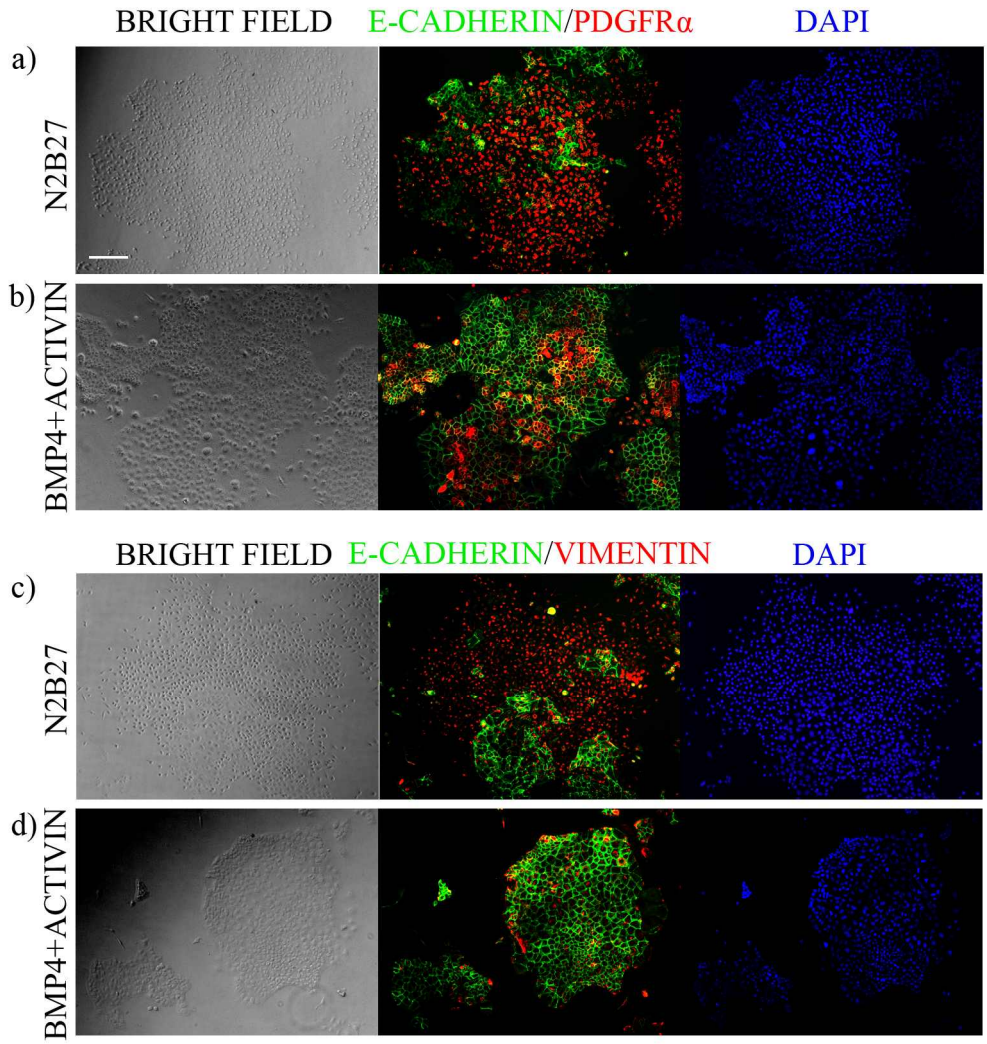

Figure 8.20 Combined BMP4 and Activin A effect on XEN cells. Immunostaining of **a-b**) E-CADHERIN and PDGFRα and **c-d**) E-CADHERIN and VIMENTIN of XEN1.3 XEN cells cultured on laminin in N2B27 or N2B27 supplemented with BMP4 and Activin (BMP4+Activin) for 4 days of culture; scale bar: 200μm.

8.7.3 qRT-PCR analysis of BMP4 and Activin A treated XEN cells

I then performed qRT-PCR analysis (Fig. 8.21). I compared the combined BMP4 and Activin A against BMP4 or Activin A only treatments. Similarly, as for the immunostaining experiment, cells for qRT-PCR analysis were cultured for 4 days in BMP4, Activin A or BMP4+Activin.

For IM8A1-GFP (Fig. 8.21a) *Gata4* levels varies only slightly between the cells in N2B27 or supplemented N2B27. *Gata6* expression is lower in the cells exposed to BMP4, but the levels of *Gata6* are comparable between control sample (N2B27 only) and N2B27+Activin A. I only observed reduced expression of *Snail*

in cells treated with BMP4 only. The levels of *Snail* are unchanged in the presence of BMP4 and Activin A, but are upregulated in Activin A only conditions. *Thbd* is downregulated in all of the treatment, though it's expressed at lowest levels in BMP4 only sample. *FoxA2* levels are decreased in BMP4, unaffected by Activin A and upregulated in BMP4+Activin A conditions. *Hex* clearly responds to the presence of BMP4 (BMP4 only or BMP4+Activin A) by increased expression. In Activin A samples *Hex* is expressed at similar levels as in control. *Afp* expression is the highest in BMP4 or Activin A only samples and is moderately upregulated in BMP4 and Activin A combined treatment. *Hnf4a* levels remain at similar levels between all the samples, but BMP4 followed by Activin A where modest downregulation is observed. *Ihh* is moderately downregulated in BMP4 sample, but its expression is halved in the presence of Activin A with or without BMP4. *Dkk1* and *Fgf8* are all downregulated in the treated samples, though least in the Activin A only conditions.

XEN1.3 cells (Fig. 8.21b) upregulate *Gata4* in all of the treatments. *Gata6* expression is lower in the cells exposed to BMP4, but the levels of *Gata6* are higher in condition where Activin A was present. Similarly, *Snail* expression is upregulated in all of the treatment, albeit the upregulation is the highest in presence of Activin A. *Thbd* is upregulated in all of the treatments, though it's expressed at highest level in BMP4+Activin A sample. *FoxA2* levels are unchanged between control and ligand treated samples. *Hex* expression is increased in presence of BMP4, but remains at the same level in presence of Activin A. *Afp* expression is the highest in BMP4 only samples and is moderately upregulated in BMP4 and Activin A combined treatment. *Hnf4a* and *Ihh* levels are upregulated in the presence of BMP4 only. *Dkk1* is downregulated in response to BMP4. And finally last but not least, expression of *Fgf8* is constant and very low between samples.

Combining BMP4 and Activin A treatment once again underlies the differences in response to ligands between XEN1.3 and IM8A1-GFP cell lines. However, in spite of differences between these cell lines it is clear that Activin A, even in the presence of BMP4, upregulates expression of *Snail*. Interestingly, addition of Activin A to BMP4 attenuates upregulation of *Afp*.

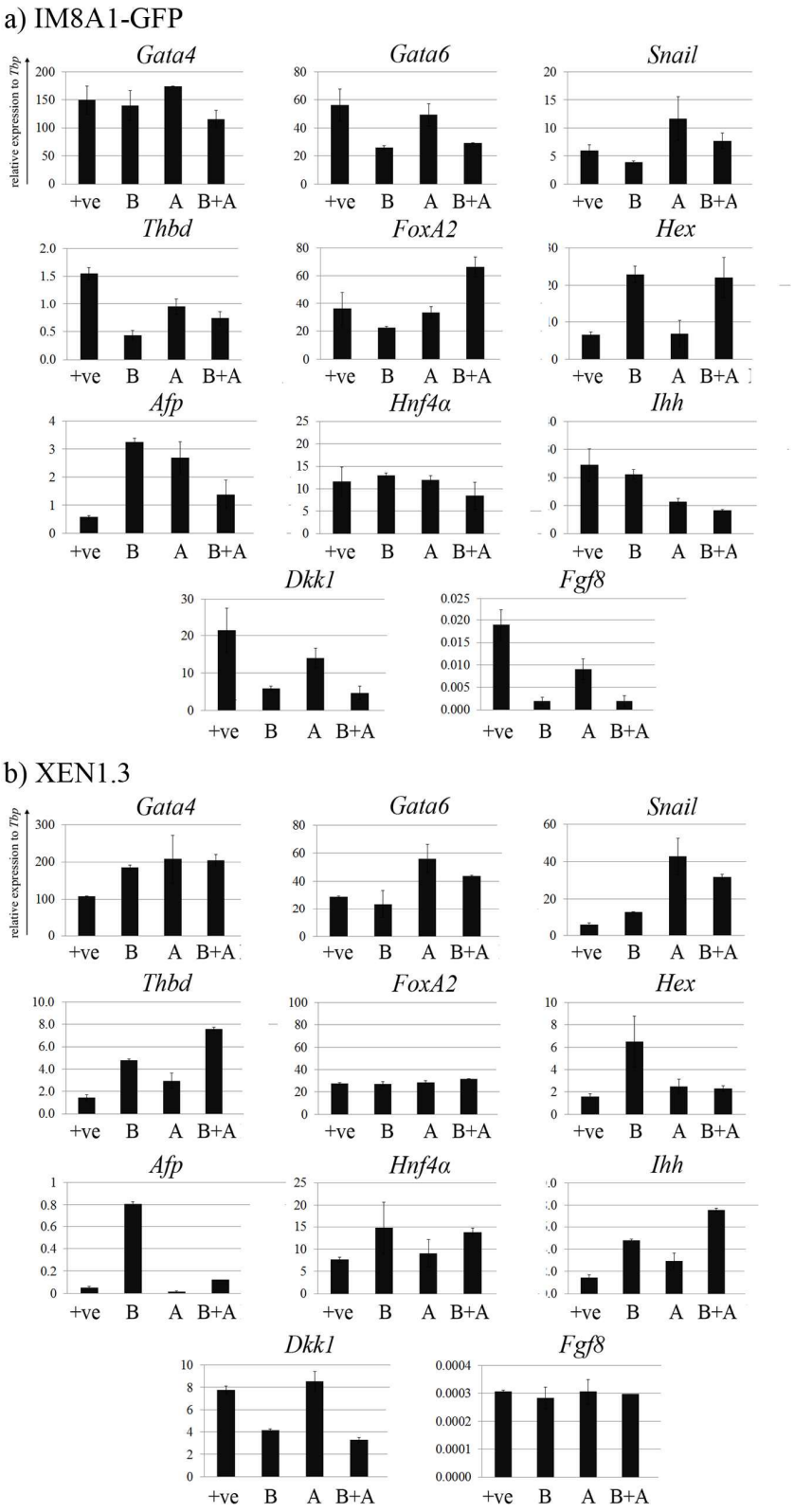

Figure 8.21 BMP4 and Activin A effect on XEN cells. Cells were cultured on laminin in the presence of DMSO (vehicle) alone (+ve), Activin A (50ng/ml; A), BMP4 (50ng/ml; B), BMP4+Activin (B+A); **a**) IM8A1-GFP, **b**) XEN1.3 cell line. The qRT-PCR results were normalised to *Tbp* expression and represent an average of biological duplicates, error bars are standard deviations of biological duplicates.

8.7.4 Sequential BMP4 and Activin A treatment

Seeing that combined BMP4 and Activin A treatment did not enhance VE differentiation of XEN cells I subsequently treated cells with BMP4 and then with Activin A.

Cells were plated at low density and after initial overnight culture in N2B27+1%FBS the media was changed to N2B27, N2B27+BMP4 and N2B27+Activin A. After 4 days in some of the wells BMP4 was replaced with Activin A for another 2 days. Following this qRT-PCR analysis was performed (Fig. 8.22).

Expression of *Gata4* is decreased by BMP4 only, unchanged by Activin A only and slightly upregulated by BMP4 followed by Activin A. *Gata6* is downregulated by BMP4 only and Activin A only, but the expression is at the similar level between combined BMP4 and Activin A treated and control sample. *Snail* is expressed at similar levels between control, BMP4 only and Activin A only samples, however Snail is remarkably upregulated by combined BMP4 and Activin A. *Hex* is upregulated in all of the treatments, with BMP4 alone inducing highest (8-fold) upregulation. *Afp* levels are strongly increased when BMP4 was present. The fold change between N2B27 and N2B27+BMP4 equals 100. And there is another 10-fold increase between N2B27+BMP4 and N2B27+BMP4→Activin A. *Hnf4a* expression is upregulated (2.5-fold change) in the presence of BMP4 with or without Activin A and by less than 2-fold in Activin A only sample. *Dkk1* is downregulated in all of the treatment, however the lowest downregulation (5-fold change) is observed in BMP4 only conditions. *Fgf8* is upregulated in the combined BMP4 and Activin A treatment, albeit the levels of expression remain at very low level between the samples. *Fgf5* is outstandingly upregulated in Activin A in response to Activin A only treatment.

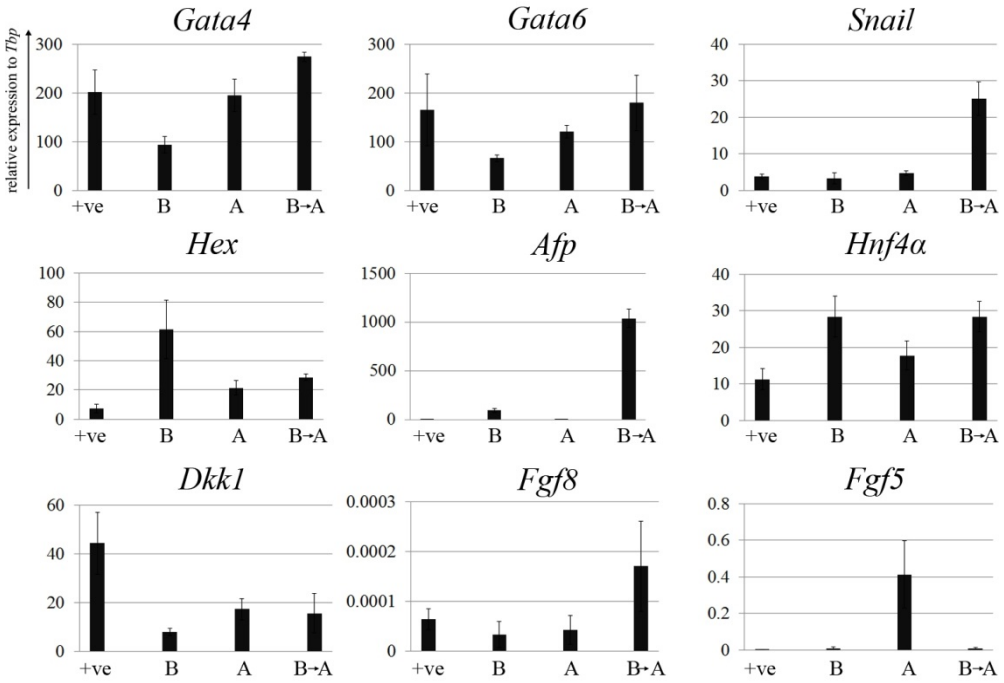

Figure 8.22 BMP4 and Activin A effect on IM8A1-GFP XEN cells. Cells were cultured on laminin in N2B27 only (+ve), or BMP4 (B), or Activin A (A) for 6 days, or BMP4 for 4 days followed by Activin A (B→A) for another 2 days. The qRT-PCR results were normalised to *Tbp* expression and represent an average of biological duplicates, error bars are standard deviation between biological duplicates.

The high *Afp* upregulation in qRT-PCR analysis prompted me to analyse the cells for the expression of AFP protein. Cell cultured in N2B27 only and N2B27 + Activin A do not express AFP (Fig. 8.23a,c). In N2B27 supplemented with BMP4 just a few cells upregulate AFP up to the levels detectable by an antibody (Fig. 8.23b). In N2B27+BMP4→Activin A highest levels of AFP were observed, however it is still only a portion of XEN cells that upregulates AFP (Fig. 8.23d).

Replacement of BMP4 with Activin A after 4 days very robustly upregulates expression of *Afp*. This has not been observed in continuous presence of Activin A (Fig. 8.18 and Fig. 8.22) or in BMP4 only treatments (Fig. 8.15 and Fig. 8.22). Basing on Afp expression sequential BMP4 and Activin A treatment promotes most efficient VE differentiation of XEN cells.

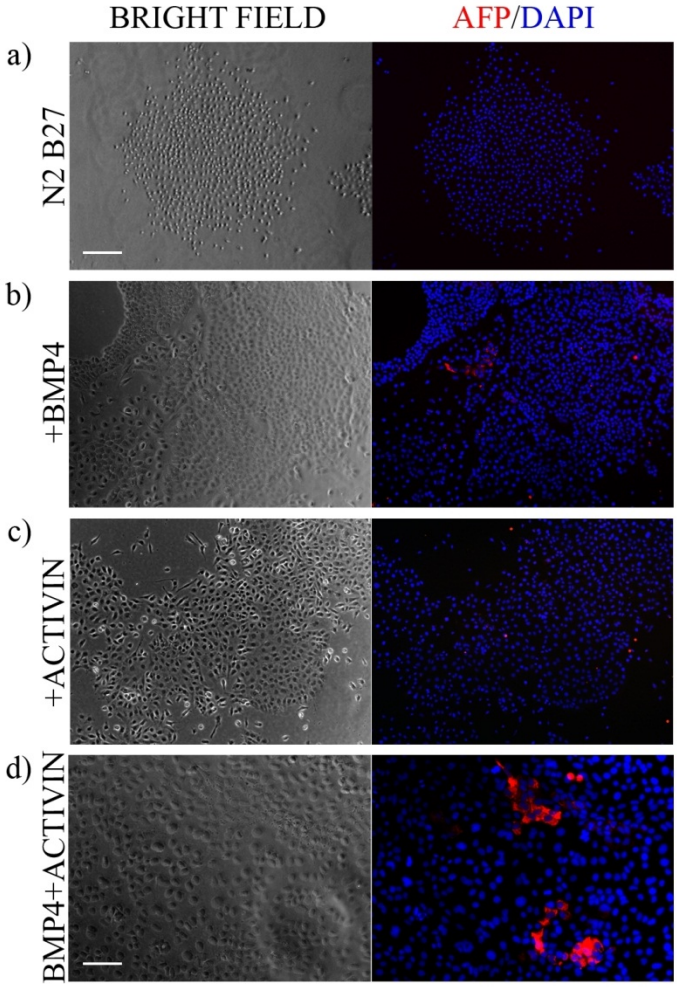

Figure 8.23 BMP4 and Activin A effect on the expression of AFP in XEN cells. Immunostaining of AFP inIM8A1-GFP XEN cells cultured on laminin in (**a**) N2B27 or (**b**) N2B27 supplemented with BMP4, or (**c**) Activin A for 6 days, or (**d**) N2B27+BMP4 for 4 days followed by N2B27+Activin A for another 2 days ; Scale bar: 200µm (a-c), 100µm (d).

8.8 Inhibition of Erk1/2, BMP and Activin A pathways

8.8.1 Introduction

To complement laminin, BMP4, Activin and driven differentiation of XEN cells and to further understand the effect of these factors on XEN cells I used well characterized inhibitors of particular signalling pathways.

8.8.2 Inhibition of Erk1/2 pathway

Laminin is known to activate the Erk1/2 signalling pathway (Ahmed et al., 2005; Hood and Cheresh, 2002; Mruthyunjaya et al., 2010). I therefore examined the

effect of inhibition of this pathway on XEN cell differentiation. I chose PD0325901 (PD03) Mek (Erk kinase) inhibitor (Thompson and Lyons, 2005). Firstly, I confirmed the specificity of PD03 in XEN cells by measuring expression of *Egr1*, an immediate-early gene induced by the Mek-Erk pathway. *Egr1* was induced by FBS, but not by FGF2 (Fig. 8.24a). Upregulation of Egr1 was attenuated by addition of PD03 (Fig. 8.24a)

Following this XEN cells either on gelatin or laminin were treated with PD03 for 4 days. After that cells were counted and compared to control. Either on gelatin or laminin PD03 reduced the number of cells by half when related to DMSO control sample (Fig. 8.24b). Of note, interestingly there were 30% less cells on laminin than on gelatin (Fig. 8.24b).

I then examined expression of E-CADHERIN in PD03 treated cells. On gelatin a few cells are E-CADHERIN positive, but there are no E-CADHERIN expressing cells in the cells cultured in the presence of PD03 (Fig. 8.24c-d). PD03 also inhibited expression of E-CADHERIN in cells cultured on laminin (Fig. 8.24e-f).

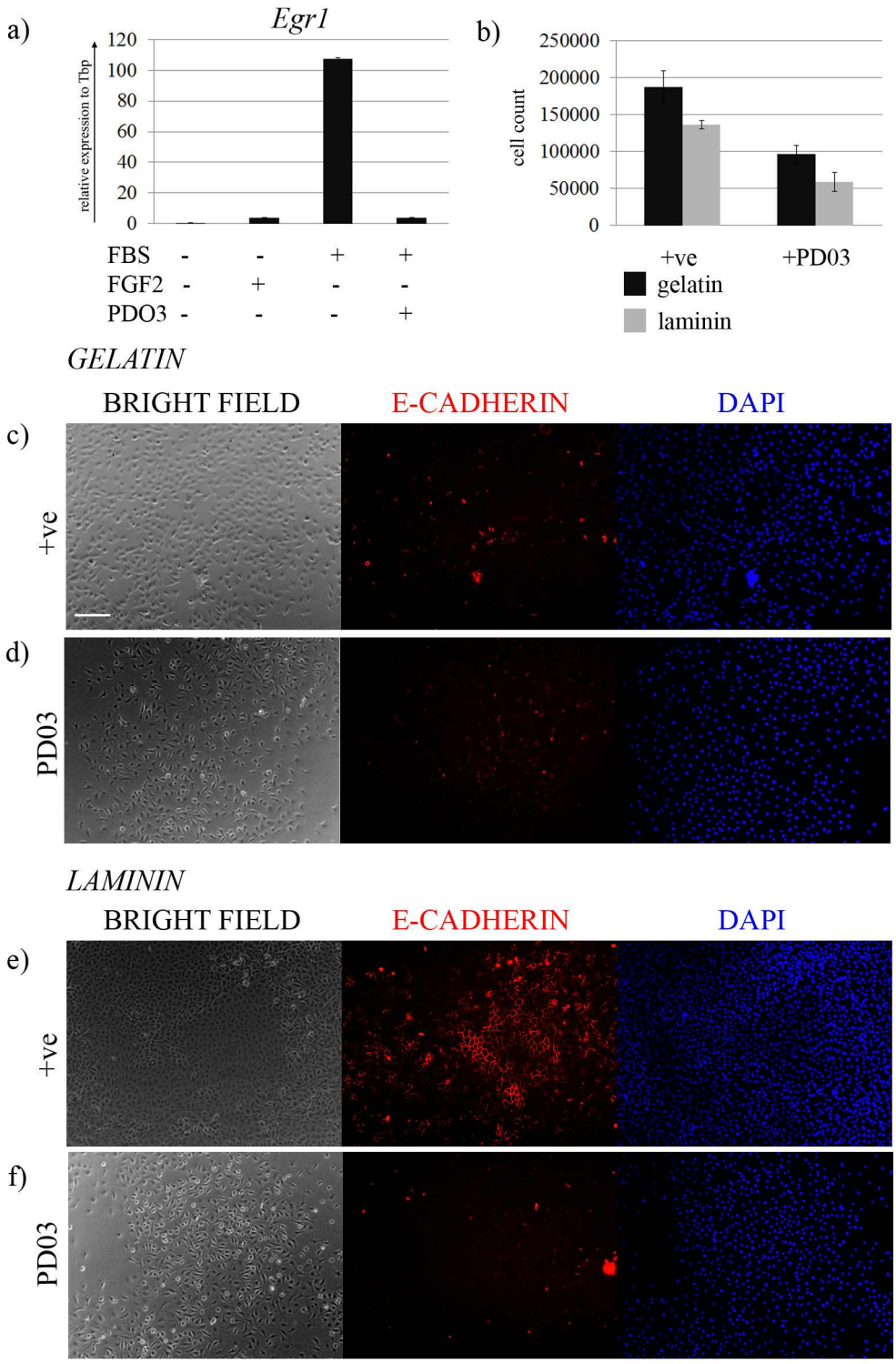

Figure 8.24 PD03, Mek inhibitor, suppressed expression of E-CADHERIN in XEN cells. a) qRT-PCR analysis of expression of *Egr1* in response to FBS in the presence of PD0325901 (PD03) in XEN cells. **b**) IM8A1-GFP cell count of cells cultured either on gelatin or laminin in presence of DMSO (+ve) or PD03 on day 4 of treatment. **c–f**) Immunostaining of E-CADHERIN in IM8A1-GFP XEN cells cultured in GMEM+10% FBS on gelatin (c-d) or laminin (e-f) in the presence of DMSO (+ve) (c, e) or PD03 (d, f) for 4 days.

After 4 days of PD03 treatment I examined expression of ExEn markers (Fig. 8.25). Presence of PD03 increases expression of *Gata4* and *Gata6*. PE markers, *Snail* and *Thbd*, are also upregulated by PD03. Conversely, VE markers such as *Hex*, *Afp*, *Hnf4α* and *Ihh* are downregulated.

Inhibition of MEK, possible integrin effector, results in reduced expression of VE markers and upregulation of PE markers.

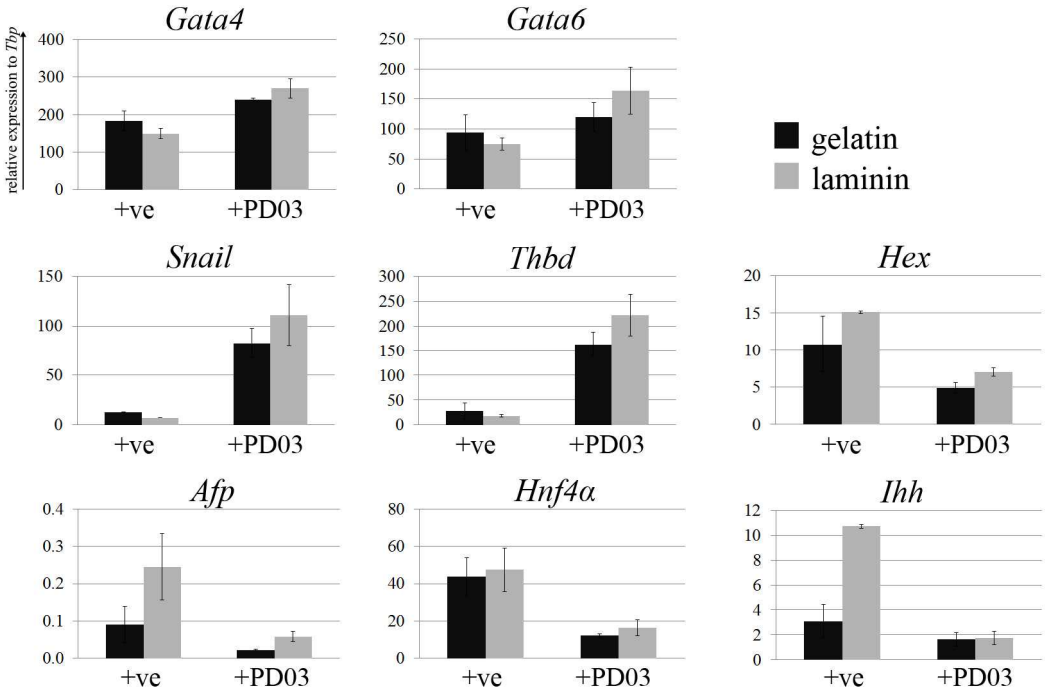

Figure 8.25 Inhibition of Erk signalling pathway increases expression of PE associated markers and decreases expression of VE markers. IM8A1-GFP cells were cultured on gelatin or laminin in presence of DMSO (+ve) or PD03 for 4 days. qRT-PCR results were normalised to *Tbp* expression and represent an average of biological duplicates, error bars are standard deviation between biological duplicates.

8.8.3 Inhibition of BMP signalling

BMP4 has an outstanding effect on XEN cells by inducing expression of E-CADHERIN, *Hex* and *Afp* and thus driving VE-like differentiation of XEN cells. The major transducers of BMP4 signalling are Smad1/5/8 proteins. To further investigate the role of BMP4I used Dorsomorphin (DM), Bmpr1a inhibitor. I started by validating DM specificity. DM successfully blocked BMP-mediated *Id3* induction (Fig. 8.26a).

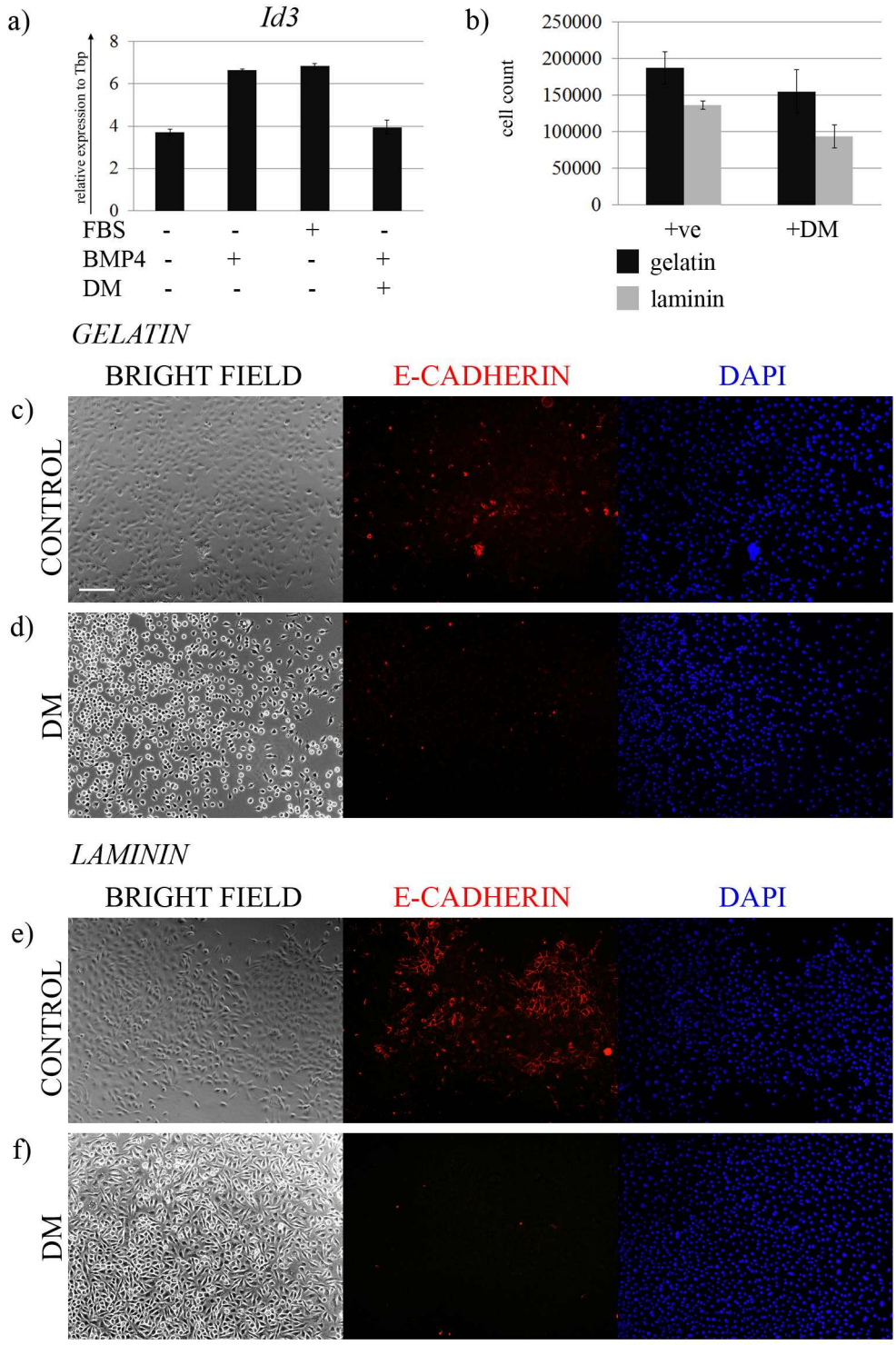

Figure 8.26 Dorsomorphin, Bmpr1a inhibitor, suppressed expression of E-CADHERIN in XEN cells. a) qRT-PCR analysis of Id3 induction in response to BMP4 or FBS in the presence of DMSO (+ve) or Dorsomorphin (DM). **b** IM8A1-GFP cell count of cells cultured either on gelatin or laminin in presence of DMSO (+ve) or DM on day 4 of treatment. **c**–**f**) Immunostaining of E-CADHERIN in IM8A1-GFP XEN cells cultured in GMEM+10% FBS on gelatin (c-d) or laminin (e-f) in the presence of DMSO (c, e; control) or DM (d, f) for 4 days.

After 4 days treatment DM reduces the number of cells on gelatin by 20% and by 30% on laminin when compared to control conditions (Fig. 8.26b). When XEN cells are cultured on gelatin sporadically they express E-CADHERIN, but in the presence of DM cells even low expression E-CADHERIN is inhibited (Fig. 8.26c-d). On laminin XEN cells become more epithelial and upregulate expression of E-CADHERIN, however they fail to do so in the presence of DM and remain mesenchymal (Fig. 8.26e-f). Moreover, qRT-PCR analysis showed that expression of *Gata4* is slightly upregulated by DM (Fig. 8.27). DM also increased expression of *Gata6*. PE markers, *Snail* and *Thbd*, are very strongly upregulated (10-20 fold increase) in the presence of DM. And correspondingly VE markers, such as *Hex*, *Afp*, *Hnf4α*, and *Ihh* are downregulated.

Similarly to PD03, DM suppressed expression of E-CADHERIN and VE markers, while upregulating *Snail* and *Thbd*, PE markers.

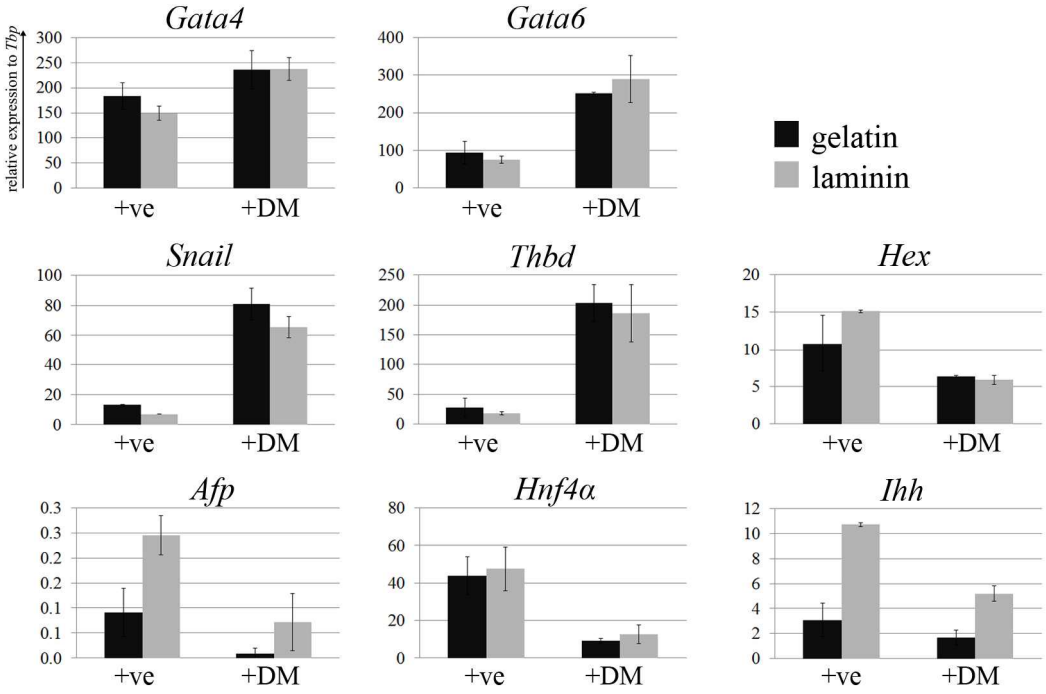

Figure 8.27 Inhibition of BMP4 signalling pathway increases expression of PE associated markers and decreases expression of VE markers. IM8A1-GFP cells were cultured either on gelatin or laminin in presence of DMSO (+ve) or DM for 4 days. qRT-PCR results were normalised to *Tbp* expression and represent an average of biological duplicates, error bars are standard deviation between biological duplicates.

8.8.4 Inhibition of Activin A signalling

Even though Activin A on its own did not drive efficient VE-like differentiation of XEN cells, I nevertheless decided to test the effect of inhibition of Activin A signalling. I examined the effect of Activin type 1 receptors (Alk2, Alk4 or Alk7) inhibitor SB431542 (SB43).

First, I confirmed the specificity of SB43 in XEN cells by measuring induction of *Lefty1*, an immediate-early gene. Upregulation of *Lefty1* was reduced by addition of SB43 (Fig. 8.28a)

Following this XEN cells either on gelatin or laminin were cultured with SB43 for 4 days and then cells were counted and compared to control. On gelatin SB43 reduced the number of cells by a quarter, whereas on laminin in the presence of SB43 the number of cells is doubled when related to DMSO control sample (Fig. 8.28b). Addition of SB43 does not change expression of E-CADHERIN in XEN cells either on gelatin or laminin (Fig. 8.28c-f). SB43 also does not alter expression of *Gata4* or *Gata6* in XEN cells (Fig. 8.29). *Snail* expression is upregulated by SB43, but *Thbd* is downregulated by SB43 on gelatin and unchanged on laminin. *Hex* decreases slightly in the presence of SB43. Interestingly, *Afp* is upregulated by SB43 on laminin by 3-fold, but is unchanged on gelatin. *Hnf4α* is unchanged on laminin in presence of SB43, and is downregulated on gelatin. And finally *Ihh* is upregulated by SB43 on gelatin and is unaffected by SB43 on laminin.

In contrast to DM or PD03, inhibition of Smad2/3 signalling does not affect expression of E-CADHERIN and most of the analysed ExEn markers.

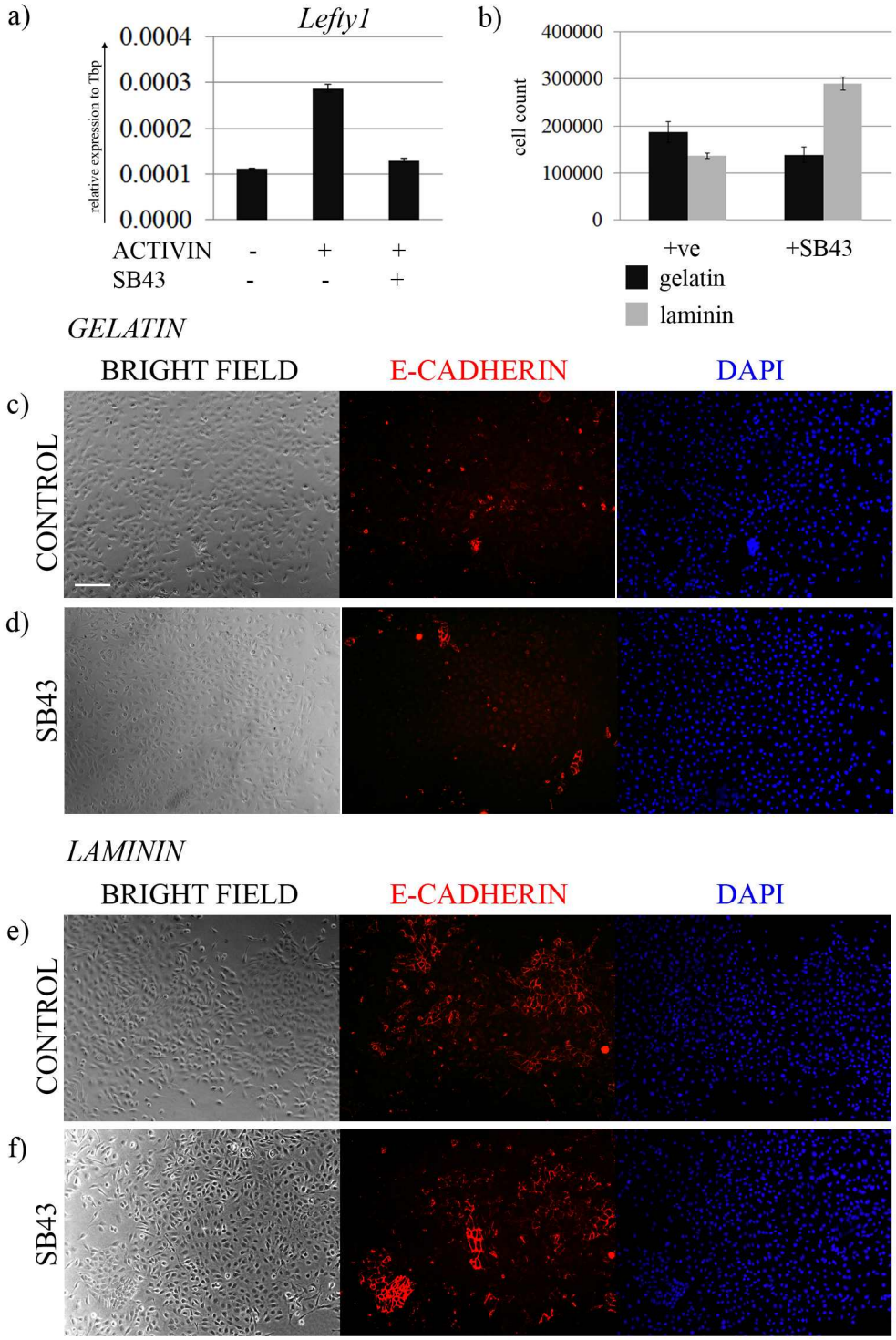

Figure 8.28 Inhibition of Activin A signalling does not alter E-CADHERIN expression in XEN cells. a) qRT-PCR analysis of Lefty 1 induction in response to BMP4 in the presence or absence of SB431542 (SB43); **b**) IM8A1-GFP cell count of cells cultured either on gelatin or laminin in presence of DMSO (+ve) or SB43 on day 4 of treatment; **c**–**f**) Immunostaining of E-CADHERIN in IM8A1-GFP XEN cells cultured in GMEM+10% FBS on gelatin (c-d, control) or laminin (e-f) in the presence of DMSO (c, e, control) or SB43 (d, f) for 4 days.

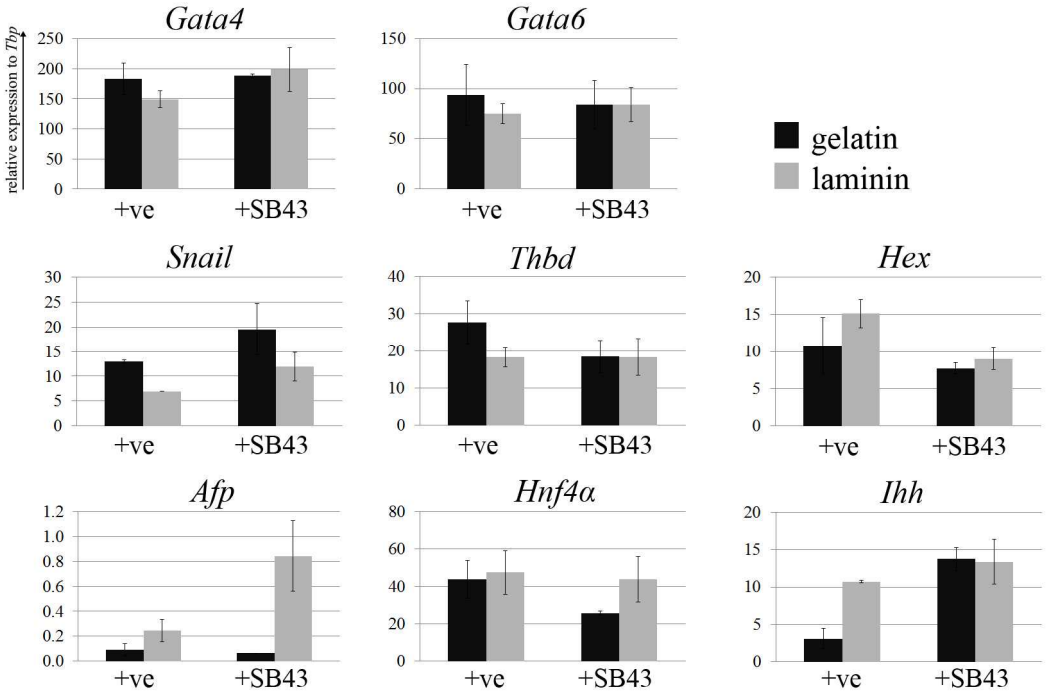

Figure 8.29 The effect of Activin A signalling pathway inhibition on the expression of various ExEn markers in XEN cells. IM8A1-GFP cells were cultured either on gelatin or laminin in presence of DMSO (+ve) or SB43 for 4 days. qRT-PCR results were normalised to *Tbp* expression and represent an average of biological duplicates, error bars are standard deviation between biological duplicates.

8.8.5 Dual inhibition of Erk1/2 and BMP4 signalling in XEN cells

Both Erk1/2 andSmad1/5/8 pathways are essential for epithelialisation of XEN cells and promoting VE phenotype (Fig. 8.24-27). I decided to expand the inhibition analysis by simultaneous PD03 and DM treatment.

After 4 days of culture in PD03 and DM on laminin I performed qRT-PCR analysis (Fig. 8.30). I compared the dual inhibition of Erk1/2 and Smad1/5/8 signalling against single inhibitor treatment or control conditions. Combined treatment with PD03 and DM even further increases expression of *Gata4* and *Gata6*. The upregulation of PE markers, *Snail* is reinforced by dual inhibition and DM induces higher expression of *Snail* than PD03 does. On the other hand PD03 is driving higher upregulation of *Thbd* than DM is and the levels *Thbd* after dual inhibitor treatment are similar to those induced by PD03 only. Both inhibitors have similar downregulating effect on *Hex* and *Afp*. The level of expression of *Hex* and *Afp* are similar between single and double inhibitor treatments. Dual inhibition results in further reduction of expression of *Hnf4α*are *Ihh*.

Collectively these data demonstrate that the effect of inhibitors is additive and dual inhibition reinforces downregulation of VE markers and enhances upregulation of PE markers.

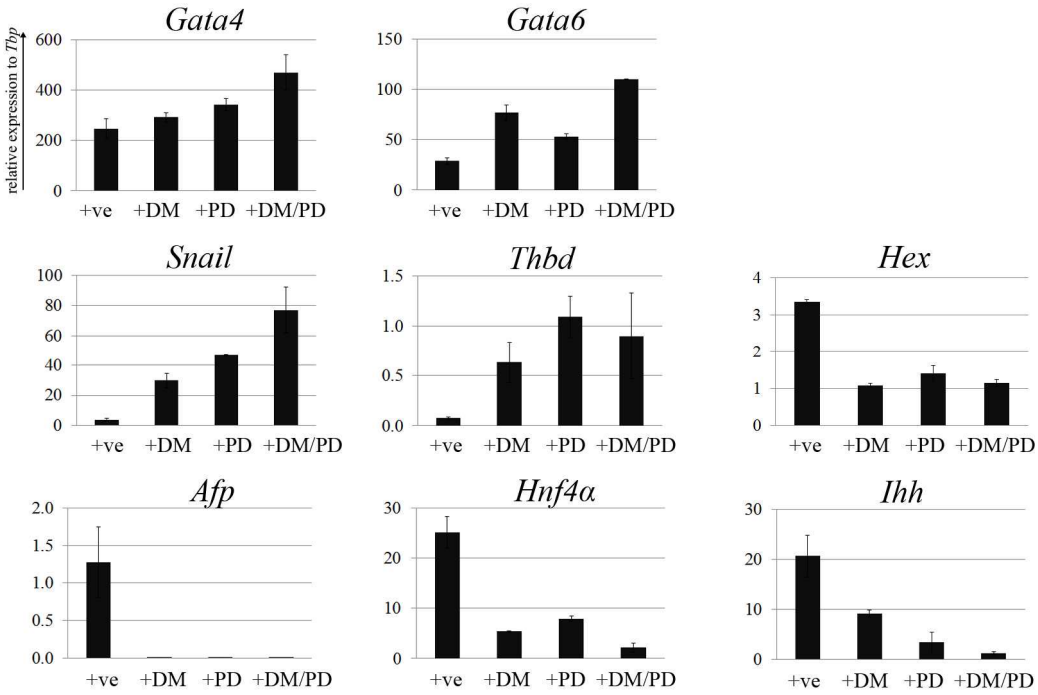

Figure 8.30 Dual inhibition of Erk1/2 and Smad1/5/8 signalling pathways increases expression of PE associated markers and decreases expression of VE markers. IM8A1-GFP cells were cultured on laminin in presence of DMSO (+ve) or DM or PD03 or DM+PD03 for 4 days. qRT-PCR results were normalised to *Tbp* expression and represent an average of biological duplicates, error bars are standard deviation between biological duplicates.

8.8.6 BMP4 differentiation in the presence of DM and PD03

Previous inhibitor experiments showed that blocking either Erk1/2 or Smad1/5/8 pathways results in parietal-like endoderm differentiation of XEN cells. To further understand the relationship between these two signalling pathways it was conceivable to add inhibitors during BMP4 treatment.

Cells were cultured on laminin in N2B27 supplemented with BMP4 in presence or absence of inhibitors. The treatment was extended up to 7 days. Presence of inhibitors, especially of PD03, severely reduced cell growth (Fig. 8.31b-d). Addition of DM only results in the reduction of epithelial morphology and appearance of highly refractile cells (Fig. 8.31b). Similarly to DM cells exposed to PD03 also change their morphology (Fig. 8.31c). Cells still grow in colonies, but

these colonies are no longer as tight as in BMP4 only. Cell in presence of both DM and PD03 during BMP4 treatment are most affected and lose completely their epithelial character (Fig. 8.31d).

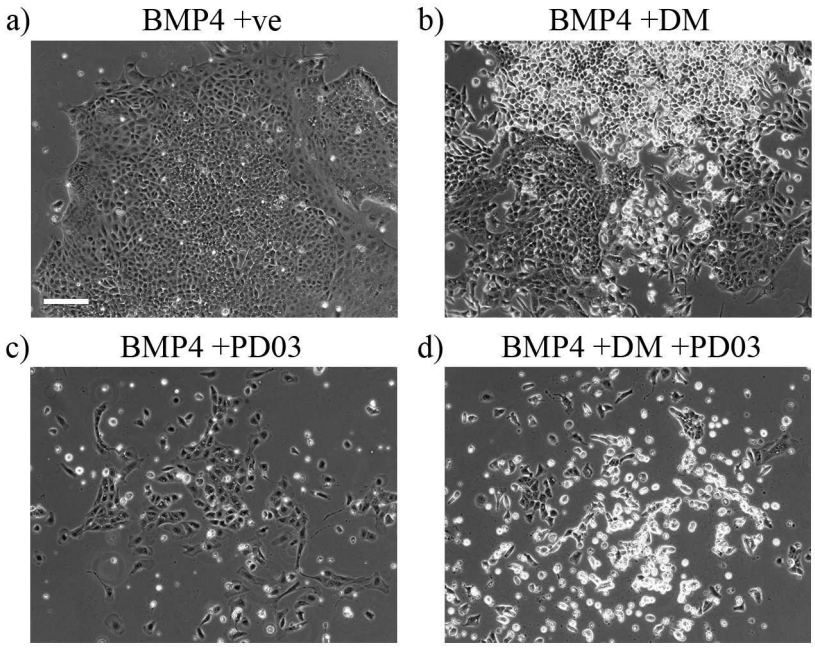

Figure 8.31 Inhibition of Erk1/2 and BMP4 signalling pathway distorts BMP4 and laminin driven VE-like differentiation of XEN cells. Bright field images of IM8A1-GFP XEN cells cultured on laminin in N2B27+BMP4 (+ve) (**a**) supplemented with DM (**b**), PD03 (**c**) or DM and PD03 (**d**) on day 7 of culture ; scale bar: 200µm.

Following 7 days of culture on laminin in N2B27+BMP4 in presence of inhibitors I analysed expression of ExEn markers (Fig. 8.32). *Gata4* and *Gata6*are upregulated in the presence of inhibitors. In the presence of PD03 it is a moderate upregulation: 1.5-fold for *Gata4* and 2-fold for *Gata6*. When DM was present (either on its own or together with PD03) *Gata4* was increased by 5-fold and *Gata6* by 3-fold. PE markers, *Snail* and *Thbd*, are both upregulated by inhibitors. However, the upregulation of *Snail* and *Thbd* is modest by PD03 only (2- and 3-fold, respectively). DM increased the expression of *Snail* and *Thbd* by 12-fold and 9-fold, respectively. Expression of *Afp* is reduced to lower level by DM (12% of BMP4 only) than by PD03 (50% of BMP4 only). Surprisingly, *Hnf4α* is slightly upregulated in the presence of PD03. The expression of *Hex* is downregulated in presence of inhibitors to comparable levels similar levels (40%, 50%, 60% of BMP4 only levels for +DM, +PD03 and +DM+PD03 respectively).

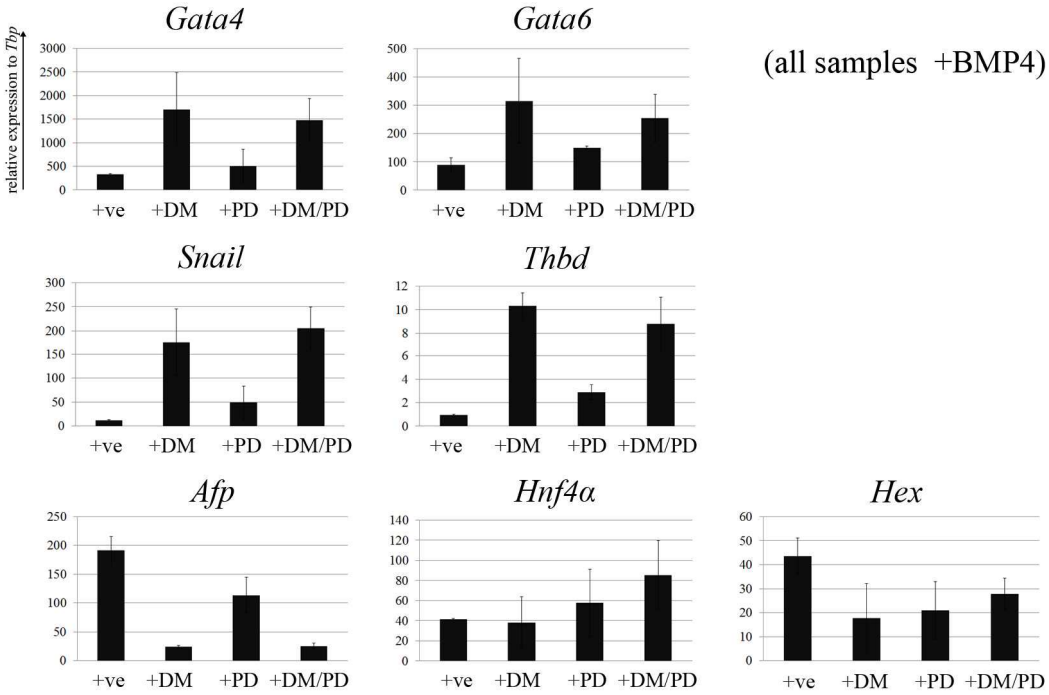

Figure 8.33 Inhibition of Erk1/2 or BMP4 signalling pathway during VE differentiation of XEN cells increases expression of PE associated markers and decreases expression of VE markers. IM8A1-GFP cells were cultured on laminin in N2B27 + BMP4 in presence or absence of inhibitors for 7 days. qRT-PCR results were normalised to *Tbp* expression and represent an average of biological duplicates, error bars are standard deviation between biological duplicates.

When during BMP4 and laminin driven VE differentiation of XEN cells Erk1/2 signalling is inhibited, it only has a moderate effect on the differentiation. However, in the presence of DM, Bmpr1a inhibitor, PE markers are strongly upregulated. This observation indicates that BMP4/laminin mediated induction of VE properties in XEN cells is promoted through Bmpr1a,and not through the Erk1/2 pathway. However, Erk1/2 signalling enhances the differentiation. Apparent upregulation of Hnf4α in DM/PD03 treated sample can reflect the type of cell that survives inhibitor treatment.

8.9 Discussion

XEN cells derived from PrE of pre-implantation embryo in standard culture conditions possess many characteristics of PE (Kunath et al., 2005). In this chapter I show that XEN cells, though seemingly represent a differentiated type of ExEn, have retained the ability to respond appropriately to developmentally relevant cues, such as ECM components and the signalling molecules BMP4 or Activin A.

E-CADHERIN is a marker of epithelial cells and hence is only expressed in PrE and VE as is absent in mesenchymal PE cells (Chen et al., 2005; Kadokawa et al., 1989). Consequently, PE cells express high levels of VIMENTIN (Lane et al 1983). E-CADHERIN hence not only marks PrE and VE, but its high expression also indicated low Snail expression as Snail is known to directly repress expression of E-cadherin (Batlle et al., 2000; Cano et al., 2000). E-CADHERIN upregulation was observed in cells cultured laminin and in the presence of BMP4 or Activin A (but only for one XEN cell lines) (Fig. 8.12, 8.13, 8.17, 8.18).

Upon BMP4 treatment XEN cells not only upregulate E-CADHERIN, but also *Afp*, *Hnf4α* and *Hex* and downregulate expression of VIMENTIN, *Dkk1* and *Fgf8* (Fig. 8.12-8.14). These results would indicate that XEN cells differentiate into VE. The precise classification of differentiated cells into a subtype of VE is not straightforward. BMP4-treated XEN cells downregulate expression of PDGFRα, an E6.5 exVE marker (Fig. 8.12a), but admittedly at the same time only portion of emVE markers is upregulated (Fig. 8.14). Upregulated markers are expressed in PrE and DVE (*Hex*) or emVE (*Afp, Hnf4α*). Afp and Hnf4α are also expressed during gastrulation in exVE domain, but this is most likely due definitive endoderm replacing emVE. Artus et al. suggest that BMP4 directs XEN cells towards exVE (Artus et al., 2011a). However, dynamic nature of markers makes it difficult to precisely classify type of differentiated ExEn. I would however argue that neither emVE nor exVE as such are formed, but rather more generic VE is established. This is also supported by an observation that during a complete loss of phosphorylated Smad1 emVE differentiation is affected, but exVE is successfully specified (Yamamoto et al., 2009). Moreover, heterogeneity of starting XEN population adds a

challenge to classification. It is possible that these various types of ExEn would respond distinctly to differentiation cues.

BMP4 is expressed in the ICM of an E3.5 embryo during PrE differentiation (Coucouvanis and Martin, 1999). BMP/Smad1 signalling is later required for emVE, but not for exVE or PE differentiation (Yamamoto et al., 2009). However, DVE formation requires downregulation of BMP signalling in distal portion of emVE (Mesnard et al., 2006; Yamamoto et al., 2009). Moreover, addition of BMP4 to in vitro culture of pre-gastrulation embryo downregulates expression of DVE markers (Yamamoto et al., 2009). In vivo removal of ExEc from E5.5 embryo, source of BMP4, causes upregulation of *Hex, Cer1* expression, but downregulation of *Afp* (Mesnard et al., 2006; Rodriguez et al., 2005). BMP4 can drive emVE differentiation of PrE cells, but at the same time would inhibit further differentiation of emVE cells into DVE or AVE. Hence, addition of BMP4 may also have various effects on XEN cells. Indeed, upon BMP4 treatment emVE and PrE markers such as Afp, Hnf4α and Hex is observed, but also downregulation of Dkk1, DVE markers is detected (Fig. 8.14).

Remarkably, *Hex* - PrE and DVE/AVE marker - is upregulated in response to BMP4 treatment and correspondingly is downregulated in the presence of DM (Fig. 8.14, Fig. 8.21, and Fig. 8.27). Also addition of DM during VE differentiation reduces expression of *Hex* (Fig. 8.32). The consistent upregulation of *Hex* in response to BMP4 does not agree with embryological data showing that Hex is repressed by BMP signals from the ExEc (Mesnard et al., 2006; Rodriguez et al., 2005). However, the expression may be indicative of the early wave of Hex expression in the PrE at E4.5 and not representative of Hex in the DVE/AVE. In fact, BMP4 is expressed in the ICM at E3.5 (Coucouvanis and Martin, 1999) which suggests it could be inducing Hex at this early stage. Furthermore, Hex has several characterised BMP-responsive elements and Smads have been shown to directly bind its promoter (Zhang et al., 2002).

Interestingly, explant culture of exVE and ExEc (source of BMP4 in an embryo) causes exVE differentiation into PE (Hogan and Tilly, 1981). AFP positive emVE explants co-cultured with ExEc downregulate expression of AFP and

conversely AFP negative exVE tissue cultured on its own upregulates AFP (Dziadek, 1978). Similarly, PrE ICM outgrowths preferentially give rise to PE cells (Behrendtsen et al., 1995). Because BMP4 is expressed in both early epiblast and ExEc (Coucouvanis and Martin, 1999) it is possible that BMP4 may facilitate PE differentiation. However, the results of this chapter show that BMP in fact promotes a very robust VE differentiation of XEN cells (Fig. 8.12-14). It is possible that other signalling pathway than BMP could play a role in PE differentiation of exVE. It is known that the PTHrP/cAMP pathway induces EMT and PE differentiation (van de Stolpe et al., 1993; Verheijen and Defize, 1999; Verheijen et al., 1999a). In fact, it was shown that even though EB expresses BMP2 and BMP4 addition of cAMP during differentiation enhances PE differentiation of the outer layer (Coucouvanis and Martin, 1999; Maye et al., 2000).

Another potential candidate promoting PE differentiation of exVE and exVE differentiation of emVE is PDGF signalling. After embryo implantation PDGF-A is expressed in emVE, epiblast and TE, but the initial PrE expression of PDGFRα is now limited to exVE and PE, with only low levels of PDGFRα being observed in emVE (Orr-Urtreger and Lonai, 1992; Plusa et al., 2008; Takakura et al., 1997). XEN cells with high E-CADHERIN levels show low expression of PDGFRα. And consequently, low levels of E-CADHERIN are observed in the PDGFRα high expressing cells (Fig. 7.3b, 8.6d, 8.12a). Interestingly, PTHr expression closely follows that of PDGFRα (Takakura et al., 1997; Verheijen et al., 1999a). Should PDGFRα signalling upregulate expression of PTHr this would be a possible link between PDGFRα and PE differentiation. Inhibition of Bmpr and Mek, a possible PDGFRα signalling effector (Artus et al., 2011a), (with DM or PD03 inhibitors, respectively), uniformly guides XEN differentiation towards PE fate (Fig. 8.24-27 and Fig. 8.30). The Bmpr inhibition agrees with the proposed role of BMP in VE differentiation. However, the effect of Mek inhibitor contradicts potential function of PDGFRα signalling in PE differentiation. Presumably, inhibition of Mek/PDGFRα signalling would sustain VE phenotype. Unless, PDGFRα induced PE differentiation of exVE in vivo is driven by other effector pathway than Mek/Erk (Artus et al., 2010). Levels of phosphorylated Erk are undetectable in emVE and exVE of E5.5-E6.5 implying that Erk signalling is not necessary for VE differentiation (Corson et

al., 2003; Yamamoto et al., 2009). Indeed, inhibition of Mek during BMP4/laminin VE-differentiation of XEN cells causes only mild upregulation of PE markers and moderate downregulation of *Afp* suggesting only secondary role of Erk signalling in VE differentiation (Fig. 8.32). Interestingly, PDGF was shown to be required for XEN cell derivation and expansion, but not differentiation of PrE from ES cells and PDGFRα mutant embryos show if any then late ExEn differentiation defect (Artus et al., 2010; Ogura et al., 1998). Moreover, Artus et al. proposed that XEN dependence on PDGF signalling is an in vitro acquired property (Artus et al., 2010). Accordingly, during subclone derivation expansion of PE and XEN like subclones, that presumably express higher levels of PDGFRα, was more efficient than that of epithelial like subclones as some of the epithelial clones were lost.

BMP role in emVE differentiation, does not explain why PE-like subclones upregulate expression of E-CADHERIN in response to BMP4 treatment (Fig. 8.16). However, it has recently been reported that BMP signalling drives mesenchymal-to-epithelial transition via microRNA mediated down-regulation of Zeb proteins (Korpal et al., 2008; Samavarchi-Tehrani et al., 2010). Zeb1 and Zeb2 are repressors of E-cadherin transcription, and their down-regulation leads to increased E-cadherin and transition to an epithelial cell type (Comijn et al., 2001; Korpal et al., 2008). It was interesting that microarray studies of BMP4-treated XEN cells identified *Zeb1* as a significantly down-regulated gene in BMP-treated XEN cells (Artus et al., 2011a; Paca et al., 2012) and that miRNAs are critical for the maintenance of XEN cells (Spruce et al., 2010). Alternatively, since PE-like subclones continue to express *Hnf4α* and *Ihh*, VE markers (Fig. 7.6) this could imply that the PE-like subclones either are not fully committed PE cells and can respond to BMP treatment in a similar manner like a naive cells or that these subclones can spontaneously give rise to VE like cells.

In summary, BMP4 can potentially differentiate XEN towards VE by different mechanisms:

1. by inducing VE differentiation of PrE and VE XEN cell progenitors;
2. by inhibiting DVE differentiation of rare emVE-like XEN cells;
3. by driving mesenchymal to epithelial transition of PE-like XEN cells.

In contrast to BMP4, Activin A treatment did not promote robust XEN cell differentiation (Fig. 8.13-14, Fig. 8.18). Activin signalling is required for emVE and DVE/AVE specification, but not for exVE or PE differentiation (Gu et al., 1998; Mesnard et al., 2006; Sirard et al., 1998). Activin A was shown to upregulate *Hex* and *Lim1* expression during embryo in vitro culture in a Cripto-independent manner (Mesnard et al., 2006). And embryos treated with Activin A receptor inhibitor (SB43) lose expression of *Dkk1*, *Lim1*, *Cer1* and upregulate *Hnf4α*(Stuckey et al., 2011). Moreover, emVE explants cultured together with epiblast, that expresses Nodal, maintain their VE character (Nichols et al., 1998a). Nodal has been recently reported to successfully differentiate XEN cells towards AVE (Kruithof-de Julio et al., 2011). Nodal-treated XEN cells upregulate expression of DVE/AVE markers and can contribute to DVE and VE in the chimeric embryos. Also Cripto, independently of Nodal signalling, had similar effect. In my hands however Activin A did not have such effect. In Activin A treated XEN cells expression of *FoxA2* and *Hnf4α* is unchanged, *Ihh* is downregulated and unexpectedly *Snail* expression is upregulated (Fig. 8.19). Correspondingly, SB43 treatment of XEN cells had very little effect on the expression of various markers and only *Afp* was upregulated in XEN cells cultured on laminin in the presence of SB43 (Fig. 8.28c-f and Fig. 8.29). *Afp* upregulation could be related to increased cell density of cells cultured in the presence of SB43 (Fig. 8.28b and Fig. 8.1c). I believe that the main reason for contradictory results in Activin A/Nodal treatment lies within use of different cell lines in respective experiments. Kruithof-de Julio et al. conducted their experiments on an earlier passage XEN cells and also modified the derivation procedure (Kruithof-de Julio et al., 2011). It is likely then that their starting population was then more of a primitive character. It is then possible, that unlike BMP4 that acts through different mechanisms but guides cells towards common fate, Activin A can only induce differentiation of certain pre-guided XEN emVE-like cells. Yamamoto et al. showed that specification of emVE required Smad1 and Smad2 signalling (Yamamoto et al., 2009). For this reason, experiments of combined BMP4 and Activin A treatments were designed. BMP4 was used as an a factor priming cells for emVE differentiation that is then specified by Activin A. Upregulation of emVE marker (*Fgf8*) was observed, but remarkably *Afp* was upregulated by 1000-fold when

compared to control condition (Fig. 8.21). Also, AFP expression could have been detected with an antibody (Fig. 8.22d). Without a doubt combined treatment of BMP4 and Activin A enhanced VE differentiation of XEN cells. In all of the treatments where Activin A was present recurring upregulation of *Snail* was observed (Fig. 8.19, Fig. 8.21). This is rather unexpected. One plausible explanation could be that during differentiation DVE cells need to downregulate E-Cadherin expression in order to migrate towards the anterior portion of the embryo. However, stable E-cadherin expression in DVE/AVE cells was recently reported (Trichas et al., 2011). Activin A is known to enhance proliferation of mES cells (Ogawa et al., 2007). It is possible then that in response to Activin A PE-like cells increase their proliferation rate and expand unproportionately in bulk culture.

It is worth noting that Activin A has different effects on IM8A1-GFP and XEN1.3 cell lines. Activin A treated IM8A1-GFP cells upregulated expression of E-CADHERIN (Fig. 8.18), in contrast E-CADHERIN was unchanged in XEN1.3 cells (Fig. 8.17). *Afp* was upregulated in IM8A1-GFP cells, but was downregulated in XEN1.3 cells (Fig. 8.19). *Hex* and *Thbd* were unaltered in IM8A1-GFP, whilst their expression was increased in XEN1.3 (Fig. 8.19). XEN cell lines respond already differently to serum-free conditions – expression of E-CADHERIN is unaltered XEN1.3, but reduced in IM8A1-GFP when cells are cultured in serum-free medium (Fig. 8.4). Moreover, XEN1.3 cells upregulates Snail and Thbd in response to BMP4 whilst IM8A1-GFP cells downregulate (Fig. 8.14). Combined BMP4 and Activin A treatment further underlines differences between XEN1.3 and IM8A1 (Fig. 8.21). Such differences between cell lines are further emphasised by lack of AVE differentiation upon Activin A treatment in my hands which has been observed elsewhere (Kruithof-de Julio et al., 2011).

In vivo various types of ExEn produce and are exposed to a diverse range of basement membrane proteins. The basement membrane between VE and epiblast is rich in laminin α1,β1, and γ1 chains (laminin-1), but not other laminins, whilst the basement membrane between PE and trophoblast giant cells, Reichert's membrane, contains a wider range of laminins (Gersdorff et al., 2005; Hogan et al., 1980). Both basement membranes contain nidogens, collagen IV, and perlecan. Fibronectin is

produced by the trophoblast of Reichert's membrane, but is less abundant than other ECM components (Leivo and Wartiovaara, 1989; Semoff et al., 1982; Wartiovaara et al., 1979). XEN cells cultured on laminin-1, but not fibronectin, adopted an epithelial structure and upregulated markers of visceral endoderm (Fig. 8.3). Laminin was reported to inhibit the formation of PE from PrE in ICM explants, while fibronectin had no such effect (Behrendtsen et al., 1995). It has also been observed that laminin, but not fibronectin, can induce terminal differentiation of ES cells into visceral endoderm (Takito and Al-Awqati, 2004). In vivo, laminin is also essential for proper differentiation of VE and PE, as a homozygous null mutation of *LAMC1*, encoding for laminin γ1 chain, leads to embryonic lethality due to the failure of the parietal yolk sac formation (Smyth et al., 1999). PrE from EB lacking expression of laminin γ1 chain quickly differentiates into PE (Murray and Edgar, 2001). Furthermore, mutant embryos for laminin α1 C-terminal globular domain have mildly disorganised VE and the expression of Afp and Dab2 is reduced (Akerlund et al., 2009). Moreover, F9, EC cells, that were cultured in presence of anti-laminin failed to form an organized epithelium and lack expression of Afp (Grover et al., 1983). Cells bind to ECM components, such as laminin, via integrins. The predominant integrins expressed in visceral endoderm areα5β1 (fibronectin receptor) and α6β1 integrin (laminin receptor) and interaction with laminin was found to activate Erk1/2 signalling in VE (Liu et al., 2009). Even earlier in embryo development signalling downstream of integrin β1 is required for PrE differentiation (Stephens et al., 1995). Similarly, expression of α5, α6 and β1 is also detected in XEN cells (Kunath et al., 2005). Integrin mediated Erk1/2 activation may promote VE character of XEN cells, as treatment with the Mek inhibitor, PD03, enhanced parietal endoderm characteristics (Fig. 8.24-25). However, also Mek/Erk signalling through PDGFRα may also be important (Artus et al., 2010).

FGF signalling, that is essential for PrE differentiation, does not seem to be involved in VE formation, as treatment of XEN cells with the FGF receptor inhibitors, PD173074 or SU5403, did not affect cell morphology or alter expression of extraembryonic endoderm genes (Spruce et al., 2010). Also, addition of FGF2 did not induce expression of immediate early Mek/Erk induction of *Egr1* expression

(Fig. 8.24a). This is in agreement with reported lack of FgfR2 expression in VE (Arman et al., 1998).

In brief, XEN cells are able to respond to developmentally relevant differentiation cues. Especially, BMP4 induces robust differentiation of XEN cells towards VE. In comparison, Activin A enhances VE differentiation of only BMP4-pretreated XEN cells. The expression of various ExEn markers indicates that PE character dominates. Yet, XEN cells reaction to differentiation stimuli is similar to that of PrE and not exVE or PE.

9. BMP4 promotes transdifferentiation of parietal endoderm to visceral endoderm**.**

9.1 Introduction

XEN cells are derived from mouse blastocyst and represent an in vitro model of extraembryonic endoderm. In previous chapters I showed that these cell lines are heterogeneous and express various types of extraembryonic endoderm markers that are not co-expressed in an embryo. To be able to better relate some of the results and to complement the analysis I analysed freshly dissected PrE, VE and PE.

9.2 Expression of E-CADHERIN, GATA4 and PDGFRα in explant cultures of primitive, visceral and parietal endoderm cells

Firstly, expression pattern of E-CADHERIN and Gata4 and E-CADHERIN and PDGFRαin was examined in different types of ExEn explants. In vivo E-CADHERIN is only expressed in epithelial cells of VE and PrE and not mesenchymal PE cells (Chen et al., 2005; Kadokawa et al., 1989). E-CADHERIN was used throughout XEN cell characterisation and differentiation experiments as a marker of VE.

Primitive endoderm was obtained from diapause embryos. Diapause embryos were subjected to immunosurgery and cultured overnight and then primitive endoderm was removed away from epiblast with fine glass pulled pipettes (Fig. 9.1a-b). Visceral endoderm was obtained from E6.5 embryos by enzymatically treating dissected epiblast tissue. Parietal endoderm was dissected from E7.5 and E8.5 embryos. To obtain parietal endoderm cells and to ensure that no visceral endoderm cells were carried over, a cut was first made at the embryonic and extraembryonic boundary. After this Reichert's membrane was removed for a brief treatment with Accutase (Fig. 9.2c). Following dissections explant tissue was deposited on γMEFs in GMEM+10%FBS and cultured for 5 days.

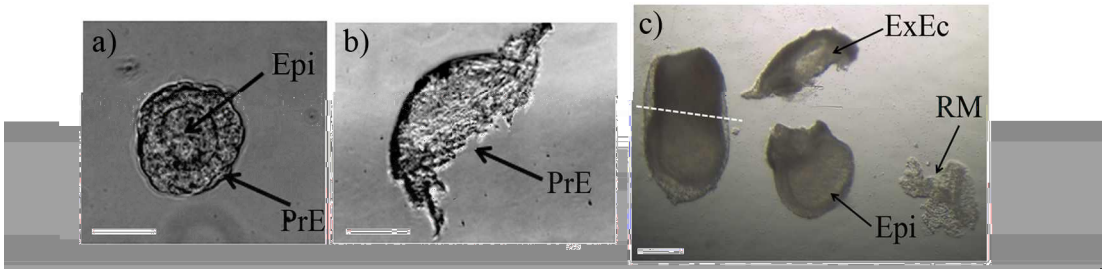

Figure 9.1 Primitive and parietal endoderm dissections. Bright field pictures of dissections. **a-b**) Primitive endoderm (b) dissected from diapause embryo after immunosurgery and overnight culture; Epi – epiblast, PrE – primitive endoderm; scale bar: 20µm (a), 10µm (b).**c**) Reichert's membrane (RM) dissected from an E7.5 embryo. ExE; extraembryonic ectoderm, scale bar: 400µm.

E-CADHERIN is expressed in PrE (Fig. 9.2a,c) and in VE (Fig. 9.2b,d), but not in PE (Fig. 9.2c,f). Already on day 5 of explant culture majority of PrE and VE cells lost E-CADHERIN expression. GATA4 continues to be expressed by all of the explants (Fig. 9.2a-c). This finding together with the loss of E-CADHERIN observation in the PrE and VE explants indicates that cells readily differentiate into PE.

As observed previously in XEN cells (Fig 7.3b), expression of PDGFRα is heterogeneous. Same is true for explant tissues. Similarly as in XEN cells, PDGFRα expression is higher in E-CADHERIN negative cells (Fig. 9.2d-f). Most of the PE cells derived from Reichert's membrane are positive for PDGFRα (Fig. 9.2c). This observation suggests that PDGFRα is marking PE cells, and not PrE and VE.

ExEn explants exhibit similar expression patterns of E-CADHERIN, GATA4 and PDGFRα as XEN cells do.

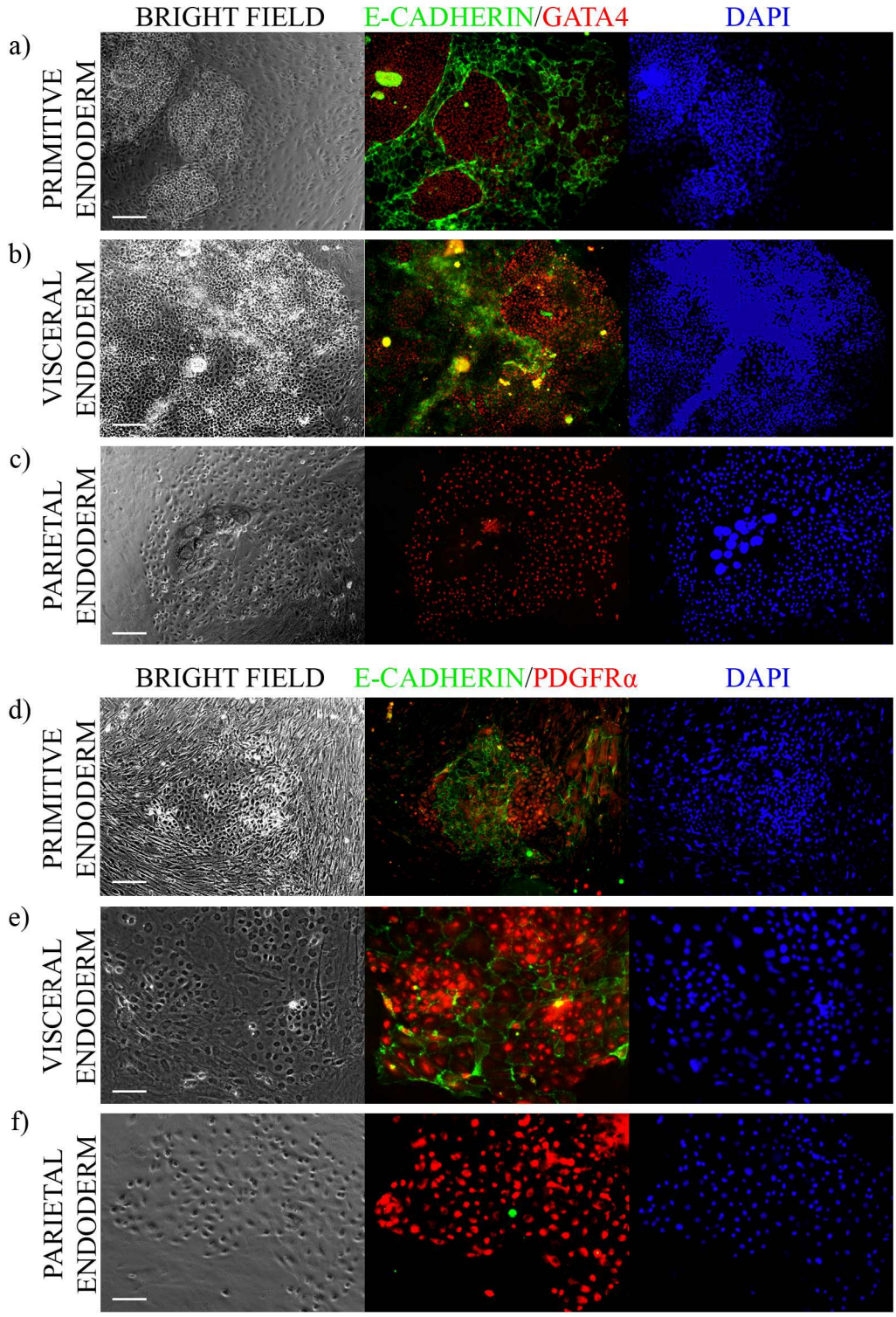

Figure 9.2 Primitive and visceral endoderm cells lose expression of E-CADHERIN in in vitro culture. PrE, VE and PE explants were cultured on MEFs for 5 days before immunostaining with appropriate antibodies.; scale bar: 200µm (a-d), 100µm (e-f).

9.3 Bmp4 treatment of parietal endoderm cells

Finally, to determine if BMP4 and laminin could transdifferentiate embryo derived PE to a VE state I applied the culture conditions that promoted VE differentiation of XEN cells to freshly isolated PE cells from post-implantation embryos. Reichert's membrane dissected from E7.5 and E8.5 embryos was placed on either laminin or gelatin coated plates in MEF-CM for 5 days. This step ensured that outgrowths used in subsequent experiments contained only PE and trophoblast giant cells. After initial 5 days of culture explants were cultured for another 5 days in either MEF-CM, or N2B27 or N2B27+BMP4.

Gelatin or laminin and N2B27 or MEF-CM very rarely produced double-positive E-CADHERIN/GATA4 cells (Fig. 9.3a,b and Fig. 9.4a,b, Table 9.1). However, BMP4 was able to induce E-CADHERIN/GATA4 double positive VE cells independent of the substrate used (Fig. 9.3c and Fig. 9.4c, two images are shown). I only observed a significant induction of E-CADHERIN in cells that were also GATA4 positive (Fig. 9.3 and Fig. 9.4). Sporadically in MEF-CM and in N2B27 (1 in 8 and 1 in 6 explants, respectively) a small number of E-CADHERIN/GATA4 double positive cells was present (Table 9.1). However, in the presence of BMP4 5 out 5 on gelatin and 7 out 8 on laminin explants gave rise to E-CADHERIN/GATA4 double positive cells (Table 9.1).

The difference between observed E-CADHERIN/GATA4 double-positive cells in MEF-CM or N2B27 conditions versus N2B27+BMP4 condition is statistically different (Fisher exact test, $p=0.0005$ and $p=0.0029$, respectively for combined results of cells grown on laminin or gelatin).

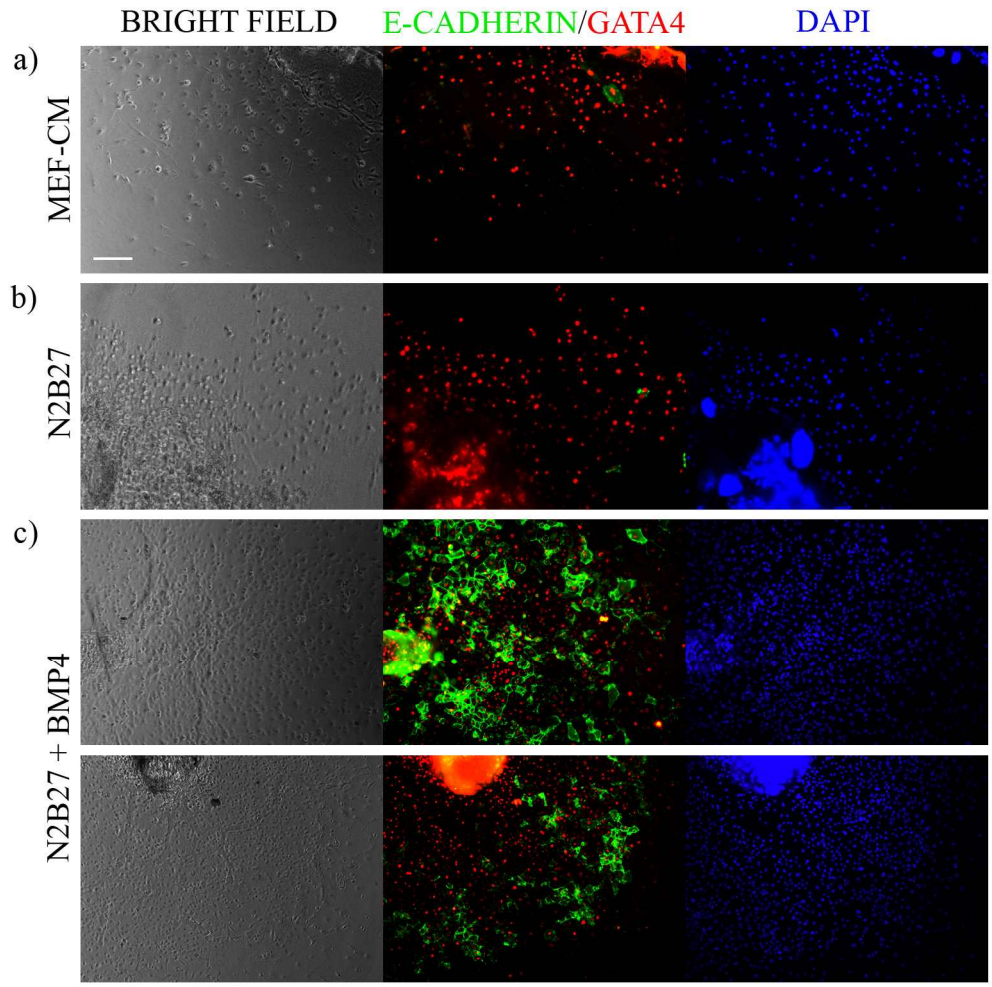

Figure 9.3 BMP4 induces E-cadherin expression in parietal endoderm cells on gelatin. Immunostaining of E-cadherin and Gata4 in parietal endoderm cells cultured on gelatin in MEF-CM for 5 days and then for an additional 5 days in either MEF-CM (**a**), N2B27 (**b**) or N2B27 supplemented with BMP4 (50ng/ml) (**c**); scale bar: 200µm.

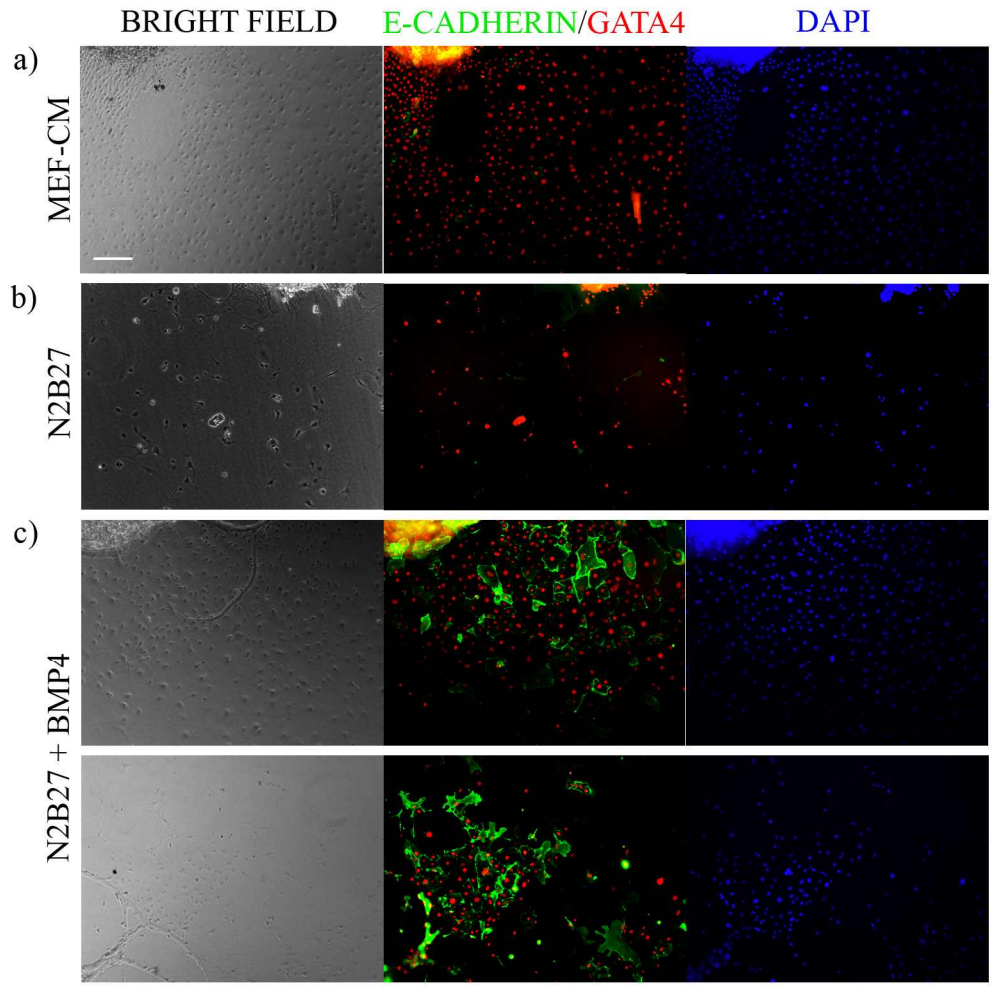

Figure 9.4 BMP4 induces E-cadherin expression in parietal endoderm cells on gelatin. Immunostaining of E-cadherin and Gata4 in parietal endoderm cells cultured on laminin in MEF-CM for 5 days and then for an additional 5 days in either MEF-CM (**a**), N2B27 (**b**) or N2B27 supplemented with BMP4 (50ng/ml) (**c**); scale bar: 200µm.

	70% MEF-CM	N2B27	N2B27 + 50ng/ml BMP4
Gelatin	0/3	1*/2	5/5
Laminin	1/5	0/4	7/8

Table 9.1 BMP4 induces E-CADHERIN expression in parietal endoderm cells from E7.5 and E8.5 Reichert's membrane. Number of explants, where E-CADHERIN/GATA4 double positive cells were present, per total number of explants treated. *A small minority of cells were E-CADHERIN/GATA4 double-positive.

9.4 Discussion

In the previous chapter BMP4 was shown to induce VE differentiation, marked by E-CADHERIN upregulation, of XEN-derived PE cells (Fig. 8.16). Remarkably, embryo derived PE cells also initiate expression of E-CADHERIN upon BMP4 treatment (Fig. 9.3-4). The fact that PE cells, isolated from as E7.5 and E8.5 embryos, can also respond to BMP4 and differentiate into VE, suggests that PE is not a terminally-differentiated cell type or that it can be easily transdifferentiated into VE.

Epithelial ExEn explants – PrE and VE – lose expression of E-CADHERIN in the culture (Fig. 9.2). Rapid and default PrE and VE differentiation into PE suggests that PE is a default phenotype of ExEn (Gardner, 1993; Gardner and Davies, 1992; Hogan and Tilly, 1981; Nichols et al., 1998a; Ninomiya et al., 2005). Even though some of the results were validated by chimaera contribution that I argued earlier is not an appropriate analysis to test for XEN cell character (see discussion Chapter 7), observed downregulation of E-CADHERIN for PrE and VE explants (Fig. 9.2) further supports predisposition of ExEn towards PE differentiation. Similarly, XEN cells express PE markers at high levels and most of the cells in standard culture conditions do not express E-CADHERIN (Fig. 7.3-4, Fig. 8.3). Patterns of expression of E-CADHERIN, GATA4 and PDGFRα in various explants are similar to those observed earlier in XEN cells (Fig. 9.2 and Fig.8.6). In particular, high PDGFRα expression is detected in PE cells and PrE and VE cells that lost E-CADHERIN expression (Fig. 9.2d-f).

In order for a PE cell to upregulate E-CADHERIN expression, cell needs to undergo mesenchymal to endothelial transition (MET). Analogous process happens during induced pluripotent stem cell derivation. Fibroblasts similarly need to change their mesenchymal character into an epithelial one and BMP signalling has been reported to facilitate this process (Korpal et al., 2008; Samavarchi-Tehrani et al., 2010). Another characteristic of induced pluripotent stem cell derivation are global changes in chromatin methylation (Hochedlinger and Plath, 2009). In fact addition of histone deacetylase inhibitors enhances reprogramming efficiency (Huangfu et al., 2008). Extraembryonic tissues have been reported to be hypomethylated when

compared to the embryonic tissue (Chapman et al., 1984; Gardner and Davies, 1992; Monk et al., 1987). Low methylation of ExEn could potentially give this tissue a significant competence to easily undergo differentiation or transdifferentiation.

The remarkable ability of BMP4 to induce epithelial character upon PE cells suggests that BMP4 could be added throughout the derivation of XEN cells. Addition of BMP4 should prevent PE-like differentiation and maintain epithelial character of newly derived cells. This is also supported by expression pattern of BMP4 during early embryo development.

In summary, the results of this chapter supports following ideas:

1. that the lack of signalling from epiblast or ExEc causes PE differentiation, as PrE and VE explants lose expression of E-CADHERIN and E-CADHERIN negative cells upregulate expression of PDGFRα (Fig. 9.2);
2. and thus the current standard culture conditions are unable to fully sustain epithelial phenotype of ExEn (Fig. 9.2);
3. BMP4 treatment of PE cells shows that even differentiated types of ExEn retain developmental plasticity (Fig 9.3 and Fig 9.4).

10. General discussion and summary

The ability to differentiate VE subtypes from XEN cells opens new opportunities to investigate this ExEn lineage. Combinatorial application of the key signals present between blastocyst formation and gastrulation, such as Activin/Nodal, FGF, WNT, and BMP signalling, will provide new ways to direct XEN cell differentiation. The variability between cell lines and sometimes low differentiation efficiency most likely arises from heterogeneous nature of XEN cells. However, it is necessary to recognise this heterogeneity, just as ZEN philosophy accepts and embraces the true nature of things. In this regard, the work with XEN cells truly lives up to its name.

Here I showed that:

1. XEN are heterogeneous cell lines and contain mixtures of primitive endoderm derivatives at different stages of development;
2. XEN cells respond to developmentally relevant signal and can be induced to differentiate into VE by BMP4. This differentiation can be further enhanced by Activin A;
3. Laminin enhances the ability of BMP4 to induce visceral endoderm differentiation, but also on its own induce VE differentiation of XEN cells;
4. BMP4 can induce PE cells to become like VE.

Importantly, this research further validates stem cell nature of XEN cells. Various stem cells are defined by two characteristics: self-renewal and the ability to differentiate into specialised cell types. The stem cell properties of XEN cells have not been clear so far (Kunath et al., 2005). This work proved that:

1. a single XEN cell can give rise to a subclonal cell line of identical properties as a parental one;
2. XEN cells can respond to developmentally relevant differentiation cues.

In the current understanding of stemness this qualifies XEN cells as stem cells. This is also supported by evidence coming from other research groups (Artus et al., 2011a; Kruithof-de Julio et al., 2011).

Chromatin of extraembryonic tissues was shown to be hypomethylated (Chapman et al., 1984; Gardner and Davies, 1992; Monk et al., 1987). Similarly, XEN cells have been recently reported to express low levels of repressive chromatin modifications, such as H3K23me3 (Rugg-Gunn et al., 2010). Interestingly, PrE-progenitors already expressing Oct4 exhibit greater developmental plasticity than Oct4-expressing epiblast progenitors at a similar stage (Grabarek et al., 2012). It is possible then that low methylation gives ExEn cells a remarkable plasticity and susceptibility to various signals. Therefore, I'd like to propose that XEN cells in an vitro culture are not only maintained by PrE-like progenitors, but also that such naïve cells can arise from more differentiate progeny and that XEN cells within culture constantly oscillate between PrE, VE and PE-like state.

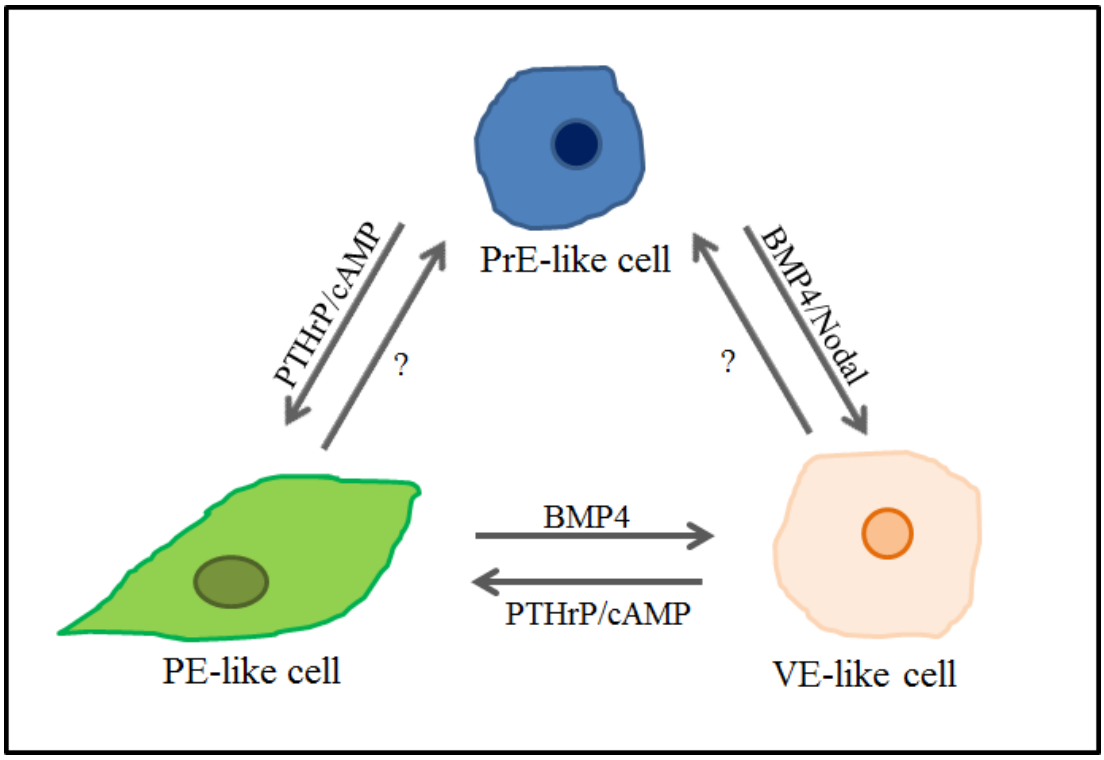

Figure 10.1 XEN cell culture model. Proposed model of XEN cell line maintenance where various extraembryonic endoderm cell types constantly interchange during the culture. The differentiation towards PE-like cells is probably driven by PTHrP/cAMP signalling (van de Stolpe et al., 1993). VE-like cell types are induced by Nodal and BMP signalling (Artus et al., 2011a; Kruithof-de Julio et al., 2011; Paca et al., 2012)

The hypothesis that XEN cells can alternate between VE and PE is supported by:

1. efficient VE differentiation of embryo and XEN-derived PE cells;
2. responsiveness of XEN-derived, but not embryo derived PE cells to laminin;

However, further experiments should be carried out to validate the hypothesis of interchanging cell types within XEN cell culture. Such experiments might include derivation of subclonal cell lines in conditions driving homogeneous XEN cell differentiation either towards VE or PE and then after removal of such stimuli observations could be carried out to assess whether a phenotype similar to the parental cell line can be obtained. Alternatively, XEN cells modified to carry a dynamic fluorescent marker for either one of the VE markers (E-cadherin or Afp) or PE markers (Snail) could be employed to carry out studies on the downregulation and upregulation of these markers in a particular cell.

Recently, XEN cells have been shown to facilitate mES cell differentiation into cardiomyocytes (Brown et al., 2010a). I imagine that manipulation of other pathways and application of different matrices will provide the means to generate all subtypes of VE, study the VE-epiblast and VE-ExEc interactions outside of the embryo and could lead to the de novo derivation of epithelial ExEn cell lines that are truly primitive in nature.

11. Appendix

11.1 SIX3 hES reporter cell line

11.1.1 Introduction

Human embryonic stem (hES) cells, like mouse embryonic stem (mES) cells, were derived from blastocysts (Martin, 1981; Thomson et al., 1998). However, hES cells share the same requirements for maintaining the undifferentiated state in culture with mouse stem cells derived from early-post implantation embryos, epiblast stem cells, but not with mES cells. Activin A and FGF2, but not LIF and BMP4, are required to maintain pluripotency of hES and epiblast stem cells (Brons et al., 2007; James et al., 2005; Tesar et al., 2007; Vallier et al., 2005; Xu et al., 2005). Analogously to mES cells, hES were found to differentiate to all germ layers (Thomson et al., 1998). The initial neural differentiation of hES involved either formation of EBs in the presence of FGF2 (Zhang et al., 2001) or prolonged culture without replacing mouse embryonic fibroblast feeder layer (Reubinoff et al., 2001). Another method of neural differentiation relies on a co-culture of hES cells with stromal-feeder cells (Hong et al., 2008). Neural monolayer protocols, initially developed for mES cells, have also been successfully applied to hES cells (Itsykson et al., 2005; Lowell et al., 2006; Pollard et al., 2006). It was shown that Nodal/Activin inhibits neural differentiation (Vallier et al., 2004) and conversely that SB431542, Nodal/Activin receptor inhibitor, promoted neural differentiation (Smith et al., 2008). Also addition of Noggin, a BMP4 inhibitor, to the differentiation media enhanced neural induction efficiency (Itsykson et al., 2005). Recently combination of both inhibitors – SB431542 and Noggin - resulted in a very effective inhibition of SMAD signalling and showed an impressive proportion of neural conversion of hES with over 80% of cells expressing early neural differentiation marker - PAX6 (Chambers et al., 2009).

SIX3 (sine oculis homeobox homolog 3) is a highly conserved gene with an important function in forebrain development (Inbal et al., 2007; Lagutin et al., 2003). Six3 plays an important role in neural induction already in sea urchins (Wei et al., 2009). *Six3* is expressed in murine early neural plate at E7.5 and its expression is

maintained throughout the development of the anterior ectoderm (Kurokawa et al., 2004; Oliver et al., 1995; Yang and Klingensmith, 2006). However, later in development Six3 expression is restricted to mainly central forebrain and eye field (Oliver et al., 1995). *Six3*$^{-/-}$ embryos die at birth and lack forebrain structures (Lagutin et al., 2003). SIX3 directly upregulates expression of SHH, ventralizing factor (Geng et al., 2008; Jeong et al., 2008). SIX3 also represses expression of Wnt3b or Wnt1 shielding forebrain from posteriorising signals (Lagutin et al., 2003; Lavado et al., 2008; Liu et al., 2010). Six3 is required during retinal development and eventually in the adult mouse its expression is restricted to the retina outer cell layer and the expression in retina pigmented epithelium is downregulated (Appolloni et al., 2008; Idelson et al., 2009; Lamba et al., 2006; Liu et al., 2010; Manavathi et al., 2007). Moreover, Six3 overexpression can induce ectopic formation of retina, whilst Wnt3b overexpression suppresses retina specification (Liu et al., 2010; Loosli et al., 1999). Although Six3 is dispensable for mouse retina pigmented epithelium specification (Liu et al., 2010). In humans and mice various mutations in *SIX3* have been linked to holoprosencephaly, a failure of rostral forebrain to develop into two hemispheres, as a result of Shh signalling insufficiency (Cohen, 2006; Domene et al., 2008; Geng et al., 2008; Jeong et al., 2008; Wallis et al., 1999). *Six3* haploinsufficiency in mice also leads to holoprosencephaly, but only in an inbred background (Geng et al., 2008; Lagutin et al., 2003). Similarly, a mutation of *SIX3* in humans may have variable penetrance in a family (Ribeiro et al., 2006; Solomon et al., 2009). Recently, Zhang et al. showed that PAX6 is required for neural differentiation of hES cells by directly downregulating expression of pluripotent markers and promoting expression of neuroectoderm genes (Zhang et al., 2010). Moreover, overexpression of PAX6 in hES cultured in self-renewal conditions initiates their neural differentiation (Zhang et al., 2010). SIX3 expression is tightly correlated with expression of PAX6 (Zhang et al., 2010). Also Six3 expression is reduced in Pax6 heterozygous mice in a dosage dependent manner (Goudreau et al., 2002). Yet, Six3 is known to activate expression of *Pax6* (Goudreau et al., 2002) and the troika of Pax6, Six3 and Sox2 is involved in lens induction and specification (Liu et al., 2006)

The efficient production of neural tissue from ES cells is important for the potential applications in pharmaceutical screening, disease modelling and cell-based transplantation therapies. As the current focus of in vitro neural differentiation protocols lies within improving their efficiency, aiming towards xeno-free culture and scaling up of the process establishment of hES reporter cell line would greatly facilitate these efforts. A SIX3 hES reporter line, obtained through homologous recombination or random integration of a transgene, would not only faithfully report early steps of neural differentiation, but also assist in developing efficient differentiation protocols towards retina lineages. In particular, this cell line could be used to investigate the neural inducing properties of XEN cells and its derivatives.

11.1.2 Materials and Methods

11.1.2.1 DNA constructs for targeting vectors and transgene

To generate DNA constructs BAC clone (RP11-672G8, BacPac Resources Centre) containing the human SIX3 gene was engineered by recombineering in *E.coli* DH5α cells using pSC101-BAD-γβαA-tet plasmid following Gene Bridges RED/ET recombineering protocol (Zhang et al., 1998; Zhang et al., 2000). This enabled insertion of a cassette consisting of a GFP-ires-Puro-mPGK after ATG start codon, or Venus-mPGK/EM7 –neo also after ATG start codon, or gtx-IRES-Venus-mPGK/EM7-neo before TAA stop codon of exon 2. The modified BAC was once again engineered by recombineering with p15-DTA-amp (for GFP-ires-Puro-mPGK and gtx-IRES-Venus-mPGK-neo modified BAC) or p15-amp-DTA retrieval cassette (for Venus-mPKG-neo modified BAC). Neomycin resistance gene is flanked by *frt*-F5 recombination sites. Final DNA constructs (Fig. 11.3) were verified by sequencing and restriction enzyme digest analysis. p15-SIX3:GFP-DTA, p15-SIX3-Venus-DTA and p15-SIX3:Venus plasmids were named as SIX3:GFP, SIX3-Venus and 12kb-SIX3:Venus, respectively

The pSC101-BAD-γβαA-tet plasmid, and plasmid with GFP-ires-Puro-mPGK-neo and p15-DTA-amp cassettes were a kind gift from Dr Andrew J. Smith, plasmid with gtx-ires-Venus sequence from Dr J. Brickman, pCAD-eGFP (control plasmid) from Dr Ian Chambers. The gtx-ires-Venus-mPGK/EM7-neo cassette was generated by standard molecular biology techniques. BamHI/HindIII excised

mPGK/EM7-neo sequence was ligated into BamHI/HindIII cut pACYC177. Correct pACYC177-mPGK-neo clone was identified, cut with PsiI and ligated with gtx-ires-Venus fragment. Cassettes used for the BAC recombineering were amplified using primers and conditions stated in Table 11.1. Amplification and sequencing primers were ordered from Integrated DNA Technologies, Belgium.

PRIMER PAIR	AMPLIFICATION CONDITIONS
SIX3:GFP cassette	Pfx Platinum polymerase 3x enhancer 94°C for 2min 20cycles: 15s for 98oC 72°C for 4min
CTTCCTCCCCTCTCTCTTCCTCTCCCTGAATTTTCTCCTCTCC TCTCAGGTCAGTCCATGGTGAGCAAGGGCGAGGAGCT	
TTGGGGTAGGGGTCCTGTAGGTACCACTCCCGCAACAGGC TCCGAGTCCGCTCCTTGAAGGTTCTTTCCGCCTCAGAAAA	
SIX3:GFP/p15-DTA-amp cassette	Phusion polymerase + 10% DMSO 98°C for 30s 20cycles: 98°C for 10s 72°C for 60s
TTTTGCATCCGTTTCCAAACTAATTTTGACTTCCGATTTCCT TTTGTCCCCATCCCCAGCCCTTAGGGCGATCGCGACCC	
GACTGGCGCTCCAAGCAATTGTCGCCCCGGACAGTAAACA CAGCTCAGTTGCCTCAACTTGCCCGGGCTACGTAGACTTA	
SIX3-Venus cassette	Phusion polymerase + 5% DMSO 98°C for 2min 20cycles: 98°C for 15s 54°C for 20s 72°C for 60s
GCAGACACCGGCACCTCCATCCTCTCGGTAACCTCCAGCG ACTCGGAATGTGATGTATGActccctctcaaaagcgggca	
AGGCGGAGGGGAAGGAGTGGGGGAGGAGGGGAAGGAGA GGGAGGAGGGCGGCCTTGGCTAAGCTTGAATTCGAAGTTC CT	
SIX3-Venus/p15-DTA-amp cassette	Phusion polymerase + 10% DMSO 98°C for 30s 20cycles: 98°C for 10s 72°C for 60s
GAGCAGTCTCTTCTCCCTCTCTTCTTCCTCTGCCTCCGTGGC CCTGTCAGTCCCGCCTAACCTTAGGGCGATCGCGACCC	
GAGGGAAGAGAGAAAGAGAGGTTGAGAGAGAATTTAAAT GGGAAACCTAACGTGACTGGGGCCCGGGCTACGTAGACTT A	
SIX3:Venus cassette	Pfx Platinum polymerase 3x enhancer 94°C for 2min 20cycles: 15s for 94°C 68°C for 3 min
CTTCCTCCCCTCTCTCTTCCTCTCCCTGAATTTTCTCCTCTCC TCTCAGGTCAGTCCATGGTGAGCAAGGGCGAGGAGCT	
CGCGCTGGGGATGGGGACAAAAGGAAATCGGAAGTCAAA ATTAGTTTGGAAACGGATGCAAGCTTGAATTCGAAGTTCCT	
12kb-SIX3:Venus/p15-amp cassette	Phusion polymerase + 10% DMSO 98°C for 30s 20cycles: 98°C for 10s 72°Cfor 70s
TCTATTCCTCCCTTTTGCATCCGTTTCCAAACTAATTTTGAC TTCCGATTTCCTTTTGTCCCTTAGGGCGATCGCGACCC	
TTATCTGATTGTGTAATGAAATATGTATGAGGAACAGCTCA ACTTCTCGCCGGAGCAGGTGCCCGGGCTACGTAGACTTA	

(all amplification cycles were followed by 5min final extension at 68°C or 72°C)

Table 11.1 Primers' sequence and PCR conditions used for cassette amplification.

11.1.2.2 hES cell culture

Shef4 and Shef1 hES cells were routinely cultured in mTeSR1 media (StemCell Technologies, #05850) on Matrigel (BD, #85351) coated plates. Cells were passaged in clumps after 3min of dispase (10µg/ml Sigma. D4818) treatment and were split at 1:3-1:4 ratio every 3-4 days. Shef4 unpublished and optimized electroporation protocol was kindly provided by Dr Andrew J. Smith. For electroporation Shef4 cells were treated with 10µM ROCK inhibitor (Y-27632, Ascent, Asc-129) for 1h before lifting with Accutase (Millipore, SCR005) for 10min at 37^{o}C. Use of ROCK inhibitor greatly enhances survival of hES cells as single cells (Watanabe et al., 2007). Cells were then pipetted up and down to ensure single cell suspension and after spinning down resuspended in small volume of mTeSR1. 50µg of SnaBI linearized DNA was added to ~18x10^{6} cells and mixed thoroughly. Electroporation was conducted using BIO-RAD Gene Pulser II (800V, 3µF). Transfected cells were then plated on Matrigel-coated plates in mTeSR1+ROCK inhibitor and 2 days later selection with G418 (50µg/ml) was started. Surviving colonies were individually picked and expanded in 96-well plate. For AMAXA nucleofection Shef1 cells were first treated with 10µM ROCK inhibitor for 1h before lifting with Accutase (Millipore, SCR005) for 10min at 37^{o}C. Cells were then pipetted up and down to achieve single cell suspension and after spinning down 8x10^{5} cells were resuspended in 100µl of Nucleofector solution. Nucleofection protocol was optimised using 2µg pCAG-EGFP following manufacturer's protocol and percentage of GFP expressing cells was quantified using flow cytometer. For 12kb-SIX3:Venus plasmid nucleofection 2µg of SnaBI linearized DNA was added to 8x10^{5}cells and selected program (A23, solution 1) was applied. Cells were plated on matrigel coated plates in mTeSR1+ROCK inhibitor and selection with G418 (20µg/ml) 2 days was started. For lipofection Shef1 cells were passaged in small clumps and were incubated overnight with Lipofectamine2000:DNA mix (6µl/2µg) in OPTIMEM. Following day fresh media was added and selection with G418 (20µg/ml) was started on day 2.

11.1.2.3 Monolayer dual Smad inhibition neural differentiation

Shef1 or Shef4 cells were incubated in 10μM ROCK inhibitor for 1h. Cells were lifted with Accutase and pipetted up and down until single cell suspension was achieved. Cells were plated as single cell in 96-well plate at ~$2x10^5$ cells per well in a 96-well plate in presence of 10μM ROCK inhibitor in mTeSR1 or TeSR2 (StemCell Technologies) until confluent (approx. 2-3 days). Media was changed then to 20% K/O serum-replacement (KSR, Gibco 10828) medium with SB431542 (SB43, 10μM, Ascent Asc-163) + LDN-193189 (LDN, 100nM, Stemgent 04-0074). Cells were fed every other day and after day 5 N2B27medium was gradually introduced.

Cells cultured in 96-well plate were pre-treated with 10μM ROCK inhibitor for 1h and then lifted with Accutase. Cells were pipetted up and down using multi-channel pipette and half of the cells' suspension was transferred to a new 96-well plate and once cells in majority of wells were confluent neural differentiation was started as for Shef1 and Shef4. To the remaining half of the cell suspension 20% DMSO in KSR was added and plates were transferred to -80^{o}C.

11.1.2.4 Immunofluorescence

Cells were fixed in 4% paraformaldehyde (room temperature, 8-10 minutes), washed three times with PBS, then incubated for 30min at room temperature in blocking buffer (PBS, 2% donkey serum, 0.1% Triton X-100). Primary antibodies PAX6 (DSHB, mouse IgG1, 1:50) and SIX3 (kind gift from O.Guillermo, rabbit, 1:300) were diluted in blocking buffer and applied overnight at 4^{o}C, followed by three washes in PBS. Donkey secondary antibodies conjugated to AlexaFluor dyes (Molecular Probes) were diluted at 1:1000 in blocking buffer and applied for 1-1.5 hours at room temperature. The cells were then washed twice in PBS and a third time in PBS containing DAPI (10μg/ml) prior to imaging using an Olympus IX51 inverted fluorescence microscope.

11.1.3 Results

11.1.3.1 Efficiency of hES cell neural differentiation in 96-well plate

Firstly, current very efficient neural differentiation protocol was adapted for 96-well format(Chambers et al., 2009). Shef1 and Shef4 hES cells were plated either as single cell suspension or clumps and differentiated for 8 days. On day 8 cells were fixed and immunostained using PAX6 antibody.

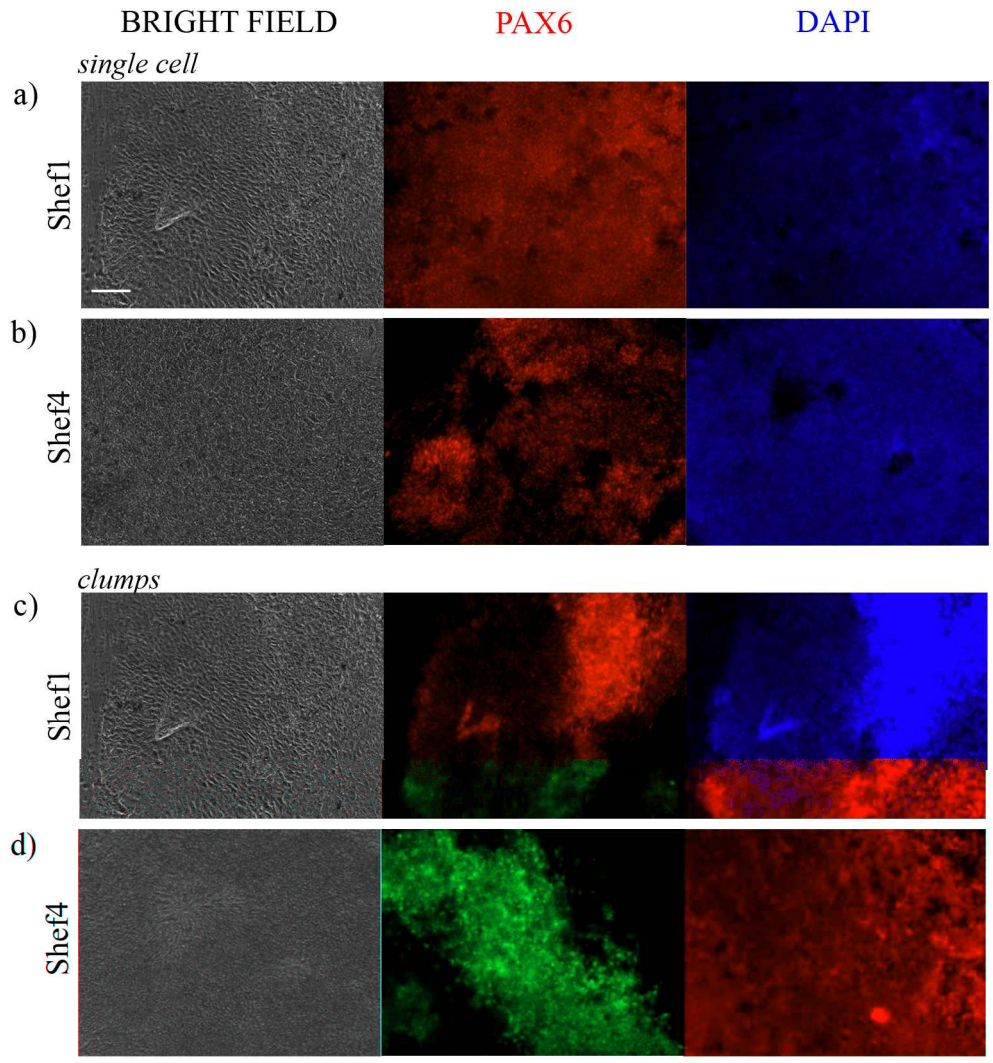

Figure 11.1 PAX6 expression on day 8 of neural differentiation. hES cells (Shef1 and Shef4) were plated either as single cell suspension or clumps and were differentiated for 8 days; scale bar: 200µm.

hEScells do not express PAX6 in self-renewing conditions (Chambers et al., 2009). After 8 days of neural differentiation hES cells upregulate PAX6 (Fig. 11.1).

Both Shef1 and Shef4 plated as single cell upregulate expression of PAX6 (Fig. 11.1a,b). In clumps the differentiation is slightly less efficient, but patches of PAX6 positive cells were still present (Fig. 11.1c,d). Single cell plating seems to be more efficient. Nevertheless, PAX6 expressing cells are also present in less favourable conditions.

Next expression of SIX3 was assessed on day 8 and day 14 of neural differentiation. On day 8 of neural differentiation PAX6 and SIX3 are co-expressed by Shef1 and Shef4 hES cells (Fig. 11.2a,b). Interestingly, SIX3 expression is dose-dependent and only PAX6-high positive cells express SIX3 at detectable levels. By day 14 in Shef1 cell line not only SIX3/PAX6 double positive cells are present, but also PAX6 only and SIX3 only positive colonies appear (Fig. 11.2c). In Shef4 cell line PAX6 and SIX3 continue to be co-expressed (Fig. 11.2d).

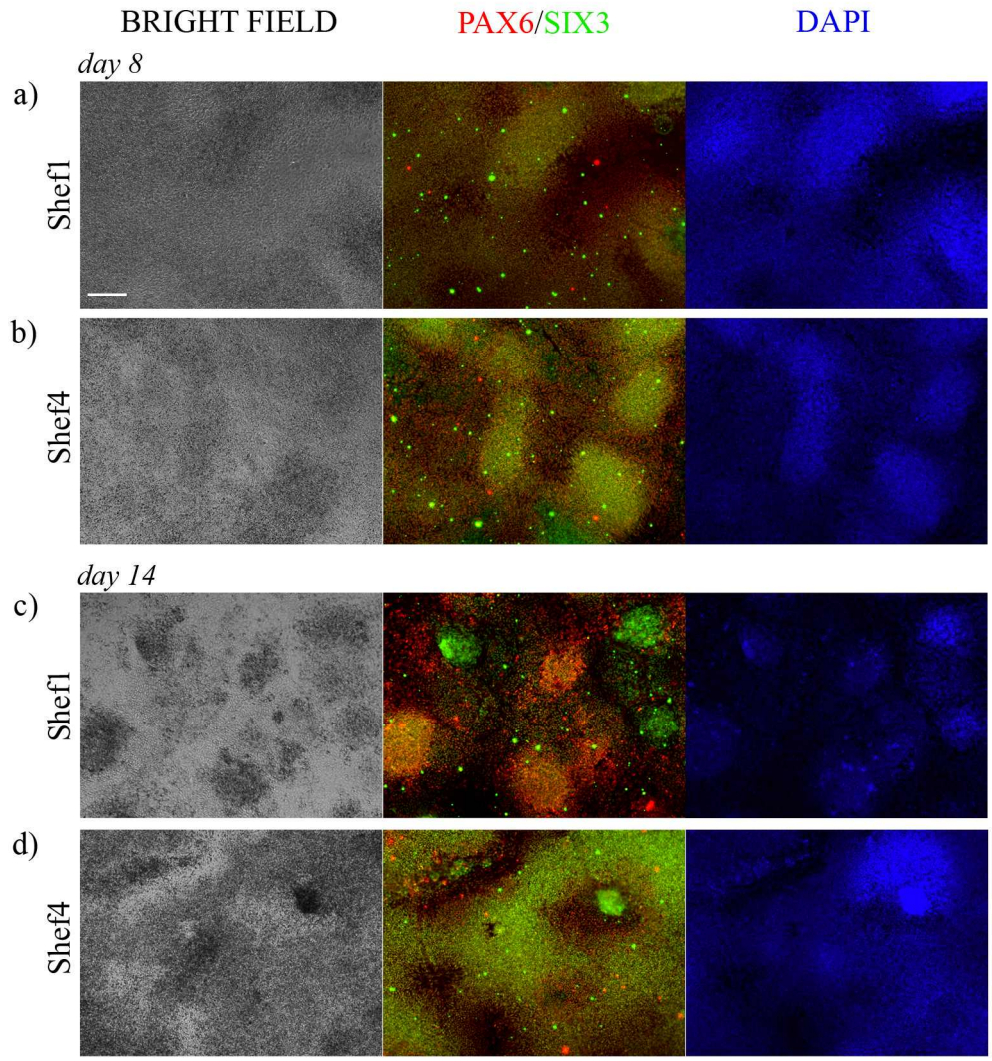

Figure 11.2 PAX6 and SIX3 expression during neural differentiation of Shef1 and Shef4 hES cells. Cells were differentiated toward neural lineages for 8 or 14 days and stained with appropriate antibodies; scale bar: 200µm.

The dual Smad inhibition neural differentiation protocol is also very efficient for cells cultured in 96-well plates and the efficiency seems to be related to density and quality of cells' plated. The remarkable efficiency of the differentiation prompted me to use this differentiation protocol for screening for SIX3 hES reporter cell line arising from not only random integration, but also targeting experiments.

11.1.3.2 SIX3 targeted Shef4 hES cell line

In order to make SIX3 Shef4 hES reporter cell line two targeting vectors were constructed (Fig. 11.3a-b). First SIX3:GFP vector, where GFP-neo cassette was introduced after start codon and a correct targeting event would result in an allele

knock-out (Fig. 11.3a). Second vector was SIX3-Venus vector with gtxIRES-Venus-neo cassette following last exon (exon 2) of *SIX3* and correct targeting event arising from this vector should not affect endogenous *SIX3* expression levels (Fig. 11.3b). Both construct contained very efficient 3' negative selection cassette with DTA (diphtheria toxin subunit A).

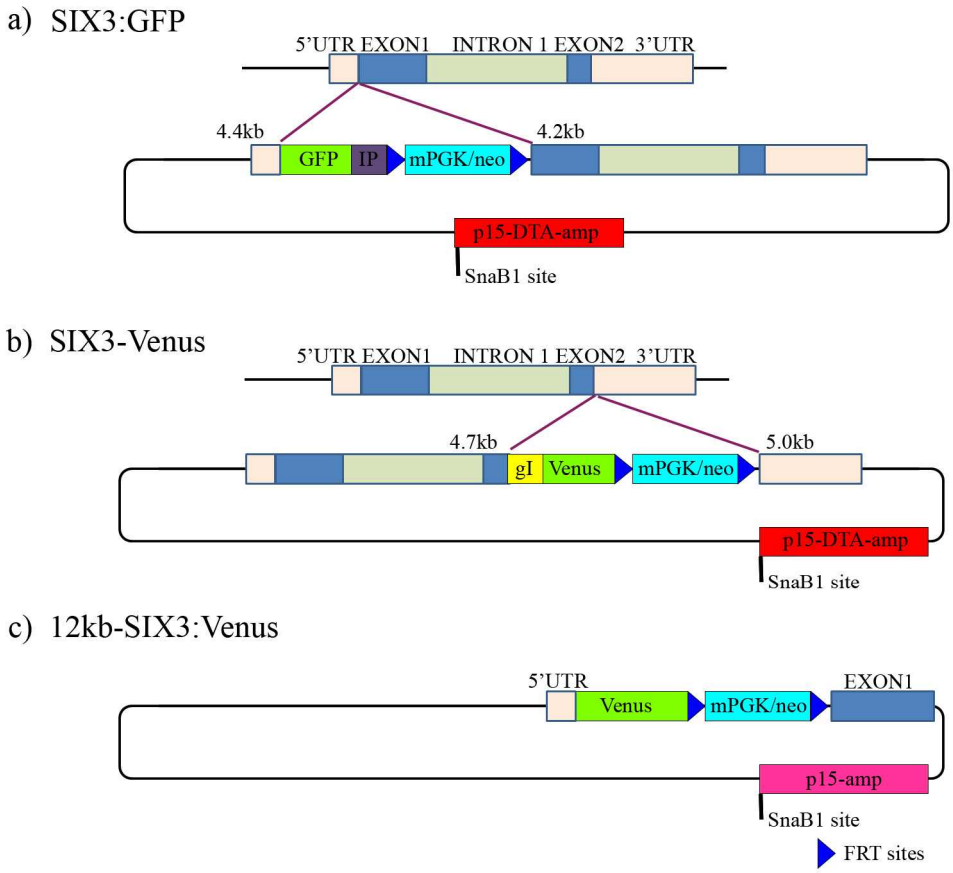

Figure 11.3 Various DNA constructs used for generation of SIX3 hES reporter cell line. a-b) targeting vectors, **c)** random integration vector.

Restriction enzyme SnaBI linearized constructs were introduced by electroporation using Bio-Rad Gene PulserII. And after 14days G418 selection 4x96 colonies were picked for each vector. Once the majority of clones reached confluence cells were split between two plates and one plate was frozen and cells within the other plate underwent neural differentiation for 12 days. Cells were observed daily under fluorescent microscope for the presence of GFP positive cells. For SIX3:GFP vector only 1 GFP positive clone appeared, whilst for the SIX3-Venus a total of 15 Venus positive clones was observed (Table 11.2). However, only 8 clones had GFP positive cells on day 8.

The GFP/Venus expression pattern varied from single GFP positive cells dispersed around the well to GFP positive cells forming neural rosette like patterns. On day 12 cells were immunostained with PAX6 antibody and only cells where an overlap between GFP/Venus and PAX6 expression was observed were thawed for further investigation. One clone for SIX3:GFP and 11 clones for SIX3-Venus vector were expanded in presence of G418 and second round of neural differentiation was carried out. Single cells were plated and differentiated for 8 days. In these more favourable neural differentiation conditions there was very little and if any non-specific co-expression of PAX6 and GFP/Venus (Fig. 11.4). Regrettably, none of the clones faithfully reported neural differentiation.

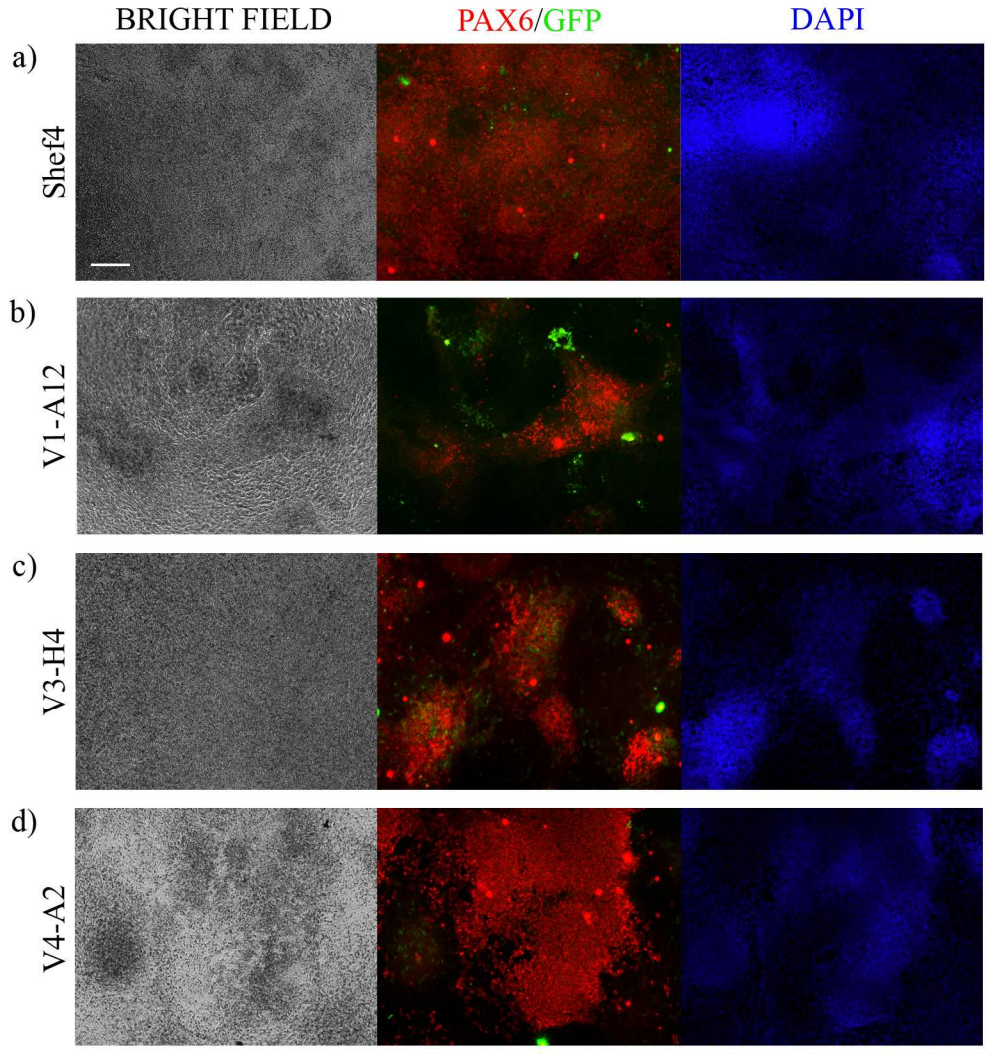

Figure 11.4 PAX6 expression on day 8 of neural differentiation of SIX3-Venus Shef4 clones. PAX6 expression in 3 representative clones is presented; scale bar: 200µm

11.1.3.3 SIX3 random integration reporter Shef1 hES cell line

Another approach carried out to derive SIX3 reporter line based on random integration of SIX3 reporter transgene. SIX3:Venus vector consisted of 12kb of SIX3 5' upstream sequence driving expression of Venus-mPGK-neo cassette (Fig. 11.3c). Linearized vector was introduced into Shef1 hES cells using AMAXA nucleofector or through lipofection.

To begin with, AMAXA nucleofection optimization for hES cells was carried out using pCAG-EGFP plasmid and manufacturer's instructions. Two different cell suspension buffers (1 and 2) and 5 suggested nucleofection conditions were used. The following day the number of cells was compared between control condition (no DNA) and GFP transfected samples. Also levels of GFP expression were quantified. Depending on the conditions cell survival varied between 30% and 95% and the proportion of GFP-positive cells spanned between 20% and 65% (Fig. 11.5). Taking into account cell survival and the efficiency of GFP transfection A23 nucleofector setting and buffer 1 were chosen.

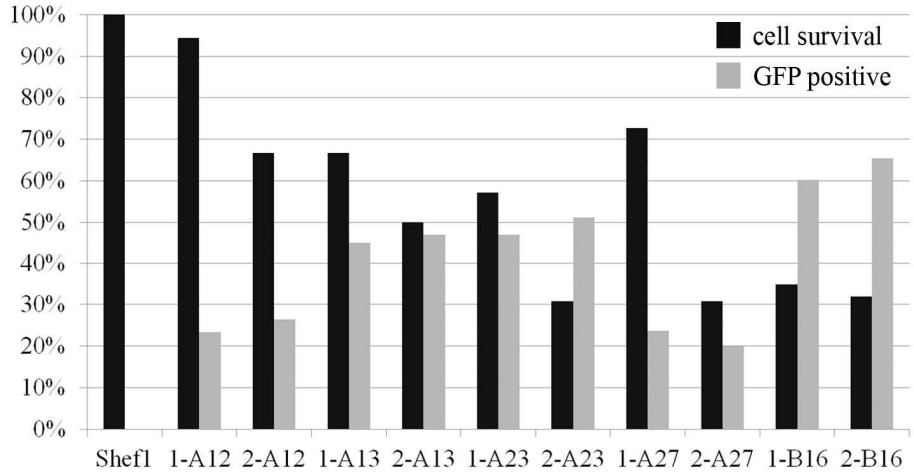

Figure 11.5 Optimization of AMAXA nucleofection for Shef1 hES cells. Shef1 hES were AMAXA nucleofected with pCAG-EGFP and the following day number of surviving cells was counted and compared to control sample and GFP expression was quantified. Two suspension buffers (1 and 2) and 5 nucleofection conditions (A12, A13, A23, A27, and B16) were used.

For linearized 12kb-SIX3-Venus construct 5 individual AMAXA nucleofection reactions were carried out. Cells were plated and on day 2 of culture G418 (20µg/ml) was added. Cells were cultured for 14 days. Even though initially a

lot of colonies were observed only minority (15 colonies) expanded. Similarly as to the targeting experiments 12kb-SIX3-Venus clones were differentiated towards neural lineages and were observed daily under a fluorescent microscope for the presence of GFP expressing cells. On day 8 of neural differentiation cells were immunostained with PAX6 antibody. Though PAX6 expression was detected, no Venus positive cells were observed (Table 11.2).

Another approach to introduce 12kb-SIX3:Venus used Lipofectamine 2000 as means of DNA delivery to the cells. Cells were also transfected with pCAG-EGFP control plasmid (Fig. 11.6b) or SnabI linearized SIX3:Venus transgene (Fig. 11.6a). Notably most of the control GFP expressing cells were present in the edges of colonies (Fig. 11.6b,c). Also, after adding G418 (15µg/ml) on day 2 the first cells to lift off and die were in the centre of the colony.

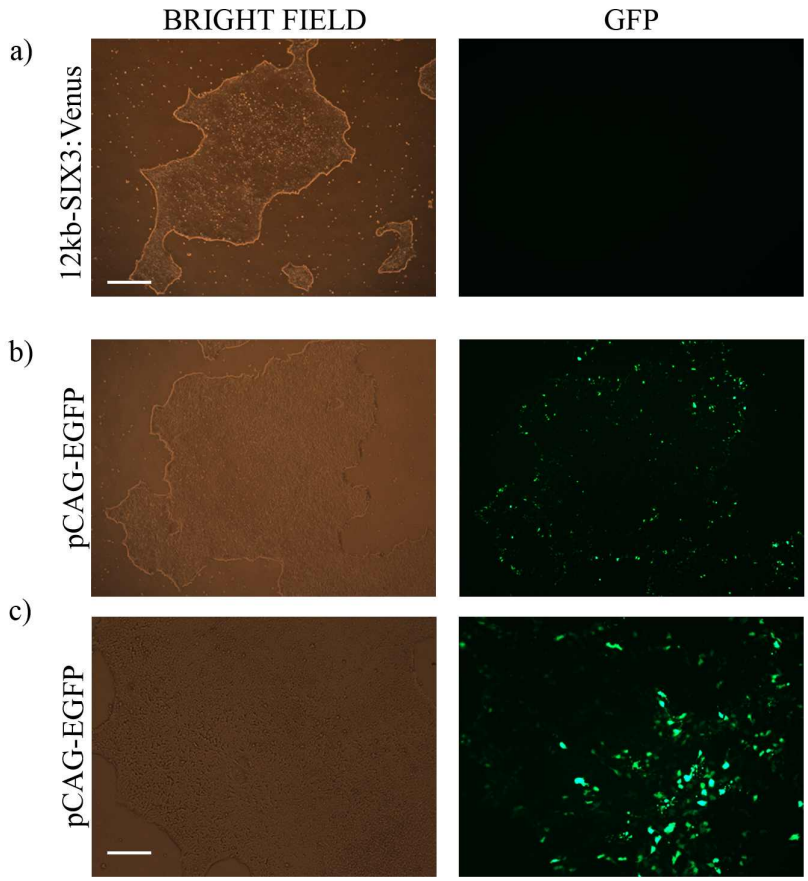

Figure 11.6 pCAG-EGFP and 12kb-SIX3:Venus lipofection of Shef1 hES cells. Cells were transfected overnight and pictures were taken 16hrs post-transfection; scale bar: 200µm (a, b), 100µm (c).

From 11 wells after 2 weeks of culture 96 colonies were picked. The number of colonies varied between 2 and 15per well. Eighty-five colonies expanded and after splitting into them 2 plates one plate was frozen at -80^{o}C and the cells in the other one were differentiated for 7 days. On day 7 71 out of 85 wells contained PAX6 expressing cells, but none contained Venus expressing cells (Table 11.1).

In summary, random integration experiments also failed to deliver SIX3 hES reporter cell line.

	construct	clones picked	clones expanded	PAX6+ clones	GFP+ clones	PAX6/GFP double positive
BIO-RAD electroporation	SIX3:GFP	384	348	-	1	0 (day 12) 0 (day 8)
	SIX3-Venus	384	314	-	13	0 (day 12) 0 (day 8)
AMAXA (A-23) nucleofection	12kb-SIX3:Venus	15	15	15	0	0
lipofection	12kb-SIX3:Venus	96	85	71	0	0

Table 11.1 Summary of SIX3 hES reporter cell line derivation attempts.

11.1.4 Discussion

In order to derive hES neural differentiation reporter cell line two different approaches were carried out: homologous recombination and random integration of transgene. Unfortunately, none of these proved to be successful (Table 11.2).

mES cells are easily amendable to genetic manipulations and use of homologous recombination as means of introducing recombinant DNA is now routine (Evans, 2011). In contrast to mES targeting of hES cells is characterised by low efficiency of homologous recombination in a range of 0.1%-0.5% for non-expressed genes (Wang et al., 2011a; Zou et al., 2009). However, targeting efficiency of an expressed gene *OCT4*, hES cell marker, reaches 27-40% depending on the size of homology arms (Zwaka and Thomson, 2003). SIX3 is not expressed in hES cells and even during overexpression of PAX6, direct SIX3 regulator, it takes 3-5 days to upregulate expression of SIX3 (Zhang et al., 2010). This would therefore suggest that chromatin modifications obstruct accessibility to SIX3 locus and the

locus is inactive. Assuming that the efficiency of traditional homologous recombination based targeting of *SIX3* should be in a range of 0.1-0.5%, 1 to 4 correctly targeted clones between 2 constructs could have been expected. Only one GFP positive clone arose from SIX3:GFP construct, but 15 from SIX3-Venus (Table 11.2). Yet, none of the clones reported SIX3 expression. Expression of Venus in SIX3-Venus construct was multiplied by gtx-IRES sequence, that was shown to be efficiently amplify levels of expression of primitive endoderm marker in mES cells (Canham et al., 2010). Also, Venus is a brighter protein than GFP(Rekas et al., 2002).The efficiency of neural differentiation in 96-well plate of expanded subclones was around 80% (Table 11.2). The 20% of wells did not differentiate most likely due to insufficient cell density or high non-specific differentiation of starting population (Chambers et al., 2009). Using Southern blot, a traditional method of screening could have increased the efficiency of screening to 100%. However, SIX3 expression is tightly controlled by PAX6 (Lengler and Graw, 2001; Zhang et al., 2010) and the expression of SIX3 closely follows expression of PAX6 during in vitro neural differentiation (Fig. 11.2). Hence, even though screening sensitivity was lowered by 20% that should have not affected the outcome, and neural differentiation based screening additionally allowed for early functional assessment of potential reporter cell line.

Due to low efficiency of targeting of hES cells various new approaches have been developed. One of them includes using BAC, where one of the homology arms is extremely long (in a range of 100-200kb). Though few colonies were obtained the efficiency of targeting of expressed genes (p53 and ATM) is between 20-30% (Song et al., 2010). Another type of targeting vector based on non-integrating adenoviral vector showed a remarkable targeting efficiency of 45% for HPRT1 gene (Suzuki et al., 2008). However, within the last few years zinc-finger nucleases (ZFN) have been gaining more ground and recognition. ZFN are enzymes that generate specific double strand breaks. Such breaks can be then repaired by non-homologous end joining or homologous recombination mechanisms (Kim et al., 1996; Mani et al., 2005). ZFN have been successfully employed in hES and induced pluripotent stem (iPS) cells for targeting of OCT4 (95-100% efficiency), α-synuclein (18% efficiency) and hES non-expressed gene PITX3 (8-11% efficiency) (Hockemeyer et al., 2009; Soldner et al.,

2011). They have also proven to be effective in targeting other organisms like zebrafish, tobacco or A.*thaliana* (Lloyd et al., 2005; Meng et al., 2008; Townsend et al., 2009). Yet, the greatest limitation for using ZFN is either laborious testing of ZFN from an open source (Maeder et al., 2008) or the price of commercially available ZFN from CompoZr® (Sigma). Nucleases of similar properties like ZFN, but instead of ZF domain to identify sequence they have transcription activator-like effector domain that allows for recognition of longer DNA sequence than ZFN, have also been shown to efficiently target hES cells (Hockemeyer et al., 2011).

SIX3 comprises only two exons and its expression regulation was studied (Chao et al., 2010; Lengler and Graw, 2001; Liu et al., 2006; Suh et al., 2010). The length of reporter transgene was based on analysis of zebrafish six3a promoter region that recapitulates embryonic expression of six3a (Chao et al., 2010; Suh et al., 2010). Also, luciferase assay of 800bp 5' upstream region of SIX3 showed that this region contains binding sites for PAX6, PROX1, SIX3 and MSX2, transcription factors that regulate SIX3 expression (Lengler and Graw, 2001). Already SIX3:GFP targeting vector has 4.4kb 5' upstream SIX3 sequence (Fig. 11.3a) and yet neomycin resistant clones cultured expanded after SIX3:GFP electroporation failed to report SIX3 expression during neural differentiation. For this reason the 5' upstream region in transgene vector was expanded to 12kb covering all of the zebrafish six3a regulatory sequences and highly conserved regions. In addition GFP was exchanged for its brighter version – Venus. 12kb transgene also did not report SIX3 expression. It is likely that because clones were resistant to neomycin and therefore transgene was integrated in a transcriptionally active site, once the differentiation process started and global changes in chromatin structure occurred the transcriptional availability of transgene was affected. Alternatively, 12kb of upstream sequence is maybe insufficient to drive SIX3 specific Venus expression. Previously, it was shown that BAC transgenesis, based on mouse modified BAC library, could also report expression of a gene of interest in hES cells (Chambers et al., 2009; Placantonakis et al., 2009; Tomishima et al., 2007). Such modified BAC includes most if not all regulatory elements, but they could also result in expression of an additional copy of genes surrounding gene of interest locus.

In order to derive SIX3 hES reporter cell line traditional methods of targeting and transgenics have proven to be insufficient. It is then advisable to apply more recently developed efficient techniques for hES cells modifications.

11.2 Negative control antibody staining

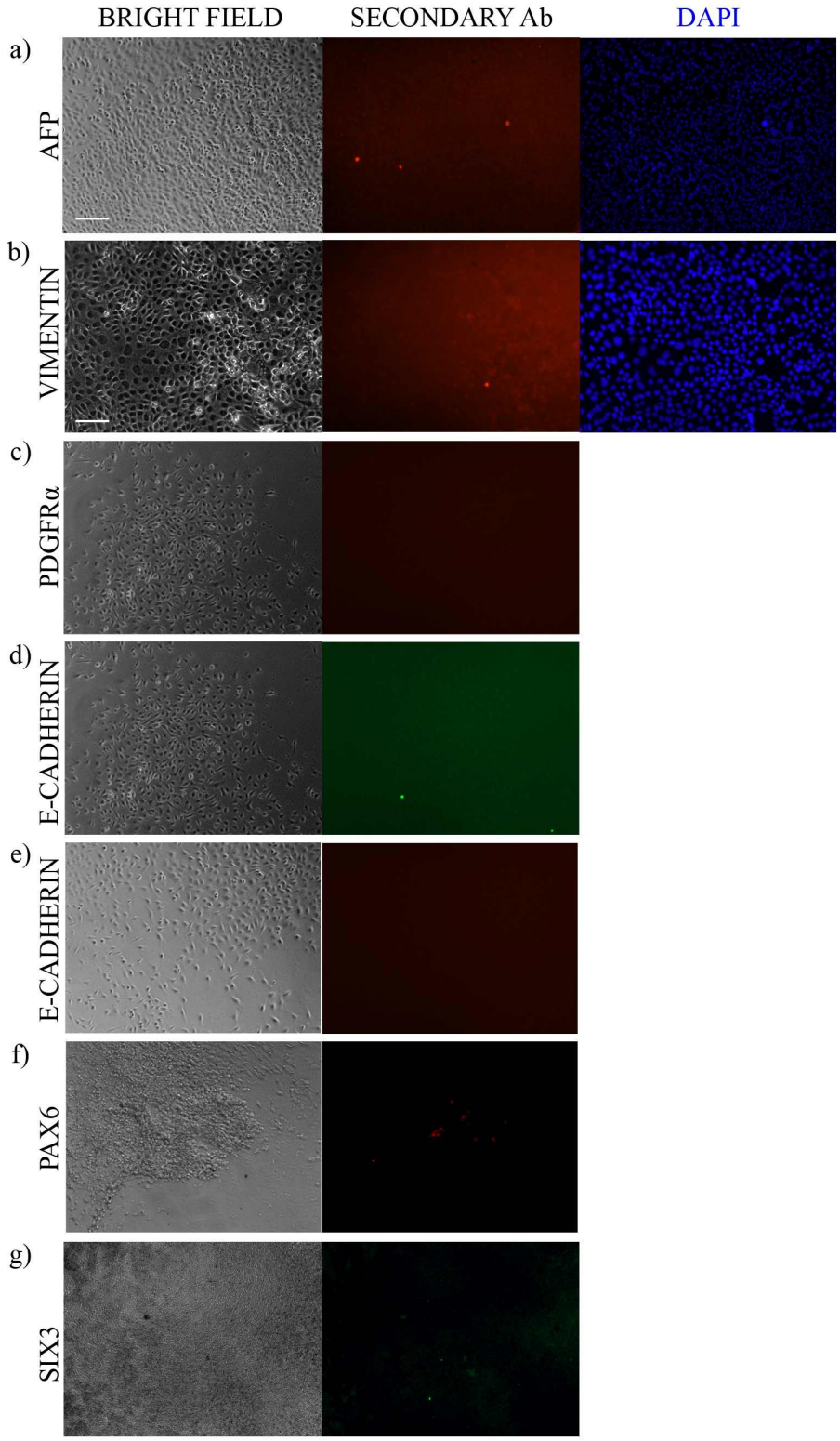

Figure 11.7 Negative staining, i.e. incubation with secondary antibody only, for various antibodies used throughout the thesis.

12. Publications

During my PhD studies I contributed towards two publications.

1. Kaji, K., Norrby, K., **Paca, A.**, Mileikovsky, M., Mohseni, P., Woltjen, K., 2009.Virus-free induction of pluripotency and subsequent excision of reprogramming factors. Nature. 458, 771-5

I performed qRT-PCR analysis and in vitro differentiation of various iPS cell lines.

2. **Paca, A.**, Séguin, C. A, Clements, M., Ryczko, M., Rossant, J., Rodriguez, T. A., Kunath T., 2012. BMP signaling induces visceral endoderm differentiation of XEN cells and parietal endoderm. Dev Biol. 361, 90-102

This published paper has arisen from this thesis and sections of it have been used throughout the thesis.

13. References

Ahmed, N., Riley, C., Rice, G., Quinn, M., 2005. Role of integrin receptors for fibronectin, collagen and laminin in the regulation of ovarian carcinoma functions in response to a matrix microenvironment. Clin Exp Metastasis. 22**,** 391-402.

Akerlund, M., Carmignac, V., Scheele, S., Durbeej, M., 2009. Laminin alpha1 domains LG4-5 are essential for the complete differentiation of visceral endoderm. Cell Tissue Res. 338**,** 129-37.

Albazerchi, A., Stern, C. D., 2007. A role for the hypoblast (AVE) in the initiation of neural induction, independent of its ability to position the primitive streak. Dev Biol. 301**,** 489-503.

Ang, S. L., Conlon, R. A., Jin, O., Rossant, J., 1994. Positive and negative signals from mesoderm regulate the expression of mouse Otx2 in ectoderm explants. Development. 120**,** 2979-89.

Appolloni, I., Calzolari, F., Corte, G., Perris, R., Malatesta, P., 2008. Six3 controls the neural progenitor status in the murine CNS. Cereb Cortex. 18**,** 553-62.

Arceci, R. J., King, A. A., Simon, M. C., Orkin, S. H., Wilson, D. B., 1993. Mouse GATA-4: a retinoic acid-inducible GATA-binding transcription factor expressed in endodermally derived tissues and heart. Mol Cell Biol. 13**,** 2235-46.

Arman, E., Haffner-Krausz, R., Chen, Y., Heath, J. K., Lonai, P., 1998. Targeted disruption of fibroblast growth factor (FGF) receptor 2 suggests a role for FGF signaling in pregastrulation mammalian development. Proc Natl Acad Sci U S A. 95**,** 5082-7.

Arnold, S. J., Robertson, E. J., 2009. Making a commitment: cell lineage allocation and axis patterning in the early mouse embryo. Nat Rev Mol Cell Biol. 10**,** 91-103.

Artus, J., Douvaras, P., Piliszek, A., Isern, J., Baron, M. H., Hadjantonakis, A. K., 2011a. BMP4 signaling directs primitive endoderm-derived XEN cells to an extraembryonic visceral endoderm identity. Dev Biol.

Artus, J., Panthier, J. J., Hadjantonakis, A. K., 2010. A role for PDGF signaling in expansion of the extra-embryonic endoderm lineage of the mouse blastocyst. Development. 137**,** 3361-72.

Artus, J., Piliszek, A., Hadjantonakis, A. K., 2011b. The primitive endoderm lineage of the mouse blastocyst: sequential transcription factor activation and regulation of differentiation by Sox17. Dev Biol. 350**,** 393-404.

Barbacci, E., Reber, M., Ott, M. O., Breillat, C., Huetz, F., Cereghini, S., 1999. Variant hepatocyte nuclear factor 1 is required for visceral endoderm specification. Development. 126**,** 4795-805.

Barrow, J. R., Howell, W. D., Rule, M., Hayashi, S., Thomas, K. R., Capecchi, M. R., McMahon, A. P., 2007. Wnt3 signaling in the epiblast is required for proper orientation of the anteroposterior axis. Dev Biol. 312**,** 312-20.

Batlle, E., Sancho, E., Franci, C., Dominguez, D., Monfar, M., Baulida, J., Garcia De Herreros, A., 2000. The transcription factor snail is a repressor of E-cadherin gene expression in epithelial tumour cells. Nat Cell Biol. 2**,** 84-9.

Beck, S., Le Good, J. A., Guzman, M., Ben Haim, N., Roy, K., Beermann, F., Constam, D. B., 2002. Extraembryonic proteases regulate Nodal signalling during gastrulation. Nat Cell Biol. 4**,** 981-5.

Beddington, R. S., 1994. Induction of a second neural axis by the mouse node. Development. 120**,** 613-20.

Beddington, R. S., Robertson, E. J., 1989. An assessment of the developmental potential of embryonic stem cells in the midgestation mouse embryo. Development. 105**,** 733-7.

Beddington, R. S., Robertson, E. J., 1998. Anterior patterning in mouse. Trends Genet. 14**,** 277-84.

Behrendtsen, O., Alexander, C. M., Werb, Z., 1995. Cooperative interactions between extracellular matrix, integrins and parathyroid hormone-related peptide regulate parietal endoderm differentiation in mouse embryos. Development. 121**,** 4137-48.

Belo, J. A., Bouwmeester, T., Leyns, L., Kertesz, N., Gallo, M., Follettie, M., De Robertis, E. M., 1997. Cerberus-like is a secreted factor with neutralizing activity expressed in the anterior primitive endoderm of the mouse gastrula. Mech Dev. 68**,** 45-57.

Ben-Haim, N., Lu, C., Guzman-Ayala, M., Pescatore, L., Mesnard, D., Bischofberger, M., Naef, F., Robertson, E. J., Constam, D. B., 2006. The nodal precursor acting via activin receptors induces mesoderm by maintaining a source of its convertases and BMP4. Dev Cell. 11**,** 313-23.

Berg, D. K., Smith, C. S., Pearton, D. J., Wells, D. N., Broadhurst, R., Donnison, M., Pfeffer, P. L., 2011. Trophectoderm lineage determination in cattle. Dev Cell. 20**,** 244-55.

Bertocchini, F., Stern, C. D., 2002. The hypoblast of the chick embryo positions the primitive streak by antagonizing nodal signaling. Dev Cell. 3**,** 735-44.

Bielinska, M., Narita, N., Wilson, D. B., 1999. Distinct roles for visceral endoderm during embryonic mouse development. Int J Dev Biol. 43**,** 183-205.

Bin, Z., Sheng, L. G., Gang, Z. C., Hong, J., Jun, C., Bo, Y., Hui, S., 2006. Efficient cardiomyocyte differentiation of embryonic stem cells by bone morphogenetic protein-2 combined with visceral endoderm-like cells. Cell Biol Int. 30**,** 769-76.

Bradley, A., Evans, M., Kaufman, M. H., Robertson, E., 1984. Formation of germ-line chimaeras from embryo-derived teratocarcinoma cell lines. Nature. 309**,** 255-6.

Brennan, J., Lu, C. C., Norris, D. P., Rodriguez, T. A., Beddington, R. S., Robertson, E. J., 2001. Nodal signalling in the epiblast patterns the early mouse embryo. Nature. 411**,** 965-9.

Brinster, R. L., 1974. The effect of cells transferred into the mouse blastocyst on subsequent development. J Exp Med. 140**,** 1049-56.

Brons, I. G., Smithers, L. E., Trotter, M. W., Rugg-Gunn, P., Sun, B., Chuva de Sousa Lopes, S. M., Howlett, S. K., Clarkson, A., Ahrlund-Richter, L., Pedersen, R. A., Vallier, L., 2007. Derivation of pluripotent epiblast stem cells from mammalian embryos. Nature. 448**,** 191-5.

Brown, K., Doss, M. X., Legros, S., Artus, J., Hadjantonakis, A. K., Foley, A. C., 2010a. eXtraembryonic ENdoderm (XEN) stem cells produce factors that activate heart formation. PLoS One. 5**,** e13446.

Brown, K., Legros, S., Artus, J., Doss, M. X., Khanin, R., Hadjantonakis, A. K., Foley, A., 2010b. A comparative analysis of extra-embryonic endoderm cell lines. PLoS One. 5**,** e12016.

Byrd, N., Becker, S., Maye, P., Narasimhaiah, R., St-Jacques, B., Zhang, X., McMahon, J., McMahon, A., Grabel, L., 2002. Hedgehog is required for murine yolk sac angiogenesis. Development. 129**,** 361-72.

Canham, M. A., Sharov, A. A., Ko, M. S., Brickman, J. M., 2010. Functional heterogeneity of embryonic stem cells revealed through translational amplification of an early endodermal transcript. PLoS Biol. 8**,** e1000379.

Cano, A., Perez-Moreno, M. A., Rodrigo, I., Locascio, A., Blanco, M. J., del Barrio, M. G., Portillo, F., Nieto, M. A., 2000. The transcription factor snail controls epithelial-mesenchymal transitions by repressing E-cadherin expression. Nat Cell Biol. 2**,** 76-83.

Capo-Chichi, C. D., Rula, M. E., Smedberg, J. L., Vanderveer, L., Parmacek, M. S., Morrisey, E. E., Godwin, A. K., Xu, X. X., 2005. Perception of differentiation cues by GATA factors in primitive endoderm lineage determination of mouse embryonic stem cells. Dev Biol. 286**,** 574-86.

Carver, E. A., Jiang, R., Lan, Y., Oram, K. F., Gridley, T., 2001. The mouse snail gene encodes a key regulator of the epithelial-mesenchymal transition. Mol Cell Biol. 21**,** 8184-8.

Chambers, S. M., Fasano, C. A., Papapetrou, E. P., Tomishima, M., Sadelain, M., Studer, L., 2009. Highly efficient neural conversion of human ES and iPS cells by dual inhibition of SMAD signalling. Nature Biotechnology. 27**,** 275-280.

Chang, H., Huylebroeck, D., Verschueren, K., Guo, Q., Matzuk, M. M., Zwijsen, A., 1999. Smad5 knockout mice die at mid-gestation due to multiple embryonic and extraembryonic defects. Development. 126**,** 1631-42.

Chao, C. H., Wang, H. D., Yuh, C. H., 2010. Complexity of cis-regulatory organization of six3a during forebrain and eye development in zebrafish. BMC Dev Biol. 10**,** 35.

Chapman, S. C., Schubert, F. R., Schoenwolf, G. C., Lumsden, A., 2003. Anterior identity is established in chick epiblast by hypoblast and anterior definitive endoderm. Development. 130**,** 5091-101.

Chapman, V., Forrester, L., Sanford, J., Hastie, N., Rossant, J., 1984. Cell lineage-specific undermethylation of mouse repetitive DNA. Nature. 307**,** 284-6.

Chazaud, C., Rossant, J., 2006. Disruption of early proximodistal patterning and AVE formation in Apc mutants. Development. 133**,** 3379-87.

Chazaud, C., Yamanaka, Y., Pawson, T., Rossant, J., 2006. Early lineage segregation between epiblast and primitive endoderm in mouse blastocysts through the Grb2-MAPK pathway. Dev Cell. 10**,** 615-24.

Chen, H. W., Chen, J. J., Yu, S. L., Li, H. N., Yang, P. C., Su, C. M., Au, H. K., Chang, C. W., Chien, L. W., Chen, C. S., Tzeng, C. R., 2005. Transcriptome analysis in blastocyst hatching by cDNA microarray. Hum Reprod. 20**,** 2492-501.

Chen, W. S., Manova, K., Weinstein, D. C., Duncan, S. A., Plump, A. S., Prezioso, V. R., Bachvarova, R. F., Darnell, J. E., Jr., 1994. Disruption of the HNF-4 gene, expressed in visceral endoderm, leads to cell death in embryonic

ectoderm and impaired gastrulation of mouse embryos. Genes Dev. 8**,** 2466-77.

Cheng, A. M., Saxton, T. M., Sakai, R., Kulkarni, S., Mbamalu, G., Vogel, W., Tortorice, C. G., Cardiff, R. D., Cross, J. C., Muller, W. J., Pawson, T., 1998. Mammalian Grb2 regulates multiple steps in embryonic development and malignant transformation. Cell. 95**,** 793-803.

Chung, Y., Klimanskaya, I., Becker, S., Marh, J., Lu, S. J., Johnson, J., Meisner, L., Lanza, R., 2006. Embryonic and extraembryonic stem cell lines derived from single mouse blastomeres. Nature. 439**,** 216-9.

Chuykin, I., Lapidus, I., Popova, E., Vilianovich, L., Mosienko, V., Alenina, N., Binas, B., Chai, G., Bader, M., Krivokharchenko, A., 2010. Characterization of trophoblast and extraembryonic endoderm cell lineages derived from rat preimplantation embryos. PLoS One. 5**,** e9794.

Clements, M., Pernaute, B., Vella, F., Rodriguez, T. A., 2011. Crosstalk between Nodal/activin and MAPK p38 signaling is essential for anterior-posterior axis specification. Curr Biol. 21**,** 1289-95.

Coffinier, C., Barra, J., Babinet, C., Yaniv, M., 1999. Expression of the vHNF1/HNF1beta homeoprotein gene during mouse organogenesis. Mech Dev. 89**,** 211-3.

Cohen, M. M., Jr., 2006. Holoprosencephaly: clinical, anatomic, and molecular dimensions. Birth Defects Res A Clin Mol Teratol. 76**,** 658-73.

Comijn, J., Berx, G., Vermassen, P., Verschueren, K., van Grunsven, L., Bruyneel, E., Mareel, M., Huylebroeck, D., van Roy, F., 2001. The two-handed E box binding zinc finger protein SIP1 downregulates E-cadherin and induces invasion. Mol Cell. 7**,** 1267-78.

Corson, L. B., Yamanaka, Y., Lai, K. M., Rossant, J., 2003. Spatial and temporal patterns of ERK signaling during mouse embryogenesis. Development. 130**,** 4527-37.

Coucouvanis, E., Martin, G. R., 1995. Signals for death and survival: a two-step mechanism for cavitation in the vertebrate embryo. Cell. 83**,** 279-87.

Coucouvanis, E., Martin, G. R., 1999. BMP signaling plays a role in visceral endoderm differentiation and cavitation in the early mouse embryo. Development. 126**,** 535-46.

Cross, J. C., Werb, Z., Fisher, S. J., 1994. Implantation and the placenta: key pieces of the development puzzle. Science. 266**,** 1508-18.

Damert, A., Miquerol, L., Gertsenstein, M., Risau, W., Nagy, A., 2002. Insufficient VEGFA activity in yolk sac endoderm compromises haematopoietic and endothelial differentiation. Development. 129**,** 1881-92.

de Sousa Lopes, S. M., Hayashi, K., Surani, M. A., 2007. Proximal visceral endoderm and extraembryonic ectoderm regulate the formation of primordial germ cell precursors. BMC Dev Biol. 7**,** 140.

de Sousa Lopes, S. M., Roelen, B. A., Monteiro, R. M., Emmens, R., Lin, H. Y., Li, E., Lawson, K. A., Mummery, C. L., 2004. BMP signaling mediated by ALK2 in the visceral endoderm is necessary for the generation of primordial germ cells in the mouse embryo. Genes Dev. 18**,** 1838-49.

Debeb, B. G., Galat, V., Epple-Farmer, J., Iannaccone, S., Woodward, W. A., Bader, M., Iannaccone, P., Binas, B., 2009. Isolation of Oct4-expressing extraembryonic endoderm precursor cell lines. PLoS One. 4**,** e7216.

Derynck, R., Zhang, Y. E., 2003. Smad-dependent and Smad-independent pathways in TGF-beta family signalling. Nature. 425**,** 577-84.

Di-Gregorio, A., Sancho, M., Stuckey, D. W., Crompton, L. A., Godwin, J., Mishina, Y., Rodriguez, T. A., 2007. BMP signalling inhibits premature neural differentiation in the mouse embryo. Development. 134**,** 3359-69.

Dickson, A. D., 1979. The disappearance of the decidua capsularis and Reichert's membrane in the mouse. J Anat. 129**,** 571-7.

Ding, J., Yang, L., Yan, Y. T., Chen, A., Desai, N., Wynshaw-Boris, A., Shen, M. M., 1998. Cripto is required for correct orientation of the anterior-posterior axis in the mouse embryo. Nature. 395**,** 702-7.

Domene, S., Roessler, E., El-Jaick, K. B., Snir, M., Brown, J. L., Velez, J. I., Bale, S., Lacbawan, F., Muenke, M., Feldman, B., 2008. Mutations in the human SIX3 gene in holoprosencephaly are loss of function. Hum Mol Genet. 17**,** 3919-28.

Dufort, D., Schwartz, L., Harpal, K., Rossant, J., 1998. The transcription factor HNF3beta is required in visceral endoderm for normal primitive streak morphogenesis. Development. 125**,** 3015-25.

Duncan, S. A., Manova, K., Chen, W. S., Hoodless, P., Weinstein, D. C., Bachvarova, R. F., Darnell, J. E., Jr., 1994. Expression of transcription factor HNF-4 in the extraembryonic endoderm, gut, and nephrogenic tissue of the developing mouse embryo: HNF-4 is a marker for primary endoderm in the implanting blastocyst. Proc Natl Acad Sci U S A. 91**,** 7598-602.

Duncan, S. A., Nagy, A., Chan, W., 1997. Murine gastrulation requires HNF-4 regulated gene expression in the visceral endoderm: tetraploid rescue of Hnf-4(-/-) embryos. Development. 124**,** 279-87.

Dyer, M. A., Farrington, S. M., Mohn, D., Munday, J. R., Baron, M. H., 2001. Indian hedgehog activates hematopoiesis and vasculogenesis and can respecify prospective neurectodermal cell fate in the mouse embryo. Development. 128**,** 1717-30.

Dziadek, M., 1978. Modulation of alphafetoprotein synthesis in the early postimplantation mouse embryo. J Embryol Exp Morphol. 46**,** 135-46.

Dziadek, M., Adamson, E., 1978. Localization and synthesis of alphafoetoprotein in post-implantation mouse embryos. J Embryol Exp Morphol. 43**,** 289-313.

Enders, A. C., Given, R. L., Schlafke, S., 1978. Differentiation and migration of endoderm in the rat and mouse at implantation. Anat Rec. 190**,** 65-77.

Evans, M., 2011. Discovering pluripotency: 30 years of mouse embryonic stem cells. Nat Rev Mol Cell Biol. 12**,** 680-6.

Evans, M. J., Kaufman, M. H., 1981. Establishment in culture of pluripotential cells from mouse embryos. Nature. 292**,** 154-6.

Feldman, B., Poueymirou, W., Papaioannou, V. E., DeChiara, T. M., Goldfarb, M., 1995. Requirement of FGF-4 for postimplantation mouse development. Science. 267**,** 246-9.

Fleming, T. P., 1987. A quantitative analysis of cell allocation to trophectoderm and inner cell mass in the mouse blastocyst. Dev Biol. 119**,** 520-31.

Fowler, K. J., Mitrangas, K., Dziadek, M., 1990. In vitro production of Reichert's membrane by mouse embryo-derived parietal endoderm cell lines. Exp Cell Res. 191**,** 194-203.

Fujikura, J., Yamato, E., Yonemura, S., Hosoda, K., Masui, S., Nakao, K., Miyazaki Ji, J., Niwa, H., 2002. Differentiation of embryonic stem cells is induced by GATA factors. Genes Dev. 16**,** 784-9.

Futaki, S., Hayashi, Y., Emoto, T., Weber, C. N., Sekiguchi, K., 2004. Sox7 plays crucial roles in parietal endoderm differentiation in F9 embryonal carcinoma cells through regulating Gata-4 and Gata-6 expression. Mol Cell Biol. 24**,** 10492-503.

Gardner, R. L., 1982. Investigation of cell lineage and differentiation in the extraembryonic endoderm of the mouse embryo. J Embryol Exp Morphol. 68**,** 175-98.

Gardner, R. L., 1993. Extrinsic factors in cellular differentiation. Int J Dev Biol. 37**,** 47-50.

Gardner, R. L., Davies, T. J., 1992. Environmental factors and the stability of differentiation in mammalian development. C R Acad Sci III. 314**,** 67-9.

Gasperowicz, M., Natale, D. R., 2011. Establishing three blastocyst lineages--then what? Biol Reprod. 84**,** 621-30.

Geng, X., Speirs, C., Lagutin, O., Inbal, A., Liu, W., Solnica-Krezel, L., Jeong, Y., Epstein, D. J., Oliver, G., 2008. Haploinsufficiency of Six3 fails to activate Sonic hedgehog expression in the ventral forebrain and causes holoprosencephaly. Dev Cell. 15**,** 236-47.

Gerbe, F., Cox, B., Rossant, J., Chazaud, C., 2008. Dynamic expression of Lrp2 pathway members reveals progressive epithelial differentiation of primitive endoderm in mouse blastocyst. Dev Biol. 313**,** 594-602.

Gersdorff, N., Muller, M., Otto, S., Poschadel, R., Hubner, S., Miosge, N., 2005. Basement membrane composition in the early mouse embryo day 7. Dev Dyn. 233**,** 1140-8.

Glinka, A., Wu, W., Delius, H., Monaghan, A. P., Blumenstock, C., Niehrs, C., 1998. Dickkopf-1 is a member of a new family of secreted proteins and functions in head induction. Nature. 391**,** 357-62.

Goudreau, G., Petrou, P., Reneker, L. W., Graw, J., Loster, J., Gruss, P., 2002. Mutually regulated expression of Pax6 and Six3 and its implications for the Pax6 haploinsufficient lens phenotype. Proc Natl Acad Sci U S A. 99**,** 8719-24.

Grabarek, J. B., Zyzynska, K., Saiz, N., Piliszek, A., Frankenberg, S., Nichols, J., Hadjantonakis, A. K., Plusa, B., 2012. Differential plasticity of epiblast and primitive endoderm precursors within the ICM of the early mouse embryo. Development. 139**,** 129-39.

Granier, C., Gurchenkov, V., Perea-Gomez, A., Camus, A., Ott, S., Papanayotou, C., Iranzo, J., Moreau, A., Reid, J., Koentges, G., Saberan-Djoneidi, D., Collignon, J., 2011. Nodal cis-regulatory elements reveal epiblast and primitive endoderm heterogeneity in the peri-implantation mouse embryo. Dev Biol. 349**,** 350-62.

Grover, A., Andrews, G., Adamson, E. D., 1983. Role of laminin in epithelium formation by F9 aggregates. J Cell Biol. 97**,** 137-44.

Gu, Z., Nomura, M., Simpson, B. B., Lei, H., Feijen, A., van den Eijnden-van Raaij, J., Donahoe, P. K., Li, E., 1998. The type I activin receptor ActRIB is required for egg cylinder organization and gastrulation in the mouse. Genes Dev. 12**,** 844-57.

Gu, Z., Reynolds, E. M., Song, J., Lei, H., Feijen, A., Yu, L., He, W., MacLaughlin, D. T., van den Eijnden-van Raaij, J., Donahoe, P. K., Li, E., 1999. The type I serine/threonine kinase receptor ActRIA (ALK2) is required for gastrulation of the mouse embryo. Development. 126**,** 2551-61.

Guo, G., Huss, M., Tong, G. Q., Wang, C., Li Sun, L., Clarke, N. D., Robson, P., 2010. Resolution of cell fate decisions revealed by single-cell gene expression analysis from zygote to blastocyst. Dev Cell. 18**,** 675-85.

Hamazaki, T., Kehoe, S. M., Nakano, T., Terada, N., 2006. The Grb2/Mek pathway represses Nanog in murine embryonic stem cells. Mol Cell Biol. 26**,** 7539-49.

Harris, T. M., Childs, G., 2002. Global gene expression patterns during differentiation of F9 embryonal carcinoma cells into parietal endoderm. Funct Integr Genomics. 2**,** 105-19.

Hochedlinger, K., Plath, K., 2009. Epigenetic reprogramming and induced pluripotency. Development. 136**,** 509-23.

Hockemeyer, D., Soldner, F., Beard, C., Gao, Q., Mitalipova, M., DeKelver, R. C., Katibah, G. E., Amora, R., Boydston, E. A., Zeitler, B., Meng, X., Miller, J. C., Zhang, L., Rebar, E. J., Gregory, P. D., Urnov, F. D., Jaenisch, R., 2009. Efficient targeting of expressed and silent genes in human ESCs and iPSCs using zinc-finger nucleases. Nat Biotechnol. 27**,** 851-7.

Hockemeyer, D., Wang, H., Kiani, S., Lai, C. S., Gao, Q., Cassady, J. P., Cost, G. J., Zhang, L., Santiago, Y., Miller, J. C., Zeitler, B., Cherone, J. M., Meng, X., Hinkley, S. J., Rebar, E. J., Gregory, P. D., Urnov, F. D., Jaenisch, R., 2011. Genetic engineering of human pluripotent cells using TALE nucleases. Nat Biotechnol. 29**,** 731-4.

Hogan, B. L., Cooper, A. R., Kurkinen, M., 1980. Incorporation into Reichert's membrane of laminin-like extracellular proteins synthesized by parietal endoderm cells of the mouse embryo. Dev Biol. 80**,** 289-300.

Hogan, B. L., Newman, R., 1984. A scanning electron microscope study of the extraembryonic endoderm of the 8th-day mouse embryo. Differentiation. 26**,** 138-43.

Hogan, B. L., Tilly, R., 1981. Cell interactions and endoderm differentiation in cultured mouse embryos. J Embryol Exp Morphol. 62**,** 379-94.

Hong, S., Kang, U. J., Isacson, O., Kim, K. S., 2008. Neural precursors derived from human embryonic stem cells maintain long-term proliferation without losing the potential to differentiate into all three neural lineages, including dopaminergic neurons. J Neurochem. 104**,** 316-24.

Hood, J. D., Cheresh, D. A., 2002. Role of integrins in cell invasion and migration. Nat Rev Cancer. 2**,** 91-100.

Huangfu, D., Maehr, R., Guo, W., Eijkelenboom, A., Snitow, M., Chen, A. E., Melton, D. A., 2008. Induction of pluripotent stem cells by defined factors is greatly improved by small-molecule compounds. Nat Biotechnol. 26**,** 795-7.

Huelsken, J., Vogel, R., Brinkmann, V., Erdmann, B., Birchmeier, C., Birchmeier, W., 2000. Requirement for beta-catenin in anterior-posterior axis formation in mice. J Cell Biol. 148**,** 567-78.

Idelson, M., Alper, R., Obolensky, A., Ben-Shushan, E., Hemo, I., Yachimovich-Cohen, N., Khaner, H., Smith, Y., Wiser, O., Gropp, M., Cohen, M. A., Even-Ram, S., Berman-Zaken, Y., Matzrafi, L., Rechavi, G., Banin, E.,

Reubinoff, B., 2009. Directed differentiation of human embryonic stem cells into functional retinal pigment epithelium cells. Cell Stem Cell. 5**,** 396-408.
Inbal, A., Kim, S. H., Shin, J., Solnica-Krezel, L., 2007. Six3 represses nodal activity to establish early brain asymmetry in zebrafish. Neuron. 55**,** 407-15.
Itsykson, P., Ilouz, N., Turetsky, T., Goldstein, R. S., Pera, M. F., Fishbein, I., Segal, M., Reubinoff, B. E., 2005. Derivation of neural precursors from human embryonic stem cells in the presence of noggin. Mol Cell Neurosci. 30**,** 24-36.
James, D., Levine, A. J., Besser, D., Hemmati-Brivanlou, A., 2005. TGFbeta/activin/nodal signaling is necessary for the maintenance of pluripotency in human embryonic stem cells. Development. 132**,** 1273-82.
Jensen, M. A., Koszalka, T. R., Brent, R. L., 1975. Production of congenital malformations using tissue antisera. Dev Biol. 42**,** 1-12.
Jeong, Y., Leskow, F. C., El-Jaick, K., Roessler, E., Muenke, M., Yocum, A., Dubourg, C., Li, X., Geng, X., Oliver, G., Epstein, D. J., 2008. Regulation of a remote Shh forebrain enhancer by the Six3 homeoprotein. Nat Genet. 40**,** 1348-53.
Johansson, S., Gustafson, A. L., Donovan, M., Romert, A., Eriksson, U., Dencker, L., 1997. Retinoid binding proteins in mouse yolk sac and chorio-allantoic placentas. Anat Embryol (Berl). 195**,** 483-90.
Johnson, M. H., Ziomek, C. A., 1981. Induction of polarity in mouse 8-cell blastomeres: specificity, geometry, and stability. J Cell Biol. 91**,** 303-8.
Jollie, W. P., 1990. Development, morphology, and function of the yolk-sac placenta of laboratory rodents. Teratology. 41**,** 361-81.
Kadokawa, Y., Fuketa, I., Nose, A., Takeichi, M., Nakatsuji, N., 1989. Expression pattern of E- and P-cadherin in mouse embryos and uteri during the periimplantation period. Development, growth & differentiation. 31**,** 23-30.
Kanai-Azuma, M., Kanai, Y., Gad, J. M., Tajima, Y., Taya, C., Kurohmaru, M., Sanai, Y., Yonekawa, H., Yazaki, K., Tam, P. P., Hayashi, Y., 2002. Depletion of definitive gut endoderm in Sox17-null mutant mice. Development. 129**,** 2367-79.
Karaplis, A. C., Kronenberg, H. M., 1996. Physiological roles for parathyroid hormone-related protein: lessons from gene knockout mice. Vitam Horm. 52**,** 177-93.
Kawano, Y., Kypta, R., 2003. Secreted antagonists of the Wnt signalling pathway. J Cell Sci. 116**,** 2627-34.
Kelly, S. J., 1977. Studies of the developmental potential of 4- and 8-cell stage mouse blastomeres. J Exp Zool. 200**,** 365-76.
Kim, Y. G., Cha, J., Chandrasegaran, S., 1996. Hybrid restriction enzymes: zinc finger fusions to Fok I cleavage domain. Proc Natl Acad Sci U S A. 93**,** 1156-60.
Kimura-Yoshida, C., Nakano, H., Okamura, D., Nakao, K., Yonemura, S., Belo, J. A., Aizawa, S., Matsui, Y., Matsuo, I., 2005. Canonical Wnt signaling and its antagonist regulate anterior-posterior axis polarization by guiding cell migration in mouse visceral endoderm. Dev Cell. 9**,** 639-50.
Kimura-Yoshida, C., Tian, E., Nakano, H., Amazaki, S., Shimokawa, K., Rossant, J., Aizawa, S., Matsuo, I., 2007. Crucial roles of Foxa2 in mouse anterior-

posterior axis polarization via regulation of anterior visceral endoderm-specific genes. Proc Natl Acad Sci U S A. 104**,** 5919-24.

Kimura, C., Yoshinaga, K., Tian, E., Suzuki, M., Aizawa, S., Matsuo, I., 2000. Visceral endoderm mediates forebrain development by suppressing posteriorizing signals. Dev Biol. 225**,** 304-21.

Korpal, M., Lee, E. S., Hu, G., Kang, Y., 2008. The miR-200 family inhibits epithelial-mesenchymal transition and cancer cell migration by direct targeting of E-cadherin transcriptional repressors ZEB1 and ZEB2. J Biol Chem. 283**,** 14910-4.

Koutsourakis, M., Langeveld, A., Patient, R., Beddington, R., Grosveld, F., 1999. The transcription factor GATA6 is essential for early extraembryonic development. Development. 126**,** 723-32.

Kovacs, C. S., Chafe, L. L., Woodland, M. L., McDonald, K. R., Fudge, N. J., Wookey, P. J., 2002. Calcitropic gene expression suggests a role for the intraplacental yolk sac in maternal-fetal calcium exchange. Am J Physiol Endocrinol Metab. 282**,** E721-32.

Kruithof-de Julio, M., Alvarez, M. J., Galli, A., Chu, J., Price, S. M., Califano, A., Shen, M. M., 2011. Regulation of extra-embryonic endoderm stem cell differentiation by Nodal and Cripto signaling. Development. 138**,** 3885-95.

Kunath, T., Arnaud, D., Uy, G. D., Okamoto, I., Chureau, C., Yamanaka, Y., Heard, E., Gardner, R. L., Avner, P., Rossant, J., 2005. Imprinted X-inactivation in extra-embryonic endoderm cell lines from mouse blastocysts. Development. 132**,** 1649-61.

Kurimoto, K., Yabuta, Y., Ohinata, Y., Ono, Y., Uno, K. D., Yamada, R. G., Ueda, H. R., Saitou, M., 2006. An improved single-cell cDNA amplification method for efficient high-density oligonucleotide microarray analysis. Nucleic Acids Res. 34**,** e42.

Kurokawa, D., Takasaki, N., Kiyonari, H., Nakayama, R., Kimura-Yoshida, C., Matsuo, I., Aizawa, S., 2004. Regulation of Otx2 expression and its functions in mouse epiblast and anterior neuroectoderm. Development. 131**,** 3307-17.

Kwon, G. S., Fraser, S. T., Eakin, G. S., Mangano, M., Isern, J., Sahr, K. E., Hadjantonakis, A. K., Baron, M. H., 2006. Tg(Afp-GFP) expression marks primitive and definitive endoderm lineages during mouse development. Dev Dyn. 235**,** 2549-58.

Kwon, G. S., Viotti, M., Hadjantonakis, A. K., 2008. The endoderm of the mouse embryo arises by dynamic widespread intercalation of embryonic and extraembryonic lineages. Dev Cell. 15**,** 509-20.

Lagutin, O. V., Zhu, C. C., Kobayashi, D., Topczewski, J., Shimamura, K., Puelles, L., Russell, H. R., McKinnon, P. J., Solnica-Krezel, L., Oliver, G., 2003. Six3 repression of Wnt signaling in the anterior neuroectoderm is essential for vertebrate forebrain development. Genes Dev. 17**,** 368-79.

Lamba, D. A., Karl, M. O., Ware, C. B., Reh, T. A., 2006. Efficient generation of retinal progenitor cells from human embryonic stem cells. Proc Natl Acad Sci U S A. 103**,** 12769-74.

Lane, E. B., Hogan, B. L., Kurkinen, M., Garrels, J. I., 1983. Co-expression of vimentin and cytokeratins in parietal endoderm cells of early mouse embryo. Nature. 303**,** 701-4.

Lanske, B., Karaplis, A. C., Lee, K., Luz, A., Vortkamp, A., Pirro, A., Karperien, M., Defize, L. H., Ho, C., Mulligan, R. C., Abou-Samra, A. B., Juppner, H., Segre, G. V., Kronenberg, H. M., 1996. PTH/PTHrP receptor in early development and Indian hedgehog-regulated bone growth. Science. 273**,** 663-6.

Lavado, A., Lagutin, O. V., Oliver, G., 2008. Six3 inactivation causes progressive caudalization and aberrant patterning of the mammalian diencephalon. Development. 135**,** 441-50.

Lawson, K. A., Dunn, N. R., Roelen, B. A., Zeinstra, L. M., Davis, A. M., Wright, C. V., Korving, J. P., Hogan, B. L., 1999. Bmp4 is required for the generation of primordial germ cells in the mouse embryo. Genes Dev. 13**,** 424-36.

Lawson, K. A., Meneses, J. J., Pedersen, R. A., 1986. Cell fate and cell lineage in the endoderm of the presomite mouse embryo, studied with an intracellular tracer. Dev Biol. 115**,** 325-39.

Lawson, K. A., Pedersen, R. A., 1987. Cell fate, morphogenetic movement and population kinetics of embryonic endoderm at the time of germ layer formation in the mouse. Development. 101**,** 627-52.

Leivo, I., Wartiovaara, J., 1989. Basement membrane matrices in mouse embryogenesis, teratocarcinoma differentiation and in neuromuscular maturation. Int J Dev Biol. 33**,** 81-9.

Lengler, J., Graw, J., 2001. Regulation of the human SIX3 gene promoter. Biochem Biophys Res Commun. 287**,** 372-6.

Li, J., Zhang, J. V., Cao, Y. J., Zhou, J. X., Liu, W. M., Fan, X. J., Duan, E. K., 2005. Inhibition of the beta-catenin signaling pathway in blastocyst and uterus during the window of implantation in mice. Biol Reprod. 72**,** 700-6.

Li, L., Arman, E., Ekblom, P., Edgar, D., Murray, P., Lonai, P., 2004. Distinct GATA6- and laminin-dependent mechanisms regulate endodermal and ectodermal embryonic stem cell fates. Development. 131**,** 5277-86.

Lim, C. Y., Tam, W. L., Zhang, J., Ang, H. S., Jia, H., Lipovich, L., Ng, H. H., Wei, C. L., Sung, W. K., Robson, P., Yang, H., Lim, B., 2008. Sall4 regulates distinct transcription circuitries in different blastocyst-derived stem cell lineages. Cell Stem Cell. 3**,** 543-54.

Liu, J., He, X., Corbett, S. A., Lowry, S. F., Graham, A. M., Fassler, R., Li, S., 2009. Integrins are required for the differentiation of visceral endoderm. J Cell Sci. 122**,** 233-42.

Liu, P., Wakamiya, M., Shea, M. J., Albrecht, U., Behringer, R. R., Bradley, A., 1999. Requirement for Wnt3 in vertebrate axis formation. Nat Genet. 22**,** 361-5.

Liu, W., Lagutin, O., Swindell, E., Jamrich, M., Oliver, G., 2010. Neuroretina specification in mouse embryos requires Six3-mediated suppression of Wnt8b in the anterior neural plate. J Clin Invest. 120**,** 3568-77.

Liu, W., Lagutin, O. V., Mende, M., Streit, A., Oliver, G., 2006. Six3 activation of Pax6 expression is essential for mammalian lens induction and specification. Embo J. 25**,** 5383-95.

Lloyd, A., Plaisier, C. L., Carroll, D., Drews, G. N., 2005. Targeted mutagenesis using zinc-finger nucleases in Arabidopsis. Proc Natl Acad Sci U S A. 102**,** 2232-7.

Loosli, F., Winkler, S., Wittbrodt, J., 1999. Six3 overexpression initiates the formation of ectopic retina. Genes Dev. 13**,** 649-54.

Lowell, S., Benchoua, A., Heavey, B., Smith, A. G., 2006. Notch promotes neural lineage entry by pluripotent embryonic stem cells. PLoS Biol. 4**,** e121.

MacDonald, B. T., Tamai, K., He, X., 2009. Wnt/beta-catenin signaling: components, mechanisms, and diseases. Dev Cell. 17**,** 9-26.

Madabhushi, M., Lacy, E., 2011. Anterior Visceral Endoderm Directs Ventral Morphogenesis and Placement of Head and Heart via BMP2 Expression. Dev Cell. 21**,** 907-19.

Maeder, M. L., Thibodeau-Beganny, S., Osiak, A., Wright, D. A., Anthony, R. M., Eichtinger, M., Jiang, T., Foley, J. E., Winfrey, R. J., Townsend, J. A., Unger-Wallace, E., Sander, J. D., Muller-Lerch, F., Fu, F., Pearlberg, J., Gobel, C., Dassie, J. P., Pruett-Miller, S. M., Porteus, M. H., Sgroi, D. C., Iafrate, A. J., Dobbs, D., McCray, P. B., Jr., Cathomen, T., Voytas, D. F., Joung, J. K., 2008. Rapid "open-source" engineering of customized zinc-finger nucleases for highly efficient gene modification. Mol Cell. 31**,** 294-301.

Manavathi, B., Peng, S., Rayala, S. K., Talukder, A. H., Wang, M. H., Wang, R. A., Balasenthil, S., Agarwal, N., Frishman, L. J., Kumar, R., 2007. Repression of Six3 by a corepressor regulates rhodopsin expression. Proc Natl Acad Sci U S A. 104**,** 13128-33.

Mani, M., Smith, J., Kandavelou, K., Berg, J. M., Chandrasegaran, S., 2005. Binding of two zinc finger nuclease monomers to two specific sites is required for effective double-strand DNA cleavage. Biochem Biophys Res Commun. 334**,** 1191-7.

Martin, G. R., 1981. Isolation of a pluripotent cell line from early mouse embryos cultured in medium conditioned by teratocarcinoma stem cells. Proc Natl Acad Sci U S A. 78**,** 7634-8.

Martin, G. R., Evans, M. J., 1975. Differentiation of clonal lines of teratocarcinoma cells: formation of embryoid bodies in vitro. Proc Natl Acad Sci U S A. 72**,** 1441-5.

Massague, J., 2008. A very private TGF-beta receptor embrace. Mol Cell. 29**,** 149-50.

Maurer, M. E., Cooper, J. A., 2005. Endocytosis of megalin by visceral endoderm cells requires the Dab2 adaptor protein. J Cell Sci. 118**,** 5345-55.

Maye, P., Becker, S., Kasameyer, E., Byrd, N., Grabel, L., 2000. Indian hedgehog signaling in extraembryonic endoderm and ectoderm differentiation in ES embryoid bodies. Mech Dev. 94**,** 117-32.

McGrath, K. E., Palis, J., 2005. Hematopoiesis in the yolk sac: more than meets the eye. Exp Hematol. 33**,** 1021-8.

Meehan, R. R., Barlow, D. P., Hill, R. E., Hogan, B. L., Hastie, N. D., 1984. Pattern of serum protein gene expression in mouse visceral yolk sac and foetal liver. Embo J. 3**,** 1881-5.

Meng, X., Noyes, M. B., Zhu, L. J., Lawson, N. D., Wolfe, S. A., 2008. Targeted gene inactivation in zebrafish using engineered zinc-finger nucleases. Nat Biotechnol. 26**,** 695-701.

Mesnard, D., Guzman-Ayala, M., Constam, D. B., 2006. Nodal specifies embryonic visceral endoderm and sustains pluripotent cells in the epiblast before overt axial patterning. Development. 133**,** 2497-505.

Migeotte, I., Omelchenko, T., Hall, A., Anderson, K. V., 2010. Rac1-dependent collective cell migration is required for specification of the anterior-posterior body axis of the mouse. PLoS Biol. 8**,** e1000442.

Mishina, Y., Suzuki, A., Ueno, N., Behringer, R. R., 1995. Bmpr encodes a type I bone morphogenetic protein receptor that is essential for gastrulation during mouse embryogenesis. Genes Dev. 9**,** 3027-37.

Miura, S., Mishina, Y., 2007. The DVE changes distal epiblast fate from definitive endoderm to neurectoderm by antagonizing nodal signaling. Dev Dyn. 236**,** 1602-10.

Miura, S., Singh, A. P., Mishina, Y., 2010. Bmpr1a is required for proper migration of the AVE through regulation of Dkk1 expression in the pre-streak mouse embryo. Dev Biol. 341**,** 246-54.

Monk, M., Boubelik, M., Lehnert, S., 1987. Temporal and regional changes in DNA methylation in the embryonic, extraembryonic and germ cell lineages during mouse embryo development. Development. 99**,** 371-82.

Morris, S. A., Grewal, S., Barrios, F., Patankar, S. N., Strauss, B., Buttery, L., Alexander, M., Shakesheff, K. M., Zernicka-Goetz, M., 2012. Dynamics of anterior-posterior axis formation in the developing mouse embryo. Nat Commun. 3**,** 673.

Morris, S. A., Teo, R. T., Li, H., Robson, P., Glover, D. M., Zernicka-Goetz, M., 2010. Origin and formation of the first two distinct cell types of the inner cell mass in the mouse embryo. Proc Natl Acad Sci U S A. 107**,** 6364-9.

Morris, S. M., Tallquist, M. D., Rock, C. O., Cooper, J. A., 2002. Dual roles for the Dab2 adaptor protein in embryonic development and kidney transport. Embo J. 21**,** 1555-64.

Morrisey, E. E., Ip, H. S., Lu, M. M., Parmacek, M. S., 1996. GATA-6: a zinc finger transcription factor that is expressed in multiple cell lineages derived from lateral mesoderm. Dev Biol. 177**,** 309-22.

Morrisey, E. E., Musco, S., Chen, M. Y., Lu, M. M., Leiden, J. M., Parmacek, M. S., 2000. The gene encoding the mitogen-responsive phosphoprotein Dab2 is differentially regulated by GATA-6 and GATA-4 in the visceral endoderm. J Biol Chem. 275**,** 19949-54.

Morrisey, E. E., Tang, Z., Sigrist, K., Lu, M. M., Jiang, F., Ip, H. S., Parmacek, M. S., 1998. GATA6 regulates HNF4 and is required for differentiation of visceral endoderm in the mouse embryo. Genes Dev. 12**,** 3579-90.

Morrison, G. M., Oikonomopoulou, I., Migueles, R. P., Soneji, S., Livigni, A., Enver, T., Brickman, J. M., 2008. Anterior definitive endoderm from ESCs reveals a role for FGF signaling. Cell Stem Cell. 3**,** 402-15.

Mruthyunjaya, S., Manchanda, R., Godbole, R., Pujari, R., Shiras, A., Shastry, P., 2010. Laminin-1 induces neurite outgrowth in human mesenchymal stem cells in serum/differentiation factors-free conditions through activation of FAK-MEK/ERK signaling pathways. Biochem Biophys Res Commun. 391**,** 43-8.

Murakami, K., Araki, K., Ohtsuka, S., Wakayama, T., Niwa, H., 2011. Choice of random rather than imprinted X inactivation in female embryonic stem cell-derived extra-embryonic cells. Development. 138**,** 197-202.

Murray, P., Edgar, D., 2001. Regulation of the differentiation and behaviour of extra-embryonic endodermal cells by basement membranes. J Cell Sci. 114**,** 931-9.

Narita, N., Bielinska, M., Wilson, D. B., 1997. Wild-type endoderm abrogates the ventral developmental defects associated with GATA-4 deficiency in the mouse. Dev Biol. 189**,** 270-4.

Ng, R. K., Dean, W., Dawson, C., Lucifero, D., Madeja, Z., Reik, W., Hemberger, M., 2008. Epigenetic restriction of embryonic cell lineage fate by methylation of Elf5. Nat Cell Biol. 10**,** 1280-90.

Niakan, K. K., Ji, H., Maehr, R., Vokes, S. A., Rodolfa, K. T., Sherwood, R. I., Yamaki, M., Dimos, J. T., Chen, A. E., Melton, D. A., McMahon, A. P., Eggan, K., 2010. Sox17 promotes differentiation in mouse embryonic stem cells by directly regulating extraembryonic gene expression and indirectly antagonizing self-renewal. Genes Dev. 24**,** 312-26.

Nichols, J., Silva, J., Roode, M., Smith, A., 2009. Suppression of Erk signalling promotes ground state pluripotency in the mouse embryo. Development. 136**,** 3215-22.

Nichols, J., Smith, A., Buehr, M., 1998a. Rat and mouse epiblasts differ in their capacity to generate extraembryonic endoderm. Reprod Fertil Dev. 10**,** 517-25.

Nichols, J., Zevnik, B., Anastassiadis, K., Niwa, H., Klewe-Nebenius, D., Chambers, I., Scholer, H., Smith, A., 1998b. Formation of pluripotent stem cells in the mammalian embryo depends on the POU transcription factor Oct4. Cell. 95**,** 379-91.

Niimi, T., Hayashi, Y., Futaki, S., Sekiguchi, K., 2004. SOX7 and SOX17 regulate the parietal endoderm-specific enhancer activity of mouse laminin alpha1 gene. J Biol Chem. 279**,** 38055-61.

Ninomiya, Y., Davies, T. J., Gardner, R. L., 2005. Experimental analysis of the transdifferentiation of visceral to parietal endoderm in the mouse. Dev Dyn. 233**,** 837-46.

Nishioka, N., Inoue, K., Adachi, K., Kiyonari, H., Ota, M., Ralston, A., Yabuta, N., Hirahara, S., Stephenson, R. O., Ogonuki, N., Makita, R., Kurihara, H., Morin-Kensicki, E. M., Nojima, H., Rossant, J., Nakao, K., Niwa, H., Sasaki, H., 2009. The Hippo signaling pathway components Lats and Yap pattern Tead4 activity to distinguish mouse trophectoderm from inner cell mass. Dev Cell. 16**,** 398-410.

Nishioka, N., Yamamoto, S., Kiyonari, H., Sato, H., Sawada, A., Ota, M., Nakao, K., Sasaki, H., 2008. Tead4 is required for specification of trophectoderm in pre-implantation mouse embryos. Mech Dev. 125**,** 270-83.

Niwa, H., Toyooka, Y., Shimosato, D., Strumpf, D., Takahashi, K., Yagi, R., Rossant, J., 2005. Interaction between Oct3/4 and Cdx2 determines trophectoderm differentiation. Cell. 123**,** 917-29.

Nomura, M., Li, E., 1998. Smad2 role in mesoderm formation, left-right patterning and craniofacial development. Nature. 393**,** 786-90.

Norris, D. P., Brennan, J., Bikoff, E. K., Robertson, E. J., 2002. The Foxh1-dependent autoregulatory enhancer controls the level of Nodal signals in the mouse embryo. Development. 129**,** 3455-68.

Ogawa, K., Saito, A., Matsui, H., Suzuki, H., Ohtsuka, S., Shimosato, D., Morishita, Y., Watabe, T., Niwa, H., Miyazono, K., 2007. Activin-Nodal signaling is involved in propagation of mouse embryonic stem cells. J Cell Sci. 120**,** 55-65.

Ogura, Y., Takakura, N., Yoshida, H., Nishikawa, S. I., 1998. Essential role of platelet-derived growth factor receptor alpha in the development of the intraplacental yolk sac/sinus of Duval in mouse placenta. Biol Reprod. 58**,** 65-72.

Oliver, G., Mailhos, A., Wehr, R., Copeland, N. G., Jenkins, N. A., Gruss, P., 1995. Six3, a murine homologue of the sine oculis gene, demarcates the most anterior border of the developing neural plate and is expressed during eye development. Development. 121**,** 4045-55.

Orr-Urtreger, A., Lonai, P., 1992. Platelet-derived growth factor-A and its receptor are expressed in separate, but adjacent cell layers of the mouse embryo. Development. 115**,** 1045-58.

Paca, A., Seguin, C. A., Clements, M., Ryczko, M., Rossant, J., Rodriguez, T. A., Kunath, T., 2012. BMP signaling induces visceral endoderm differentiation of XEN cells and parietal endoderm. Dev Biol. 361**,** 90-102.

Papaioannou, V. E., McBurney, M. W., Gardner, R. L., Evans, M. J., 1975. Fate of teratocarcinoma cells injected into early mouse embryos. Nature. 258**,** 70-73.

Pauken, C. M., Capco, D. G., 2000. The expression and stage-specific localization of protein kinase C isotypes during mouse preimplantation development. Dev Biol. 223**,** 411-21.

Perea-Gomez, A., Lawson, K. A., Rhinn, M., Zakin, L., Brulet, P., Mazan, S., Ang, S. L., 2001a. Otx2 is required for visceral endoderm movement and for the restriction of posterior signals in the epiblast of the mouse embryo. Development. 128**,** 753-65.

Perea-Gomez, A., Meilhac, S. M., Piotrowska-Nitsche, K., Gray, D., Collignon, J., Zernicka-Goetz, M., 2007. Regionalization of the mouse visceral endoderm as the blastocyst transforms into the egg cylinder. BMC Dev Biol. 7**,** 96.

Perea-Gomez, A., Rhinn, M., Ang, S. L., 2001b. Role of the anterior visceral endoderm in restricting posterior signals in the mouse embryo. Int J Dev Biol. 45**,** 311-20.

Perea-Gomez, A., Shawlot, W., Sasaki, H., Behringer, R. R., Ang, S., 1999. HNF3beta and Lim1 interact in the visceral endoderm to regulate primitive streak formation and anterior-posterior polarity in the mouse embryo. Development. 126**,** 4499-511.

Perea-Gomez, A., Vella, F. D., Shawlot, W., Oulad-Abdelghani, M., Chazaud, C., Meno, C., Pfister, V., Chen, L., Robertson, E., Hamada, H., Behringer, R. R., Ang, S. L., 2002. Nodal antagonists in the anterior visceral endoderm prevent the formation of multiple primitive streaks. Dev Cell. 3**,** 745-56.

Pereira, P. N., Dobreva, M. P., Graham, L., Huylebroeck, D., Lawson, K. A., Zwijsen, A. N., 2011. Amnion formation in the mouse embryo: the single amniochorionic fold model. BMC Dev Biol. 11**,** 48.

Pfister, S., Steiner, K. A., Tam, P. P., 2007. Gene expression pattern and progression of embryogenesis in the immediate post-implantation period of mouse development. Gene Expr Patterns. 7**,** 558-73.

Piccolo, S., Agius, E., Leyns, L., Bhattacharyya, S., Grunz, H., Bouwmeester, T., De Robertis, E. M., 1999. The head inducer Cerberus is a multifunctional antagonist of Nodal, BMP and Wnt signals. Nature. 397**,** 707-10.

Placantonakis, D. G., Tomishima, M. J., Lafaille, F., Desbordes, S. C., Jia, F., Socci, N. D., Viale, A., Lee, H., Harrison, N., Tabar, V., Studer, L., 2009. BAC transgenesis in human embryonic stem cells as a novel tool to define the human neural lineage. Stem Cells. 27**,** 521-32.

Plachta, N., Bollenbach, T., Pease, S., Fraser, S. E., Pantazis, P., 2011. Oct4 kinetics predict cell lineage patterning in the early mammalian embryo. Nat Cell Biol. 13**,** 117-23.

Plusa, B., Piliszek, A., Frankenberg, S., Artus, J., Hadjantonakis, A. K., 2008. Distinct sequential cell behaviours direct primitive endoderm formation in the mouse blastocyst. Development. 135**,** 3081-91.

Pollard, S. M., Benchoua, A., Lowell, S., 2006. Neural stem cells, neurons, and glia. Methods Enzymol. 418**,** 151-69.

Ralston, A., Cox, B. J., Nishioka, N., Sasaki, H., Chea, E., Rugg-Gunn, P., Guo, G., Robson, P., Draper, J. S., Rossant, J., 2010. Gata3 regulates trophoblast development downstream of Tead4 and in parallel to Cdx2. Development. 137**,** 395-403.

Ralston, A., Rossant, J., 2008. Cdx2 acts downstream of cell polarization to cell-autonomously promote trophectoderm fate in the early mouse embryo. Dev Biol. 313**,** 614-29.

Rekas, A., Alattia, J. R., Nagai, T., Miyawaki, A., Ikura, M., 2002. Crystal structure of venus, a yellow fluorescent protein with improved maturation and reduced environmental sensitivity. J Biol Chem. 277**,** 50573-8.

Reubinoff, B. E., Itsykson, P., Turetsky, T., Pera, M. F., Reinhartz, E., Itzik, A., Ben-Hur, T., 2001. Neural progenitors from human embryonic stem cells. Nat Biotechnol. 19**,** 1134-40.

Ribeiro, L. A., El-Jaick, K. B., Muenke, M., Richieri-Costa, A., 2006. SIX3 mutations with holoprosencephaly. Am J Med Genet A. 140**,** 2577-83.

Richardson, L., Torres-Padilla, M. E., Zernicka-Goetz, M., 2006. Regionalised signalling within the extraembryonic ectoderm regulates anterior visceral endoderm positioning in the mouse embryo. Mech Dev. 123**,** 288-96.

Rivera-Perez, J. A., Mager, J., Magnuson, T., 2003. Dynamic morphogenetic events characterize the mouse visceral endoderm. Dev Biol. 261**,** 470-87.

Robertson, E. J., Norris, D. P., Brennan, J., Bikoff, E. K., 2003. Control of early anterior-posterior patterning in the mouse embryo by TGF-beta signalling. Philos Trans R Soc Lond B Biol Sci. 358**,** 1351-7; discussion 1357.

Rodriguez, T. A., Casey, E. S., Harland, R. M., Smith, J. C., Beddington, R. S., 2001. Distinct enhancer elements control Hex expression during gastrulation and early organogenesis. Dev Biol. 234**,** 304-16.

Rodriguez, T. A., Srinivas, S., Clements, M. P., Smith, J. C., Beddington, R. S., 2005. Induction and migration of the anterior visceral endoderm is regulated by the extra-embryonic ectoderm. Development. 132**,** 2513-20.

Rossant, J., 1976. Postimplantation development of blastomeres isolated from 4- and 8-cell mouse eggs. J Embryol Exp Morphol. 36**,** 283-90.

Rossant, J., Tam, P. P., 2004. Emerging asymmetry and embryonic patterning in early mouse development. Dev Cell. 7**,** 155-64.

Rugg-Gunn, P. J., Cox, B. J., Ralston, A., Rossant, J., 2010. Distinct histone modifications in stem cell lines and tissue lineages from the early mouse embryo. Proc Natl Acad Sci U S A. 107**,** 10783-90.

Sakuma, R., Ohnishi Yi, Y., Meno, C., Fujii, H., Juan, H., Takeuchi, J., Ogura, T., Li, E., Miyazono, K., Hamada, H., 2002. Inhibition of Nodal signalling by Lefty mediated through interaction with common receptors and efficient diffusion. Genes Cells. 7**,** 401-12.

Salamat, M., Miosge, N., Herken, R., 1995. Development of Reichert's membrane in the early mouse embryo. Anat Embryol (Berl). 192**,** 275-81.

Samavarchi-Tehrani, P., Golipour, A., David, L., Sung, H. K., Beyer, T. A., Datti, A., Woltjen, K., Nagy, A., Wrana, J. L., 2010. Functional genomics reveals a BMP-driven mesenchymal-to-epithelial transition in the initiation of somatic cell reprogramming. Cell Stem Cell. 7**,** 64-77.

Sato, M., Ozawa, M., Hamada, H., Kasai, M., Tokunaga, T., Muramatsu, T., 1985. Cell surface markers to monitor the process of visceral endoderm differentiation from embryonal carcinoma cells: identification of the stage sensitive to high concentration of retinoic acid. J Embryol Exp Morphol. 88**,** 165-82.

Sekiya, S., Suzuki, A., 2011. Direct conversion of mouse fibroblasts to hepatocyte-like cells by defined factors. Nature. 475**,** 390-3.

Semoff, S., Hogan, B. L., Hopkins, C. R., 1982. Localization of fibronectin, laminin-entactin, and entactin in Reichert's membrane by immunoelectron microscopy. Embo J. 1**,** 1171-5.

Shawlot, W., Wakamiya, M., Kwan, K. M., Kania, A., Jessell, T. M., Behringer, R. R., 1999. Lim1 is required in both primitive streak-derived tissues and visceral endoderm for head formation in the mouse. Development. 126**,** 4925-32.

Shen, M. M., 2007. Nodal signaling: developmental roles and regulation. Development. 134**,** 1023-34.

Shi, W. K., Heath, J. K., 1984. Apolipoprotein expression by murine visceral yolk sac endoderm. J Embryol Exp Morphol. 81**,** 143-52.

Shimoda, M., Kanai-Azuma, M., Hara, K., Miyazaki, S., Kanai, Y., Monden, M., Miyazaki, J., 2007. Sox17 plays a substantial role in late-stage differentiation of the extraembryonic endoderm in vitro. J Cell Sci. 120**,** 3859-69.

Shimosato, D., Shiki, M., Niwa, H., 2007. Extra-embryonic endoderm cells derived from ES cells induced by GATA factors acquire the character of XEN cells. BMC Dev Biol. 7**,** 80.

Singh, A. M., Hamazaki, T., Hankowski, K. E., Terada, N., 2007. A heterogeneous expression pattern for Nanog in embryonic stem cells. Stem Cells. 25**,** 2534-42.

Sirard, C., de la Pompa, J. L., Elia, A., Itie, A., Mirtsos, C., Cheung, A., Hahn, S., Wakeham, A., Schwartz, L., Kern, S. E., Rossant, J., Mak, T. W., 1998. The tumor suppressor gene Smad4/Dpc4 is required for gastrulation and later for anterior development of the mouse embryo. Genes Dev. 12**,** 107-19.

Smith, J. R., Vallier, L., Lupo, G., Alexander, M., Harris, W. A., Pedersen, R. A., 2008. Inhibition of Activin/Nodal signaling promotes specification of human embryonic stem cells into neuroectoderm. Dev Biol. 313**,** 107-17.

Smith, K. K., Strickland, S., 1981. Structural components and characteristics of Reichert's membrane, an extra-embryonic basement membrane. J Biol Chem. 256**,** 4654-61.

Smyth, N., Vatansever, H. S., Murray, P., Meyer, M., Frie, C., Paulsson, M., Edgar, D., 1999. Absence of basement membranes after targeting the LAMC1 gene results in embryonic lethality due to failure of endoderm differentiation. J Cell Biol. 144**,** 151-60.

Soares, M. L., Haraguchi, S., Torres-Padilla, M. E., Kalmar, T., Carpenter, L., Bell, G., Morrison, A., Ring, C. J., Clarke, N. J., Glover, D. M., Zernicka-Goetz, M., 2005. Functional studies of signaling pathways in peri-implantation development of the mouse embryo by RNAi. BMC Dev Biol. 5**,** 28.

Soares, M. L., Torres-Padilla, M. E., Zernicka-Goetz, M., 2008. Bone morphogenetic protein 4 signaling regulates development of the anterior visceral endoderm in the mouse embryo. Dev Growth Differ. 50**,** 615-21.

Soldner, F., Laganiere, J., Cheng, A. W., Hockemeyer, D., Gao, Q., Alagappan, R., Khurana, V., Golbe, L. I., Myers, R. H., Lindquist, S., Zhang, L., Guschin, D., Fong, L. K., Vu, B. J., Meng, X., Urnov, F. D., Rebar, E. J., Gregory, P. D., Zhang, H. S., Jaenisch, R., 2011. Generation of isogenic pluripotent stem cells differing exclusively at two early onset Parkinson point mutations. Cell. 146**,** 318-31.

Solomon, B. D., Lacbawan, F., Jain, M., Domene, S., Roessler, E., Moore, C., Dobyns, W. B., Muenke, M., 2009. A novel SIX3 mutation segregates with holoprosencephaly in a large family. Am J Med Genet A. 149A**,** 919-25.

Song, H., Chung, S. K., Xu, Y., 2010. Modeling disease in human ESCs using an efficient BAC-based homologous recombination system. Cell Stem Cell. 6**,** 80-9.

Spemann, H., Mangold, H., 1924. Über induktion von Embryonalagen durch Implantation Artfremder Organisatoren. Roux' Arch. Entw. Mech. 100**,** 599–638.

Spruce, T., Pernaute, B., Di-Gregorio, A., Cobb, B. S., Merkenschlager, M., Manzanares, M., Rodriguez, T. A., 2010. An early developmental role for miRNAs in the maintenance of extraembryonic stem cells in the mouse embryo. Dev Cell. 19**,** 207-19.

Srinivas, S., 2006. The anterior visceral endoderm-turning heads. Genesis. 44**,** 565-72.

Srinivas, S., Rodriguez, T., Clements, M., Smith, J. C., Beddington, R. S., 2004. Active cell migration drives the unilateral movements of the anterior visceral endoderm. Development. 131**,** 1157-64.

Stephens, L. E., Sutherland, A. E., Klimanskaya, I. V., Andrieux, A., Meneses, J., Pedersen, R. A., Damsky, C. H., 1995. Deletion of beta 1 integrins in mice results in inner cell mass failure and peri-implantation lethality. Genes Dev. 9**,** 1883-95.

Strickland, S., Smith, K. K., Marotti, K. R., 1980. Hormonal induction of differentiation in teratocarcinoma stem cells: generation of parietal endoderm by retinoic acid and dibutyryl cAMP. Cell. 21**,** 347-55.

Strumpf, D., Mao, C. A., Yamanaka, Y., Ralston, A., Chawengsaksophak, K., Beck, F., Rossant, J., 2005. Cdx2 is required for correct cell fate specification and differentiation of trophectoderm in the mouse blastocyst. Development. 132**,** 2093-102.

Stuckey, D. W., Clements, M., Di-Gregorio, A., Senner, C. E., Le Tissier, P., Srinivas, S., Rodriguez, T. A., 2011. Coordination of cell proliferation and anterior-posterior axis establishment in the mouse embryo. Development. 138**,** 1521-30.

Suh, C. S., Ellingsen, S., Austbo, L., Zhao, X. F., Seo, H. C., Fjose, A., 2010. Autoregulatory binding sites in the zebrafish six3a promoter region define a new recognition sequence for Six3 proteins. FEBS J. 277**,** 1761-75.

Suzuki, K., Mitsui, K., Aizawa, E., Hasegawa, K., Kawase, E., Yamagishi, T., Shimizu, Y., Suemori, H., Nakatsuji, N., Mitani, K., 2008. Highly efficient transient gene expression and gene targeting in primate embryonic stem cells with helper-dependent adenoviral vectors. Proc Natl Acad Sci U S A. 105**,** 13781-6.

Takagi, N., Sasaki, M., 1975. Preferential inactivation of the paternally derived X chromosome in the extraembryonic membranes of the mouse. Nature. 256**,** 640-2.

Takakura, N., Yoshida, H., Ogura, Y., Kataoka, H., Nishikawa, S., 1997. PDGFR alpha expression during mouse embryogenesis: immunolocalization analyzed by whole-mount immunohistostaining using the monoclonal anti-mouse PDGFR alpha antibody APA5. J Histochem Cytochem. 45**,** 883-93.

Takaoka, K., Yamamoto, M., Hamada, H., 2011. Origin and role of distal visceral endoderm, a group of cells that determines anterior-posterior polarity of the mouse embryo. Nat Cell Biol. 13**,** 743-52.

Takaoka, K., Yamamoto, M., Shiratori, H., Meno, C., Rossant, J., Saijoh, Y., Hamada, H., 2006. The mouse embryo autonomously acquires anterior-posterior polarity at implantation. Dev Cell. 10**,** 451-9.

Takito, J., Al-Awqati, Q., 2004. Conversion of ES cells to columnar epithelia by hensin and to squamous epithelia by laminin. J Cell Biol. 166**,** 1093-102.

Tam, P. P., Loebel, D. A., 2007. Gene function in mouse embryogenesis: get set for gastrulation. Nat Rev Genet. 8**,** 368-81.

Tam, P. P., Steiner, K. A., 1999. Anterior patterning by synergistic activity of the early gastrula organizer and the anterior germ layer tissues of the mouse embryo. Development. 126**,** 5171-9.

Tanaka, S., Kunath, T., Hadjantonakis, A. K., Nagy, A., Rossant, J., 1998. Promotion of trophoblast stem cell proliferation by FGF4. Science. 282**,** 2072-5.

Tao, H., Suzuki, M., Kiyonari, H., Abe, T., Sasaoka, T., Ueno, N., 2009. Mouse prickle1, the homolog of a PCP gene, is essential for epiblast apical-basal polarity. Proc Natl Acad Sci U S A. 106**,** 14426-31.

Tarkowski, A. K., Wroblewska, J., 1967. Development of blastomeres of mouse eggs isolated at the 4- and 8-cell stage. J Embryol Exp Morphol. 18**,** 155-80.

Tesar, P. J., Chenoweth, J. G., Brook, F. A., Davies, T. J., Evans, E. P., Mack, D. L., Gardner, R. L., McKay, R. D., 2007. New cell lines from mouse epiblast share defining features with human embryonic stem cells. Nature. 448**,** 196-9.

Thomas, P., Beddington, R., 1996. Anterior primitive endoderm may be responsible for patterning the anterior neural plate in the mouse embryo. Curr Biol. 6**,** 1487-96.

Thomas, P. Q., Brown, A., Beddington, R. S., 1998. Hex: a homeobox gene revealing peri-implantation asymmetry in the mouse embryo and an early transient marker of endothelial cell precursors. Development. 125**,** 85-94.

Thompson, N., Lyons, J., 2005. Recent progress in targeting the Raf/MEK/ERK pathway with inhibitors in cancer drug discovery. Curr Opin Pharmacol. 5**,** 350-6.

Thomson, J. A., Itskovitz-Eldor, J., Shapiro, S. S., Waknitz, M. A., Swiergiel, J. J., Marshall, V. S., Jones, J. M., 1998. Embryonic stem cell lines derived from human blastocysts. Science. 282**,** 1145-7.

Toles, J. F., Chui, D. H., Belbeck, L. W., Starr, E., Barker, J. E., 1989. Hemopoietic stem cells in murine embryonic yolk sac and peripheral blood. Proc Natl Acad Sci U S A. 86**,** 7456-9.

Tomishima, M. J., Hadjantonakis, A. K., Gong, S., Studer, L., 2007. Production of green fluorescent protein transgenic embryonic stem cells using the GENSAT bacterial artificial chromosome library. Stem Cells. 25**,** 39-45.

Torres-Padilla, M. E., Richardson, L., Kolasinska, P., Meilhac, S. M., Luetke-Eversloh, M. V., Zernicka-Goetz, M., 2007. The anterior visceral endoderm of the mouse embryo is established from both preimplantation precursor cells and by de novo gene expression after implantation. Dev Biol. 309**,** 97-112.

Townsend, J. A., Wright, D. A., Winfrey, R. J., Fu, F., Maeder, M. L., Joung, J. K., Voytas, D. F., 2009. High-frequency modification of plant genes using engineered zinc-finger nucleases. Nature. 459**,** 442-5.

Tremblay, K. D., Dunn, N. R., Robertson, E. J., 2001. Mouse embryos lacking Smad1 signals display defects in extra-embryonic tissues and germ cell formation. Development. 128**,** 3609-21.

Tremblay, K. D., Hoodless, P. A., Bikoff, E. K., Robertson, E. J., 2000. Formation of the definitive endoderm in mouse is a Smad2-dependent process. Development. 127**,** 3079-90.

Trichas, G., Joyce, B., Crompton, L. A., Wilkins, V., Clements, M., Tada, M., Rodriguez, T. A., Srinivas, S., 2011. Nodal dependent differential localisation of dishevelled-2 demarcates regions of differing cell behaviour in the visceral endoderm. PLoS Biol. 9**,** e1001019.

Vallier, L., Alexander, M., Pedersen, R. A., 2005. Activin/Nodal and FGF pathways cooperate to maintain pluripotency of human embryonic stem cells. J Cell Sci. 118**,** 4495-509.

Vallier, L., Reynolds, D., Pedersen, R. A., 2004. Nodal inhibits differentiation of human embryonic stem cells along the neuroectodermal default pathway. Dev Biol. 275**,** 403-21.

van de Stolpe, A., Karperien, M., Lowik, C. W., Juppner, H., Segre, G. V., Abou-Samra, A. B., de Laat, S. W., Defize, L. H., 1993. Parathyroid hormone-related peptide as an endogenous inducer of parietal endoderm differentiation. J Cell Biol. 120**,** 235-43.

Veltmaat, J. M., Orelio, C. C., Ward-Van Oostwaard, D., Van Rooijen, M. A., Mummery, C. L., Defize, L. H., 2000. Snail is an immediate early target gene

of parathyroid hormone related peptide signaling in parietal endoderm formation. Int J Dev Biol. 44**,** 297-307.

Verheijen, M. H., Defize, L. H., 1999. Signals governing extraembryonic endoderm formation in the mouse: involvement of the type 1 parathyroid hormone-related peptide (PTHrP) receptor, p21Ras and cell adhesion molecules. Int J Dev Biol. 43**,** 711-21.

Verheijen, M. H., Karperien, M., Chung, U., van Wijuen, M., Heystek, H., Hendriks, J. A., Veltmaat, J. M., Lanske, B., Li, E., Lowik, C. W., de Laat, S. W., Kronenberg, H. M., Defize, L. H., 1999a. Parathyroid hormone-related peptide (PTHrP) induces parietal endoderm formation exclusively via the type I PTH/PTHrP receptor. Mech Dev. 81**,** 151-61.

Verheijen, M. H., Wolthuis, R. M., Bos, J. L., Defize, L. H., 1999b. The Ras/Erk pathway induces primitive endoderm but prevents parietal endoderm differentiation of F9 embryonal carcinoma cells. J Biol Chem. 274**,** 1487-94.

Verheijen, M. H., Wolthuis, R. M., Defize, L. H., den Hertog, J., Bos, J. L., 1999c. Interdependent action of RalGEF and Erk in Ras-induced primitive endoderm differentiation of F9 embryonal carcinoma cells. Oncogene. 18**,** 4435-9.

Vinot, S., Le, T., Ohno, S., Pawson, T., Maro, B., Louvet-Vallee, S., 2005. Asymmetric distribution of PAR proteins in the mouse embryo begins at the 8-cell stage during compaction. Dev Biol. 282**,** 307-19.

Waddington, C. H., 1932. Experiments on the development of chick and duck embryos, cultivated in vitro. Phil. Trans. R. Soc. B. 221**,** 179-230.

Waddington, C. H., 1933. Induction by the primitive streak and its derivatives in the chick. J. Exp. Biol. 10**,** 38-46.

Waldrip, W. R., Bikoff, E. K., Hoodless, P. A., Wrana, J. L., Robertson, E. J., 1998. Smad2 signaling in extraembryonic tissues determines anterior-posterior polarity of the early mouse embryo. Cell. 92**,** 797-808.

Wallis, D. E., Roessler, E., Hehr, U., Nanni, L., Wiltshire, T., Richieri-Costa, A., Gillessen-Kaesbach, G., Zackai, E. H., Rommens, J., Muenke, M., 1999. Mutations in the homeodomain of the human SIX3 gene cause holoprosencephaly. Nat Genet. 22**,** 196-8.

Wang, P., Rodriguez, R. T., Wang, J., Ghodasara, A., Kim, S. K., 2011a. Targeting SOX17 in human embryonic stem cells creates unique strategies for isolating and analyzing developing endoderm. Cell Stem Cell. 8**,** 335-46.

Wang, Y., Smedberg, J. L., Cai, K. Q., Capo-Chichi, D. C., Xu, X. X., 2011b. Ectopic expression of GATA6 bypasses requirement for Grb2 in primitive endoderm formation. Dev Dyn. 240**,** 566-76.

Wartiovaara, J., Leivo, I., Vaheri, A., 1979. Expression of the cell surface-associated glycoprotein, fibronectin, in the early mouse embryo. Dev Biol. 69**,** 247-57.

Watanabe, K., Ueno, M., Kamiya, D., Nishiyama, A., Matsumura, M., Wataya, T., Takahashi, J. B., Nishikawa, S., Nishikawa, S., Muguruma, K., Sasai, Y., 2007. A ROCK inhibitor permits survival of dissociated human embryonic stem cells. Nat Biotechnol. 25**,** 681-6.

Wei, Z., Yaguchi, J., Yaguchi, S., Angerer, R. C., Angerer, L. M., 2009. The sea urchin animal pole domain is a Six3-dependent neurogenic patterning center. Development. 136**,** 1179-89.

Willnow, T. E., Hilpert, J., Armstrong, S. A., Rohlmann, A., Hammer, R. E., Burns, D. K., Herz, J., 1996. Defective forebrain development in mice lacking gp330/megalin. Proc Natl Acad Sci U S A. 93**,** 8460-4.

Xu, R. H., Peck, R. M., Li, D. S., Feng, X., Ludwig, T., Thomson, J. A., 2005. Basic FGF and suppression of BMP signaling sustain undifferentiated proliferation of human ES cells. Nat Methods. 2**,** 185-90.

Yamamoto, H., Flannery, M. L., Kupriyanov, S., Pearce, J., McKercher, S. R., Henkel, G. W., Maki, R. A., Werb, Z., Oshima, R. G., 1998. Defective trophoblast function in mice with a targeted mutation of Ets2. Genes Dev. 12**,** 1315-26.

Yamamoto, M., Beppu, H., Takaoka, K., Meno, C., Li, E., Miyazono, K., Hamada, H., 2009. Antagonism between Smad1 and Smad2 signaling determines the site of distal visceral endoderm formation in the mouse embryo. J Cell Biol. 184**,** 323-34.

Yamamoto, M., Meno, C., Sakai, Y., Shiratori, H., Mochida, K., Ikawa, Y., Saijoh, Y., Hamada, H., 2001. The transcription factor FoxH1 (FAST) mediates Nodal signaling during anterior-posterior patterning and node formation in the mouse. Genes Dev. 15**,** 1242-56.

Yamamoto, M., Saijoh, Y., Perea-Gomez, A., Shawlot, W., Behringer, R. R., Ang, S. L., Hamada, H., Meno, C., 2004. Nodal antagonists regulate formation of the anteroposterior axis of the mouse embryo. Nature. 428**,** 387-92.

Yamanaka, Y., Lanner, F., Rossant, J., 2010. FGF signal-dependent segregation of primitive endoderm and epiblast in the mouse blastocyst. Development. 137**,** 715-24.

Yang, Y. P., Klingensmith, J., 2006. Roles of organizer factors and BMP antagonism in mammalian forebrain establishment. Dev Biol. 296**,** 458-75.

Yeo, C., Whitman, M., 2001. Nodal signals to Smads through Cripto-dependent and Cripto-independent mechanisms. Mol Cell. 7**,** 949-57.

Ying, Q. L., Nichols, J., Chambers, I., Smith, A., 2003. BMP induction of Id proteins suppresses differentiation and sustains embryonic stem cell self-renewal in collaboration with STAT3. Cell. 115**,** 281-92.

Zhang, H., Bradley, A., 1996. Mice deficient for BMP2 are nonviable and have defects in amnion/chorion and cardiac development. Development. 122**,** 2977-86.

Zhang, S. C., Wernig, M., Duncan, I. D., Brustle, O., Thomson, J. A., 2001. In vitro differentiation of transplantable neural precursors from human embryonic stem cells. Nat Biotechnol. 19**,** 1129-33.

Zhang, W., Yatskievych, T. A., Cao, X., Antin, P. B., 2002. Regulation of Hex gene expression by a Smads-dependent signaling pathway. J Biol Chem. 277**,** 45435-41.

Zhang, X., Huang, C. T., Chen, J., Pankratz, M. T., Xi, J., Li, J., Yang, Y., Lavaute, T. M., Li, X. J., Ayala, M., Bondarenko, G. I., Du, Z. W., Jin, Y., Golos, T. G., Zhang, S. C., 2010. Pax6 is a human neuroectoderm cell fate determinant. Cell Stem Cell. 7**,** 90-100.

Zhang, Y., Buchholz, F., Muyrers, J. P., Stewart, A. F., 1998. A new logic for DNA engineering using recombination in Escherichia coli. Nat Genet. 20**,** 123-8.

Zhang, Y., Muyrers, J. P., Testa, G., Stewart, A. F., 2000. DNA cloning by homologous recombination in Escherichia coli. Nat Biotechnol. 18**,** 1314-7.

Zhou, J., Hernandez, G., Tu, S. W., Scholes, J., Chen, H., Tseng, C. P., Hsieh, J. T., 2005. Synergistic induction of DOC-2/DAB2 gene expression in transitional cell carcinoma in the presence of GATA6 and histone deacetylase inhibitor. Cancer Res. 65**,** 6089-96.

Zou, J., Maeder, M. L., Mali, P., Pruett-Miller, S. M., Thibodeau-Beganny, S., Chou, B. K., Chen, G., Ye, Z., Park, I. H., Daley, G. Q., Porteus, M. H., Joung, J. K., Cheng, L., 2009. Gene targeting of a disease-related gene in human induced pluripotent stem and embryonic stem cells. Cell Stem Cell. 5**,** 97-110.

Zwaka, T. P., Thomson, J. A., 2003. Homologous recombination in human embryonic stem cells. Nat Biotechnol. 21**,** 319-21.